UNIVERSITÉ DU QUÉBEC À MONTRÉAL

PRÉTRAITEMENT ET TRAITEMENT PASSIF DU DRAINAGE MINIER ACIDE FERRIFÈRE

THÈSE

PRÉSENTÉE

COMME EXIGENCE PARTIELLE

DU DOCTORAT EN SCIENCES DE L'ENVIRONNEMENT

PAR

TSIVERIHASINA VAVAKA RAKOTONIMARO

AOÛT 2017

À ma famille, à mon frère qui a été avec nous jusqu'à l'âge de 14 ans.

REMERCIEMENTS

Je tiens premièrement à adresser mes sincères remerciements à mon directeur de thèse, Prof. Carmen Mihaela Neculita, pour avoir été toujours présente et avec qui j'ai beaucoup appris durant les cinq années où j'ai travaillé avec elle au sein de l'Institut de recherche en mines et en environnement (IRME), à l'Université du Québec en Abitibi-Témiscamingue (UQAT). Ses précieux conseils, ses encouragements et son soutien m'ont forgé et m'ont permis de m'enrichir et de me dépasser sur le plan professionnel. Toujours disponible et passionnée, elle a été plus qu'un simple professeur à mes côtés.

Je tiens également à remercier mon codirecteur de thèse, Prof. Bruno Bussière, pour m'avoir permis d'intégrer son équipe et de pouvoir travailler sur ce projet. Sa confiance et son appui me sont précieux.

Mes remerciements vont également au Prof. Gérald J. Zagury, mon codirecteur, dont les suggestions et commentaires constructifs m'ont permis de bien poursuivre ce projet.

J'aimerais remercier le Dr Thomas Genty pour sa disponibilité, son aide et ses conseils bien appréciés et de qui j'ai hérité un beau projet.

J'adresse également mes remerciements aux professeurs Mostapha Benzaazoua et Vincent Cloutier ainsi qu'au Dr Robin Potvin pour leur implication lors de la synthèse environnementale qui m'a permis de publier un article de revue scientifique.

Je remercie aussi tous les membres de l'équipe du laboratoire de l'Unité de recherche et de technologie minérale (URSTM) qui ont contribué de près ou de loin à la réalisation de ce projet, particulièrement, Marc Paquin, Patrick Bernèche, Mélanie Bélanger, Alain Perreault, Yvan Poirier, Dr Bruno Bossé et Joël Beauregard.

Mes remerciements vont également aux stagiaires/étudiants qui ont contribué aux travaux de laboratoire durant cette étude : Thomas Lux, Houssem Eddine Ben Ali, Bryce Le Bourre, Tomy Roy et Marouen Jouini.

J'adresse mes remerciements aux partenaires de l'IRME UQAT- Polytechnique ainsi qu'au CRSNG pour avoir financé cette étude.

J'aimerais exprimer mes remerciements à mes évaluateurs externes, à savoir le Dr Tobias Rötting, le Prof. Jean-François Blais et la Prof. Cécile Bulle, pour leur vif intérêt pour ce projet.

Enfin, je remercie ma famille, tous mes amis ainsi que mes collègues de l'IRME et du Comité des étudiants en recherche mines et environnement (CERME).

AVANT-PROPOS

Cette thèse est présentée sous forme d'articles scientifiques. Les articles concernés sont les chapitres 3, 4 et 5, rédigés en anglais selon les exigences des revues, tandis que le reste de la thèse est rédigé en français. Je suis le premier auteur de ces articles et mon directeur de thèse, Carmen Mihaela Neculita, ainsi que mes codirecteurs Bruno Bussière et Gérald J. Zagury, sont les coauteurs des trois articles. Ils ont également contribué étroitement à la réalisation de l'ensemble de la thèse, depuis l'établissement du projet jusqu'à la rédaction de ce rapport final.

Chapitre 3- **Rakotonimaro, T.V.**, Neculita, C.M., Bussière, B., Zagury, G.J., 2016. Effectiveness of various dispersed alkaline substrates for the pretreatment of ferriferous acid mine drainage. *Applied Geochemistry* 73: 13−23.

Chapitre 4- **Rakotonimaro, T.V.**, Neculita, C.M., Bussière, B., Zagury, G.J., 2017a. Comparative column testing of three reactive mixtures for the bio-chemical treatment of iron-rich acid mine drainage. *Minerals Engineering* 111: 79−89.

Chapitre 5- **Rakotonimaro, T.V**., Neculita, C.M., Bussière, B., Genty, T., Zagury, G.J., 2017b. Scale effect assessment of passive multi-step treatment system and new design criteria for the treatment of iron-rich acid mine drainage. (soumis pour publication potentielle dans *Environmental Science and Pollution Research*).

TABLE DES MATIÈRES

LISTE DES FIGURES

LISTE DES TABLEAUX

LISTE DES ABRÉVIATIONS, SIGLES ET ACRONYMES

APHA	American Public Health Association
ASTM	American Society for Testing and Materials
BFR/IRB	Bactéries ferri-réductrices/Iron Reducing Bacteria
BSR/SRB	Bactéries sulfato-réductrices/Sulfate Reducing Bacteria
CB/WA	Cendres de bois/Wood Ash
CE/EC	Conductivité électrique/Electrical Conductivity
CIT/TIC	Carbone inorganique total/Total Inorganic Carbon
COD/DOC	Carbone organique dissous/Dissolved Organic Carbon
COT/TOC	Carbone organique total/Total Organic Carbon
Cu	Coefficient d'uniformité
DAC/ALD	Drain anoxique calcaire/Anoxic Limestone Drain
DMA/AMD	Drainage minier acide/Acid Mine Drainage
DRX/XRD	Diffraction des rayons X/X-Ray Diffraction
DOC/OLD	Drain oxique calcaire/Oxic Limestone Drain
ESH/SHE	Électrode standard à hydrogène/Standard Hydrogen Electrode
i.e	C'est-à-dire/id est
k_{sat}	Conductivité hydraulique saturée / Saturated Hydraulic Conductivity

MEB/SEM-EDS	Microscope à balayage électronique/ Scanning Electron Microscopy with X-Ray Energy Dispersion
n	Porosité/Porosity
OD/DO	Oxygène dissous/Dissolved Oxygen
POR/ORP	Potentiel d'oxydo-réduction/Oxydo-Reduction Potential
SAD/DAS	Substrat alcalin dispersé/Dispersed Alkaline Substrate
TRH/HRT	Temps de résidence hydraulique/Hydraulic Retention Time
USEPA	United States Environmental Protection Agency/Agence de protection de l'environnement des États-Unis
Via	Par
vs	Versus

RÉSUMÉ

La combinaison de plusieurs unités de traitement passif, dite connue comme filière de traitement passif, est présentement une technologie de plus en plus utilisée pour traiter le drainage minier acide (DMA) fortement contaminé, incluant le DMA riche en fer (>500 mg/L) ou le DMA ferrifère lors de la restauration des sites miniers abandonnés/fermés. Les technologies passives les plus fréquemment utilisées dans les filières sont les réacteurs passifs biochimiques (RPB) et les drains calcaires (oxique/anoxique). En général, les essais de laboratoire ont montré des résultats satisfaisants, à l'exception des problèmes d'écoulement en surface, qui surviennent sur le terrain (surtout dans le cas du traitement du DMA ferrifère), montrant qu'une recherche plus approfondie est nécessaire. L'utilisation de mélanges réactifs à haute porosité et à forte alcalinité, de type substrats alcalins dispersés (SAD), composés de copeaux de bois et d'agent neutralisant (p. ex. : $CaCO_3$, MgO) est présentement l'alternative qui pourrait limiter les problèmes d'enrobage et de colmatage (problèmes hydrauliques) communément constatés dans les systèmes de traitements passifs.

Dans ce contexte, les principaux objectifs de cette thèse sont les suivants : 1) évaluer l'efficacité des unités composées de mélanges à haute porosité et forte alcalinité sur le traitement du DMA ferrifère; 2) évaluer la performance à long terme d'une unité de prétraitement du Fe dans une filière; et 3) réaliser une étude comparative des résultats de laboratoire et sur le terrain, afin de proposer de nouveaux critères de design utiles pour construire une filière de traitement passif efficace du DMA ferrifère. Pour atteindre ces objectifs, des travaux de laboratoire (essais en batch- sans écoulement et en colonnes- avec écoulement) et de terrain ont été réalisés. Les travaux de terrain étaient réalisés sur le site Lorraine (pilote de terrain) pendant la période estivale de 2012–2016. L'approche méthodologique générale a été réalisée en trois étapes consécutives/complémentaires.

La première étape consistait à caractériser et à évaluer l'efficacité des mélanges de type SAD, afin d'en sélectionner le(s) mélange(s) le(s) plus efficace(s) pour le prétraitement du Fe dans le DMA ferrifère (pH 4, 2500 mg/L Fe et 5000 mg/L SO_4^{2-}). Ainsi, trois types de SAD composés de matériaux alcalins naturels (cendres de bois, calcite, dolomite), à différentes proportions (20, 50% et 80% v/v) et des substrats à grande surface spécifique (copeaux de bois) ont été testés dans neuf réacteurs batch. Les essais ont été réalisés en duplicata pendant une période de 91 j. Les résultats ont montré que les mélanges composés de cendre de bois (CB-SAD) présentaient une surface spécifique 17–60 fois supérieure aux mélanges composés de calcite ou de dolomite (calcite-SAD et dolomite-SAD, respectivement). De plus, tous les mélanges pouvaient

enlever jusqu'à 99,9% de Fe et 40% de SO_4^{2-}, tandis que la calcite-SAD et la dolomite-SAD avaient une efficacité comparable à long terme (16–27% Fe et <10% SO_4^{2-}). Le mélange avec 50% de cendre de bois (CB50) a été sélectionné en compromis, étant donné le contenu trop élevé en fines de CB80 (80% cendre de bois), et que l'efficacité de CB20 (20% cendre de bois) risquerait de diminuer rapidement. Les mélanges calcite-SAD et/ou dolomite-SAD étaient plutôt suggérés pour être utilisés dans des unités de polissage.

Par la suite, en deuxième étape, deux des mélanges les plus performants testés lors des essais batch, i.e., CB50 et C20 (20% calcite), ont été sélectionnés pour prétraiter le Fe dans des réacteurs de type colonne de 1,5 L. Un troisième mélange, composé de matériaux organiques (70%) et inorganiques (30%), a également été testé pour être utilisé dans un RPB, surtout pour traiter les SO_4^{2-} en raison de l'efficacité limitée du traitement des SO_4^{2-} par les mélanges SAD. L'efficacité et la performance hydraulique de ces trois mélanges, qui étaient exploités à différents temps de résidence hydraulique (TRH) (1–5 j), ont alors été évaluées. Les résultats ont montré qu'un TRH minimum de 2 j est nécessaire pour traiter un DMA ferrifère (pH 2–4, Fe 500–2500 mg/L et ~5000 mg/L SO_4^{2-}). Les réacteurs CB50 ont montré une meilleure efficacité d'enlèvement du Fe et des SO_4^{2-} (17–62% et de 7,5–37%, respectivement) à un TRH de 5 j (CB50-5), tandis que les réacteurs C20 étaient efficaces seulement à très court terme (les premiers 7 j) à un TRH de 2 j. L'efficacité des RPB augmentait de 77% à 91% lorsque le TRH était doublé de 2,5 à 5 j. Cette partie de l'étude a aussi permis de trouver qu'une compétition potentielle entre les bactéries ferri-réductrices et les bactéries sulfato-réductrices a pu entraîner une diminution de l'enlèvement des SO_4^{2-} de 91% à moins de 14% dans les RPB. L'évolution de la conductivité hydraulique (k_{sat}) dans tous les réacteurs a montré des changements peu significatifs et qu'effectivement, le problème de colmatage était limité, même avec un TRH de 5 j.

Dans la troisième étape de l'étude, les résultats obtenus durant les essais batch et en petites colonnes ont été utilisés pour monter trois scénarios de filières de traitement du DMA ferrifère dans des réacteurs colonnes de 10,7 L. Cette dernière étape consistait à comparer la performance des filières de laboratoire et de la filière de terrain, afin d'évaluer l'effet d'échelle et d'identifier les facteurs et paramètres qui ont un impact sur la performance à long terme. Les résultats des études ont montré que les paramètres qui pourraient influencer la performance des expériences au laboratoire et sur le terrain, sont la conductivité électrique, le débit (Q), la conductivité hydraulique saturée (k_{sat}) et la concentration en Fe et SO_4^{2-}. Au laboratoire, une filière intégrant une unité de prétraitement du Fe et utilisant des mélanges SAD, pouvait enlever 52–98% de Fe. Les meilleures performances ont été obtenues lorsque deux unités de prétraitement ont été utilisées. Les unités de prétraitement les plus efficaces étaient les deux CB50 avec, en moyenne, un enlèvement de 82% de Fe et 79% de SO_4^{2-}. Par conséquent, le RPB qui les succédait, pouvait traiter, en moyenne, 86% de Fe et 98% de SO_4^{2-}. Sur le terrain, l'efficacité d'une filière à base de RPB était d'environ 75%. Le prétraitement du Fe a

amélioré la performance globale d'une filière de traitement passif du DMA ferrifère. De plus, la comparaison des essais en laboratoire et sur le terrain a permis de déterminer que le débit Q est le paramètre qui affecte le plus la performance à long terme d'une filière de traitement du DMA ferrifère. Enfin, de nouveaux critères de design pour la conception d'une filière de traitement du DMA ferrifère ont été proposés et visent les concentrations du Fe et des SO_4^{2-}, ainsi que le k_{sat}. De plus, un RPB est plus efficace avec une charge en Fe <26 g/m^{3}substrat/j et en SO_4^{2-} <110 g/m^{3}substrat/j. Cette partie de l'étude a également permis de suggérer l'utilisation d'un mélange avec un k_{sat} >10^{-3}cm/s pour traiter un DMA ferrifère. Par ailleurs, un facteur de correction de 0,2–0,8 pourrait être pris en compte sur la valeur de Q et l'enlèvement du Fe, ainsi que 1/100 sur le k_{sat} mesuré au laboratoire pour prédire la durabilité du traitement sur le terrain.

Le présent projet a donc permis d'approfondir les connaissances liées au traitement du DMA ferrifère (Fe >500 mg/L) au moyen des filières de traitement passif. De plus, les cendres de bois, qui étaient utilisés comme substitution de matériaux moins coûteux dans la composition des SAD, se sont montrés aussi efficaces que les matériaux conventionnels ($CaCO_3$, MgO) utilisés dans les SAD. Les nouveaux critères de design proposés dans cette étude constituent également un apport scientifique innovant. Enfin, les connaissances et les approches méthodologiques acquises durant cette étude pourront être applicables à d'autres qualités d'eau pour la restrauration d'autres sites miniers abandonnés ou fermés.

Mots clés : Drainage minier acide (DMA), Substrat alcalin dispersé (SAD), fer, traitement passif, filière, Réacteur passif biochimique (RPB), critères de design

ABSTRACT

The combination of several units of passive treatment, known as multi-step passive treatment is presently an increasingly technology used to treat highly contaminated acid mine drainage (AMD), including iron-rich AMD (>500 mg/L) or ferriferous AMD, during rehabilitation of abandoned/closed mine sites. The most commonly used passive technologies in multi-step systems are the passive biochemical reactors (PBRs) and limestone drains (oxic/anoxic, respectively). In general, laboratory testing has shown satisfactorily results except surface runoff problems in the field (especially in the case of the treatment of ferriferous AMD), showing that further research is needed. The use of highly porous reactive mixtures type dispersed alkaline substrate (DAS), composed of wood chips and neutralizing agent (e.g. $CaCO_3$, MgO), is presently the alternative that limit the coating and clogging problems (hydraulic problems) commonly found in passive treatment systems.

In this context, the main objectives of this thesis are the following: 1) to evaluate the efficiency of DAS units for the treatment of Fe-rich AMD; 2) to evaluate the long-term performance of a Fe pretreatment unit in a multi-step system; and 3) to carry out a comparative study of laboratory and field experiments in order to propose new design criteria useful for constructing an efficient multi-step treatment passive of Fe-rich AMD.

To achieve these objectives, laboratory (batch-without flow and column-with continuous flow) and field experiments were carried out. The fieldwork was performed on Lorraine mine site (field pilot) during the summer period of 2012-2016. The experimental approaches (laboratory and field experiments) were undertaken into three consecutive/complementary steps.

The first step consists of characterizing and evaluating the effectiveness of the DAS mixtures in order to select the most efficient for Fe pretreatment in ferriferous AMD (pH 4, 2500 mg/L Fe, and 5000 mg/L SO_4^{2-}). To do so, three types of DAS composed of natural alkaline materials (wood ash, calcite, dolomite), at different proportions (20% v/v, 50% v/v, 80% v/v) and materials with high specific surface area (wood chips) were tested in 9 batch reactors. The tests were performed in duplicate for a period of 91 days. Results showed that wood-ash mixtures (WA-DAS) had a specific surface area 17–60 times higher than the mixtures composed of calcite or dolomite (calcite-DAS and dolomite-DAS, respectively). In addition, all mixtures could remove up to 99.9% Fe and 40% SO_4^{2-}, while calcite-DAS and dolomite-DAS had comparable long-term efficiency (16–27% Fe and <10% SO_4^{2-}). A compromise had to be made by selecting the mixture with 50% wood ash (WA50) due to high content in fine grain size

particles in WA80 (80% wood ash), and that a rapid decline in effectiveness of WA20 (20% wood ash) could occur. The calcite- and/or dolomite-DAS were rather suggested to be used in polishing units.

Thereafter, in the second step, two of the most efficient mixtures tested during batch testing i.e. WA50 and C20 (20% calcite) were selected for Fe pretreatment in continuous column reactors of 1.5 L. A third mixture, composed of organic (70%) and inorganic (30%) materials, was also tested to be used in PBR, especially to treat SO_4^{2-} because of the limited SO_4^{2-} removal by the DAS. The efficiency and the hydraulic performance of these three mixtures, operated at different hydraulic residence times (HRT) (1–5 d), were then evaluated. Results showed that a minimum HRT of 2 d is required to treat a ferriferous AMD (with about 5000 mg/L SO_4^{2-}). WA50 reactors showed better Fe and SO_4^{2-} removal (17–62% and 7.5–37%, respectively) at a 5-day HRT (WA50-5), while the C20 reactors were only effective in a very short term (first 7 days) with a HRT of 2 d. The efficiency of the PBR increased from 77% to 91% when HRT was doubled from 2.5 d to 5 d. This part of the study also found that a potential competition between iron-reducing bacteria and sulfate reducing bacteria might have led to a decrease in the SO_4^{2-} removal from 91% to less than 14% in PBRs. The evolution of hydraulic conductivity (k_{sat}) in all reactors showed insignificant changes, meaning that clogging problem was indeed limited even at 5 d HRT.

In the third step of the study, the results obtained during the batch and small column testing were used to set up three scenarios of multi-step treatment of Fe-rich AMD by using 10.7 L column reactors. This last step consists of comparing the lab-based and field-based experiments performance in order to assess the scale effects as well as to identify the factors and parameters that have an impact on the long-term performance. Results of the studies showed that the parameters that could influence the differences in the performance of the laboratory-scale and field-scale systems are the electrical conductivity, Q, k_{sat}, and Fe and SO_4^{2-} concentrations. In the laboratory, a system including a Fe-pretreatment unit and using DAS mixtures could remove 52–98% Fe. The best performance was obtained when two pretreatment units were used. The most effective pretreatment units were the two WA50s, with a mean Fe removal of 82% and 79% SO_4^{2-}. Consequently, the immediate succeeding PBR unit could treat on average Fe removal of 86% Fe and 98% SO_4^{2-}. In the field, the efficiency of the system was about 75%. The Fe-pretreatment has improved the overall performance of a passive multi-step system for the treatment of ferriferous AMD. In addition, the comparison of laboratory and field experiments showed that flow rate Q is the parameter that affects the most the long-term performance of the multi-step treatment for Fe-rich AMD. Finally, new design criteria for the construction of a multi-step treatment for Fe-rich AMD consider Fe and SO_4^{2-} concentrations, as well as k_{sat}. Moreover, a PBR is more efficient with a Fe load <26 g/m^3 substrates/d and SO_4^{2-} <110 g/m^3 substrate/d. This part of the study also suggested the use of a mixture with a k_{sat} >10^{-3}cm/s to treat Fe-rich AMD. In addition, a correction factor of 0.2–0.8 could be taken into account on

the Q value and Fe removal, as well as 1/100 on the measured k_{sat} during laboratory testing in order to predict the on-site treatment lifespan.

The present project allows then to deepen the knowledge related to the treatment of Fe-rich AMD (Fe >500 mg L) with multi-step passive systems. In addition, the wood ash, used as a substitute of low cost material in the DAS mixtures components, was as effective as the conventional materials ($CaCO_3$, MgO) used in these types of mixtures. The new design criteria proposed in this study also constitutes an innovative scientific contribution. Finally, the knowledge and methodological approaches acquired during this study may be applied to different water qualities for the rehabilitation of other abandoned or closed mine sites.

Key words: Acid Mine Drainage (AMD), Dispersed Alkaline Substrate (DAS), Iron, Passive treatment, Multi-step treatment, Passive Biochemical Reactor (PBR), Design criteria

CHAPITRE I

INTRODUCTION

1.1 Contexte de l'étude

Le drainage minier acide (DMA) est considéré comme l'un des impacts environnementaux majeurs associés à l'exploitation minière. Le DMA est une eau contaminée résultant de l'exposition à l'eau et à l'air des minéraux sulfureux contenus dans les matériaux miniers ; l'équation générale exprimant ce phénomène peut s'écrire de la façon suivante (Kleinmann et al., 1981; Aubertin et al., 2002; Bussière et al., 2005) :

$$FeS_2 + 15/4\ O_2 + 7/2\ H_2O \rightarrow Fe(OH)_3 + 2H_2SO_4 \qquad (1.1)$$

Le DMA est caractérisé par un pH bas (jusqu'à -3,6) et, en raison de la forte acidité, les concentrations de métaux et de sulfates (SO_4^{2-}) peuvent être très élevées, allant jusqu'à 200 et >900 g/L, respectivement (Nordstrom et Alpers, 1999 ; Nordstrom et al., 2000, 2015). Les méthodes de traitement du DMA (et éventuellement du drainage neutre contaminé- DNC), sont généralement divisées en actifs et passifs, chimiques et biochimiques (USEPA, 2014 ; Skousen et al., 2017). Présentement, le traitement passif (chimique et biochimique) est de plus en plus utilisé pour ses avantages de générer des boues stables et ses faible coûts d'installation et d'opération (Aubertin et al., 2002, 2010). Également, il a l'avantage d'être un moyen de valorisation des matériaux résiduels et consomme moins d'énergie (Neculita et al., 2007; Clyde et al., 2016; Zhang

et al., 2017). Dans le contexte québécois, ce type de traitement est la seule méthode reconnue par la législation pour le traitement des eaux contaminées lors de la restauration des sites miniers abandonnés (MERN, 1997). Le traitement passif, dont plusieurs types ont été repertoriés dans diverses études intégratrices (Johnson et Hallberg, 2005 ; Taylor et al., 2005; Neculita et al., 2007; USEPA, 2014 ; Haakensen et al., 2015 ; Skousen et al., 2017), est souvent utilisé pour traiter le DMA avec une faible acidité (<800 mg $CaCO_3$/L) et à faibles débits (<50 L/s) (Skousen et Ziemkiewicz, 2005; Hedin et al., 2013). Généralement, les limites de performance des systèmes passifs sont liées surtout au colmatage attribuable à l'enrobage des grains de calcaire et à la production de gypse (Johnson et Hallberg, 2005a; Neculita et al., 2007). Ainsi, chaque type de traitement passif (chimique ou biochimique), utilisé seul, a une performance limitée lorsqu'il s'agit de traiter du DMA fortement contaminé. D'où l'importance de l'utilisation d'une combinaison de plusieurs types de traitement passif connue comme filière (Champagne et al., 2005; Caraballo et al., 2009; Macías et al., 2012a; Genty, 2012). Dans cette étude, un DMA fortement contaminé fera référence à un DMA riche en Fe ou DMA ferrifère dont les concentrations du Fe excèdent 500 mg/L (Neculita et al., 2008a; Potvin, 2009).

Bien que les travaux de recherche effectués au laboratoire et sur le terrain sur une filière de traitement passif du DMA ferrifère aient donné des résultats satisfaisants (Genty, 2012 ; Genty et al., 2016), des améliorations sont encore nécessaires. En effet, des problèmes d'écoulement de surface ont été constatés sur un système pilote de terrain (site Lorraine, Abitibi-Témiscamingue, Québec), où une filière de traitement composée de deux unités de réacteur passif biochimique (RPB) séparées par une unité composée de cendres de bois, a été installé en 2011. Les problèmes de performance sont potentiellement engendrés par : 1- un colmatage lié à la diminution de la porosité (n) et de la conductivité hydraulique saturée (k_{sat}) des mélanges réactifs qui composent les unités de la filière. Jusqu'ici, le choix des mélanges réactifs qui composent le RPB était basé sur leur efficacité à augmenter le pH et à enlever les métaux et les sulfates (Zagury

et al., 2006; Neculita et al., 2007, 2008a; 2011); 2- un problème de conception (design). Présentement, les critères de design imposés pour construire les unités composantes d'une filière sont le temps de résidence hydraulique (TRH) et l'épaisseur du mélange réactif. La conception d'un système de traitement passif est aussi basée sur le débit et la qualité de l'eau à traiter (Hedin et al., 1994). À son tour, le TRH dépend du débit (Q) qui, par définition est le volume des pores par unité de temps ($Q=V_{pores}/TRH= (V_{total} \times n) /TRH$). La qualité de l'eau (dans ce cas-ci, le pH faible et la forte contamination en Fe et en SO_4^{2-}) et le débit d'eau à traiter peuvent éventuellement changer le volume des pores, mais l'étude de cette corrélation n'a pas été approfondie ; 3- un problème d'effet d'échelle (transposition de résultats de l'échelle du laboratoire vers le site). À l'instar des essais de laboratoire, le contrôle des conditions environnementales lors des essais de terrain pose toujours des défis.

1.2 Hypothèses de recherche

Dans ce contexte, les hypothèses posées dans cette étude sont les suivantes :

- L'utilisation des mélanges réactifs à grande porosité et à forte alcalinité peut améliorer l'écoulement et réduire le problème de colmatage dans la filière de traitement passif du DMA ferrifère ;
- Le prétraitement du DMA peut améliorer l'efficacité et la stabilité (fonctionnement à l'état stationnaire) à long terme de la filière ;
- La comparaison des résultats obtenus aux laboratoires et sur le terrain (la filière) peut aider à évaluer, comprendre et pallier au problème d'effet d'échelle ;
- De nouveaux critères de design intégrant la porosité et la charge en fer, en plus de ceux déjà utilisés, peuvent améliorer la conception d'une filière de traitement du DMA ferrifère.

1.3 Objectifs

Basé sur ces hypothèses, l'objectif général de ce projet est donc de réaliser des investigations plus poussées pour améliorer la performance à long terme des filières de traitement, dans le but de proposer de nouveaux critères de design pour la construction d'un système efficace. Dans ce contexte, la performance entend à la fois efficacité et stabilité, c'est-à-dire la capacité de traiter l'eau contaminée de manière stationnaire ou sans déclin au cours du temps.

Afin de vérifier les hypothèses énumérées précédemment, trois objectifs spécifiques sont proposés :

1. Évaluer l'efficacité des unités composées de mélanges à haute porosité et forte alcalinité sur le traitement du DMA ferrifère ;
2. Évaluer la performance à long terme d'une unité de prétraitement du Fe dans une filière ;
3. Réaliser une étude comparative des résultats de laboratoire et sur le terrain, afin de proposer de nouveaux critères de design utiles pour construire une filière de traitement passif efficace du DMA ferrifère.

1.4 Originalité de l'étude

Une filière de traitement passif permet de traiter du DMA fortement contaminé (Champagne et al., 2005; Prasad et Henry, 2009; Caraballo et al., 2011; Macìas et al., 2012). De précédentes études ont alors donné lieu à la construction sur un site pilote d'une filière à base de (bio)filtres pour traiter le DMA ferrifère (Genty, 2012). Cette thèse s'inscrit dans l'amélioration de la performance à long terme de ce système.
Parmi l'originalité de cette thèse, on retrouve l'utilisation des mélanges réactifs à haute porosité et à forte alcalinité communément appelés substrat alcalin dispersé (SAD), pour prétraiter du DMA à une concentration de Fe >2000 mg/L. La particularité de

l'étude est la substitution des composants de ces mélanges par des matériaux peu coûteux (dolomite et cendres) par rapport à ceux utilisés généralement dans les SAD. L'intégration d'une unité de prétraitement du Fe constituée de tels mélanges, combinée avec un RPB pour le traitement du DMA ferrifère, n'a pas encore été testée.

Une autre originalité de cette étude réside dans l'identification des paramètres et facteurs en condition réelle qui ont pu influencer la performance *in situ* de la filière. Par la comparaison des études de terrain ainsi que celles effectuées au laboratoire, une évaluation des problèmes d'effet d'échelle (transposition des essais de laboratoire vers le terrain) a été réalisée ; peu d'études sur ce sujet ont été retrouvées dans la littérature. Cette approche a par la suite permis de suggérer des critères supplémentaires pour la conception et la construction d'une filière de traitement passif du DMA ferrifère efficace. À noter que les critères de design pour la conception d'une filière sont généralement basés sur ceux des systèmes de traitement passifs conventionnels, pouvant être variables selon la qualité d'eau, et ne sont donc pas forcément adaptés pour le DMA ferrifère.

1.5 Organisation de la thèse et principales contributions

La thèse est composée de 7 chapitres, dont 3 sont rédigés sous forme d'articles scientifiques, publiés ou soumis dans des revues avec comité de lecture.

Le présent chapitre, introductif, présente le contexte général et la problématique du DMA ferrifère. Les types de traitement passifs du DMA sont brièvement rappelés ainsi que les limites du traitement passif conventionnel pour traiter le DMA fortement contaminé. Cette première partie présente également les hypothèses de recherche, les objectifs de l'étude (généraux et spécifiques) et son originalité, ainsi que les différentes contributions apportées tout au long du projet.

Le chapitre 2 présente une brève revue de la problématique du DMA fortement contaminé, notamment le DMA ferrifère, et l'impact du Fe sur l'environnement. Une

synthèse sur le traitement passif du DMA fortement contaminé est ensuite présentée. Les critères de design des systèmes de traitement passifs, qui sont les bases de conception d'une filière, sont après décrits. Enfin, les avantages et les limites des filières utilisant les SAD pour traiter le DMA fortement contaminé sont présentés.

Le chapitre 3, présenté sous forme d'un article publié dans la revue *Applied Geochemistry* (2016), traite le premier objectif de la thèse, réalisé par des essais en batch et portant sur :

- la caractérisation physicochimique des mélanges réactifs type SAD, susceptibles d'être utilisés dans une unité composant une filière de traitement passif ;
- l'évaluation de l'efficacité de ces mélanges à prétraiter le Fe dans le DMA ferrifère et d'en sélectionner le(s) plus efficace(s).

Pour ce faire, l'efficacité de neuf mélanges réactifs à base de SAD a été testée pour prétraiter le Fe. Ces mélanges sont composés de copeaux de bois et d'agents alcalins, soit de la calcite (calcite-SAD), de la dolomite (dolomite-SAD) ou encore de la cendre de bois (CB-SAD). Les proportions des agents alcalins sont variées de 20, 50 et 80% v/v. Les tests ont été réalisés en utilisant des réacteurs batch (sans écoulement), pour une durée de 91 j.
Le(s) mélange(s) qui montrerait/montreraient un meilleur enlèvement du Fe (concentration initiale d'environ 2500 mg/L et la cible finale à moins de 500 mg/L) a/ont été alors sélectionné(s) afin de le(s) tester par la suite dans des réacteurs avec écoulement de type colonne.

Le chapitre 4, rédigé sous forme d'un article publié dans la revue *Minerals Engineering* (2017), répond au second objectif qui discute plus spécifiquement de :

- l'évaluation de l'efficacité des mélanges réactifs les plus performants, sélectionnés lors des essais batch, en système colonne pour prétraiter le Fe ;

- l'évaluation de l'efficacité d'un mélange réactif utilisé dans les RPB pour traiter les sulfates ;
- le suivi de l'évolution de k_{sat} selon le TRH ;
- la caractérisation des solides récupérés après le démantèlement des réacteurs.

Le travail présente le montage de quatre réacteurs en colonne remplis de mélanges sélectionnés pendant les tests batch : deux réacteurs sont remplis du mélange CB50 (50% cendres de bois) et les deux autres, de C20 (20% calcite). Ensuite, un RPB rempli d'un mélange de 70% de matière organique (copeaux de bois, fumier de volaille et compost) et de 30% de matière inorganique (sable et calcite) ont également été construits. Le suivi de l'évolution de la qualité de l'eau et du k_{sat} a été effectué tout le long des expériences (16–63 j) avec des TRH de 1–5 j pour les réacteurs CB50, 1 et 2 j pour C20 et 2,5 j et 5 j pour RPB.

Afin de pouvoir construire une filière, le TRH optimal de chaque réacteur pour un prétraitement/traitement du Fe, l'évolution des caractéristiques hydrauliques de tous les réacteurs et l'efficacité de l'enlèvement des SO_4^{2-} par les RPB ont été évalués.

Le chapitre 5, présenté aussi sous forme d'un article, soumis dans la revue *Environmmental Science and Pollution Research* (2017), traite l'objectif 3 de la thèse, notamment le comportement d'une filière de traitement passif du DMA ferrifère, soit :

- l'évaluation du changement des caractéristiques hydrauliques des mélanges réactifs composant les unités d'une filière de traitement du DMA ferrifère ;
- l'évaluation d'un prétraitement du Fe sur l'efficacité et la performance de la filière afin de valider la charge en Fe comme un critère de design ;
- la comparaison d'une filière de traitement passif au laboratoire et sur le terrain ;
- l'identification des facteurs et paramètres qui influencent la performance d'une filière de traitement du DMA ferrifère.

La comparaison de filières testées au laboratoire et sur un pilote de terrain est mise en évidence dans cette partie du travail. Trois scénarios de filières à base de réacteurs SAD et de RPB construites au laboratoire et une filière de terrain à base de RPB et de cendre bois ont été évalués. La durée totale des tests menés au laboratoire a été de 36 semaines (252 j), tandis que le suivi de la performance de la filière de terrain a été de 5 ans (2011–2016). Cependant, pour faire une comparaison de deux séries de données homogènes, les données traitées ont été considérées comme indépendantes du temps. De nouveaux critères de design, utiles pour construire une filière de traitement passif du DMA ferrifère, sont proposés à la fin de ce chapitre.

Il est à noter que ces travaux sont concentrés sur l'amélioration de la qualité de l'eau à traiter et des aspects hydrauliques. Toutefois, la caractérisation des solides récupérés après les tests batch (chapitre 3) et petites colonnes (chapitre 4) a été effectuée. Afin d'évaluer la stabilité des solides après traitement, ainsi que de déterminer les mécanismes d'enlèvement des métaux, des travaux plus approfondis seront réalisés dans le cadre d'une maîtrise en cours (Marouen Jouini).

Le chapitre 6 discute des points essentiels traités durant l'étude, à savoir le prétraitement du Fe et l'enlèvement des SO_4^{2-}, l'évaluation de l'effet d'échelle, ainsi qu'une évaluation préliminaire de la faisabilité technico-économique d'une éventuelle construction de filière de terrain basée sur des réacteurs SAD et RPB.

Enfin, le dernier chapitre présente les conclusions et recommandations en lien avec les travaux réalisés dans cette étude.

En plus des trois articles de revues scientifiques, les contributions scientifiques apportées dans le cadre de cette thèse sont les suivantes :

Publications de conférences

- Rakotonimaro, T.V., Neculita, C.M., Bussière, B., Genty, T., Zagury, G.J., 2017. Iron and sulfate removal in highly contaminated acid mine drainage using passive multi-step systems. *International Mine Water Association (IMWA) Congress*, June 25-30, Rauha, Lappeeranta, Finland.
- Neculita, C.M., Rakotonimaro, T.V., Bussière, B., Zagury, G.J., 2017. Passive treatment of highly contaminated iron-rich acid mine drainage. *National Meeting of the American Society of Mining and Reclamation (ASMR)*, April 9-13, Morgantown, WV, USA.
- Rakotonimaro, T.V., Neculita, C.M., Bussière, B., Zagury, G.J., 2015. Comparative efficiency of calcite- and dolomite-based dispersed alkaline substrate for the pre-treatment of highly contaminated acid mine drainage. In: Proc. of the 4th *International Seminar on Environmental Issues in Mining – ENVIROMINE 2015*, December 2-4, Lima, Peru.
- Rakotonimaro, T.V., Neculita, C.M., Bussière, B., Zagury, G.J., 2015. Efficacité de divers substrats alcalins dispersés pour traiter le drainage minier acide ferrifère (Poster). 5ème édition du *Symposium sur l'environnement et les mines*, 14-17 Juin, Rouyn-Noranda, QC, Canada.

Enfin, d'autres contributions scientifiques ont été également produites durant les études de doctorat, incluant les suivantes :

Autres publications

- Foudhaili, T., Rakotonimaro, T.V., Babi, K., Lefebvre, O., Neculita, C.M., 2017. Iron and sulfate removal in acid mine drainage by electrocoagulation and microbial fuel cells. *Journal of Applied Electrochemistry* (to be submitted).
- Rakotonimaro, T.V., Guittonny-Larchevêque, M., Neculita, C.M., 2017. Reclamation of metal-contaminated tailings with organic amendments: pore water quality control and phytostabilization. *5th International Conference on Sustainable Solid Waste Management,* June 21-24, Athens, Greece. (Paper selected for consideration in the Special Issue on the Athens 2017 of the journal *Desalination and Water Treatment*).
- Rakotonimaro, T.V., Neculita, C.M., Bussière, B., Zagury, G.J., 2016. Recovery and reuse of sludge from active and passive treatment of mine drainage-impacted waters: a review. *Environmental Science and Pollution Research* 24 (1): 73–91.
- Rakotonimaro T., Lacroix, R., Trudel, S., Neculita, C.M., 2015. East Sullivan mine site restoration: Current success and perspectives. *Goldschmidt*, August 16-21, Prague, Czech Republic.

Les copies des articles publiés sont présentées dans les annexes du présent document.

CHAPITRE II

REVUE DE LITTÉRATURE

Ce court chapitre est un complément des revues de littératures qui ont été rédigées dans chaque introduction des trois grandes sections (chapitres 3, 4 et 5) de la thèse.

2.1 Problématiques du DMA ferrifère

Le DMA ferrifère est non seulement riche en Fe, mais également en SO_4^{2-} et en plusieurs autres métaux selon la minéralisation du gisement. Puisque les sulfures métalliques les plus rencontrés sur les sites miniers abandonnés sont la pyrite (FeS_2) et la pyrrhotite ($Fe_{(1-x)}S$; x=0−0,2), la concentration du Fe dans le DMA est généralement plus élevée, pouvant atteindre jusqu'à 141 g/L (Hustwit et al., 1992; Nordstrom et al., 2000; Moncur et al., 2005). Dans le même temps, la concentration des autres métaux peut aller jusqu'à 6,68 g/L Al, 49 g/L Zn et 9,8 g/L Cu (Nordstrom et al., 1999; 2000). Dans la plupart des sites miniers abandonnés/fermés au Canada, le DMA peut contenir une concentration en Fe jusqu'à 5 g/L et 12,5 g/L de SO_4^{2-} (Zinck et Griffith, 2013). La forte concentration en métaux dans le DMA ferrifère est associée à l'oxydation suivie de l'hydrolyse du Fe^{2+} en Fe^{3+}, qui entraîne une augmentation de l'acidité (en l'absence ou insuffisance de matériaux neutralisants), favorisant une plus grande solubilité des éléments métalliques (Éq. 2.1) (King et al., 1993; Bernier, 2005).

$$Fe^{3+} + 3H_2O \rightarrow Fe(OH)_3 + 3H^+ \qquad (2.1)$$

Ainsi, le Fe contrôle souvent la concentration des autres éléments dans le DMA,

représentant ainsi un important défi, tel que l'enlèvement du Mn (Neculita et Rosa, 2017).

Dans l'eau, l'état d'oxydation du Fe se présente sous deux formes : Fe^{2+} (soluble en milieu réducteur) et Fe^{3+} (insoluble en milieu oxydant Eh ≥0,77V) (USGS, 1962 ; Moore, 1991). Pour les animaux et les plantes, le Fe est considéré comme un élément trace essentiel. Toutefois, il peut être toxique pour la vie aquatique à certaines concentrations (Moore, 1991). Par exemple, la concentration létale du Fe_t (CL50) pour les poissons est de 0,3−10 mg/L, dépendamment des espèces et des conditions de tests (Tableau 2.1).

Tableau 2.1 Toxicité du Fe : concentration effective 50 (CE50), concentration létale (CL50) sur des espèces aquatiques (Biesinger et Christensen, 1972 ; Martin et Holdich, 1986 ; Moore, 1991)

	CE50 (mg/L)	**CL50 (mg/L)**
Plantes		
Lemna minor	3,7	-
Poissons		
Daphnia magnia	5,2	0,3−>10
Asellus aquaticus (Fe^{3+})	-	5,9
Crangonyx pseudogracilis	-	124−183
Fe^{2+}	-	95−143
Fe^{3+}	-	120−160
Insectes	-	0,3−16

Dureté de l'eau : 50 mg/L ; pH 6,75 ; Température de l'eau 13°C

L'organisation mondiale de la santé (OMS) a établi qu'à une concentration inférieure à 2 mg/L, le Fe ne représente pas de danger pour la santé. Toutefois, l'eau potable ne devrait pas contenir plus de 0,3 mg/L de Fe (WHO, 2011). La limite acceptable de la concentration du Fe dans les effluents miniers finaux au Québec et aux États-Unis est de 3 mg/L (MDDELCC, 2012 ; USEPA, 2014).

Généralement, le traitement du DMA vise à augmenter le pH et à précipiter les métaux. Dans le cas du DMA ferrifère, le Fe est stabilisé sous forme de trois phases minérales (oxydes/hydroxydes, carbonates, et sulfures) soit par précipitation/co-précipitation, sorption, échange ionique ou par complexation (Kalin et al., 2006; Neculita et al., 2008b). Toutefois, l'enlèvement du Fe peut s'avérer complexe à cause des différentes conditions (p. ex. : pH, Eh, oxygène dissous, température) qui régissent la réduction du Fe^{3+} (photochimique, biologique ou chimique) ou l'oxydation du Fe^{2+} (biochimique/chimique). Le pH est l'un des paramètres les plus importants qui contrôlent la précipitation et la solubilité du Fe et de ses composés. À pH acide (<2), presque tous les précipités (p. ex. : $Fe(OH)_3$) sont instables. À partir d'un pH 5, les phases minérales Fe(II) oxydes/hydroxydes et sulfures (p. ex. : $Fe(OH)_3$ et FeS_2) restent relativement stables (Fig. 2.1a, 2.1b).

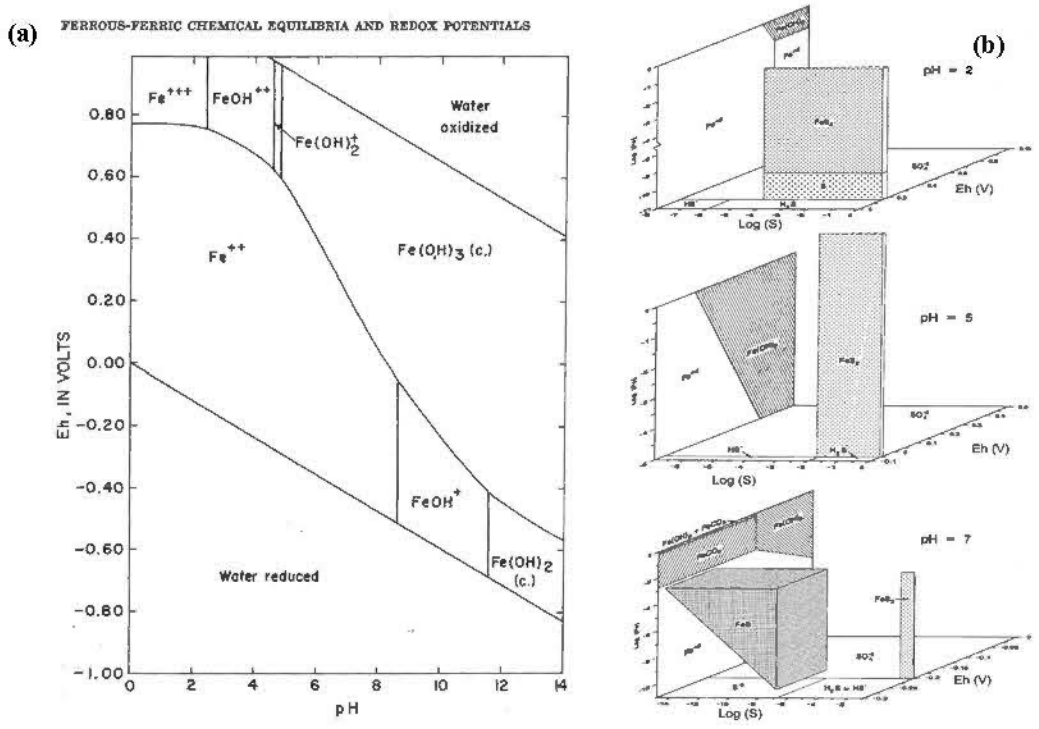

Figure 2.1 (a) Diagramme Eh-pH : conditions d'équilibre des réactions d'oxydoréduction et processus d'équilibre entre précipitation et solubilisation en solution aqueuse du Fe et de ses composés ; (b) Diagramme tridimensionnel du Fe-S-O-H (USGS, 1962 ; Kalin et al., 2006).

Lors du traitement du DMA, les oxydes/hydroxydes (p. ex. : goethite α-FeOOH et ferrihydrite $Fe_5HO_8 \cdot H_2O$) sont les phases minérales les plus fréquemment rencontrées en condition oxydante et à pH >5,5. Par contre, en condition réductrice et à pH entre 6,5–9,5, les sulfures (p. ex. : FeS) et les carbonates (p. ex. : sidérite $FeCO_3$) se forment (Bigham et al., 1996; Schwertmann et Carlson, 2005; Kalin et al., 2006). La température peut influencer également la solubilité des composés du Fe; par exemple, l'hydroxyde de Fe(III) ($Fe(OH)_3$) a une très faible solubilité (0,048 µg/L) à 18°C, par rapport à l'hydroxyde de Fe(II) ($Fe(OH)_2$) à 20°C (1420 µg/L). Par contre, le carbonate de Fe ($FeCO_3$) est beaucoup moins soluble à 18°C (0,77 g/L) (Phippen et al., 2008).
À l'issue du traitement du DMA, la quantité des précipités secondaires varie selon les

valeurs de pH et la qualité du DMA traité (concentrations spécifiques de Fe, S et H^+). Pour le DMA ferrifère, la concentration trop élevée en Fe et de SO_4^{2-} peut engendrer une grande quantité de précipités. De plus, la présence d'autres éléments, particulièrement l'Al, dont la précipitation se fait à partir d'un pH de 3,7 à 4,5, peut également entrer en concurrence avec la précipitation du Fe, qui commence à pH 3 (Kalin et al., 2006). Par conséquent, ces précipités peuvent limiter la performance des systèmes de traitement, voire entraîner leur défaillance.

Tel que souligné en introduction, les deux types de technologies utilisés pour traiter le drainage minier sont les traitements actifs et passifs. Cependant, la technologie passive est de plus en plus privilégiée, surtout sur les sites miniers abandonnés.

2.2 Traitement passif du DMA fortement contaminé

Le traitement passif est actuellement favorisé pour traiter le DMA (et/ou DNC) sur les sites miniers abandonnés ou sites orphelins, car il est économique et écologique. Il offre la possibilité de réutiliser des matériaux à faible coût (p. ex. : les déchets biologiques), consomme moins d'énergie, améliore la qualité de l'eau et produit des boues plus stables (Skousen et Ziemckiewicz, 2005 ; Zagury et al., 2007; Skousen et al., 2017). En outre, il ne nécessite pas d'assistance mécanique comme le traitement actif, mais utilise plutôt l'écoulement gravitaire (Johnson et Hallberg, 2005a). Les technologies passives peuvent être divisées en deux catégories : a) chimiques, qui s'appuient sur l'utilisation du calcaire ; et b) biochimiques qui utilisent principalement des bactéries dans le processus (Neculita et al., 2007; USEPA, 2014; Skousen et al., 2017). Différents types de traitement passif sont identifiés et décrits dans la littérature scientifique (Tableau 2.2) (Johnson et Hallberg, 2005a ; Neculita et al., 2007; USEPA, 2014; Rakotonimaro et al., 2016a; Skousen et al., 2017).

Le choix des types à adopter, pour une situation dounée, est principalement basé sur la qualité de l'eau à traiter (teneur en Fe, Al, oxygène dissous - OD) (Fig. 2.2) (Hedin et al., 1994, 2013).

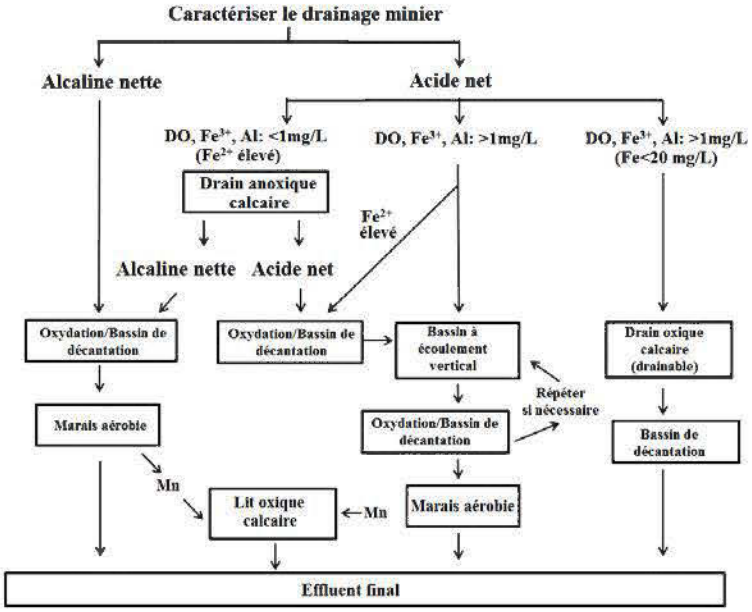

Figure 2.2 Arbre décisiounel pour le choix d'un traitement passif (adapté de Hedin et al., 1994, 2013)

Tableau 2.2 Mode opératoire, avantages et limites des technologies passives (traduit et adapté de Rakotonimaro et al., 2016a)

Technologies passives	Types de traitement	Mode opératoire	Avantages	Limites	Références
Chimiques	Drain anoxique calcaire (DAC)	Dissolution du calcaire dans des conditions anoxiques (par encapsulation en plastique et couverture d'argile ou de sol compacté)	Augmentation de l'alcalinité ; Diminution de l'acidité	Faible efficacité sur le traitement du DMA fortement contaminé (enrobage des calcaires par les précipités de fer, de soufre à la sortie du système ; Difficulté à atteindre un pH supérieur à 7 ; Utilisé uniquement pour les situations à faible débit	Hedin et al., 1994; Gazea et al., 1996; Johnson et Hallberg, 2005a; Potvin, 2009; Genty, 2012; Genty et al., 2012a; USEPA, 2014; Skousen et al., 2017
	Lit/Tranchée oxique calcaire (LOC/TOC)	Dissolution du calcaire dans des conditions aérobies	Augmentation de l'alcalinité ; Diminution de l'acidité ; Formation de précipités métalliques dans le drain ; Utilisé pour l'enlèvement de Mn ; Sorption des métaux-traces sur les oxydes de Mn et de Fe	Faible réactivité du matériau ; Dépôt de précipités dans le système	
	Cascade aération/ Bassin de décantation	Aération de l'effluent (oxydation), décantation et formation de solides	Conçu pour faciliter la minimisation des boues ; Utilisé comme unité de polissage	Risque de re-dissolution du Fe ; Mn non enlevé	
	Sorption (tourbe)	Adsorption, chélation, échange ionique	Réduction des métaux en solution	Saturation plus ou moins rapide des sites de sorption	
	Puits de déviation	Neutralisation de l'acidité, floculation	Conception simple ; Possibilité de rinçage ; Réglage facile des flocs métalliques à la surface	Nécessite un grand débit ; Neutralisation incomplète	Sibrell et al., 2013

Biochimiques	Marais aérobie	Aération des effluents par les plantes, adsorption et bioaccumulation	Diminution de la quantité de métal dans la solution par les mécanismes d'oxydation et d'hydrolyse	Utilisé davantage pour traiter les eaux de surface (alcalines nets)	Gazea et al., 1996; Johnson et Hallberg, 2005a; USEPA, 2014
	Marais anaérobie	Environnement réducteur renforcé par la présence de matière organique dans les zones humides (idem bioréacteur)	Précipitation des métaux sous forme de sulfures métalliques par des bactéries sulfato-réductrices ; Utilisé pour traiter l'eau alcaline	Requiert un grand espace	
	Réacteurs sulfato-réducteurs	Sorption, précipitation d'hydroxydes, carbonates, sulfure métallique, co-précipitation, échange d'ions	Augmentation de l'alcalinité ; Diminution de l'acidité ; Précipitations de métaux (sulfures métalliques)	Problèmes hydrauliques ; Rétention moyenne de la concentration élevée en fer ; Diminution de l'efficacité (si pH <5 ou potentiels redox trop élevés) ; Développement de bactéries fortement dépendant du TRH, pH, source organique	Neculita et al., 2007, 2008a; Genty et al., 2010; Genty, 2012 ; Vasquez et al., 2017
	Barrière réactive	Dégradation concomitante de la matière organique et réduction des sulfates en sulfure d'hydrogène	Utilisé dans le cas de la contamination des eaux souterraines avec une large gamme de concentrations de contaminants		
	Systèmes successifs de production d'alcalinité (SAPS) / Bassins à écoulement vertical	Combinaison de DAC et de réacteur passif biochimique (RPB), constituée d'une couche de calcaire et d'une couche de mélange réactif (y compris le substrat)	Augmentation du pH, alcalinité ; Précipitation des métaux ; Enlèvement Al (jusqu'à 100%) ; Enlèvement partiel de Fe ; Enlèvement de Cu, Zn	Mn non enlevé ; Demande d'espace très élevé ; Colmatage	Hedin et al., 2010; USEPA, 2014

Les deux types de traitement passif les plus utilisés pour traiter le DMA ferrifère sont les drains calcaires (chimiques) et les RPB (biochimiques) (Neculita et al., 2008a, 2008b; Genty, 2012).

a) Les drains calcaires (oxiques/anoxiques calcaires ou DOC/DAC) sont utilisés pour augmenter le pH et l'alcalinité du DMA (Eq. 2.2), et pour précipiter les métaux tels le Pb, Cd, Al (Hedin et al., 1994).

$$CaCO_3 + H^+ \rightarrow HCO_3^- + Ca^{2+} \qquad (2.2)$$

Le traitement consiste à permettre à l'eau contaminée d'être en contact ou de traverser un drain/tranchée (lit/canal) rempli de matériaux neutralisants. Les DAC peuvent traiter de l'eau contaminée avec une acidité <500 mg $CaCO_3$/L et un débit <20 L/s (Taylor et al., 2005). Toutefois, à partir d'une concentration de 270 mg/L Fe (et à plus de 1 mg/L d'Al), ils ne sont pratiquement plus efficaces (Watzlaf et al., 2004; Taylor et al., 2005). En effet, un DAC traitant une eau contenant 75 mg/L de Fe et 21 mg/L d'Al ne durerait que huit mois (Watzlaf et al., 2000), car les précipités secondaires enrobent les grains calcaires et entraînent le colmatage (Watzlaf et al., 1992; Ziemkiewicz et al., 1997). Cependant, il a été démontré que les calcaires enrobés étaient seulement 2–45% moins efficaces que les calcaires non enrobés. Ces calcaires enrobés étaient reportés 90% autant performants que ceux non enrobés pour neutraliser le DMA (Ziemckiewicz et al., 1997; Genty et al., 2012a).

b) Le principe de fonctionnement d'un RPB est basé sur l'oxydation du carbone organique et la réduction des sulfates. Cette réaction d'oxydo-réduction est catalysée par les bactéries sulfato-réductrices (BSR) en conditions anaérobies, où le bicarbonate formé augmente le pH et l'alcalinité de l'eau (Éq. 2.3), alors que les sulfures solubles réagissent avec les ions métalliques et forment des sulfures métalliques peu solubles (Éq. 2.4) (Widdel, 1988; Hao et al., 1996).

$$2\ CH_2O + SO_4^{2-} \rightarrow H_2S + 2\ HCO_3^- \qquad (2.3)$$

$$H_2S + M^{2+} \rightarrow MS_{(s)} + 2H^+ \qquad (2.4)$$

Dans les RPB, des mélanges réactifs composés de matière organique biodégradable (p. ex. : compost, champignons, fumiers, coquilles de moules/crabes) et de matériaux plus récalcitrants à la dégradation (p. ex. : tourbe, paille, sciure) sont utilisés pour traiter l'eau contaminée (Neculita et al., 2007; 2011; Song et al., 2012a, 2012b; Jeen et Mattson, 2016; Grembi et al., 2015; Diloreto et al., 2016; Clyde et al., 2016).
L'efficacité d'un RPB pour traiter le DMA ferrifère est limitée par sa forte concentration en Fe (et/ou la production excessive de H_2S) qui peut inhiber les BSR. Une diminution de l'efficacité d'enlèvement des SO_4^{2-} de 39–100% peut survenir car le dépôt de FeS peut entraver l'activité des cellules (Utgikar et al., 2002; Neculita et al., 2007; Zhang et al., 2009; Lewis, 2010), alors que le Fe^{3+} peut concurrencer les donneurs d'électrons (Lovley et Phillips, 1986; Van Bodegum et al., 2004).

Bien que les technologies passives aient des coûts d'exploitation inférieurs à ceux actives, la plupart d'entre elles sont soumises à des problèmes importants, tels que la passivation (enrobage) et/ou le colmatage, principalement lorsqu'elles sont utilisées en une seule unité pour traiter le DMA fortement contaminé (Neculita et al., 2008a; Skousen et al., 2017). Différentes techniques ont été développées pour minimiser ces problèmes. Par exemple, le lavage du système (Hedin et al., 2010; Skousen et al., 2017), le prétraitement (p. ex. : oxydation de Fe par lagune ou aération en cascade) (Caraballo et al., 2009; Macías et al., 2012a) et l'utilisation de mélanges à haute porosité et à forte alcalinité pour améliorer la perméabilité et pour éliminer les éléments acidogènes (Fe et Al) avant d'autres métaux tels que les SAD (Rötting et al., 2008a; Ayora et al., 2013). Le lavage a été trouvé coûteux (Hedin, 2010), tandis que le prétraitement du Fe et les systèmes à réacteurs SAD pourraient donner des résultats prometteurs (Caraballo et al., 2011; Ayora et al, 2013).
Ainsi, une amélioration des critères de design, indispensables pour concevoir un système de traitement passif efficace du DMA fortement contaminé, est nécessaire. La section suivante présente une revue des critères de design des traitements passifs conventionnels.

2.3 Critères de design de base des traitements passifs conventionnels

La construction d'un système de traitement passif s'appuie sur des critères de design en lien avec le temps de séjour et la charge d'acide (Tableau 2.3). Le concept de base de la technologie passive consiste à construire un système de traitement qui ne requiert pas l'utilisation d'électricité ou de produits chimiques et qui minimise les maintenances, tout en conservant une plus longue durée de vie. En général, la réhabilitation et la maintenance des systèmes de traitements passifs devraient se faire seulement 5–10 ans après sa construction (Skousen et al., 2017).

Les traitements passifs sont souvent configurés en série (filière) suite à la performance limitée d'une seule unité. Ainsi, les critères de design d'une unité de traitement passif sont également adoptés comme paramètres et/ou facteurs de base pour construire une filière de traitement passif du DMA fortement contaminé.

Tableau 2.3 Critères de design des systèmes de traitement passifs (traduit et adapté de Zipper et Skousen, 2010 ; Skousen et al., 2017)

Types de technologies	Critères de design	Références
Biochimiques		
Marais aérobie	10 g Fe/m^2 /j; 1 g Mn/m^2 /j	Hedin et al., 1994; Skousen et Ziemkiewicz, 2005
Marais anaérobie	3,5 g acidité/m^2/j ; 10 g Fe/m^2 /j	Hedin et al., 1994; Skousen et Ziemkiewicz, 2005
Marais à écoulement vertical	35 g acidité/m^2/j	Kepler et McCleary, 1997
Lit d'enlèvement du Mn	2–10 g Mn/m^2/j	Rose et al., 2003a, 2003b
RPB	Faible débit ; carbone organique facilement dégradable ; 0,3 mol SO_4^{2-}/m^3 substrat/j	Neculita et al., 2008a; McCauley et al., 2009;
Chimiques		
DAC	15 h temps de séjour	Watzlaf, 2004; Watzlaf et al., 2004
DOC	Charge acide et temps de séjour ; 30 g acidité/t/j	Ziemckiewicz et al., 1997; Skousen et Ziemkiewicz, 2005;
Chéneaux calcaires ouverts	2 h temps de séjour ; 10 g acidité/t/j	Skousen et Ziemkiewicz, 2005
Lit de lixiviation à scories d'acier	1000 g acidité/t/j	Skousen et Ziemkiewicz, 2005
Puits de déviation	Équivalence en charge d'acide	Arnold, 1991; Ziemkiewicz et Brant, 1997
Lit calcaire	2 h temps de séjour ; 2 fois charge d'acide (appliquée 2–4 fois /an)	Skousen et Ziemkiewicz, 2005 McClurg et al., 2007
Chéneaux d'oxydation du Fe à pH bas	Faible pH ; pente pour aération	Hilton, 2005; Burgos et al., 2008
SAD	Temps de séjour	Rötting et al., 2008a

2.4 Filière de traitement passif du drainage minier acide fortement contaminé

Plusieurs types de filière de traitement du DMA moyennement à fortement contaminé présentent une efficacité variable (Tableau 2.4). Pour une concentration de Fe <500 mg/L, l'efficacité des filières (en termes d'enlèvement du Fe) est pratiquement stable et très élevée (>96%). Toutefois, plus d'incertitudes sont relevées lorsque la concentration en Fe est >500 mg/L, dépendamment des types d'unités utilisés et particulièrement lors d'une transposition à grande échelle. Néanmoins, l'utilisation de filières à réacteurs SAD se distingue par leur performance dans l'enlèvement des métaux et également dans leur caractéristique à réduire le problème de colmatage. Comme tout type de traitement, les réacteurs SAD ont toutefois leurs limites et leurs avantages.

Tableau 2.4 Performance de quelques filières de traitement passif du DMA réalisées au laboratoire et sur le terrain

Types de filière	Qualité du DMA	Composant des unités	Objectifs	Efficacité
Laboratoire	pH= 5,2; **Fe= 40 mg/L**; Zn=65–75 mg/L ; SO_4^{2-}=700 mg/L ; Acidité=3500 mg $CaCO_3$/L	DAC	Enlèvement Fe, Al	pH= 5,8; **Fe= >99,7** %; Zn= 27– 31% ; SO_4^{2-}= 14% (0,13 mol/m^3/j)
		RPB	Enlèvement SO_4^{2-}	
	pH=3,2±0,34; **Fe=189±17 mg/L**; Al=91,3±4,98 mg/L; Zn=101±7,58 mg/L; Mn=25,2±1,39 mg/L; Ni=20,2±0,91 mg/L ; Cu=19,6±1,45 mg/L ; Cd=6±0,26 mg/L; SO_4^{2-}=3140 mg/L; Acidité=1440±159 mg $CaCO_3$/L	Aération/ Décanteur	Précipitation Fe	pH=7,2 ; **Fe= 95–97%**; Al=99,9%; Zn=99,9%; Mn=98,6% ; Ni=98,2%; Cu=99,9%; Cd=66,5%; SO_4^{2-}=70%; Alcalinité=1340 mg $CaCO_3$/L
		Biofiltre à tourbe	Sorption métaux lourds et condition anoxique	
		RPB	Génération alcalinité et réduction deSO_4^{2-}	
		DAC	Addition d'alcalinité	
	pH= 2,02; **Fe= 500 mg/L**; Mn=50 mg/L; Zn=100 mg/L; Cu=50 mg/L ; SO_4^{2-}=2580 mg/L ; Acidité=3500 mg $CaCO_3$/L	RPB	Production d'alcalinité et précipitation de snlfures	pH=6,34; **Fe= 96,6%**; Mn, Zn, Cu=95,5–97,5%; SO_4^{2-}=53%; Acidité=0 mg $CaCO_3$/L ; Alcalinité=965 mg $CaCO_3$/L ; (Pourcentage optimal DMA/ Liquide snlfidogène anaérobie : 60/40)
		Réacteur chimique	Augmentation du pH, production d'alcalinité et précipitation du Fe	
		Réacteur alcalin	Augmentation de l'alcalinité	

	pH=3; **Fe= 2000 mg/L**; Al=0,5 mg/L; Zn=40 mg/L; Mn=6 mg/L ; Ni=0,5 mg/L ; Pb=0,1 mg/L ; SO_4^{2-}=5000 mg/L ; Acidité=1440±159 mg $CaCO_3$/L	RPB (1)	Neutralisation d'acide et enlèvement partiel de métaux	pH=6,5 ; **Fe= 37–97%**; Al=98%; Zn=98%; Mn=16%; Ni= 98 %; Pb=95%; SO_4^{2-}=50–72%; Acidité≈ 83%
		Cendres de bois	Filtre du Fe (Rétention du Fe par sorption et précipitation)	
		RPB (2)	Enlèvement métaux résiduels	
Terrain	pH=3–3,9 ; **Fe= 315 mg/L** ; Al=75 mg/L; Zn=270 mg/L; Mn=20 mg/L ; Cu=1,5 mg/L ; SO_4^{2-}=3200 mg/L ; Acidité=1590 mg $CaCO_3$/L	Réacteur calcite-SAD	Enlèvement Al, Fe, Pb, Cu	pH=6,2 ; **Fe= 48%**; Al=90–98%; Zn=5%; Cu=90–99%; Acidité=43%
		Cascade aération + bassin (1)	Oxydation Fe^{2+}	
		Cascade aération + bassin (2)	Oxydation Fe^{2+}	
		Cascade aération + bassin (3)	Oxydation Fe^{2+}	
	pH=2,35–2,96 ; **Fe= 755-1100 mg/L**; Al=128–167 mg/L; Zn=19–33 mg/L ; Mn=4–6 mg/L ; Cu=12–24 mg/L ; SO_4^{2-}=3324–4515 mg/L ; Acidité=2500 mg $CaCO_3$/L	Chéneaux ouverts +cascades	Oxydation Fe^{2+}	pH=5–6; **Fe= 40–77%**; Al=100%; Zn=-60–80%; Cu=89%; Acidité=60%
		Réacteur calcite-SAD	Augmentation pH et enlèvement métaux trivalents	
		Bassins de décantations + cascades aérations	Oxydation Fe^{2+}	
	pH= 3,55–3,61 ; **Fe=237–281 mg/L** ; Al=70–91 mg/L ; Zn= 342–364 mg/L ; Cu= 2,1–3,4 mg/L ; Acidité= 1404–1609 mg $CaCO_3$/L	Réacteur calcite-SAD (T1)	Enlèvement Al, As, et partiellement Fe	pH= 9,33–10,35 ; **Fe= 99,96%**; Mn=99,2%; Cu=99,9%; Al=99,9%; 99,99%
		Bassin+ cascade aération (D1)	Oxydation Fe^{2+}	
		Bassin+ cascade aération (D2)	Oxydation Fe^{2+}	
		Réacteur calcite-SAD (T2)	Augmentation pH et enlèvement Al et Fe	
		Deux bassins de décantation (D3+D4)	Oxydation Fe^{2+}	
		Réacteur MgO-SAD (T3)	Enlèvement éléments bivalents	

2.5 Avantages et limites des filières à base de substrat alcalin dispersé dans le traitement du DMA fortement contaminé

Le SAD est un mélange de matériaux alcalins fins (1−5 mm) et de matrices grossières, généralement des copeaux de bois (Rötting et al., 2006 ; Macìas et al., 2012). La taille des grains a été choisie de façon à ce qu'ils fournissent une plus grande surface réactive et qu'ils puissent être dissous avant que le phénomène d'enrobage ne survienne. En effet, les grains plus fins offrent une plus grande réactivité, et sont donc non enclins à l'enrobage, mais ils peuvent augmenter les précipités et diminuer la perméabilité, tandis que les grossiers risquent d'être plus susceptibles à la passivation (Rötting et al., 2008c). La matrice grossière sert plutôt à fixer les précipités, retardant ainsi le colmatage (Rötting et al., 2008b). Les agents alcalins de base utilisés sont la calcite (calcite-SAD) (p. ex. : Rötting et al., 2008a, 2008b; Caraballo et al., 2011) ou l'oxyde de magnésium (MgO-SAD) (Rötting et al., 2006; Caraballo et al., 2009). La calcite dans le mélange lui confère l'avantage d'augmenter le pH autour de 7 pour précipiter les métaux trivalents ; et à un pH plus de 8,5 avec le MgO, permettant de précipiter les métaux bivalents (Rötting et al., 2008c; Caraballo et al., 2009).

La caractéristique « dispersive » du mélange SAD lui donne l'avantage d'avoir des meilleures propriétés hydrauliques (Rötting et al., 2008b). En effet, le SAD peut avoir une porosité (n) initiale de 0,62 à 0,76 (Rötting et al., 2007; Caraballo et al., 2010) et une k_{sat} de l'ordre de 10^{-2}–10^{1}cm/s (p. ex. : Rötting et al., 2007; 2008a; Caraballo et al., 2011). Ces valeurs sont plus élevées par rapport à celles des autres types de traitement passif, comme le RPB, dont n varie typiquement de 0,34–0,53 (Neculita et al., 2008a; Vasquez et al., 2016a, 2016b) et la k_{sat}, de 10^{-4}–10^{-2} cm/s (URS, 2003; Neculita et al., 2008a; Genty, 2012). Ce qui amène à une diminution moins élevée du k_{sat} de l'ordre de 10^{-2}–10^{-1} cm/s (Rötting et al., 2008a; 2008b) lors d'un traitement d'eau fortement contaminée (en raison du colmatage), tandis que celle du RPB arborait une diminution jusqu'à un ordre de 10^{-5}cm/s par rapport à la valeur initiale (Neculita et al., 2008b).

Toutefois, les facteurs et paramètres pouvant entraîner la réduction du k_{sat} ne sont pas encore bien connus et devraient être évalués plus en profondeur dans le futur.

Généralement, un enlèvement du Fe de 48–85% pour une concentration initiale de 290–1100 mg/L a été obtenu avec une filière utilisant des réacteurs à calcite- et MgO-SAD (Rötting et al., 2008b; Caraballo et al., 2009, 2011). Les autres métaux, tels l'Al, le Cu, l'As, et le Pb, étaient enlevés jusqu'à 100%, et à environ 25–65% pour le Zn et 80% pour l'acidité (Rötting et al., 2008c; Caraballo et al., 2009). Une filière à calcite-SAD a permis de traiter un débit élevé (entre 43–86 m^3/jour) pendant 20 mois sans éprouver des problèmes significatifs de colmatage. De plus, 44–77% d'efficacité (Fe initial de 755–1100 mg/L) a été obtenue (Caraballo et al., 2011). Une filière à MgO-SAD a montré un enlèvement de Fe de >99,9% (concentration initiale 231–281 mg/L) à un débit de 0,5 L/min (Macías et al., 2012a).

La performance des filières de traitement à base de SAD est limitée en présence de concentration élevée d'Al (et éventuellement du Mn) qui, comme mentionné précédemment, peut concurrencer l'enlèvement du Fe (Neculita et al., 2017). En effet, l'Al peut précipiter à partir d'un pH 5 et migre dans la partie inférieure en bouchant la proximité du port d'entrée d'eau (Caraballo et al., 2010). L'utilisation du MgO comme agent alcalin augmente considérablement, et de façon plus ou moins constante, le pH à plus de 8 (jusqu'à 12), nécessitant parfois une correction pour rencontrer les exigences règlementaires. De plus, du fait de cette valeur élevée de pH, les minéraux secondaires, résultant de la précipitation des métaux bivalents en plus des métaux trivalents, augmentent. Par conséquent, une rapide accumulation de précipités conduit à un rapide colmatage. En outre, la précipitation de $Mg(OH)_2$ peut provoquer une cimentation localisée, causant une diminution du k_{sat}, et peut subséquemment créer un chemin d'écoulement préférentiel (Caraballo et al., 2010).

Par ailleurs, l'efficacité d'enlèvement des SO_4^{2-} est inconsistante dans les filières de traitement à SAD, mais les tendances indiquaient une valeur inférieure à 9% (Rötting

et al., 2008a ; Macías et al., 2012a). Ainsi, l'ajout d'une unité supplémentaire de traitement de SO_4^{2-} serait bénéfique.

2.6 Dernières remarques

La problématique du DMA ferrifère est principalement liée à la concentration élevée en Fe (>500 mg/L) qui, à son tour, contrôle la concentration des autres éléments dans le DMA. Le DMA ferrifère est fréquemment rencontré dans les sites miniers abandonnés/fermés. La combinaison de plusieurs types de traitement passif, connue sous le nom de filière, est recommandée pour traiter le DMA ferrifère, due à la limite de performance d'une seule unité de traitement passif. D'un côté, les filières composées de réacteurs SAD ont une efficacité plus élevée dans l'enlèvement des métaux et plus particulièrement dans leurs capacités à limiter le colmatage. D'un autre côté, les filières à base de RPB sont fréquemment utilisées pour traiter le DMA riche en SO_4^{2-}. La conception des filières de traitement passif est basée sur les critères de design des traitements passifs conventionnels. Toutefois, ces critères varient selon le type d'eau à traiter et les critères adaptés au traitement du DMA ferrifère doivent donc être déterminés. En utilisant les avantages et les inconvénients des RPB et des réacteurs SAD, une filière composée de ces deux types de traitement pourrait être constituée pour améliorer le traitement du DMA ferrifère. Dans ce contexte, les trois chapitres qui suivent (chapitres 3, 4 et 5) présentent les trois grandes étapes des recherches effectuées durant cette étude.

CHAPITRE III

EFFECTIVENESS OF VARIOUS DISPERSED ALKALINE SUBSTRATES FOR THE PRE-TREATMENT OF FERRIFEROUS ACID MINE DRAINAGE[1]

Ce premier chapitre a été publié en juillet 2016 dans la revue *Applied Geochemistry*. Une copie de l'article peut être consultée dans les annexes (Annexe D).

[1] Rakotonimaro, T.V., Neculita, C.M., Bussière, B., Zagury, G.J., 2016. Effectiveness of various dispersed alkaline substrates for the pre-treatment of ferriferous acid mine drainage. *Applied Geochemistry* 73:13-23.

3.1 Résumé

Les substrats alcalins dispersés (SAD) ont été utilisés avec succès dans le traitement passif du drainage minier acide (DMA) pour limiter les problèmes d'enrobage et de colmatage. Cependant, une optimisation supplémentaire des systèmes SAD est encore nécessaire, en particulier pour leur efficacité à long terme, pour traiter le DMA ferrifère. Dans la présente étude, trois types de SAD, composés de matériaux alcalins naturels (cendres de bois, calcite, dolomie), à différentes proportions (20, 50 et 80% v/v) et des susbtrats à grande surface spécifique (copeaux de bois) ont été testés dans neuf réacteurs batch. Les essais ont été réalisés en duplicata pendant une période de 91 j, afin de comparer la performance des mélanges pour le prétraitement du Fe dans le DMA ferrifère (2500 mg/L de Fe, à pH 4). Les résultats ont montré une augmentation du pH (entre 4,15 et 7,12), quelle que soit la proportion d'agents alcalins dans les mélanges réactifs. Parmi les mélanges testés, les SAD composés de cendres de bois ont été plus efficaces pour enlever le Fe (99,9%) que les SAD composés de calcite ou de dolomite (jusqu'à 66%). Tous les SAD testés avaient une efficacité limitée pour enlever les SO_4^{2-}, et une unité de traitement supplémentaire, comme un réacteur passif biochimique, permettant de traiter les SO_4^{2-}, est nécessaire. De plus, en raison des performances similaires des mélanges calcite- et dolomite-SAD, ils pourraient être potentiellement substitués et sont plutôt suggérés pour être utilisés dans une unité de traitement de polissage. Basé sur ces résultats, le mélange le plus prometteur était le SAD composé de 50% de cendre de bois.

3.2 Abstract

Dispersed alkaline substrates (DAS) have been successfully used in passive treatment of highly contaminated acid mine drainage (AMD) to limit coating and clogging issues. However, further optimization of DAS systems is still needed, especially for their long-term efficiency during the treatment of ferriferous AMD. In the present study, three types of DAS comprised of natural alkaline materials (wood ash, calcite, dolomite), in different proportions (20%v/v, 50%v/v, 80%v/v), and a substrate with high surface area (wood chips) were tested in 9 batch reactors. The testing was carried out in duplicate, for a period of 91 days, to evaluate the comparative performance of the mixtures for iron pre-treatment in ferriferous AMD (2500 mg/L Fe, at pH 4). Results showed increasing of pH (between 4.15 and 7.12), regardless of the proportion of alkaline materials in the DAS mixtures. Among the tested mixtures, wood ash type DAS were more effective for Fe removal (99.9%) than calcite or dolomite type DAS (up to 66%). All tested DAS had limited efficiency for sulfate removal and an additional treatment unit, such as a sulfate-reducing biochemical reactor, is needed. Moreover, due to the similar performances of the calcite and dolomite DAS, they could be potentially substituted and rather be used in a polishing treatment unit. Based on these findings, the most promising mixture was the 50% wood ash type DAS (WA50-DAS).

Keywords: Ferriferous acid mine drainage, iron pre-treatment, dispersed alkaline substrate, calcite, Dolomite

3.3 Introduction

Environmental impacts of acid mine drainage (AMD), which is characterized by low pH (-3.6<pH<6) and high concentrations of dissolved metals, metalloids and sulfate (SO_4^{2-}) are largely documented (Neuman et al., 2014; Nordstrom et al, 2015). Improvement of technologies has been conducted over the last decade to limit and prevent AMD generation (Sahoo et al., 2013; Jennings and Jacobs, 2014). Several treatment technologies, including active and passive systems, have also been developed (USEPA, 2014). Passive treatment is preferred, principally for moderately contaminated water, because of its low cost, potential production of marketable sludge, and simple installation and operation (Hedin et al., 2013; Zipper and Skousen, 2014). Despite these advantages, efficiency of a single unit of passive treatment (e.g. oxic/anoxic limestone drains- OLD/ALD, passive biochemical reactor- PBR) is limited when used for the treatment of highly contaminated AMD, particularly ferriferous AMD (Fe >500 mg/L) (Neculita et al., 2008; Genty et al., 2010). Hence, combinations of two or more units of passive treatment or so-called passive multi-step treatment system have been optimized (Macías et al., 2012; Genty et al., 2012a). Nonetheless, coating/passivation (loss of reactivity) and clogging (loss of permeability) caused by precipitated minerals during treatment (e.g., gypsum, metal oxides-hydroxides) (Rötting et al., 2008a) are presently limiting the long-term performance of such systems. Their longstanding efficiency is conditioned by removal, at an early stage, of acidogenic metallic elements, such as Fe and/or Al (Ayora et al., 2013). Indeed, during precipitation of ferric iron as hydroxide [$Fe(OH)_3$] (Eq.(3.1)), which starts at pH around 3–3.5, depending on Fe total concentration, the pH decreases, and the removal of divalent metals (which precipitation requires pH >8.5), is inhibited.

$$Fe^{3+} + 3H_2O \rightarrow Fe(OH)_3 + 3H^+ \qquad (3.1)$$

Consequently, a pre-treatment unit for Fe removal in ferriferous AMD is necessary before forwarding water into a second treatment unit for the removal of other metals

and of SO_4^{2-}, if necessary. Various techniques have been developed for Fe pre-treatment, such as oxidation/precipitation (Champagne et al., 2005), oxic limestone drain (OLD) (Figueroa et al., 2007), natural Fe-oxidizing lagoon (NFOL) (Macìas et al., 2012), and cascade aeration (USEPA, 2014). Most of these techniques gave promising results, but have been mostly used for Fe pre-treatment when AMD has low to moderate concentrations (40–1000 mg/L Fe). Regarding Fe concentration, the quality of water in this study is then considered as extremely contaminated (2500 mg/L Fe).

Innovative approaches using reactive mixtures composed of a coarse, highly porous material (wood chips) and small grain size of neutralizing agents (e.g. MgO, $CaCO_3$) known as dispersed alkaline substrate (DAS) have also been investigated with the aim of overcoming the coating-clogging general issues in passive treatment (Macías et al., 2012; Ayora et al., 2013). Two main types of DAS have been used to treat AMD, one comprised of MgO (MgO-DAS), for the removal of bivalent metals (e.g. Macìas et al., 2012; Ayora et al., 2013), and one of calcite (calcite-DAS), for the removal of trivalent metals (e.g. Rötting et al., 2008b; Caraballo et al., 2011).

In passive treatment, the use of economic, available and natural materials or substitute is recommended. Other selection criteria include the reaction rate of neutralizing agents, sludge production and costs (Potgieter-Vermaak et al., 2006). Hence, the dolomite DAS could be an economic replacement of the calcite/limestone DAS because it could reduce expenses up to 23% (Potgieter-Vermaak et al., 2006). Moreover, previous studies using dolomite as a neutralizing agent in the treatment of very acidic water have shown promising results (Potgieter-Vermaak et al., 2006; Huminicki and Rimstidt, 2008; Genty, et al., 2012a). Depending on the grain size, some studies even presented comparable efficiency of calcite and dolomite when used for the treatment of moderately contaminated AMD under anoxic condition, with lower difference in alkalinity production (105–220 mg/L as $CaCO_3$) for a hydraulic residence time of 15 h (Genty et al., 2012a). Additional benefits of dolomite-DAS include the

delaying of the neoformed minerals (e.g. gypsum $CaSO_4 \cdot H_2O$) because of the belated release of Ca^{2+}.

Another potential replacement of MgO in DAS systems could be wood ash, principally used for its high pH (up to 12), metal retention, and neutralization capacity. The wood ash, which is usually considered as a waste, has in fact a good potential of reuse. It showed efficiency in the pre-treatment of ferriferous AMD (Genty et al., 2012b). Moreover, it is an economic material, relative to MgO which cost is up to ten times higher than limestone (Rötting et al., 2006). Then, wood ash-DAS (WA-DAS) could be advantageous and potentially give similar performance to MgO-DAS. Despite the satisfactory performance (in terms of Fe and SO_4^{2-} removal, as well as of hydraulic conductivity stability) of the wood ash, its long term performance remains uncertain (Genty et al., 2012b). Moreover, additional treatment units for sulfate removal are necessary.

The results of a very recent laboratory study, which compared the performance of calcite-DAS to witherite ($BaCO_3$)-DAS, in terms of SO_4^{2-} removal, showed that the last was more efficient, but became unreactive after only 40 days of operation, due to passivation (by coating with barite – $BaSO_4$) (Lozano et al., 2015).

Therefore, the objective of the present study is to evaluate the efficiency of WA-DAS, calcite-DAS and dolomite-DAS in batch testing, in the perspective of their use as pre-treatment units for Fe removal in a ferriferous AMD. The residual Fe concentration targeted for this pre-treatment is 500 mg/L. This concentration was reported as a threshold value based on the steady performance of a PBR, in a 15-month laboratory study (Neculita et al., 2008).

3.4 Materials and methods

3.4.1 Physicochemical characterization of materials composing the mixtures

Nine reactive mixtures made of natural materials, i.e. wood chips, and three neutralizing agents (wood ash, calcite and dolomite) were evaluated in batch tests. The wood ash was a by-product from a co-generation plant located at Kirkland Lake (Canada), the wood chips originated from P.W.I. industries (QC), the calcite from the quarry of Perth (ON), and the dolomite from the Temiscamingue region (QC). These three reagents were mainly composed of Ca and Mg (Table A1). Grain size of calcite and dolomite was less than 5 mm, in order to allow almost complete dissolution, before eventual armoring during the treatment of ferriferous AMD. In this study, paste pH of the nine mixtures was determined in deionized water using a solid liquid ratio of 1:10 (ASTM, 1995). Water content was evaluated in duplicate by drying samples at 40°C during 2 days. Specific surface area (Ss) of dry samples was determined by the BET method using 5-point N_2 adsorption isotherms with Micromeritics Gimini III 2375 surface analyzer. Particle size analysis was carried out using standard sieves (ISO R-20) in order to obtain size corresponding to 10% and 60% by weight of passing, as well as uniformity coefficient (D_{10}, D_{60} and $C_u = D_{60}/D_{10}$ respectively) (Aitcin et al., 2012). Loss on ignition (LOI), used as an indication of the organic matter content, was determined by weighing the samples before and after calcination (375°C for 16 h). Each mixture was grinded and sieved through 0.25 mm opening before being digested in a mixture of strong mineral acids (HNO_3, Br_2, HCl, and HF) (Potts et al., 1987). Then, the resulting digestate was analyzed for Fe, Ca, Mg and SO_4^{2-} content by Inductively Coupled Plasma-Atomic Emission Spectrometry (ICP-AES; relative precision of 5%) using a Perkin Elmer OPTIMA 3100 RL.

3.4.2 Batch testing description

The nine mixtures were set up in duplicate in 18 glass flasks of 1L, at room temperature (around 20°C). Each batch reactor was filled with 200 g dry mixture and 600 mL synthetic AMD (Neculita and Zagury, 2008). Mixtures consisted of wood chips and one of the following three neutralizing agents: wood ash (WA-DAS), calcite (calcite-DAS) or dolomite (dolomite-DAS) (Table 3.1). The batch testing was performed during a 91-day period.

Table 3.1 Composition and relative proportion of components of the nine reactive mixtures tested in batch reactors

Reactors	Wood ash	Calcite	Dolomite (%v/v)	Wood chips	Total
WA20	20	-	-	80	100
WA50	50	-	-	50	100
WA80	80	-	-	20	100
C20		20	-	80	100
C50	-	50	-	50	100
C80	-	80	-	20	100
D20	-	-	20	80	100
D50	-	-	50	50	100
D80	-	-	80	20	100

WA: Wood ash; C: Calcite; D: Dolomite

The characteristics of synthetic AMD (Table 3.2) simulated the typical water quality of ferriferous AMD encountered at several closed/abandoned mine sites in the region of Abitibi-Temiscamingue (QC, Canada), in Canada and around the world (Genty et al., 2012a; Ayora et al., 2013; Bejan and Bunce, 2015).

Table 3.2 Physicochemical quality of synthetic ferriferous AMD used in batch testing

Parameter	Concentration (mg/L, excepting for pH)	Source
Al	1.6±0.6	$Al_2(SO_4)_3 \cdot 18H_2O$
Fe	2500±300	$FeSO_4 \cdot 7H_2O$
Mg	33.5±3.8	$MgSO_4 \cdot 7H_2O$
Mn	8.2±1.0	$MnSO_4 \cdot H_2O$
Ni	0.7±0.4	$NiSO_4 \cdot 6H_2O$
Pb	0.2±0.1	$Pb(NO_3)_2$
Zn	0.2±3.0	$ZnSO_4 \cdot 7H_2O$
Ca	430±5	$CaSO_4 \cdot 2\ H_2O$
SO_4	5395±1000	$Na_2SO_4 \cdot 10H_2O$
pH	4	-

3.4.3 Sampling, analysis and geochemical modeling

Measurements of pH, redox potential (Eh), electrical conductivity (EC) and dissolved oxygen (DO), as well as analysis of alkalinity, acidity, total iron (Fe_t), ferrous iron (Fe^{2+}) and SO_4^{2-} concentrations were performed weekly, over the entire testing period. Water pH was measured with an electrode AccupHast 13-620-114 ATC/BNC, while the EC was measured with an Accumet 13-620-100 electrode. The two electrodes were connected to an Accumet Excel XL-60®. Redox potential was measured with a potentiometer (Sension1 POR HACH 51939-00) coupled with an internal Pt/Ag/AgCl electrode (dipped in acid 1N solution). The reading was then corrected relative to the standard hydrogen electrode (SHE) to calculate the Eh. The DO was measured using a LDO10103-Hach HQ30d probe, calibrated with air-saturated water. Alkalinity and acidity were determined with a Metrohm Binkmann, 716 DMS Trinitro titrator (APHA, 2005). The concentrations of Fe_t, Fe^{2+} and SO_4^{2-} were determined on filtered samples

(0.45 µm), within the first 2 hours after collection, with a DR/890 HACH colorimeter (Method 8008 – 1, 10 phenantroline, Method 8146–1, 10 phenantroline, and Method 8051– barium chloride powder pillows for Fe_t, Fe^{2+} and SO_4^{2-}, respectively). Total metal concentrations were analyzed by ICP-AES, at the beginning and at the end of the experiments, on filtered (0.45 µm) and acidified (with 2% (v/v) of nitric acid) samples. Following these analysis, relative metal removal r (%) in the supernatant was calculated using the following equation: $r = [(C_x - C_{x+7})/C_x]. 100$, where C_x and C_{x+7} are metal concentrations (mg/L) at time x and x+7 days. Precipitated Fe was calculated from the difference between the Fe_t content of water at t_x and at t_{x+7}.

Metal removal mechanisms during the batch testing were evaluated using the physicochemical quality of supernatant samples collected on days 0, 7, 14, 21, 56, 70 and 91 and the geochemical equilibrium software VMINTEQ, version 3.0 (KTH, 2013).

3.4.4 Post testing mineralogy

Samples were collected from the reactors and dried at 40°C for 48h and metallized. Afterward, the microstructure and mineralogy were observed with a scanning electron microscope (SEM) equipped with probe Energy Dispersive X-ray Spectroscopy (EDS) HITACHI S-3500N (voltage of 20 kV, amperage of 140 A, pressure around 25 kPa and work distance of 15mm). Images, element maps and chemical composition were recorded with a data processor INCA (Oxford Energy 450).

Crystalline phases of the secondary precipitates were analyzed by X-ray diffractometer (Bruker axs D8 ADVANCE) equipped with a Cu anticathode and a scintillation counter. Prior to XRD analyses, the samples were dried (at 40°C for 48 h), and grinded to 10µm (detection limit <1%w/w). Then the data was collected and interpreted for minerals identification and quantification with Bruker axs EVA and TOPAS software packages.

3.5 Results and discussion

3.5.1 Physicochemical characteristics of the substrates

Initial pH of WA-DAS was higher (7.98–9.41) than both calcite- and dolomite-DAS (6.02–8.80) (Table 3.3). In addition, water content was higher for WA-DAS (18.3–28.3%) than for calcite- or dolomite-DAS (0.3–2.2%), indicating that the materials composing these two last DAS were dry. Specific surfaces (Ss) of calcite- and dolomite-DAS were relatively low (0.16–0.55 m^2/g) comparing to that of WA-DAS (9.15–32.50 m^2/g). Nonetheless, the dolomite-DAS had double Ss relative to calcite-DAS, except for the C20 mixture (Table 3.3). The Ss of calcite-DAS was higher (0.16−0.46 m^2/g) compared to calcite alone with similar particle size, as reported in a previous study (12.07 $x10^{-4}$ m^2/g, Genty et al., 2012a). The wood chips might have contributed to this Ss increase. Calcite- and dolomite-DAS had spread grains size distribution and contained low fines (D_{10}=0.18–0.26 mm, D_{60}=0.7–1.4 mm, Cu=3.18–6.36). On the contrary, the WA-DAS contained considerable fraction of fines as the proportion of wood ash in the mixture was high (D_{10}=4–22 µm, D_{60}≈0.3–0.4 mm, Cu=1.45–150), which explain, at least in part, its high Ss value. Mixtures composed of wood ash also had higher organic contents as indicated by the results on LOI, which were 2 to 3 times higher for WA20 compared to C20 and D20, 5 times higher for WA50 compared to C50 and D50, and 7 to 13 times higher for W80 compared to C80 and D80 (Table 3.3). The results on water content and LOI indicate the presence of significant organic carbon in all mixtures, particularly in WA-DAS, originating mainly in the wood chips and probably with the contribution of unburned wood contained in the wood ash itself (Genty et al., 2012b). Thus, sorption of metallic ions on negatively charged surface of organic material components could be a resulting advantage (Asadi et al., 2009). The Ca content of WA-DAS was 2−7 times lower than of calcite- and dolomite-DAS. Mg content in dolomite-DAS was 10−130 times higher than in calcite-

DAS and 6 to 27 higher than in the WA-DAS. A higher release of Mg^{2+} from dolomite could induce higher SO_4^{2-} removal (>86% at 300 mg/L Mg^{2+}; Potgieter-Vermaak et al., 2006). This could be partially explained by potential reaction of Mg^{2+} with SO_4^{2-} and/or HCO_3^- to form either $MgSO_4$ salt or $MgCO_3/Mg(HCO_3)_2$ with respect to pH (Eq.(3.2)). Since $MgSO_4$ is soluble in water, the formation of insoluble $MgCO_3/Mg(HCO_3)_2$ would be favored. Consequently, ion Ca^{2+} is available to form $CaSO_4$ or gypsum.

$$CaMg(CO_3)_{2\,(s)} + H_2SO_4 \leftrightarrow CaCO_{3(s)} + Ca^{2+} + Mg^{2+} + SO_4^{2-} + HCO_3^- \qquad (3.2)$$

These results might give calcite- and dolomite-DAS the advantage to delay Fe-oxy (hydroxides) precipitation that entails clogging issues in comparison to WA-DAS. All substrates contain low Fe and have similar concentrations of SO_4^{2-}, except for WA50 and WA80 (Table 3.3). Noteworthy, significant SO_4^{2-} concentrations were released in control batch (set up with deionized water slightly acidified with sulphuric acid to maintain a pH around 4, for 24 h and 1 week) with respectively 220 mg/L, 540 mg/L and 1180 mg/L in WA20, WA50 and WA80 reactors.

Table 3.3 Physicochemical characteristics of substrates used in batch testing

Mixtures	pH	Ss (m^2/g)	Water content (%w/w)	LOI (%)	Ca	Mg	Fe	SO_4^{2-}
					(g/kg)			
WA20	7.98	9.15	28.3	78.6	28	2.4	<0.01*	0.9
WA50	8.79	18.63	18.3	63.4	50	5.6	<0.01	3.4
WA80	9.41	32.8	22.0	46.8	91	9.5	11.1	7.8
C20	6.51	0.46	1.8	28.3	170	0.5	<0.01	0.9
C50	7.41	0.21	0.8	12.0	224	1.3	<0.01	0.9
C80	8.73	0.16	2.0	6.6	300	5.5	<0.01	0.9
D20	6.02	0.43	2.2	44.3	115	65.0	<0.01	0.9
D50	8.02	0.43	1.0	12.6	354	55.0	<0.01	0.9
D80	8.80	0.55	0.3	3.5	182	53.0	<0.01	0.9

*Method detection limit

3.5.2 Batch tests: Comparative efficiency of dispersed alkaline substrates

Over the batch testing duration, three periods have generally been observed in the evolution of treated water quality in reactors: 1) optimal efficiency (0–21 days), 2) steady state (21–70 days), and 3) either steady state or efficiency improvement (70–91 days).

3.5.2.1 First period (0–21 days) – optimal efficiency

During this period, water pH increased in all reactors (from 4 to an average of 6.7, 5.4, 4.8 in WA-, calcite- and dolomite-DAS reactors, respectively), regardless of the proportion of neutralizing agents in the DAS mixtures. However, in the WA-DAS reactors, pH was higher than either in calcite- or dolomite-DAS, due to the higher neutralizing capacity of wood ash, especially within the first week (Fig. 3.1).

The Eh decreased from 405 mV to slightly lower values (around 290 mV) in calcite- and WA-DAS comparing to that of dolomite-DAS (326 mV), showing oxic condition (Fig. 3.1).

In the same time, the WA-DAS neutralized during the first 14 days up to 96% of acidity, whereas calcite- and dolomite-DAS neutralized only 16–27% (Fig. 3.1). After day 21, the acidity increased in WA-DAS, C20 and C80, which is partially explained by the additional acidity generated during the fast precipitation of Fe (oxy)-hydroxide. Similar results have been previously reported, when alkaline materials with small grain size were used in a limestone-DAS (Ayora et al., 2013). From the first 7 days, the alkalinity increased significantly in the WA-DAS (on average 1240 mg/L as $CaCO_3$) and calcite-DAS (230 mg/L as $CaCO_3$), but not with the dolomite-DAS (0–5 mg/L as $CaCO_3$) (Fig. 3.1).

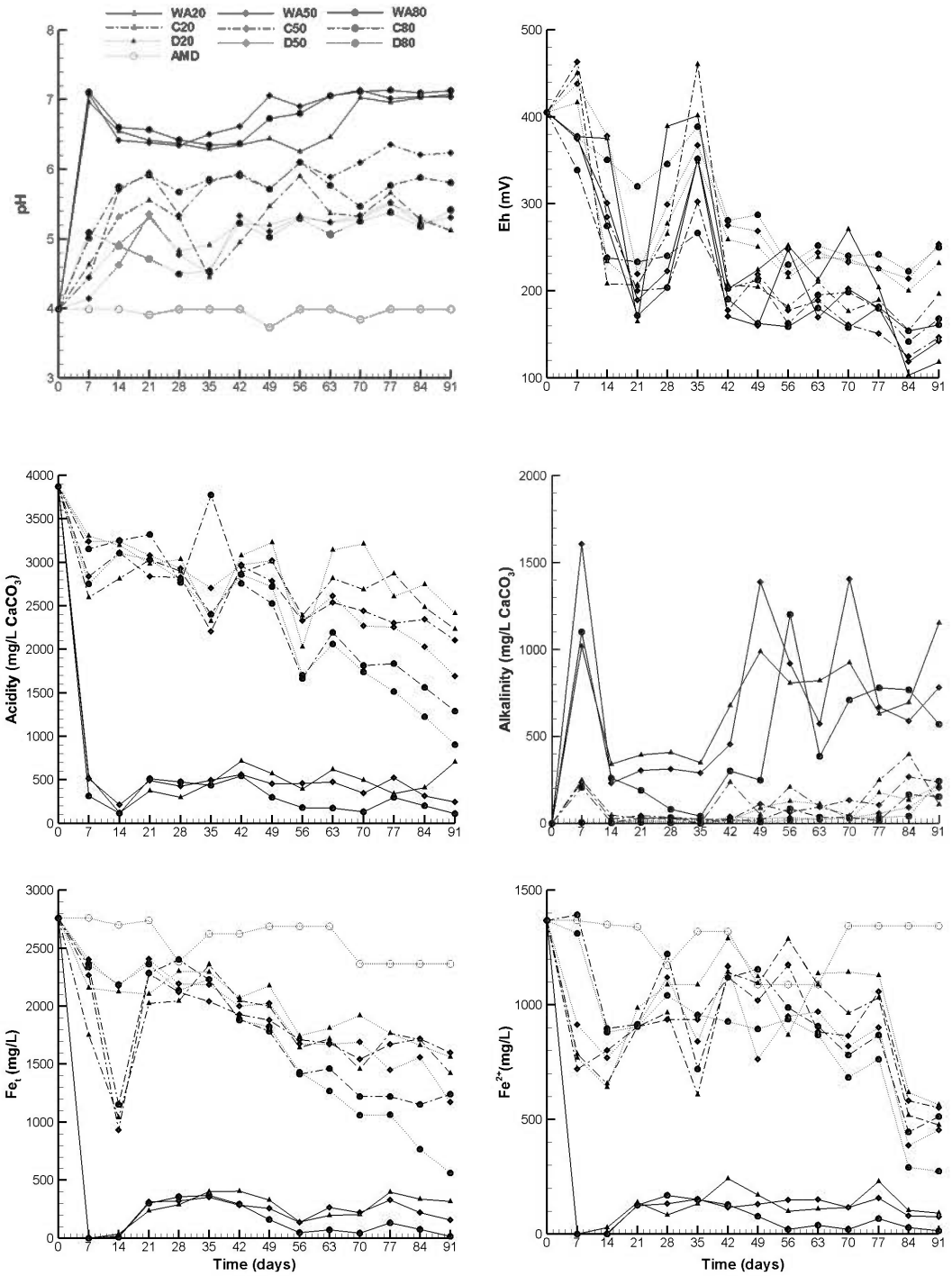

Figure 3.1 Evolution of pH, Eh, acidity, alkalinity, Fe_t and Fe^{2+} concentration in wood ash-, calcite- and dolomite-DAS batch reactors

The low value of alkalinity obtained in the last reactors is consistent with the low recorded pH values and was expected, considering the low reactivity of dolomite. However, at the end of this first period, while alkalinity decreased rapidly in the WA- and calcite-DAS (286 mg/L as $CaCO_3$ and between 17 and 37 mg/L as $CaCO_3$, respectively), it increased in the dolomite-DAS reactors (between 4.5 and 11.5 mg/L as $CaCO_3$), which means that dolomite started to be activated only after 21 days.

As the pH increased rapidly because of the fast reactivity of the wood ash, precipitates assumed to be ferric hydroxides (likewise visible as yellow, yellow-brown in the WA-DAS reactors during this experiment) appeared. In addition, because of the high Fe concentration, the precipitation of ferric hydroxide occurred firstly, thereby influencing gypsum precipitation, especially when the ratio Ca^{2+}/SO_4^{2-} was low. In such cases, Fe oxy-hydroxides (instead of gypsum) armoring could be the major issue during the passive treatment of Fe-rich AMD. However, Fe oxy-hydroxides are weakly bound precipitates and can be removed mechanically or flushed (Santomartino and Webb, 2007; Wolfe et al., 2010). Given their positive charged surfaces at pH <8, they could potentially sorb oxy-anions of As and Sb, if present in the AMD (Cornell and Schwertmann, 2003; Sparks, 2003).

The DO remained high in all reactors during the first 7 days (~8.1 mg/L), which may partially explain the optimal Fe removal of the treatment, particularly in WA-DAS reactors during this period, since it contributed to oxidation, hydrolysis and precipitation of Fe^{2+} (Strosnider et al., 2013). As a result, Fe removal with the WA-DAS was up to 99.9% (Fig. 3.1), corresponding to 1680 mg Fe, at a rate of 238 mg Fe/d (Table A2). Resultant SO_4^{2-} removal was between 25 and 44%, with WA20 and WA80 as the most and the least efficient, respectively (Fig. 3.2). However, after 21 days, the DO dropped to 0.80–1.29 mg/L in all reactors, probably due to organic matter decomposition (Sahoo et al., 2013). This was followed by a slight decrease in Fe removal to 94% (Fig. 3.1), while SO_4^{2-} removal remained constant (Fig. 3.2). Hence, Fe and/or SO_4^{2-} reduction is not excluded. Nonetheless, with a sufficient alkalinity to

buffer acid and keep high the pH value (>3.5), the main Fe removal mechanism is by precipitation in the form of oxyhydroxides and carbonates. Sorption and co-precipitation mechanisms can also occur.

The efficiency of calcite- and dolomite-DAS was related to their reactivity. The fast reactivity of calcite during the first stage of dissolution, which is correlated to the neutralization of sulfuric acid (Maree et al., 1992; Potgieter-Vermaak et al., 2006), ascribed calcite-DAS its capacity to early increase the pH, and thus precipitate metals. Accordingly, calcite-DAS allowed maximal Fe_t removal up to 66% after 14 days, whereas in this same period, dolomite-DAS removed only 22%, on average (Fig. 3.1).

Additionally, SO_4^{2-} removal was comparable for the two types of DAS (29% for C20 and D20; 40% for DAS with ≥ 50% of calcite or dolomite). Within the first 7 days of the batch testing with calcite- and dolomite-DAS, SO_4^{2-} concentration increased, except in C20. The release of SO_4^{2-} originating in the materials constituting the mixtures could contribute to this increase (Neculita and Zagury, 2008). Indeed, control batch reactor containing W20, which SO_4^{2-} content was the same as calcite- and dolomite-DAS mixtures, showed release of 220 mg/L SO_4^{2-} (Table 3.3). This could explain also the decrease of SO_4^{2-} removal in all calcite- and dolomite-DAS reactors to <12% after 21 days. Hence, a proportion of 50% of calcite or dolomite could be enough for ferriferous AMD (with Fe <1500 mg/L) pre-treatment only within short period of times because after the first 7 days, C80 and D80 showed the lowest Fe^{2+} removal (<5% efficiency) (Fig. 3.1). Gypsum precipitation probably hindered acid neutralization and, thus, Fe concentration stayed high. Geochemical modeling using water chemistry on day 7, from reactors C80 and D80, supports this hypothesis by indicating gypsum oversaturation and the possible subsequent precipitation.

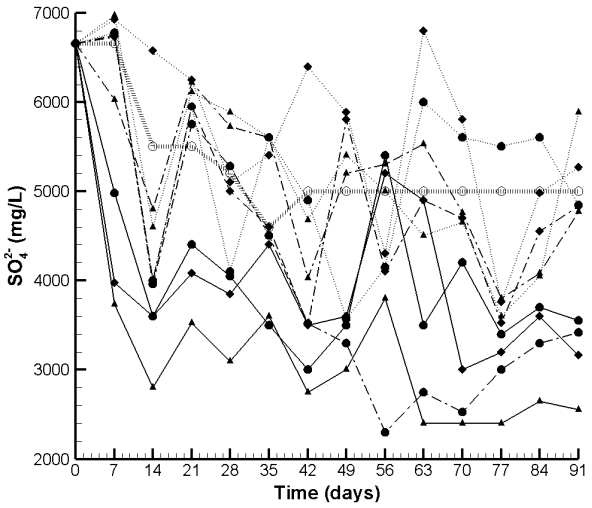

Figure 3.2 Evolution of SO_4^{2-} concentration in wood ash-, calcite- and dolomite-DAS batch reactors

Saturation indices (SI) calculated with VMINTEQ using water chemistry in all reactors on days 0,7, 14 and 21 indicated oversaturation of (oxy)hydroxide minerals, such as $Fe_3(OH)_{8(s)}$, goethite (α-FeOOH), hematite (α-Fe_2O_3), H-jarosite [$(H_3O)Fe_3(OH)_6(SO_4)_2$], lepidocrocite (γ-FeOOH) and magnetite (Fe_3O_4). Fe would be also precipitated under the form of Fe-carbonate siderite ($FeCO_3$) in the WA-DAS reactors.

3.5.2.2 Second period (21–70 days) – steady state

The pH in calcite-and WA-DAS reactors remained stable, while it increased to 5.12 in dolomite-DAS, but not in D80 (pH 4.99). The overall increase of pH value in all reactors seemed independent of the neutralizing agent proportion in the tested DAS; however, this could play a key role in the long term sustainability of their performance. Other parameters indicating water quality such as Eh, EC, and DO followed similar trends, and showed slight decrease or stability in all reactors (Table 3.4).

The alkalinity stayed high in WA-DAS reactors (81–1407 mg/L as $CaCO_3$), accompanied with a decrease in acidity down to 37.5% (final values 134–717 mg/L as $CaCO_3$). Subsequently, Fe_t removal was maintained relatively high to approximately 90%, giving a cumulative precipitation of 1700 mg Fe, at a rate of 240 mg Fe/d (Table A2). The mechanism of Fe removal in WA-DAS was mainly oxide-hydroxides precipitation. Ion exchange as well as adsorption could also occur according to previous studies on the Fe removal with wood ash (Genty et al., 2012b). At the end of the experiment, the Ss of WA20, WA50 and WA80 decreased respectively to 5.68 m^2/g, 16.76 m^2/g, and 30.08 m^2/g.

The efficiency of calcite- and dolomite-DAS was comparable, with an average removal of 28% Fe. According to Fe^{2+} removal, treatment of ferriferous AMD contaminated with Fe <1500 mg/L, was around 17% in calcite-DAS reactors, 8% in D20 and ~23% in D50 and D80 (Table 3.4).

Table 3.4 DAS systems efficiency during the steady state of ferriferous AMD treatment

Parameters	**WA-DAS**	**Calcite-DAS**	**Dolomite-DAS**
pH	6.65	5.62	5.08
Eh (mV)	232	220	274
DO (mg/L)	0.95–1.15	1.05–1.28	1.67–2.22
Alkalinity ($mgCaCO_3/L$)	423–710	33–95	23–53
Acidity ($mgCaCO_3/L$)	320–510	2600	2630
Fe removal (%)- AMD <1500mg/L	91	29	27
Fe removal (%)- AMD >1500mg/L	90	17	D20: 8%; DAS >50% dolomite: 23%
SO_4^{2-} removal (%)	18–40	<10 except C80 (31%)	<10

The similar performance of the calcite- and dolomite-DAS could be explained by the slower Fe removal in the calcite-DAS due to coating of calcite grains by precipitates, which corresponds to the second stage of calcite neutralization (Maree et al., 1992; Potgieter-Vermaak et al., 2006). The SO_4^{2-} removal was 18–40% with WA-DAS, whereas it was below 10% with calcite- and dolomite-DAS, except in C80 (31%). Irregularities in SO_4^{2-} removal are not easy to explain, but were consistent with similar DAS-based treatment systems using calcite or dolomite (e.g. Rötting et al., 2008b; Ayora et al., 2013). Nonetheless, SO_4^{2-} could be removed as calcium sulfate such as anhydrite and gypsum, as well as sorption onto Fe-oxyhydroxides. Indeed, SI calculated with VMINTEQ using water chemistry on days 21, 35, 56, 70 indicated the oversaturation of (oxy) hydroxide minerals, as well as of gypsum. The Fe-oxide-hydroxides, which were identified as the yellow-brown precipitates on the bottom of the reactors, could be responsible for calcite and dolomite armoring, and the decrease of their dissolution and reactivity.

3.5.2.3 Third period (70–91 days) – steady state or efficiency improvement

The WA-DAS maintained their performance and the steady state period was extended to the third phase, whereas the efficiency of calcite- and dolomite-DAS was enhanced. Consequently, the pH, Eh, and EC showed stability or water quality improvement. The pH remained constant in all reactors except for D80, in which it slightly increased from 4.99 to 5.33 units. The EC dropped from 2.52 mS/cm to 1.95 mS/cm and <1 mS/cm in WA-DAS and both calcite- and dolomite-DAS, respectively, presenting a decrease of the total dissolved solid. The proportion of neutralizing agents seemed to be linked with the generated alkalinity, which augmented around 13% in the reactors containing <50% of wood ash, and 40% in WA80. Consequently, the neutralized acidity was on the one hand 4% in WA20, 21% in WA50 and 36% in WA80. On the other hand, acidity in dolomite- DAS reactor was slightly lower (950–2750 mg/Las $CaCO_3$) than in calcite-DAS reactors (1287–2872 mg/L as $CaCO_3$). It is worth mentioning that alkalinity in

dolomite-DAS constantly increased until the end of the experiments (up to 86%), which could be advantageous to reduce acidity in long term (Fig. 3.1). The low value of DO (0.18–1.2 mg/L) in all reactors suggested that oxidation of Fe^{2+} was spurred by other processes for example sufficient alkalinity that buffers the acidic solution (Younger et al., 2002). Indeed, correlated with acidity neutralization rate, Fe removal slightly decreased in WA20 (85%, final value 350 mg/L), while it stayed constant in WA50 (90%, final value 235 mg/L) and increased in WA80 (97%, final value 75 mg/L) (Fig. 3.1). Generally, Fe removal of calcite- and dolomite-DAS was improved and increased to about 33% in reactors with ≤50% calcite or dolomite, 49% in C80 and 66% in D80. Based on the results of Fe^{2+} removal, all tested DAS could pre-treat Fe-rich AMD with Fe <1500 mg/L, with an efficiency of 93% (around 94 mg/L) in WA-DAS, ~50% (670 mg/L) in calcite-DAS and between 43 and 67% (440–770 mg/L) in dolomite-DAS (Fig. 3.1). The DAS systems with ≥50% of dolomite seems particularly promising because in D50 and D80, Fe concentration decreased to 386 mg/L and 290 mg/L, respectively, after day 84. However, a larger system and a longer hydraulic residence time would be necessary.

The efficiency improvement of the calcite- and dolomite-DAS reactors over time could be due to the reactivation of calcite and/or dolomite grains after passivation with Fe precipitates. The interaction of acidic solution with the calcite or dolomite grains in the DAS mixtures led to dissolution of secondary Fe minerals from the armored grains surface. Thereby, the effective surface area would be reactivated. Indeed, the surface area of the calcite- and dolomite-DAS mixture after the treatment increased up to 5 times their initial values. Hence, sorption could occur as metal removal mechanism. Moreover, the coating/dissolution phenomenon would influence the effectiveness of the DAS mixtures. Some other studies corroborated this fact and stated that efficiency of armored and unarmored limestone was comparable as dissolution of grains increases with acidity in the solution (Ziemkiewicz et al., 1997; Simón et al., 2005). In addition,

as pH remained constant (4–5), the acidity neutralization stayed constant (Ziemkiewicz et al., 1997).

Improvement of SO_4^{2-} removal required longer contact time according to the efficiency of the different mixtures (31–49% in WA-DAS, 14–35% in calcite-DAS, <10% in dolomite-DAS reactors) (Fig. 3.2). The calcite- or dolomite-DAS required also longer contact time relative to wood ash.

3.5.3 Removal of other metals

All mixtures removed up to 92 % Al. According to the modeling results (i.e. VMINTEQ) on water quality from days 0 and 91, Al-oxyhydroxides such as diaspore [AlO(OH)], ($Al(OH)_3$), and hydrated aluminium sulfate basaluminite ($Al4(OH)_{10}SO_4$) were oversaturated. The DAS composed of wood ash and those with more than 50% of calcite allowed >90% of Zn removal, while the dolomite-DAS removed only 23% and 76% of Zn in D50 and D80, respectively. The Pb removal was 88% in W20, >94% in WA50 and W80, 41–68% in calcite-DAS and 33–78% in dolomite-DAS. These results showed that at a very low concentration, Zn and Pb removal appears to be strongly linked to alkaline agent proportion in the mixtures, and pH values. The higher is the amount of alkaline agent, the longer the pH is maintained at a value that promotes higher removal rate, with respect to concentration. Moreover, since results of modeling indicated that Pb was mostly removed as $PbCO_3$, the lower Pb removal in the calcite- and dolomite-DAS could have been explained by coating of grains that limited dissolution and availability of HCO_3^-/CO_3^{2-}. The Mn was not removed except in WA50 (up to 50%). Factors such as pH, DO, surface of Mn- and Fe-oxides and the presence of reducing agents, such as Fe^{2+} could adversely impact Mn removal (Rose et al., 2003; El Gheriany et al., 2009). The evaluation of key parameters influencing Mn removal in the presence of high concentrations of Fe requires further study.

3.5.4 Post-testing mineralogy

The precipitates on the surface of the mixtures composed of 20% and 80% of neutralizing reagents (WA20, WA80, C20, C80, D20 and D80) after the batch testing have been observed with SEM-EDS. The main mineral phases consisted of calcium sulfate mainly gypsum and Fe-oxides/hydroxides. The surface of the calcite recovered from the spent mixture C20 (cal-C20) was covered by a patch-like calcium sulfate (Fig. 3.3A).

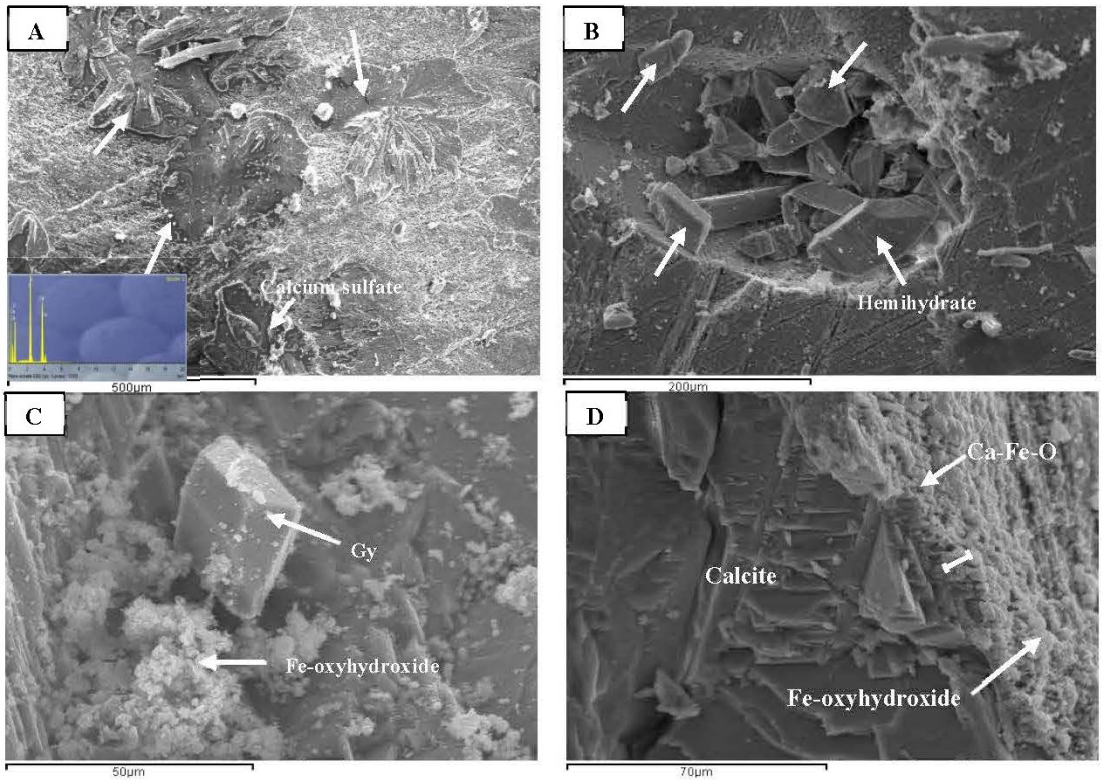

Figure 3.3 SEM-EDS images of the surface of calcite from C20 (cal-C20) and C80 (cal-C80) after the treatment: (A) Surface of cal-C20 covered by patch-like calcium sulfate on a layer of Fe/Al- oxyhydroxide, (B) Niche filled with gypsum crystals on the surface of cal-C20, (C) Monoclinic gypsum and flaky Fe-oxyhydroxides on the surface of the cal-C80, (D) Cal-C80 fouled with ~5µm of Fe-oxyhydroxides and srebrodolskite.

The formation of this latter may be due to its direct contact to sulfuric acid and organic colloids from the decomposition of organic matter which were both found to be as calcium sulfate crystal growth inhibitors (Singh and Middendorf, 2007). This hypothesis could be corroborated by the fact that gypsum crystals could grow in the niche of the calcite grains (Fig. 3.3B). It appears then that the high acidity and the pore volume of the calcite grains might influence the growth of crystal gypsum. Indeed, at a lower acidity, gypsum crystal could develop as it has been observed on the surface of the calcite from C80 (cal-80) (Fig. 3.3C).

Similarly, to what was found on cal-C20, crystals of gypsum were well formed in the hollow of dolomite grains from D20 (dol-D20) (Fig. 3.4A). Whilst gypsum reached saturation (as it has been modelled), calcite and/or dolomite continued to be dissolved, adding Ca and Mg that would become oversaturated and precipitated as portlandite [$Ca(OH)_2$]. The Fe was detected in the form of siderite, chukanovite ($Fe_2(CO_3)(OH)_2$), srebrodolskite ($Ca_2Fe_2O_5$), magnesioferrite ($MgFe_2O_4$), and hydroniumjarosite [$(H_3O)Fe_3(SO_4)_2(OH)_6$]. The layer thickness of the secondary precipitates on the surface of calcite and dolomite grains was between 5 and 50µm, which could impede further reactivity (Figs. 3.3D, 3.4B, Fig. A1).

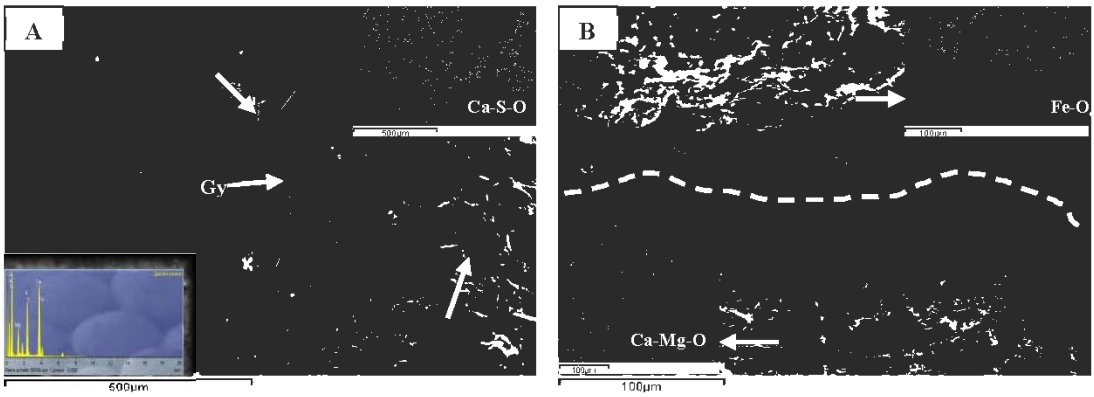

Figure 3.4 SEM-EDS images of the surface of dolomite from D20 (dol-D20) and D80 (dol-D80) after the treatment: (A) Surface of dol-D20 covered by gypsum (Gy) and Fe-oxyhydroxides, (B) Layer of ~50µm of precipitates (srebrodolskite, portlandite) and Fe-oxyhydroxides on the surface of the dol-D80

The surface of wood chips recovered from WA20 was partially enveloped by secondary precipitates of Fe-oxyhydroxides (Fig. 3.5A). On the contrary, that of WA80 was completely coated (Fig. 3.5B). This is in accordance to the amount of precipitated Fe which was higher in WA80 than in W20 reactor. Poorly crystallized, plate and small particles of hemihydrate gypsum was observed on wood chips from C20 (Fig. 3.5C). On the surface of wood chips from C80, amorphous Fe-oxyhydroxides were more abundant than gypsum (Fig. 3.5D). The hydration of calcium sulfate hemihydrate formed needle shape gypsum on the surface of wood chips from D20 (Fig. 3.5E). The particle size of gypsum precipitated in the D80 varied from 5 to 150µm. The large interlocked gypsum indicates the hydration of hemihydrate which could have been influenced by pH, acid concentration, and temperature (Fig. 3.5F).

It can be concluded that the precipitation and sorption of secondary minerals on the wood chips surface can limit coating of calcite or dolomite grains. With 20% of neutralizing agent, gypsum precipitation is favored while with 80%, Fe-oxyhydroxides are more abundant.

In order to optimize the XRD analysis (detection limit <1% w/w), two spent reactive mixtures (WA50 and D50) were selected. The presence of goethite, lepidocrocite as well as gypsum was principally the expected mineral phases. The XRD analysis showed that gypsum was the main crystallized secondary mineral. Quartz and biotite originating from the mixtures were also identified. The presence of pyrite was also detected, indicating that Fe^{3+} and SO_4^{2-} reduction occurred (Fig. A2). However, Fe-oxyhydroxides were amorphous and could not be detected.

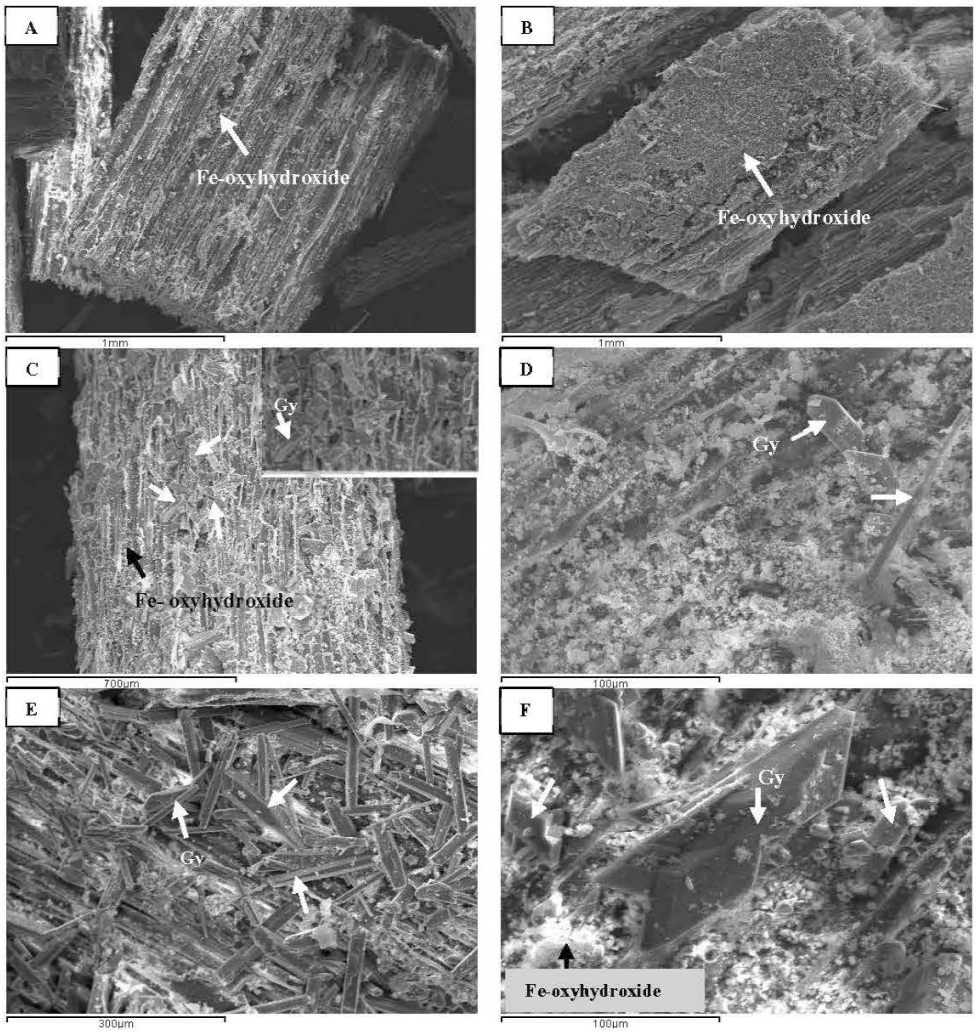

Figure 3.5 SEM-EDS images of wood chips recovered from mixtures after the batch testing and fouled with precipitates: (A) Wood chips from WA20 partially covered by Fe-oxyhydroxide, (B) Wood chips from WA80 with all the surface patched with Fe-oxyhydroxide, (C) Wood chips from C20 fouled with plate small grains of needle shaped hemihydrate gypsum (Gy) with local precipitates of Fe-oxyhydroxide, (D) Wood chips from C80 fouled with Fe-oxyhydroxides with euhedral and needle shaped gypsum, (E) Wood chips from D20 covered with needle shaped-gypsum, (F) Wood chips from D80 covered with a layer of Fe-oxyhydroxide under variable size (5µm–150µm) of euhedral gypsum

3.5.5 Performance of wood ash type DAS: Iron removal within the first 12h

As noted during the 91 days of batch testing, efficient Fe removal in mixtures containing wood ash occurred within the first 7 days. To better evaluate the critical time where Fe decreased to under 500 mg/L, and to better assess the efficiency of each of the three WA-DAS, three batch reactors containing WA20, WA50 and WA80 were set up as the previous tests (1L glass flasks filled with 200 g dry mixture and 600 mL of synthetic AMD). Two sets of tests were undertaken where Fe_t, Fe^{2+} and SO_4^{2-} removal was mainly measured within the first 12 h, using the same analysis methods as the 91-day period batch test. After the first 12h test, a second set was carried out with the AMD concentration set back at the initial concentration (2500 mg/L Fe).

During the first set of tests, the pH increased after 1h from 3.86 to 5.8, 6.14, 6.28 in WA20, WA50, and WA80, respectively and stayed stable around 6.30 in all reactors after 12h (Fig. 3.6). The Eh was around 300 mV, indicating an oxic environment (Fig. 3.6). The EC in WA20 and WA50 was 4.45 mS/cm, whereas that of WA80 was 5.4 mS/cm, which was explained by the high content in dissolved suspended solids (Fig. 3.6).

The efficiency of the three WA-DAS showed distinctive features, with Fe concentration in the reactors decreasing from 2590 mg/L to 495 mg/L after 9 h, to 440 mg/L after 4 h, and to 450 mg/L after 1 h, in WA20, WA50 and WA80, respectively (Fig. 3.6), corresponding to around 1300 mg Fe removal in each of the reactor (Table A3). The Fe^{2+} concentrations were 170 mg/L in WA20, 160 mg/L in WA50 and 240 mg/L in WA80 (Fig. 3.6), with similar precipitation rate (Table A3). After 12 h, SO_4^{2-} concentration decreased from 6500 mg/L to around 4700 mg/L.

On the second set of experiments, the pH was similar to the first set and the Eh decreased to 200 mV. The EC also decreased to around 2.4 mS/cm in all reactors (Fig. 3.6). Fe removal trend was the same as the first run for all reactors, except that Fe decreased at less than 500 mg/L only after 12 h in WA20, 11 h in WA50 and 6 h in

WA80 (Table A4). Thus, longer contact time was required for the first two DAS to decrease Fe concentration. Overall, Fe^{2+} concentration decreased to <500 mg/L after 12 h in WA20 (420 mg/L), and after 4 h in WA50 and W80 (340 mg/L and 260 mg/L) (Fig. 3.6). Thus, for the pre-treatment of ferriferous AMD, a contact time of 4 h would be enough if Fe <1500 mg/L, and 6–11h if Fe >1500 mg/L.

The SO_4^{2-} removal in WA20 (44%) was better than in WA50 (25%) and in WA80 (19%). Thus, WA20 appears to be promising. Nonetheless, alkalinity generation could be limited, therefore limiting long term performance of the treatment system. However, the use of WA80 involves higher content of fine grains, leading to a possible long term decline in hydraulic conductivity and limitation of efficiency. Given the obtained results and the advantage of WA-DAS to rise water pH around neutral (maximal 7.12), which does not require adjustment when used in a polishing or pre-treatment unit, oppositely to MgO-DAS, the WA50 seems to be the best compromise between the three WA-DAS.

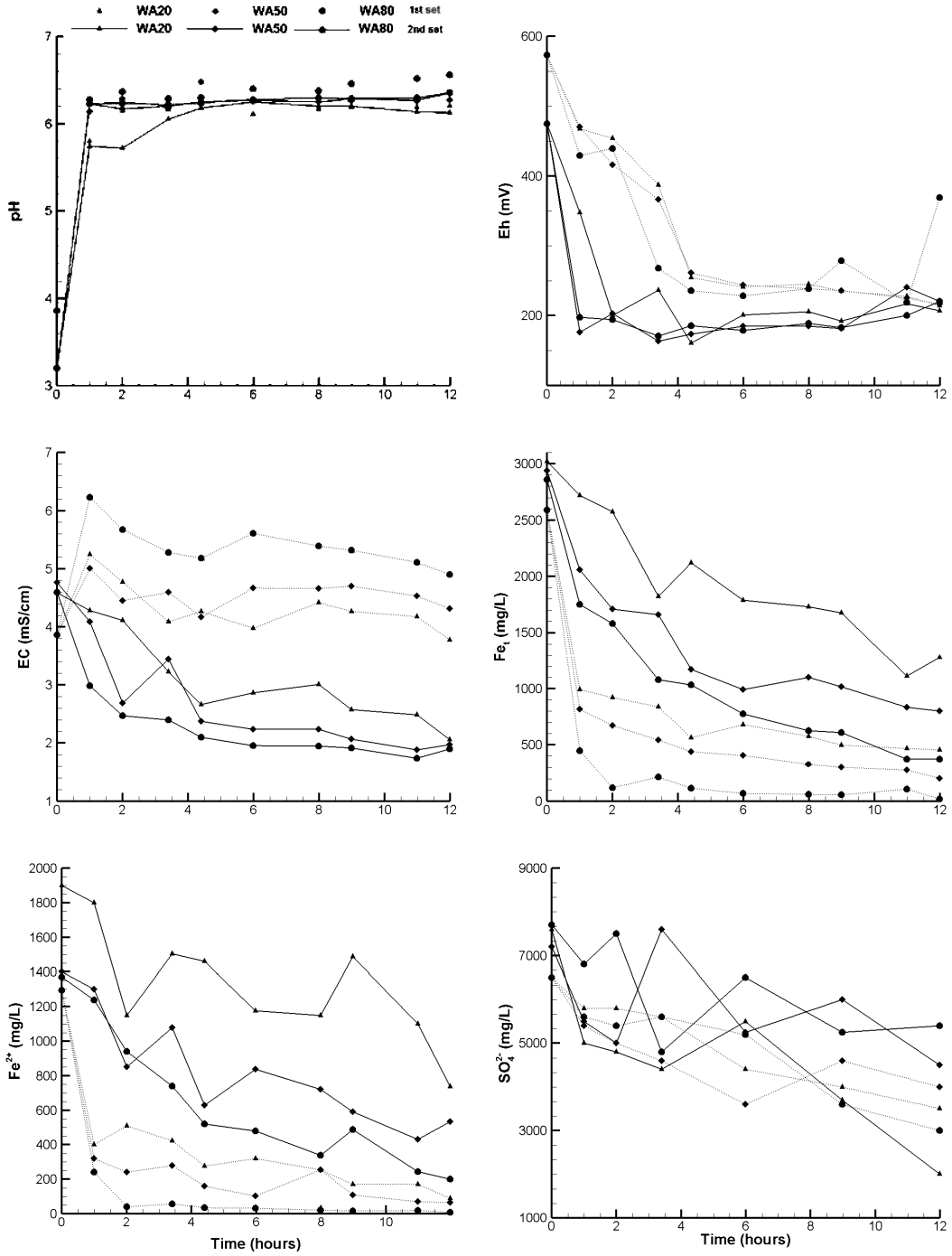

Figure 3.6 Evolution of Fe_t, Fe^{2+} and SO_4^{2-} concentrations in the first 12 hours of treatment in WA-DAS

3.6 Conclusion

The present study evaluated three types of DAS (dispersed alkalinity substrate), comprised of natural alkaline materials (wood ash, calcite, dolomite) in different proportions (20% v/v, 50% v/v, 80% v/v), and substrate with high surface area (wood chips) in 9 batch reactors, for Fe pre-treatment in ferriferous AMD (>1500 mg/L Fe), over a 91-day period. Among the tested DAS, the one composed of wood ashes (WA) was the most effective (99.9%), whereas those containing calcite or dolomite gave comparable performance. A contact time of 6–11 h was required for Fe concentrations to be decreased to below 500 mg/L. The efficiency of the WA-DAS systems was similar, regardless of the proportion of wood ash. However, the possible washing out/ clogging because of the high content of fine particles of W80, as well as the rapid alkalinity depletion of WA20, that eventually lead to limited long term performance, pointed out WA50 as the best choice for Fe pre-treatment. In a very short term run, calcite-DAS was more efficient (66%) than dolomite-DAS (22%). However, in a mid-term, calcite- and dolomite-DAS could be potentially substituted and used in a polishing unit for the passive treatment of iron-rich AMD. All DAS mixtures showed Al, Zn and Pb removal, except for Mn, which was removed up to 50% only in WA50. SO_4^{2-} removal in WA-DAS was higher (18–40%) compared to calcite- or dolomite-DAS (<10%). Nonetheless, additional treatment units for sulfate removal are necessary.

Acknowledgements

This study was funded by the NSERC (Natural Sciences and Engineering Research Council of Canada), and the industrial partners of the RIME (Research Institute on Mines and Environment) – UQAT (University of Quebec in Abitibi-Temiscamingue) – Polytechnique Montreal, Agnico Eagle, Mine Canadian Malartic, Iamgold, Raglan Mine Glencore, and Rio Tinto. The authors gratefully acknowledge the assistance of Dr Hassan Bouzahzah during mineralogy analysis. They also want to thank Marc Paquin, Mélanie Bélanger for the laboratory assistance.

References

Aitcin, P.C., Généreux, F., Jolicoeur, G., Maurice, M., 2012. Technologie des granulats, third ed. Modulo, Montréal, QC (Canada), 352p.

APHA (American Public Health Association), 2005. Titration method, in: Greenberg A. (Eds), nineteenth ed., Standard methods for the examination of water and wastewater, Washington, DC (USA), pp. 161–166.

ASTM (American Society for Testing and Materials), 1995. Standard test method for permeability of granular soils. Annual book of ASTM Standards.08. D 2434 – 68, Philadelphia, PA (USA).

Asadi, A., Huat, B.K.B., Hanafi, M.M., Mohamed, T.A., Shariatmadari, N., 2009. Role of organic matter on electroosmotic properties and ionic modification of organic soils. Geosci. J. 13 (2), 175–181.

Ayora, C., Caraballo, M.A., Macías, F., Rötting, T.S., Carrera, J., Nieto, J.-M., 2013. Acid mine drainage in the Iberian Pyrite Belt: 2. Lessons learned from recent passive remediation experiences, Environ. Sci. Pollut. Res. 20, 7837–7853.

Bejan, D. and Bunce, N.J., 2015. Acid mine drainage: Electrochemical approaches to prevention and remediation of acidity and toxic metals. J. Appl. Electrochem. 45, 1239–1254.

Caraballo, M. A., Macías, F., Rötting, T.S., Nieto, J. M., Ayora, C., 2011. Long term remediation of highly polluted acid mine drainage: A sustainable approach to restore the environmental quality of the Odiel river basin. Environ. Pollut. 159, 3613–3619.

Champagne, P., Van Geel, P., Parker, W., 2008. Impact of temperature and loading on the mitigation of AMD in peat biofilter columns. Mine Water Environ. 27, 225–240.

Cornell, R.M. and Schwertmann, U., 2003. The iron oxides: Structure, properties, reactions, occurrences, and uses, second ed. Wiley-VCH GmbH&Co. KGaA, Weinheim (Germany), 694 p.

El Gheriany, I.A., Bocioaga, D., Hay, A.G., Ghiorse, W.C., Shuler, M.L., Lion, L.W., 2009. Iron requirement for Mn(II) oxidation by *Leptothrix discophora* SS-1, Appl. Environ. Microbiol. 75(5), 1229–1235.

Figueroa, L., Miller, A., Zaluski, M., Bless, D., 2007. Evaluation of a two-stage passive treatment approach for mining influenced waters. National Meeting of the American Society of Mining and Reclamation (ASMR), Gillette, WY, 30 Years of SMCRA and Beyond. June 2-7, Barnishel, R.I., Lexington, KY (USA), pp. 238–247.

Genty, T., Bussière, B., Potvin, R., Benzaazoua, M., Zagury, G.J., 2012a, Dissolution of calcitic marble and dolomitic rock in high iron concentrated acid mine drainage: Application to anoxic limestone drains, Environ. Earth. Sci. 66, 2387–2401.

Genty, T., Bussière, B., Potvin, R., Benzaazoua, M., Zagury, G.J., 2012b. Capacity of wood ash filters to remove iron from acid mine drainage: Assessment of retention mechanism, Mine Water Environ. 31 (4), 273–286.

Hedin, R., Weaver, T., Wolfe, N., Watzlaf, G., 2013. Effective passive treatment of coal mine drainage. In: Proc. of the 35th Annual National Association of Abandoned Mine Land Programs Conference, September 22-25, Daniels, WV (USA), 13p.

Huminicki, D.M.C. and Rimstidt, J.D., 2008. Neutralization of sulfuric acid solutions by calcite dissolution and the application to anoxic limestone drain design, Appl. Geochem. 23, 148–165.

Jennings, S.R. and Jacobs, J.A., 2014. Overview of acid drainage prediction and prevention, in: Jacobs, J.A., Lehr, J.H., Testa, S. M. (Eds), Acid mine drainage, rock drainage, and acid sulfate soils: Causes, assessment, prediction, prevention, and remediation. John Wiley & Sons, Inc., Hoboken, NJ (USA), pp. 205–215.

KTH, 2013. Visual MINTEQ, Version 3.0: A Window Version of MINTEQA2, available at: http://vminteq.lwr.kth.se/ (last access: 8 August 2015).

Lozano, A., Ayora, C., Macias, F., Nieto, J.M., Gomez-Arias, A., Castillo, J., Van Heerden, E., 2015. Sulphate removal from acid mine drainage: Evaluation of granular $BaCO_3$ with column experiments. Macla 20, 83–84.

Macías, F., Caraballo, M.A., Rötting, T.S., Péréz-López, R., Nieto, J.M., Ayora, C., 2012. From highly polluted Zn-rich acid mine drainage to nonmetallic waters: Implementation of multi-step alkaline treatment system to remediate metal pollution. Sci. Total Environ. 435, 323–350.

Maree, J.P., Du Plessis, P., Van der Walt, C.J., 1992. Treatment of acidic effluents with limestone instead of lime. Water Sci. Technol. 26 (1–2), 345–355.

Neculita, C.M. and Zagury, G.J., 2008. Biological treatment of highly contaminated acid mine drainage in batch reactors: Long-term treatment and reactive mixture characterization. J. Hazard. Mater. 157, 358–366.

Neculita, C.M., Zagury, G.J., Bussiere, B., 2008. Effectiveness of sulphate-reducing passive bioreactors for treating highly contaminated acid mine drainage: I. Effect of hydraulic retention time. Appl. Geochem. 23, 3442–3451.

Neuman, D.R., Brown, P.J., Jennings, S.R., 2014. Metals associated with acid rock drainage and their effect on fish health and ecosystems, in: Jacobs, J.A., Lehr J.H., Testa S.M. (Eds), Acid mine drainage, rock drainage, and acid sulfate soils: Causes, assessment, prediction, prevention, and remediation. John Wiley & Sons, Inc., Hoboken, NJ (USA), pp.139–169.

Nordstrom, K., Blowes, D.W., Ptacek, C.J., 2015. Hydrogeochemistry and microbiology of mine drainage: An update. Appl. Geochem. 57, 3–16.

Potgieter-Vermaak, S.S., Potgieter, J.H., Monama, P., Van Grieken, R., 2006. Comparison of limestone, dolomite and fly ash as pre-treatment agents for acid mine drainage, Miner. Eng. 19, 454–462.

Potts, P.J., 1987. A handbook of silicate rock analysis, Blakie & Son Ltd., 622p.

Rötting, T.S., Jordi C., Ayora, C., 2006. Use of caustic magnesia to remove cadmium, nickel, and cobalt from water in passive treatment systems: column experiments. Environ. Sci. Technol. 40, 6438–6443.

Rötting, T.S., Thomas, R.C., Ayora, C., Carrera, J., 2008a. Passive treatment of acid mine drainage with high metal concentrations using dispersed alkaline substrate. J. Environ. Qual. 37, 1741– 1751.

Rötting, T.S., Caraballo, M.A., Serrano, J.A., Ayora, C., Carrera, J., 2008b. Field application of calcite Dispersed Alkaline Substrate (calcite-DAS) for passive treatment of acid mine drainage with high Al and metal concentrations. Appl. Geochem. 23, 1660–1674.

Rose, A.W., Means, B., Shah, P.J., 2003. Methods for passive removal of manganese from acid mine drainage. In: Proc. of West Virginia Surface Mine Drainage Task Force Symposium, Morgantown, WV (USA), 11p.

Sahoo, P.K., Kim, K., Equeenuddin, Sk. Md., Powell, M.A., 2013. Current approaches for mitigating acid mine drainage. Whitacre, D.M., Bennett, E.R., Doerge, D.R. (Eds), In: Reviews of environmental contamination and toxicology, NY (USA), pp. 1–32.

Santomartino, S. and Webb, J.A., 2007. Estimating the longevity of limestone drains in treating acid mine drainage containing high concentrations of iron. Appl. Geochem. 2, 2344–2361.

Simón, M., Martín, F., García, I., Bouza, P., Dorronsoro, C., Aguilar, J., 2005. Interaction of limestone grains and acidic solutions from the oxidation of pyrite tailings. Environ. Pollut. 135 (1), 65–72.

Singh, N.B. and Middendorf, B., 2007. Calcium sulphate hemihydrate hydration leading to gypsum crystallization. Prog. Cryst. Growth Charact. Mater. 53, 57–77.

Sparks, D.L., 2003. Environmental soil chemistry, second ed. Academic Press, San Diego, CA (USA), 352p.

Strosnider, W.H.J., Nairn, R.W., Peer, R.A.M., Winfrey, B.K., 2013. Passive co-treatment of Zn-rich acid mine drainage and raw municipal wastewater. J. Geochem. Explor. 125, 110–116.

USEPA (United States Environmental Protection Agency), 2014. Reference Guide to Treatment Technologies for Mining-influenced Water. EPA 542-R-14-001, 94p.

Wolfe, N., Hedin, B., Weaver, T., 2010. Sustained treatment of AMD containing Al and Fe^{3+} with limestone aggregate. In: Proc. of the IMWA, September 5-9, Wolkersdorfer & Freund (Eds), Sydney, NS (Canada), pp. 29–32.

Younger, P.L., Banwart, S.A., Hedin, R.S., 2002. Passive treatment of polluted mine waters, in: Mine water: Hydrology, pollution, remediation. Kluwer Academic Publishers, Norwell, MA (USA), pp. 311– 393.

Ziemkiewicz, P.F., Skousen, J.G., Brant, D.T., Sterner, P.L., Lovett, R.J., 1997. Acid mine drainage treatment with armored limestone in open channels. J. Environ. Qual. 26(4), 1017–1024.

Zipper, C. and Skousen, J., 2014. Passive treatment of acid mine drainage, in: Jacobs, J.A., Lehr, J. H., Testa, S.M. (Eds), Acid mine drainage, rock drainage, and acid sulfate soils: Causes, Assessment, prediction, prevention, and remediation, John Wiley & Sons, Inc., Hoboken, NJ (USA), pp. 339–353.

CHAPITRE IV

COMPARATIVE COLUMN TESTING OF THREE REACTIVE MIXTURES FOR THE BIO-CHEMICAL TREATMENT OF IRON-RICH ACID MINE DRAINAGE[2]

Ce chapitre a été publié en juin 2017 dans la revue *Minerals Engineering* (Annexe E).

[2] Rakotonimaro, T.V., Neculita, C.M., Bussière, B., Zagury, G.J., 2017. Comparative column testing of three reactive mixtures for the bio-chemical treatment of iron-rich acid mine drainage. *Minerals Engineering* 111: 79–89.

4.1 Résumé

L'optimisation des propriétés hydrauliques des mélanges réactifs dans les systèmes passifs peut améliorer l'efficacité de traitement du drainage minier acide (DMA) ferrifère. L'utilisation des mélanges de type substrat alcalin dispersé (SAD) pourrait limiter les problèmes de colmatage et d'écoulement. L'efficacité et l'évolution de la conductivité hydraulique (k_{sat}) de trois mélanges réactifs (deux de types SAD, composé de cendres de bois [50% v/v-CB50] ou de calcite [20% v/v-C20], et un troisième principalement utilisé dans les réacteurs passifs biochimiques (RPB) constitué de matières organiques [70% p/p], ont été testés dans des colonnes de 1,5 L. Les réacteurs étaient exploités avec 1 à 5 j de temps de résidence hydraulique (TRH), sur une période de 16–63 jours. Dans les réacteurs CB-SAD, les résultats ont montré qu'un TRH minimum de 2 j était nécessaire pour enlever 33–62% de Fe dans le DMA avec 2500 mg/L de Fe. Les réacteurs calcite-SAD ont montré une efficacité limitée d'enlèvement du Fe (<10%) dans le DMA à plus de 1500 mg/L de Fe, mais était d'environ 40% à moins de 1500 mg/L de Fe, sur une période de 7 j, à 2 j de TRH. Une légère augmentation de l'efficacité du RPB (77% et 91%) a été observée, pour une concentration initiale de 500 mg/L de Fe, lorsque le TRH a été doublé (2,5 j à 5 j). Tous les réacteurs ont enlevé d'autres métaux (37–99,9% pour l'Al, le Zn et le Pb, 20 à 98% pour le Ni, sauf dans C20) et de SO_4^{2-} (5–37%) dans le DMA. L'évolution des paramètres hydrauliques de tous les réacteurs a montré une faible variation de la porosité initiale de 0,68–0,74 et de k_{sat} de l'ordre de 10^{-2} cm/s, indiquant aucun signe de colmatage tout au long de la période d'essai, même à 5 j de TRH. Néanmoins, l'enlèvement de Fe était dépendant du TRH. Par conséquent, la qualité de l'eau, en particulier la concentration en Fe, devrait figurer parmi les critères de design pour la construction d'un traitement passif satisfaisant, à long terme, du DMA ferrifère.

4.2 Abstract

Optimization of the hydraulic properties of reactive mixtures in passive systems can improve treatment efficiency of iron-rich acid mine drainage (Fe-rich AMD). The use of highly permeable and porous substrates could limit clogging and flow-related issues. The efficiency and evolution of hydraulic conductivity (k_{sat}) of three reactive mixtures – two types of dispersed alkaline substrate (DAS), composed of wood ash (50% v/v - WA50) or calcite (20% v/v - C20), and one mixture consisting mainly of organic matter (70% w/w), typically used in passive biochemical reactors (PBRs) – were tested in 1.5 L columns.

The reactors were operated with hydraulic retention times (HRTs) of 1 to 5 d over a period of 16–63 days. In the WA-DAS reactors, results showed that a minimum HRT of 2 d was required to remove 33–62% of Fe in AMD with 2500 mg/L Fe. The calcite-DAS showed limited Fe removal (<10%) in AMD at >1500 mg/L Fe, but was around 40% at <1500 mg/L Fe, over a 7-day period, at 2 d of HRT. Slight increase of the PBRs efficiency was found (77% and 91%), at initial Fe concentration of 500 mg/L, when the HRT was doubled (from 2.5 d to 5 d). All reactors removed other metals (37–99.9% for Al, Zn, and Pb; 20–98% for Ni, except in C20) and SO_4^{2-} (5–37%). Evolution of the hydraulic parameters of all reactors showed insignificant variation of the initial porosity of 0.68–0.74 and k_{sat} around 10^{-2} cm/s, indicating no evidence of clogging throughout the testing period, even at 5 d of HRT. Nonetheless, Fe removal was HRT-dependent. Therefore, water quality, especially Fe concentration, should be among the design criteria for a long-term satisfactory treatment of Fe-rich AMD.

Keywords: Ferriferous acid mine drainage, iron pretreatment, dispersed alkaline substrate, passive biochemical reactor, hydraulic retention time

4.3 Introduction

Besides the variable content in bivalent heavy metals, metalloids (often As), and sulfate (SO_4^{2-}), acid mine drainage (AMD) can contain high concentrations of trivalent acidogenic elements, such as Fe and Al. Iron is the most common and often the predominant metal in AMD because it originates from sulfide minerals, such as the ubiquitous pyrite. The oxidation of Fe in AMD occurs as shown in Eq. 4.1 (Nordstrom and Alpers, 1999).

$$FeS_{2\,(s)} + 7/2\ O_{2\,(g)} + H_2O \rightarrow Fe^{2+}{}_{(aq)} + 2\ SO_4^{2-}{}_{(aq)} + 2\ H^{+}{}_{(aq)} \qquad (4.1)$$

The Fe-rich AMD is frequently encountered at closed and abandoned mine sites and must be treated to avoid significant environmental impacts to the surrounding ecosystems (Gazea et al., 1996; Diz et al., 1999; Genty et al., 2016). The use of passive treatment is prioritized for such mine sites because of its low cost and little maintenance requirements relative to active treatment (Johnson and Hallberg, 2005a; USEPA, 2014a). The treatment of Fe-rich AMD is particularly challenging because Fe removal is limited by the kinetics of Fe(II) to Fe(III) oxidation and subsequent hydrolysis, with consequences such as pH decrease, alkalinity exhaustion, and oxydoreduction potential (ORP) increase (Kirby et al., 1999; Neculita et al., 2008a). In addition, the rate of Fe(III) oxides/oxyhydroxides formation could be accelerated at higher pH (>4) and may lead to rapid clogging and armoring, as well as changes in the hydraulic properties of the treatment system itself (Rötting et al., 2008a; Neculita et al., 2008a; Zipper et al., 2011; Orakwue et al., 2016). Such a situation was encountered at the abandoned Lorraine mine site (Quebec, Canada), where a three-step treatment system (composed of two passive biochemical reactors [PBRs], separated by one unit of wood ash) was constructed for the treatment of Fe-rich AMD (Genty et al., 2016).

The composition of reactive mixtures used in passive systems influences the overall treatment performance. Generally, the components of mixtures are low-cost neutralizing agents and bio-wastes (Zipper and Skousen, 2014; USEPA, 2014a;

Skousen et al., 2017). Limestone/calcite are widely employed in conventional passive treatment (e.g., PBR/anoxic limestone drain), but they are not recommended to treat highly acidic Fe-rich waters because their efficiency is significantly limited by the high Fe content (Maree et al., 1992; Potgieter-Vermaak et al., 2006), and they are subjected to coating/armoring by Fe(III) oxides/oxyhydroxides minerals (Hammarstrom et al., 2003; Zipper et al., 2011). Different options were attempted to address this issue: 1) the use of alkaline materials with a slower reactivity and less Ca^{2+} release (i.e., dolomite) to retard the clogging by gypsum (Huminicki and Rimstidt, 2008; Genty et al., 2012a; Kagambega et al., 2014); 2) the use of alkaline materials capable of increasing the pH over 8.5 (e.g., MgO, wood ash) to remove simultaneously divalent and trivalent metals (Rötting et al., 2006; Genty et al., 2012b); and 3) a combination of the neutralizing agents listed above with coarse and highly porous materials (e.g., wood chips) also called dispersed alkaline substrate (DAS) to improve hydraulic properties and avoid clogging (Rötting et al., 2008a; Ayora et al., 2013).

Mixtures used in PBRs are composed of a substrate (source of electrons, organic carbon, and nutrients for microorganisms), an inoculum of sulfate-reducing bacteria (SRB), a solid support (structural agents) for microbial attachment and porosity-permeability improvement, and a neutralizing agent for pH and alkalinity increase to prevent bacterial shock in the early start-up (Cocos et al., 2002). Previous work was essentially based on the study of substrate sustainability, efficiency, and permeability (Waybrant et al., 1998; Gibert et al., 2004; Neculita et al., 2007; Vasquez et al., 2016a). Mixed biodegradable materials were more efficient substrates for anaerobic bacteria compared to individual ones (Johnson and Hallberg, 2005a; Zagury et al., 2006). The efficiency of the PBRs is mainly based on their ability to remove SO_4^{2-}, of which final concentrations vary according to the mixture components and proportions, as well as water quality (Johnson and Hallberg, 2005b; Neculita et al., 2007; Skousen et al., 2017). In addition, Fe removal is limited when influent water contains more than 500 mg Fe/L (Neculita et al., 2008a). The porosity of mixtures usually ranges between

0.34–0.53 (Neculita et al., 2008a; Vasquez et al., 2016b), while saturated hydraulic conductivity (k_{sat}) is 10^{-4}–10^{-2} cm/s and can decrease to as low as 10^{-9} cm/s due to changes in substrate properties caused by suspended solids from AMD, secondary precipitates (oxides/oxyhydroxides, carbonate, and sulfide minerals), biomass and metabolic products generated by bacterial activity (URS, 2003; Neculita et al., 2008a). At the same time, existing research emphasizes the use of DAS mixtures because their efficiency in Fe removal ranges from 20–99.9%, depending on their type (calcite, dolomite, wood ash, or MgO) and the water quality (Caraballo et al., 2009, 2011; Rakotonimaro et al., 2016). Moreover, calcite-DAS and MgO-DAS present better hydraulic properties with porosity of 0.62–0.76 (Rötting et al., 2007; Caraballo et al., 2010) and k_{sat} of 10^{-3}–10^{0} cm/s, with less decrease (down to 10^{-3} cm/s) because of the grains dissolution which increases specific surface (Ss) to allocate metal precipitates, depending on the hydraulic residence time (HRT) (Caraballo et al., 2010; Ayora et al., 2013).

Based on such knowledge, research on the passive treatment of Fe-rich AMD that is frequently encountered at coal and base metal mine sites often recommends the design of materials/mixtures that achieve satisfactory efficiency in removing Fe, other metals/metalloids (if present), and SO_4^{2-} while preserving enough permeability to accommodate input flow. However, uncertainty about SO_4^{2-} removal using only DAS units has generally led to an additional well-known SO_4^{2-} treatment reactor—namely, PBRs.

Thus, the present work aims to comparatively evaluate the efficiency and hydraulic performance of two reactive mixtures used in DAS systems for Fe pre-treatment, as well as a third reactive mixture used in PBR for SO_4^{2-} removal.

4.4 Materials and methods

4.4.1 Column design, set-up, and operating conditions

The DAS experiments were performed with six 1.5 L columns (height 22 cm, inner diameter 10 cm) equipped with perforated drainpipes placed at the bottom (as inlet) and on top (as outlet) (Fig. B1A). Four reactors were filled with WA50 [50% v/v wood ash, and 50% v/v wood chips] and operated at four different HRTs: 1 d (WA50-1), 2 d (WA50-2), 3 d (WA50-3), and 5 d (WA50-5). Each reactor was in operation for a 30-day period. Two other column reactors were used to evaluate the efficiency of C20 [20% (v/v) calcite and 80% (v/v) wood chips], at two HRTs of 1 d (C20-1) and 2 d (C20-2), for 16 days. Previous batch testing showed that the calcite-DAS had maximal efficiency only in a very short time (Rakotonimaro et al., 2016). These two types of DAS mixtures (WA50 and C20) were fully characterized prior their use to pre-treat Fe-rich AMD during batch testing (Rakotonimaro et al., 2016), while their efficiency and hydraulic performance was evaluated in continuous flow reactors. In each reactor, glass bead layers and fine-mesh geotextiles (1.66 cm) compressed and sealed off the mixtures at the top and bottom, prior to their covering. Artificial AMD (Table 4.1) was prepared (weekly/biweekly) in 20 L buckets and fed by peristaltic pumps in upward flow to the columns. This design allows uniform distribution of influent since downward and/or horizontal flow could favor early clogging and preferential flow (Neculita et al., 2007). Notably, the synthetic effluents simulate the typical quality of AMD from hard rock mines in Canada (Aubertin et al., 2002).

Table 4.1 Quality of Fe-rich AMD used in column type DAS reactors and PBRs

Parameters	Concentration (mg/L, except for pH)	Source
Al^{3+}	1.6±0.6	$Al_2(SO_4)_3 \cdot 18H_2O$
Fe^{2+}	2500±171 (DAS)	$FeSO_4 \cdot 7H_2O$
Fe^{2+}	500±33 (PBRs)	$FeSO_4 \cdot 7H_2O$
Mg^{2+}	33.5±3.8	$MgSO_4 \cdot 7H_2O$
Mn^{2+}	8.2±1.0	$MnSO_4 \cdot H_2O$
Ni^{2+}	0.7±0.4	$NiSO_4 \cdot 6H_2O$
Pb^{2+}	0.2±0.1	$Pb(NO_3)_2$
Zn^{2+}	0.2±3.0	$ZnSO_4 \cdot 7H_2O$
Ca^{2+}	430±5	$CaSO_4 \cdot 2H_2O$
SO_4^{2-}	5395±988	Na[1]
pH	3–4	Na

[1] Na- Not applicable; PBR- Passive biochemical reactors

Two columns having the same size as the DAS reactors, but equipped with a gas chamber, were used as PBRs (Fig. B1B). They were filled with reactive mixtures consisting of 70% (w/w, dry weight) organic materials (40% wood chips, 20% chicken manure, 10% leaf compost), and 30% (w/w) inorganic materials (10% sand and 20% calcium carbonate). The set-up was thereafter similar to that of DAS columns, where the mixture was slightly compressed between two layers of glass beads and geotextile at the top and bottom of the reactors, prior to their covering. After the set-up, the reactors were saturated with a Postgate B medium, prepared in distilled water, with the following composition: 3.5 g/L sodium lactate (or 4.7 mL lactate liquid 56.8%); 2.0 g/L $MgSO_4 \cdot 7H_2O$; 1.0 g/L NH_4Cl; 1.27 g/L $CaSO_4 \cdot 2H_2O$; 1.0 g/L yeast extract; 0.5 g/L KH_2PO_4; 0.5 g/L $FeSO_4 \cdot 7H_2O$; 0.1 g/L thioglycolic acid, and 0.1 g/L ascorbic acid (Postgate, 1984). Then, the columns were incubated for 3 to 4 weeks (acclimation period) before starting the continuous flow. This acclimation period allowed SRB to grow and produce enough sulfides and alkalinity to treat the initial input of AMD (Waybrant et al., 2002; Neculita et al., 2008a). Calibrated Masterflex-peristaltic pumps

were used to feed in upward flow the AMD in the PBRs. Each PBR was operated for a 63-day period, at 2.5 d (R2.5) and 5 d (R5) of HRT.

4.4.2 Hydraulic parameters monitoring

Drainpipes were equipped with manometers placed at 3.5 cm and 7.5 cm (Fig. B1A, B1B) to measure the pore water gradient and k_{sat} according to the HRT of each column during the entire operating period. Initial k_{sat} was determined using rigid wall permeameter and the constant-head method as per norm D2434 (ASTM, 1995). During the operation, the k_{sat} was determined weekly (in DAS reactors) and biweekly (in PBRs) by temporarily raising the flow rate to increase the head-loss across the column and to obtain measurable values. The piezometric head differences between adjacent ports were then read. The k_{sat} (cm/s) in the depth interval between two pressure ports was calculated using Darcy's Law:

$$k_{sat} = Q.L/\ A.\Delta h \qquad (4.1)$$

where Q (mL/s) is flow rate, A (cm^2) is the reactor cross section, L and Δh (cm) are distance and head-loss between pressure ports, respectively.

The porosity of the reactors was measured gravimetrically by saturating the column with water while filled with fresh (before set-up) and spent mixtures (at the end of the experiment).

4.4.3 Physicochemical, microbiological and geochemical modeling

The effluent quality was monitored until the steady state was reached in each column by measuring weekly the pH, oxidation-reduction (redox) potential (ORP), electrical conductivity (EC), and dissolved oxygen (DO), as well as alkalinity, acidity, total iron (Fe_t), ferrous iron (Fe^{2+}), and SO_4^{2-} concentrations. Water pH was measured with an electrode Orion 3 Star Thermo (GENEQ Inc.), while the EC was measured with a

HACH Sension 1 electrode. The ORP was determined with a potentiometer (Sension1 POR HACH 51939-00) coupled with an internal Pt/Ag/AgCl electrode. The DO was measured using a LDO10103-Hach HQ30d probe, calibrated with air-saturated water. Alkalinity and acidity were determined with a Metrohm Binkmann, 716 DMS Trinitro titrator (APHA, 2012). The concentrations of Fe_t, Fe^{2+}, and SO_4^{2-} were analyzed on filtered samples (0.45 μm) in the first 1–2 h after collection with pre-calibrated and standardized DR/890 HACH colorimeter (Method 8008 – 1, 10 phenanthroline, Method 8146 – 1, 10 phenanthroline, and Method 8051 – barium chloride powder pillows for Fe_t, Fe^{2+}, and SO_4^{2-}, respectively). The filtering through 0.45 μm pore size membrane was performed to remove particulates (total suspended solids) before analyzing water for total metal (e.g., Fe_t) concentrations. Moreover, HACH standard method for Fe_t analysis recommends the use of 0.45 (47 mm) of filter pore size (HACH, 2013). This specific method of analysis was selected for its rapidity. In addition, a comparative analysis to ICP-AES showed a difference in concentration <4.2%. The analysis was performed weekly, and relative efficiency r (%) was calculated following equation:

$$r = [(C_x - C_{x+7})/ C_x] \times 100 \qquad (4.2)$$

where C_x and C_{x+7} are concentrations (mg/L) at time (x) and (x+7) d.

Metal concentrations (in liquid phase) such as Al, Mn, Ni, Pb, and Zn were analyzed by ICP-AES, on filtered (0.45 μm) and acidified (with 2% v/v of nitric acid) samples only at the beginning and the end of the experiments. In addition, dissolved organic carbon (DOC) was determined at 680°C using a TOC analyzer (SHIMAZU, model TOC-Vcph).

Microbial counts (SRB and iron-reducing bacteria [IRB]) in non-filtered effluent from PBRs were performed at the beginning, during the steady state, and at the end of the test by using the most probable number (MPN) method (ASTM, 1990; Cochran, 1950). Tubes (5 replicates per dilution) were inoculated and incubated at 30°C for 21 d under anaerobic conditions for SRB counting. The SRB growth was indicated by the presence

of black FeS precipitate (Postgate, 1984). When the presence of black precipitate was not obvious, samples were verified using $FeCl_3$/HCl and p-aminodimethylaniline dihydrochloride/HCl (ASTM, 1990). For IRB enumeration, 1 mL of liquid was added to each of 5 replicate serum glass tubes (each tube contains 9 mL of culture medium, prepared in an anaerobic glove box). The inoculated serum tubes were then diluted tenfold using 1 mL syringes into another series of 5 serum tubes and repeated until there were 10 to 12 serial dilutions. Inoculated and diluted tubes were incubated for 28 d at 25°C in an anaerobic chamber and enumerated. To verify iron reduction, 0.2 mL of ferrozine reagent was injected into each serum tube; the development of a purple color indicated a positive result (Gould et al., 2003).

Saturation indices (SI) of the principal minerals inclined to precipitate were calculated using the code PHREEQC, version 3.35.00 (USGS, 2015). The simulation was run using the initial effluent quality, the one collected during steady state and the one at the end of the experiments. The redox potential (pe) was used to determine the distribution of the element among its oxidation states.

4.4.4 Post-testing mineralogical characterization

Samples were collected from the DAS reactor and PBR operated at 3 and 5 d of HRT, respectively, at the end of their operation. This sampling strategy was performed in order to optimize the observation of mineral phases, which might not be emphasized in columns operated at less than 2 d of HRT. The spent reactive mixtures were recovered from the first 10 cm layer at the bottom (0–10 cm) and the last 5 cm layer at the top (15–20 cm) of the columns, dried at 40°C for 48 h, and metallized. Afterward, the microstructure and mineralogy were observed with a scanning electron microscope equipped with probe Energy Dispersive X-ray Spectroscopy (SEM-EDS), HITACHI S-3500N (voltage of 20 kV, amperage of 140 A, pressure around 25 kPa, and work distance of 15 mm). Images, element maps, and chemical composition were recorded with a data processor INCA (Oxford Energy 450).

4.5 Results and discussion

The DAS reactors and PBRs had distinctive performances. The DAS reactors reached different steady states depending on HRTs, while the PBRs presented consistent efficiency until the end of the testing.

4.5.1 Iron and sulfate removal

4.5.1.1 Efficiency of the DAS reactors

Although the performance of the WA-DAS reactors showed a similar trend (gradual decrease), a significant difference was noted according to the tested HRTs. The efficiency seemed defined and delimited by the breakthrough time (where efficiency started to decline or remained stable). The highest efficiency occurred only during the first 2 days in WA50-1 and 4 days in WA50-2, whereas it lasted 12 days in WA50-3 and 16 days in WA50-5. Nonetheless, WA50-1 and WA50-2 continued to remove metals, albeit at a lower rate, until their breakthrough time, i.e., days 12 and 26, respectively. This elapsed time is considered as the steady state period for these first two reactors. On the other hand, the WA50-3 and WA50-5 maintained their effectiveness until the end of the experiment, on day 30.

During the highest peak performance, the pH increased in all reactors, from 3.83±0.19 up to 8.33±0.13 (Fig. 4.1). Thereafter, the pH dropped and remained stable at around 5.33±0.39 in WA50-1, 5.40±0.51 in WA50-2, 5.95±0.89 in WA50-3, and 6.28±0.98 in WA50-5, until the end of the experiment. The lower pH in WA50-1 and WA50-2 could be explained by the short contact time, which did not properly allow the acidic water to be neutralized. Albeit, these pH values give the advantage to the WA-DAS to be used in a pre-treatment or in a final polishing unit before a PBR, which requires an optimal pH range of 5–8 (Willow and Cohen, 2003). On the contrary, MgO-DAS and

wood ash (100%) can raise water pH between 8.5–10 and up to 11, respectively, which need to be corrected (Genty et al., 2012b; Ayora et al., 2013).

The ORP decreased from +254 mV to an average of +31mV (Fig. 4.1), which was comparable to previous studies; such values were considered as a reducing environment in full-scale experiment (Caraballo et al., 2011; Macías et al., 2012).

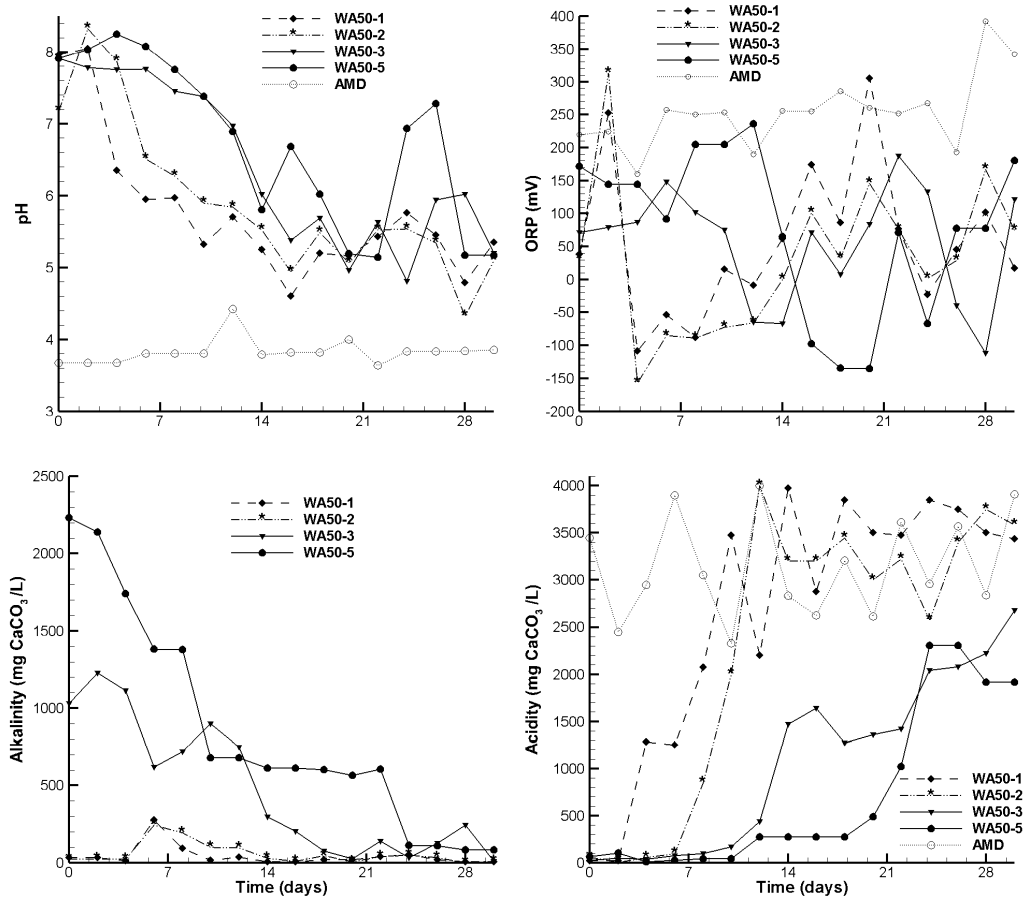

Figure 4.1 Evolution of the physicochemical parameters of the WA-DAS reactors during column testing

Moreover, the high EC value (6.12 mS/cm), which was maintained until the end of the experiment, was probably due to the total dissolved solid originating from the mixtures in addition to AMD load. The decomposition of organic materials could have

contributed to the DO decrease from 7.20±0.88 mg/L to 3.21±0.23 mg/L. During the entire operation time, the alkalinity in the reactors operated at less than 2 d of HRT was 2 to 5 times higher than in those run for more than 2 d (43–66 mg/L as $CaCO_3$ *vs* 128–346 mg/L as $CaCO_3$, respectively) (Fig. 4.1). Alkalinity in WA50-5 was 1.6 to 4 times higher than previously reported (Genty et al., 2012b) where columns were filled with wood ash (#1) or wood ash mixed with sand (#4, #5), with values of 53–80 mg/L as $CaCO_3$ (Table B1). Accordingly, 62% of acidity was neutralized (Fig. 4.1). The WA50-1 and WA50-2 failed to neutralize acidity, which means that using WA-DAS mixture might not be appropriate to treat *in situ* contaminated water with high inflow rate, as leaching of the alkaline component could take place.

Regarding Fe removal (Fe_t and Fe^{2+}), a maximal efficiency of >99.9% was noted only during the optimal efficiency period in all reactors (Fig. 4.2). Thereafter, each reactor performed differently until their breakthrough time (steady state phase) or until the end of the experiment. Indeed, the effectiveness of WA50-1 to remove Fe_t decreased to an average of 12.4% (day 2–12) and to 36.1% in WA50-2 (day 4–26) before reaching the initial concentration. This deterioration was assumed to be triggered by the insufficient contact time between the reactive mixture and the contaminated water, as well as the depletion of alkaline materials necessary to buffer the acidity, particularly in WA50-1. In WA50-3 and WA50-5, Fe_t removal continued after their optimal performance period until the end of the experiment, with respectively 44% (day 12–30) and 62% (day 16–30). The performance of WA50-5 could last longer due to Fe removal mechanisms, which would not only be precipitation and sorption, but also through filtration of nanoparticles Fe(III) that could be retained on the surface of wood chips. Similar phenomenon has been reported during pre-treatment of AMD with 95 mg Fe/L *via* vertical flow reactor composed of siliceous gravel with an average removal of 65% (Florence et al., 2015). Moreover, Fe^{2+} concentration decreased to 40–61% in all reactors (Fig. 4.2). The removal mechanism is usually by precipitation but microbial oxidation would be possible.

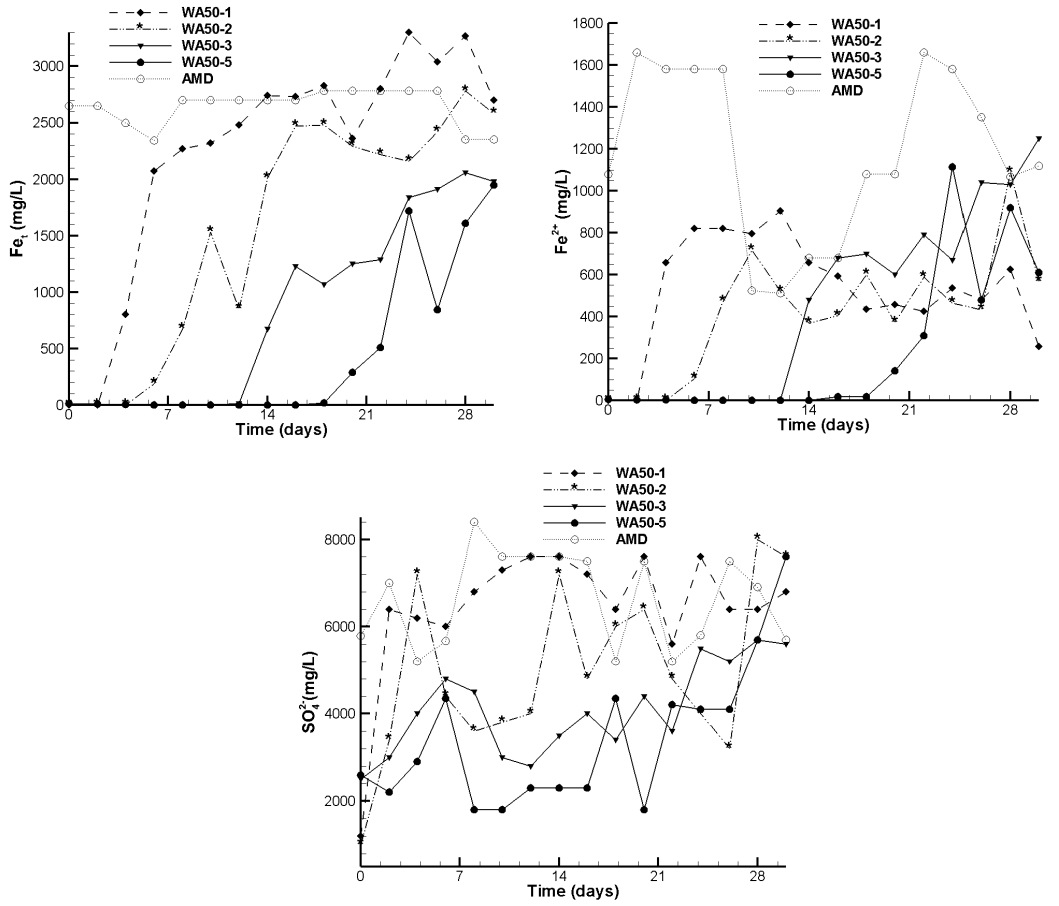

Figure 4.2 Evolution of concentrations of Fe_t, Fe^{2+} and SO_4^{2-} in the WA-DAS reactors during column testing

The SO_4^{2-} removal was <8% in WA50-1, 23% in WA50-2, and around 35% in WA50-3 and WA50-5 (Fig. 4.2). Results showed that the efficiency of the reactors was strongly HRT-dependent. The lower the HRT, the more limited the reactor's performance. Therefore, 2 d of HRT seem the minimum required criteria to efficiently treat AMD with Fe >1500 mg/L and $SO_4^{2-} \geq 5000$ mg/L.

Notably, the reactor with 3 d HRT remained in operation after the 30 days of testing to test whether increasing the HRT to 4 d would entail a performance increase, but similar results (not shown here) were obtained.

The two calcite-DAS columns (operated at 1 and 2 d of HRT) filled with C20 mixture showed comparable efficiency. The pH rose to 6–7 only at the beginning of the operation, and then remained stable to around 5±0.20 until the end of the testing (Fig. B2). An ORP of around +150 mV in all reactors suggests an oxidizing environment. The C20-1 generated 3 times lower of alkalinity relative to C20-2, with on average of 16±23 mg/L as $CaCO_3$ *vs* 50±17 mg/L as $CaCO_3$, respectively (Fig. B2). Consistently, 18% of acidity was neutralized in C20-1 while 47% was neutralized in C20-2 (Fig. B2). Coupled with the acidity neutralization and generation of alkalinity, about 47% of Fe_t was removed in C20-1 and 73% in C20-2 only during the first 7 d (Fig. B2). Then, the efficiency of both reactors dropped to less than 10% until the end of the experiment. The Fe^{2+} removal was lower than 10% in C20-1, whereas it was maintained around 47% in C20-2 during the entire testing period (Fig. B2). The SO_4^{2-} removal was <5% in C20-1, while it was around 38% during the first 8 days of the treatment in C20-2 before decreasing to the same rate as in C20-1 (Fig. B2). Previous work using calcite-DAS to treat AMD with SO_4^{2-} concentration around 3500 mg/L, found removal around 9% (Rötting et al., 2008a). These findings suggest that DAS composed of 20–25% calcite could be used as a pre-treatment unit, before a PBR treatment, only for acidic water with Fe <1500 mg/L and SO_4^{2-} <3500 mg/L at a minimum HRT of 2 d.

4.5.1.1 Efficiency of the PBRs

In general, R5 had slightly higher efficiency than R2.5. Once the AMD was fed after the acclimation period, black precipitates were observed at the outlet of the PBRs, which indicated the formation of sulfide minerals as a result of SRB activity. This is consistent with the significant SRB counting (around 10^7 cells/100 mL in R2.5 and R5) in water collected right after the feeding of the columns with AMD. Moreover, the low values of ORP, as low as –274 mV at the beginning of the experiment, indicate favorable conditions for their growth. Hence, the pH rose from the initial value of 4.11±0.24 to 6.56±0.46 in R5 and 6.15±0.51 in R2.5 (Fig. 4.3).

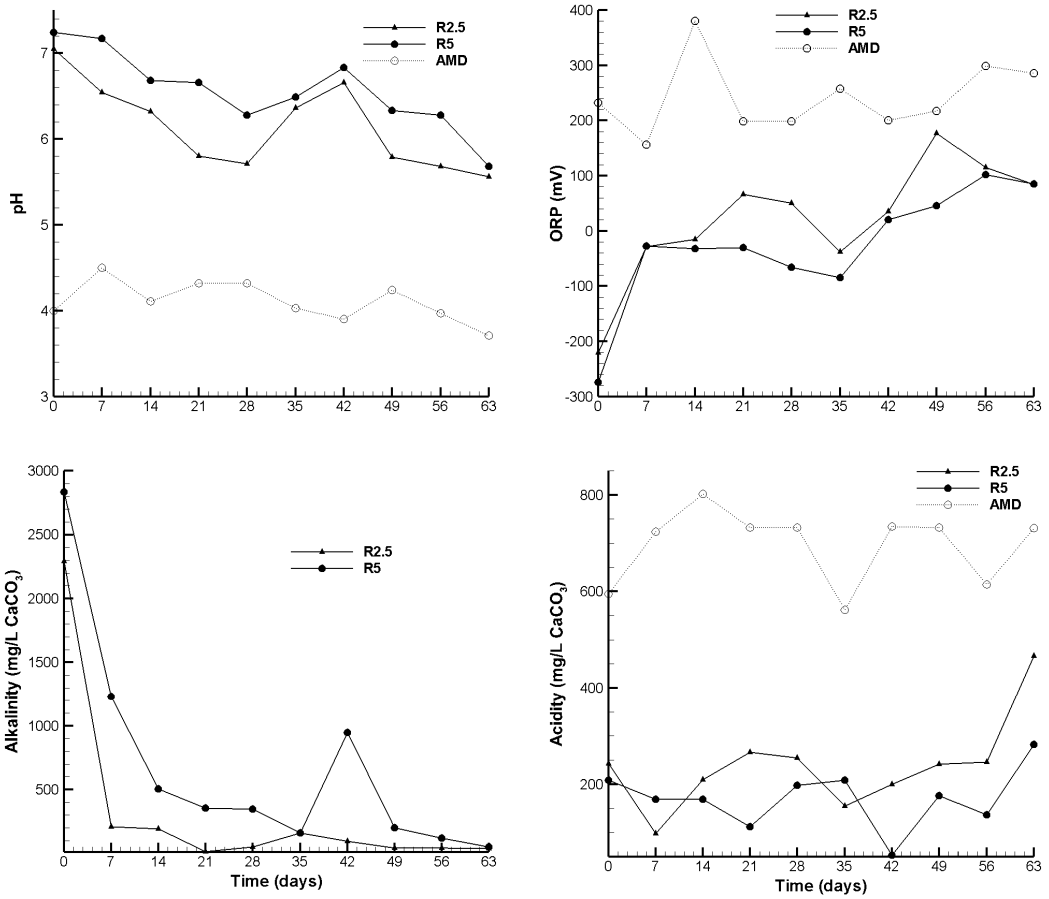

Figure 4.3 Evolution of pH, ORP, alkalinity, and acidity in the PBRs during column testing

The low DOC/SO_4^{2-} ratio at the beginning of the operation (around 0.4) would promote sulfidogenesis (Dar et al., 2008; Prasad and Henry, 2009), but the optimal value of this ratio can vary according to the type of used substrates (Neculita et al., 2007; Dar et al., 2008; Deng et al., 2016). Consequently, high SO_4^{2-} removal of around 91% in both PBRs was achieved before the first 7 days (Fig. 4.4). In addition, the alkalinity increased up to 2833 mg/L as $CaCO_3$ in R5, and 2293 mg/L as $CaCO_3$ in R2.5 (Fig. 4.3).

Thereafter, the ORP, which increased up to +177 mV after 7 days of operation (Fig. 4.3), had a visible impact on the "culturable SRB" by decreasing their number (10^5 cells/100 mL) in both PBRs. Even though the alkalinity also dropped significantly, it remained almost 5 times higher in R5 (435±288 mg/L as $CaCO_3$) than in R2.5 (90±64 mg/L as $CaCO_3$). At the same time, 76% of acidity was neutralized in R5 and 66% in R2.5 (Fig. 4.3).

The SO_4^{2-} concentrations remained high after 7 days (Fig. 4.4). Previously, it was reported that SO_4^{2-} reduction was absent or inhibited in the presence of high concentration of Fe(III) oxides/hydroxides, in anaerobic condition, until Fe(III) depletion (Chapelle and Lovley, 1992; Chapelle et al., 2009). This may explain the lowest, if not the absence, of SO_4^{2-} removal after 7 days, particularly in R2.5 where SO_4^{2-} removal dropped to <5% in R2.5 and around 13.5% in R5 (Fig. 4.4). The deterioration could also be due to the decrease of DOC/SO_4^{2-} ratio (0.003–0.01), since it was reported to be the limiting factor for supporting active biomass of SRB (Neculita and Zagury, 2008; Deng et al., 2016). In which case, SRB would be competing with other microbial communities, such as IRB. Indeed, it was found that if sufficient Fe(III) is available, IRB can outcompete the SRB and can even hinder the latter to metabolize available carbon sources; thus, SO_4^{2-} reduction was inhibited up to 86–100% (Lovley and Philipps, 1987; Deng et al., 2016). In the present study, SRB and IRB counts were comparable (Fig. 4.4).

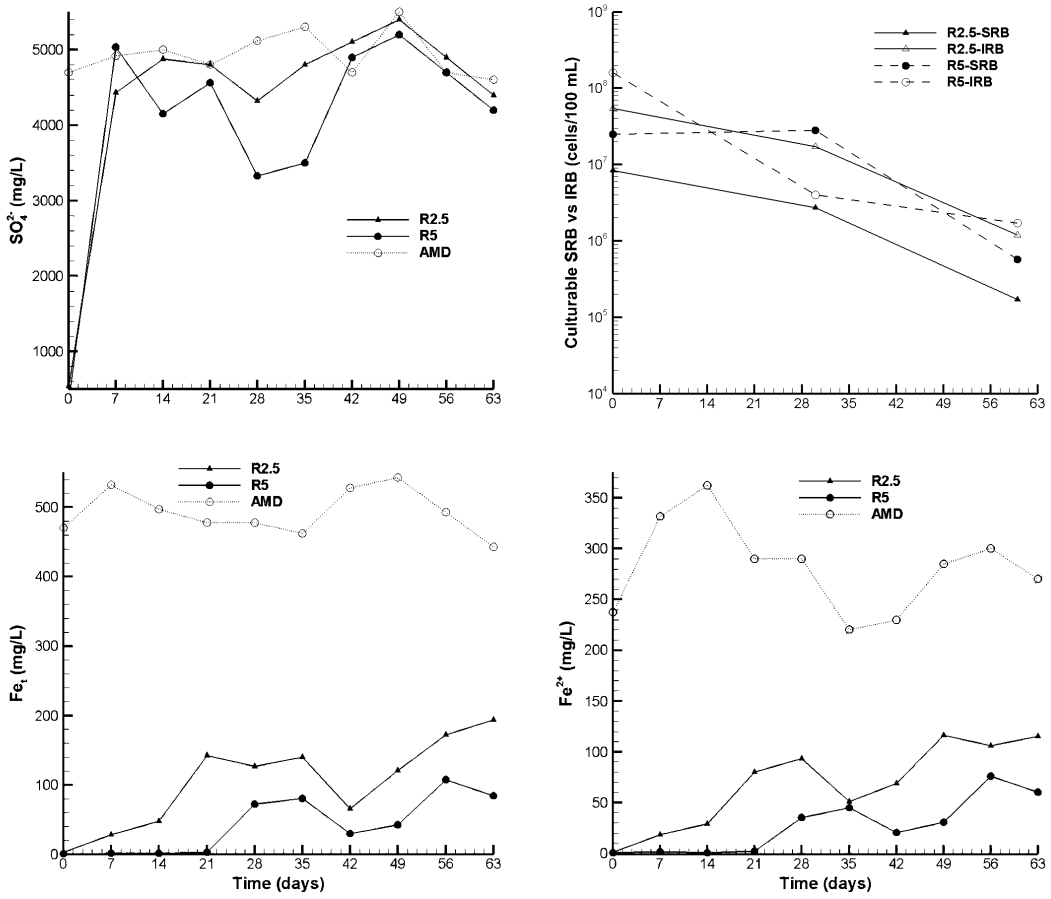

Figure 4.4 Evolution of the concentrations of Fe_t, Fe^{2+} and SO_4^{2-} as well as counting of culturable SRB and IRB from effluent collected in the R2.5 and R5 during column testing

The SRB was reported to be less active than IRB at high Fe concentrations (Lovley and Philipps, 1987; Chapelle and Lovley, 1992). These findings may explain the better removal of Fe_t, which was on average 77% (115±57 mg/L) in R2.5, and 91% (47±41 mg/L) in R5 (Fig. 4.4). The trends of Fe^{2+} and Fe_t evolution were similar, with a Fe^{2+} removal rate of 84% in R5, and 67% in R2.5 (Fig. 4.4). Iron reduction is seemingly important in R2.5 and R5 in the view of Fe^{2+} concentrations relative to Fe^{3+} and the DO (Fig. B3). The ratio of Fe^{3+}/Fe^{2+} in R.2.5 and R5 was also comparable (0.68 and 0.63, respectively).

The overall Fe removal found in this study was higher relative to previous studies that used the same components but in different proportions in typical mixtures used in PBRs, with reported efficiency of 84% *vs* 66% during laboratory testing (Genty, 2012). Given the fact that the influent concentration was not similar (1000–2000 mg/L *vs* 500 mg/L in the previous studies and the present one, respectively), Fe pre-treatment could therefore improve the performance of a PBR. However, the residual Fe concentration was still high, whereas the objective is to lower the concentration to less than 3 mg/L (USEPA, 2014b). Effluents from the R2.5 and R5 were then exposed to open air to oxidize the Fe^{2+} into Fe^{3+}, which would hydrolyze and precipitate. Results showed that only 7% of Fe was removed in R2.5 outflow, whereas up to 37% was removed from R5. It is assumed that the produced alkalinity from R2.5 (34 mg/L as $CaCO_3$) was insufficient to buffer the acidity (360 mg/L as $CaCO_3$) generated from Fe^{3+} precipitation. In addition, too short exposure of treated effluent to air along the cascade (≈ 40 cm) probably limited Fe^{2+} oxidation. Previous studies showed that a multi-cascade aeration at a higher altitude could remove 88% of Fe with initial concentration of 27.5 mg/L (Oh et al., 2015; 2016). Therefore, natural oxidation (multi-step cascade) of PBR effluent could be efficient only if Fe <25 mg/L.

4.5.2 Other metals removal

Up to 99% of Al and 95% of Zn concentrations were removed in all tested reactors (WA-DAS, calcite-DAS, and PBRs), whereas the Mn concentration increased in the treated effluent (10–50%). The additional Mn concentration could be the result of the dissolution of solid Mn bearing minerals (formed during the initial period, upon the starting-up) or from the substrate itself, consistent with previous findings (Zagury et al., 2006; Song et al., 2012). However, given the high pH (>8) in the WA-DAS reactors just after the start of the operation, probable partial removal of Mn could occur. Additionally, 37% of Pb was removed in WA50-1 and WA50-2, 72% in WA50-3, 53% in WA50-5, and >99.9% in the R2.5 and R5. Ni concentration was lowered by 20%

and 98% in WA50-3 and WA50-5, respectively, and >90% in the two PBRs, while it did not decrease in WA50-1 and WA50-2. In the calcite-DAS, 42% of Pb was removed but not the Ni.

4.5.3 Hydraulic parameters evolution

While the initial porosity was 0.74, the average flow of each DAS reactor with the selected four HRTs of 1, 2, 3, and 5 d was, respectively, 0.77 mL/min, 0.38 mL/min, 0.26 mL/min, and 0.15 mL/min. During the experiment, very little changes of k_{sat} were noted in WA50-1 and WA50-2 from the initial value of 1.4 x 10^{-2} cm/s to final values of 1.0 x 10^{-2} cm/s and 8.6 x 10^{-3} cm/s, respectively (Fig. 4.5). This was explained by the short contact time, which did not allow metals to precipitate and clog the pores. However, it can be deduced that 2 d of HRT is not enough to treat contaminated water with Fe concentration >1500 mg/L, at a high inflow rate. In WA50-3, the k_{sat} decreased in the order of 10^{-3} cm/s during the first 21 d. Then, the k_{sat} increased to a final value of 2.2 x 10^{-2} cm/s at the end of the experiment, possibly due to wood ash dissolution. In WA50-5, the k_{sat} decreased to around 1.5 x 10^{-3} cm/s during the first 7 d of the treatment (Fig. 4.5), probably due to the fast precipitation of secondary minerals filling the pores. This decrease was followed by an increase ($k_{sat} \approx 10^{-2}$ cm/s) between day 14 and 21, indicating once again a possible liberation of pores because of the dissolution of wood ash (Fig. 4.5). Finally, a rebound to a decrease of the k_{sat} ($\approx 10^{-3}$ cm/s) at the end of the experiment apparently indicates a cycle of dissolution/precipitation alternation.

Dissolution of neutralizing agent, which was linked to the increase of k_{sat} and porosity, followed by precipitation correlated to pore filling, and thus k_{sat} decrease, were often encountered during the treatment of contaminated mine water with DAS mixtures (e.g., Rötting et al., 2007; Ayora et al., 2013; Zarzo et al., 2016). The longer the dissolution/precipitation phenomenon is balanced, the better the sustainability of the treatment system. The variation of k_{sat} showed that all the tested WA-DAS reactors did

not clog during the experiment. Nonetheless, a HRT of 3 d would be suggested for a large-scale treatment to reduce precipitates' volume and space requirement.

Similar behavior was observed during operation of calcite-DAS reactors where k_{sat} evolution was comparable to WA50-1 and WA50-2 (Fig. 4.5). Insignificant variation of k_{sat} was noticed in C20-1 and C20-2 columns, from an initial value of 3.0 x 10^{-2} cm/s (for both reactors) to 2.4 x10^{-2} cm/s (C20-1) and 1.6 x10^{-2} cm/s (C20-2) at the end of testing. Mean calculated porosity, which only very slightly increased from 0.68 (comparable to previous studies on calcite-DAS: 0.65–0.70; Rötting et al., 2008a, 2008b) to 0.71, but showed that columns did not clog. Nevertheless, the efficiency in terms of Fe removal depends on the choice of HRT and the water quality (Fe concentration).

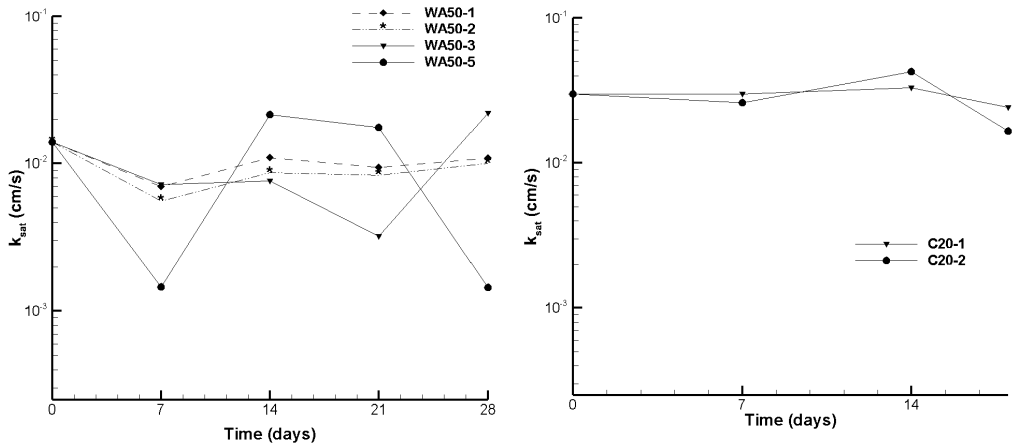

Figure 4.5 Saturated hydraulic conductivity evolution during 30 days in the WA-DAS reactors operated at HRT of 1, 2, 3, 5 d and for 18 days in the calcite-DAS reactors operated at 1 and 2 d of HRT during column experiments

The k_{sat} value noted during the Fe-rich AMD treatment with R2.5 or R5 decreased from 2.1 x 10^{-2} cm/s to around 2.4 x 10^{-3} cm/s in both PBRs (Fig. 4.6).

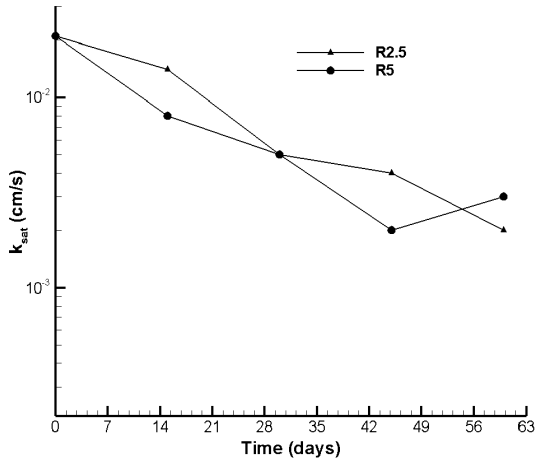

Figure 4.6 Evolution of k_{sat} over 60-day period in the two PBRs operated at HRT 2.5 d and 5 d during column experiments

The high porosity of the mixture (0.72) used in R2.5 and R5 (relative to what is found in other studies 0.34–0.53) was an advantage for the microbes to grow and develop their biofilm, thereby limiting k_{sat} decrease. Indeed, it was reported that microbial development could decrease up to 99.95% of k_{sat} causing preferential flow path (Taylor and Jaffé, 1990; Anello et al., 2005).

4.5.4 Modeling

PHREEQC modeling suggested that almost all metals were removed by precipitation under the form of oxides/hydroxides, especially in the DAS reactors. The Fe exists predominantly as Fe- oxides/hydroxides. The simulation predicted oversaturation of important phases including ferrihydrite, goethite (α-FeOOH), hematite (α-Fe_2O_3), jarosite [$KFe_3(SO_4)_2(OH)_6$], lepidocrocite [γ-FeO(OH)], magnetite (Fe_3O_4), magnesioferrite ($MgFe_2O_4$), schwertmannite [$Fe_8O_8(OH)_6(SO_4).nH_2O$] (Table B2).

Carbonate minerals could be also present in the form of siderite ($FeCO_3$). Contrary to other studies (e.g., Neculita et al., 2008b), the negative SI of Fe sulfides, such as greigite (Fe_3S_4) and mackinawite (FeS), indicated that these minerals did not reach saturation in the PBRs (Table B2). This could be due to the low ratio of Fe^{2+}/SO_4^{2-}or Fe^{3+}/SO_4^{2-} (0.006 or 0.02, respectively), meaning that although the concentration of SO_4^{2-} was high, the low concentration of Fe was not sufficient to form Fe-sulfides. Al would be removed as alunite [$KAl_3(SO_4)_2(OH)_6$], boehmite [AlO(OH)], corundum (Al_2O_3), diaspore [AlO(OH)], and gibbsite [$Al(OH)_3$]. The simulation indicated also that some Pb could be included in the jarosite [$Pb.5Fe_3(SO_4)_2(OH)_6$] or in the cerussite ($PbCO_3$). The SO_4^{2-} would be included in the precipitates of gypsum ($CaSO_4.2H_2O$), jarosite, and schwertmannite.

4.5.5 Post-testing mineralogical characterization

4.5.5.1 Solids in the DAS column reactors

Mineral phases were observed with the SEM-EDS, and, in accordance with the PHREEQC modeling, Fe was observed to be mainly as Fe-oxides/oxyhydroxides (Fig. 4.7A), but was also found as carbonates, such as siderite (Fig. 4.7B), or associated with Al and Si as Fe-Si-Al oxyhydroxides (Fig. 4.7C). Nanoparticles of oxides/hydroxides ($\leq$100 μm) were observed as well (Fig. 4.7D). The gypsum was either needle-shaped (Fig. 4.8E) or as larger euhedral particles (Fig. 4.7F).

Image mapping showed the precipitation order of Fe-oxides/hydroxides and gypsum, which in an embossed picture apparently indicated its post-Fe-oxides formation (Fig. B4A). Gypsum crystals (Fig. B4B) and excess of Ca (Fig. B4C) were then deposited on a thin layer of Fe-oxides/oxyhydroxides (Fig B4D).

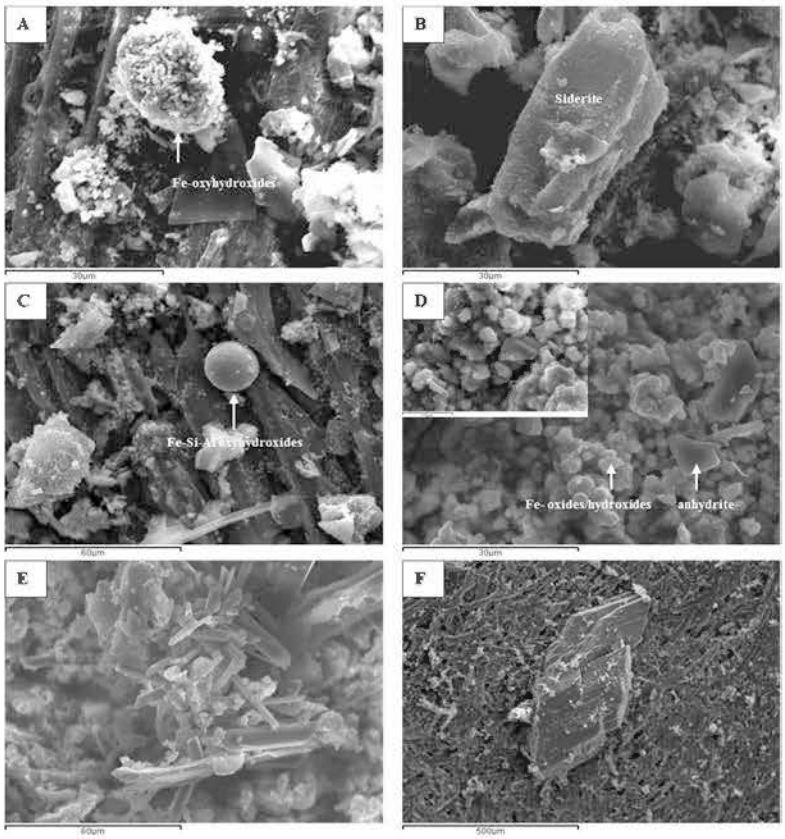

Figure 4.7 Scanning electron microscope (SEM) images of minerals in the spent reactive mixtures recovered from WA50-3, at the top layer (15–20 cm) (A) Fe-oxide/hydroxides, and the bottom layer (0–10 cm) (B) Siderite; (C) Amorphous Fe-Al-Si oxyhydroxides; (D) Poorly crystallized nanoparticle layer of Fe-oxides/hydroxides under anhydrite; (E) Needle-like gypsum with calcium bicarbonate, (F) Enhedral gypsum crystal

Other mineral phases (not pointed out by modeling) have also been observed, such as wustite (FeO), and srebrodolskite or calcined ankerite ($Ca_2Fe_2O_5$), which probably originated from the wood ash dissolution. In addition, anhydrite ($CaSO_4$) was also present and could have been a SO_4^{2-} scavenger. Possible calcite dissolution could have led to carbonation due to the liberation of bicarbonate anion (Eq. (4.3)), forming

mineral carbonates and possibly entailing a premature development of crystals or leaving an excess of calcium (Fig. B5A & 5B).

$$CaCO_3 + H^+ \rightarrow Ca^{2+} + HCO_3^- \qquad (4.3)$$

The presence of rosette-like carbonate mineral, typically encountered in the biotic environment (Power et al., 2007), could be a sign of bacterial activity (Fig. B6). Most of these precipitates were adsorbed at the surface of wood chips which acted like a natural filter (Fig. B7A & 7B).

4.5.5.1 Solids in the PBRs

Observation on the SEM-EDS of R5 showed precipitates of Fe-oxides/hydroxides, corundum (Fig. B8A) and gypsum (Fig. B8B, C & D).

Native sulfur (S^0) was also detected during SEM-EDS observation (Fig. B9), which might be formed by indirect reduction of ferric iron [Fe(III)] reacting with biogenic sulfide, as suggested by Eq. 4.4 (Johnson and Hallberg, 2005b).

$$2Fe(OH)_3 + H_2S \rightarrow 2Fe^{2+} + S^0 + 2H_2O + 4OH^- \qquad (4.4)$$

The colony of bacteria developed on wood chips instead of on sand grains, while their biofilm developed nearby (Fig. 4.8A, 8B). It appears then that the wood chips became a favorable niche for bacteria and served not only to improve k_{sat} but also as a support and/or substrate for the bacteria (Fig. 4.8C, 8D). Hence, addition of siliceous materials as a component of the substrate could be optional.

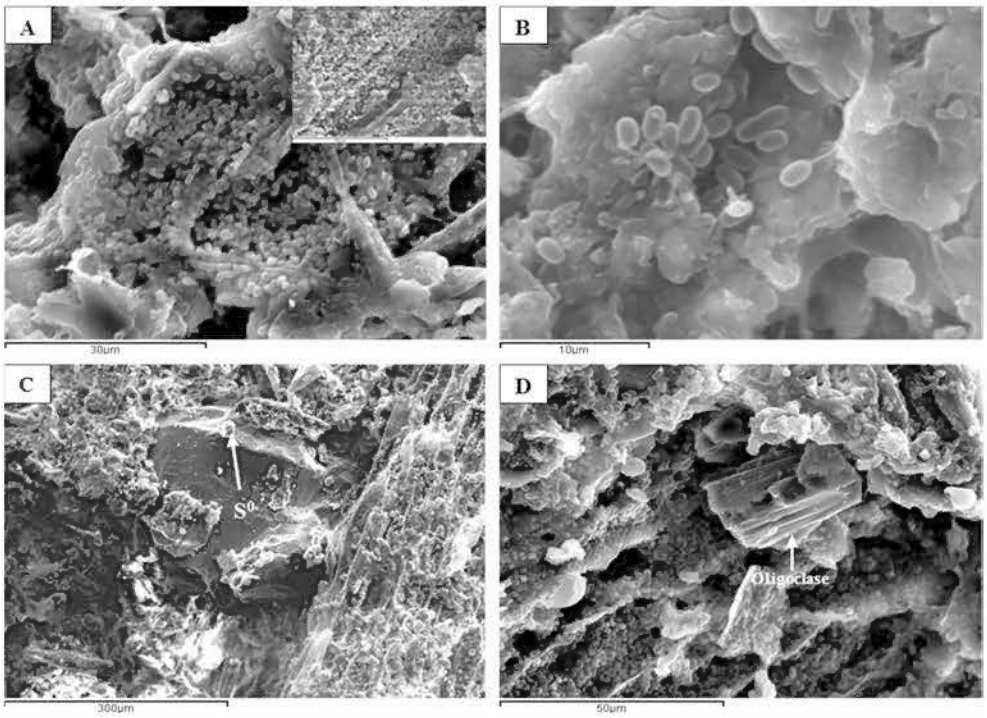

Figure 4.8 SEM images of minerals observed at the bottom layer (0–10 cm) of the spent reactive mixture recovered from R5: (A) Image of wood chips colonized by bacteria; (B) SRB on wood chips; (C) Sandstone enclosed in wood chips fouled with Fe-oxides/hydroxides, biofilm, with a deposit of native sulfur (S^0); and (D) Microorganisms colony installed on the wood chips interstices

4.6 Conclusion

The effectiveness and the hydraulic performance of three reactive mixtures were evaluated in column reactors, under different HRTs, during the passive treatment of Fe-rich AMD. Two reactive mixtures type DAS, composed of wood ash or calcite, were used for Fe pre-treatment, while a third mixture composed of organic and inorganic materials was used in a PBR for SO_4^{2-} removal. The wood ash-DAS reactors showed Fe and SO_4^{2-} removal of 17–62% and 7.5–37%, respectively. Better efficiency was found at higher HRTs, with optimal performance at 5 d of HRT (WA50-5). However, a HRT of 3 d would be proposed at field scale to limit space requirements.

The calcite-DAS reactors were efficient only in a very short term (within the first 7 days) and at 2 d of HRT, with 73% of Fe and 47% of SO_4, respectively. The calcite-DAS reactors could be used in a polishing treatment, at the exit of a PBR. The efficiency of Fe removal in the two PBRs was, respectively, 77% and 91%, in R2.5 and R5. Potential competition between IRB and SRB can occur, leading to SO_4^{2-} reduction below 14%. Other metal removal in all tested columns was 37–99.9% for Al, Zn, and Pb; 20–98% for Ni, except in C20, and ranged between 5–37% for SO_4^{2-}. Results obtained in this study suggest that optimizing the hydraulic properties of the reactive mixture used in passive treatment could improve its effectiveness and long-term performance. Hence, the columns did not show clogging issues. Larger-scale applications of DAS and PBRs units, in a multi-step treatment system, should be performed in order to identify specific design criteria for an efficient long-term treatment of Fe-rich AMD.

Acknowledgements

This study was funded by the NSERC (Natural Sciences and Engineering Research Council of Canada), grant no. 469489-14, and the industrial partners of the RIME UQAT-Polytechnique Montreal, including Agnico Eagle, Mine Canadian Malartic, Iamgold, Raglan Mine Glencore, and Rio Tinto. The authors gratefully acknowledge the assistance of Dr Hassan Bouzahzah during mineralogical analysis. They also want to sincerely thank Marc Paquin, Mélanie Bélanger, Patrick Bernèche, and Joël Beauregard for technical assistance.

References

Anello, G., Lamarche, P., Héroux, J.A., 2005. Reduction of hydraulic conductivity changes in an in-ground bioreactor. J. Environ. Eng. Sci. 4: 195–207.

APHA (American Public Health Association), 2012. Alkalinity titration, Standard methods for the examination of water and wastewater, 22nd ed. Greenberg A. (Eds), Washington DC, USA.

ASTM (American Society for Testing and Materials), 1990. Standard methods for sulphate reducing bacteria in water and water-formed deposit. In: Annual book of ASTM Standards, vol. 04.08. Section D 4412–84, Washington, DC, pp. 533–535.

ASTM (American Society for Testing and Materials), 1995. Standard test method for permeability of granular soils. Annual book of ASTM Standards. 08. D 2434–68, Philadelphia, PA, USA.

Aubertin, M., Bussière, B., Bernier, L., 2002. Environment et gestion des rejets miniers. Presses Internationales, Polytechnique Montréal, QC, Canada.

http://www.presses-polytechnique.ca/fr/environnement-et-gestion-des-rejets-miniers

Ayora, C., Caraballo, M.A., Macías, F., Rötting, T.S., Carrera, J., Nieto, J.-M., 2013. Acid mine drainage in the Iberian Pyrite Belt: 2. Lessons learned from recent passive remediation experiences, Environ. Sci. Pollut. R. 20: 7837–7853.

Caraballo, M. A., Macías, F., Nieto, J. M., Castillo, J., Quispe, D., Ayora, C., 2011. Hydrochemical performance and mineralogical evolution of a dispersed alkaline substrate (DAS) remediating the highly polluted acid mine drainage in the full-scale passive treatment of Mina Esperanza (SW Spain). Am. Mineral. 96:1270–1277.

Caraballo, M.A., Rötting, T.S., Silva, V., 2010. Implementation of an MgO-based metal removal step in the passive treatment system of Shilbottle, UK: Column experiments. J. Hazard. Mater. 181: 923–930.

Caraballo, M. A., Rötting, T.S, Macías, F., Nieto, J.M., Ayora, C., 2009. Field multi-step limestone and MgO passive system to treat acid mine drainage with high metal concentrations. Appl. Geochem. 24: 2301–2311.

Chapelle, F.H., Bradley, P.M., Thomas, M.A., McMahon, P.B., 2009. Distinguishing iron-reducing from sulfate-reducing conditions. Ground Water 47(2): 300–305.

Chapelle, F.H. and Lovley, D.R., 1992. Competitive exclusion of sulfate reduction by Fe (III) - reducing bacteria: A mechanism for producing discrete zones of high-iron. Ground Water 30 (1): 29–36.

Cochran, W.G., 1950. Estimation of bacterial densities by means of the most probable number. Biometrics 6: 105–116.

Cocos, I.A., Zagury, G.J., Clement, B., Samson, R., 2002. Multiple factor design for reactive mixture selection for use in reactive walls in mine drainage treatment. Water Res. 32:167–177.

Dar, S.A., Kleerebezem, R., Stams, A.J.M., Kuenen, J.G., Muyzer, G., 2008. Competition and coexistence of sulfate-reducing bacteria, acetogens and methanogens in a lab-scale anaerobic bioreactor as affected by changing substrate to sulfate ratio. Appl. Microbiol. Biotechnol. 78(6): 1045−1055.

Deng, D., Weidhaas, J.L., Lin, L.-S., 2016. Kinetics and microbial ecology of batch sulfidogenic bioreactors for co-treatment of municipal wastewater and acid mine drainage. J. Hazard. Mater. 305: 200–208.

Diz, H.R., Novak, J.T., Rimstidt, F.D., 1999. Iron precipitation kinetics in synthetic acid mine drainage. Mine Water Environ. 18 (1): 1−14.

Florence, K., Sapsford, D., Wolkersdorfer, C., 2015. Mechanisms of iron removal during passive treatment of AMD in a vertical flow reactor. In: Proc. of the International Conference on Acid Roch Drainage (ICARD) & International Mine Water Association (IMWA) Annual Conference, April 21-24, Santiago, Chile.

Gazea, B., Adam, K., Kontopoulos, A., 1996. A review of passive systems for the treatment of acid mine drainage. Miner. Eng. 9:23–42.

Genty, T., Bussière, B., Paradie, M., Neculita, C.M., 2016. Passive biochemical treatment of ferriferous mine drainage: Lorraine mine site, Northern Quebec, Canada. Wolkersdorfer & Freud (Eds). In: Proc. of the IMWA, July 11-15, Leipzig, Germany.

Genty, T., 2012. Comportement hydro-bio-géo-chimique de systèmes passifs de traitement du drainage minier acide fortement contaminé en fer. Ph.D diss. Research Institute on Mines and Environment (RIME)-University of Quebec in Abitibi-Temiscamingue (UQAT). Rouyn-Noranda, QC, Canada, 270p.

http://depositum.uqat.ca/id/eprint/269http://depositum.uqat.ca/id/eprint/269.

Genty, T., Bussière, B., Potvin, R., Benzaazoua, M., Zagury, G.J., 2012a. Dissolution of calcitic marble and dolomitic rock in high iron concentrated acid mine drainage: Application to anoxic limestone drains. Environ. Earth Sci. 66: 2387–2401.

Genty, T., Bussière, B., Potvin, R., Benzaazoua, M., Zagury, G.J., 2012b. Capacity of wood ash filters to remove iron from acid mine drainage: Assessment of retention mechanism. Mine Water Environ. 31(4): 273–286.

Genty, T., Bussière, B., Zagury, G.J., Benzaazoua, M., 2010. Passive treatment of high-iron acid mine drainage using sulphate reducing bacteria: Comparison between eight biofilter mixtures. Wolkersdorfer & Freud (Eds). In: Proc. of the IMWA, September 5-9, Sydney, NS, Canada.

Gibert, O., De Pablo, J., Cortina, J., Ayora, C., 2004. Chemical characterisation of natural organic substrates for biological mitigation of acid mine drainage. Water Res. 38: 4186–4196.

Gould, W. D., Stichbury, M., Francis, M., Lortie, L., Blowes, D. W., 2003. An MPN method for the enumeration of iron-reducing bacteria. In Proc. of Mining and the environment III Conference. Laurentian University, Sudbury, ON, Canada, pp. 25–28.

HACH, 2013. Colorimeter procedures manual.

http://www.hach.com/quick.search-download.search.jsa?keywords=Colorimeter%20procedures%20manual

Hammarstrom, J.M., Sibrell, P.L., Belkin, H.E., 2003. Characterization of limestone reacted with acid-mine drainage in a pulsed limestone bed treatment system at the Friendship Hill National Historical Site, Pennsylvania, USA. Appl. Geochem. 18: 1705–1721.

Huminicki, D.M.C. and Rimstidt, J.D., 2008. Neutralization of sulfuric acid solutions by calcite dissolution and the application to anoxic limestone drain design. Appl. Geochem. 23: 148–165.

Johnson, D.B. and Hallberg, K.B., 2005a. Acid mine drainage remediation options: A review. Sci. Total Environ. 338: 3–14.

Johnson, D.B. and Hallberg, K.B., 2005b. Biogeochemistry of the compost bioreactor components of a composite acid mine drainage passive remediation system. Sci. Total Environ. 338: 81–93.

Kagambega, N., Galvez, R., Ouattara, A., Laflamme, M., 2014. Assessment of the neutralizing capacity of high purity dolomite on the highly polluted acid mine drainage. Int. J. Environ. Eng. Nat. Resour. 1(3): 120–129.

Kirby, C.S., Thomas, H.M., Southam, G., Donald, R., 1999. Relative contributions of abiotic and biological factors in Fe(II) oxidation in mine drainage. Appl. Geochem. 14: 511–530.

Lovley, D.R. and Phillips, E.J.P., 1987. Competitive mechanisms for inhibition of sulfate reduction and methane production in the zone of ferric iron reduction in sediments. Appl. Environ. Microbiol. 53(11): 2636–2641.

Macías, F., Caraballo, M.A., Nieto, J.M., Rötting, T.S., Ayora, C., 2012. Natural pretreatment and passive remediation of highly polluted acid mine drainage. J. Environ. Manage. 104: 93–100.

Maree, J.P., Du Plessis, P., Van der Walt, C.J., 1992. Treatment of acidic effluents with limestone instead of lime. Water Sci. Technol. 26 (1–2): 345–355.

Neculita, C.M., Zagury, G.J., Bussière, B., 2008a. Effectiveness of sulfate-reducing passive bioreactors for treating highly contaminated acid mine drainage: I. Effect of hydraulic retention time. Appl. Geochem. 23: 3442–3451.

Neculita, C.M., Zagury, G.J., Bussière, B., 2008b. Effectiveness of sulfate-reducing passive bioreactors for treating highly contaminated acid mine drainage: II. Metal removal mechanisms and potential mobility. Appl. Geochem. 23: 3545–3560.

Neculita, C.M. and Zagury, G.J., 2008. Biological treatment of highly contaminated acid mine drainage in batch reactors: Long-term treatment and reactive mixture characterization. J. Hazard. Mater. 157: 358–368.

Neculita, C.M., Zagury, G.J., Bussière, B., 2007. Passive treatment of acid mine drainage in bioreactors using sulfate-reducing bacteria– critical review and research needs. J. Environ. Qual. 36: 1–16.

Nordstrom, D.K. and Alpers, C.N., 1999. Negative pH, efflorescent mineralogy, and consequences for environmental restoration at the Iron Mountain Superfund site, California. In: Proc. of Natl. Acad. Sci. 96: 3455–3462.

Oh, C., Ji, S., Cheong, Y., Yim, G., Hong, J.-H., 2016. Evaluation of design factors for cascade aerator to enhance efficiency of oxidation pond for ferruginous mine drainage. Environ. Technol. 37 (19): 2483–2493.

Oh, C. Yu, C., Cheong, Y., Yim, G., Song, H., Hong, J.-H., Ji, S., 2015. Efficiency assessment of cascade aerator in a passive treatment system for Fe(II) oxidation in ferruginous mine drainage of net alkaline. Environ. Earth Sci. 73 (9): 5363–5373.

Orakwue, E.O., Asokbunyarat, V., Rene, E.R., Lens, P.N.L., Annachhatre, A., 2016. Adsorption of iron (II) from acid mine drainage contaminated groundwater using coal fly ash, coal bottom ash, and bentonite clay. Water Air Soil Pollut. 227(3): 74.

Postgate, J.R., 1984. The sulfate-reducing bacteria. 2nd ed. Cambridge University Press, Cambridge.

Potgieter-Vermaak, S.S., Potgieter, J.H., Monama, P., Van Grieken, R., 2006. Comparison of limestone, dolomite and fly ash as pre-treatment agents for acid mine drainage. Miner. Eng. 19: 454–462.

Power, I.M., Wilson, S., Thom, J.M., Dipple, G.M., Southam, G., 2007. Biologically induced mineralization of dypingite by cyanobacteria from an alkaline wetland near Atlin, British Columbia, Canada. Geochem. Trans. 8:13.

Prasad, D. and Henry, J.G., 2009 Removal of sulphates, acidity and iron form from acid mine drainage in a bench scale biochemical system. Environ. Technol. 30 (2): 151–160.

Rakotonimaro T., Neculita C.M., Bussière, B., Zagury, G.J., 2016. Effectiveness of various dispersed alkaline substrates for the pre-treatment of ferriferous acid mine drainage. Appl. Geochem. 73: 13–23.

Rötting, T.S., Thomas, R.C., Ayora, C., Carrera, J., 2008a. Passive treatment of acid mine drainage with high metal concentrations using dispersed alkaline substrate. J. Environ. Qual. 37:1741–1751.

Rötting, T.S., Caraballo, M.A., Serrano, J.A., Ayora, C., Carrera, J., 2008b. Field application of calcite Dispersed Alkaline Substrate (calcite-DAS) for passive treatment of acid mine drainage with high Al and metal concentrations. Appl. Geochem. 23: 1660–1674.

Rötting, T.S., Ayora, C., Carrera, J., 2007. Chemical and hydraulic performance of "dispersed alkaline substrate" (DAS) for passive treatment of acid mine drainage with high metal concentrations. R. Cidu & F. Frau (Eds). In: Proc. of the IMWA, May 27-34, Cagliari, Italy.

Rötting, T.S., Jordi C., Ayora, C., 2006. Use of caustic magnesia to remove cadmium, nickel, and cobalt from water in passive treatment systems: column experiments. Environ. Sci. Technol. 40: 6438– 6443.

Song, H., Yim, G.J., Ji, S.W., Nam, I.-H., Neculita, C.M., Lee, G. 2012. Performance of mixed organic substrates during treatment of acidic and moderate mine drainage in column bioreactors. J. Environ. Eng. 138 (10): 1077-1084.

Taylor, S.W. and Jaffé, P.R., 1990. Biofilm growth and the related changes in the physical properties of a porous medium: 1. Experimental investigation. Water Resour. Res. 26: 2153–2159.

USEPA (United States Environmental Protection Agency), 2014a. Reference Guide to Treatment Technologies for Mining-influenced Water. EPA 542-R-14-001, 94p.

USEPA (United States Environmental Protection Agency), 2014b. Code of Federal Regulations: Part 434- Coal mining point source category BPT, BAT, BCT limitations and new source performance standards.

https://www.gpo.gov/fdsys/pkg/CFR-2014-title40-vol30/xml/CFR-2014-title40-vol30-part434.xml#seqnum434.33

URS (United Registrar of Systems), 2003. Passive and semi-active treatment of acid rock drainage from metal mines-state of the practice. Prepared for US Army Corps of Engineers, Portland, ME.

USGS (United States Geological Survey), 2015.

http://wwwbrr.cr.usgs.gov/projects/GWC_coupled/phreeqc/index.html

Vasquez, Y., Escobar, María, C., Neculita, C. M., Arbeli, Z., Roldan, F., 2016a. Biochemical passive reactors for treatment of acid mine drainage: Effect of hydraulic retention time on changes in efficiency, composition of reactive mixture, and microbial activity. Chemosphere 153: 244–253.

Vasquez, Y., Escobar, María, C., Neculita, C. M., Arbeli, Z., Roldan, F., 2016b. Selection of reactive mixture for biochemical passive treatment of acid mine drainage. Environ. Earth Sci. 75: 576.

Waybrant, K., Ptacek, C., Blowes, D., 2002. Treatment of mine drainage using permeable reactive barriers: column experiments. Environ. Sci. Technol. 36: 1349–1356.

Waybrant, K., Ptacek, C., Blowes, D., Ptacek, C.J., 1998. Selection of reactive mixtures for use in permeable reactive walls for the treatment of acid mine drainage. Environ. Sci. Technol. 32: 1972–1979.

Willow, M.A., and Cohen, R.R.H., 2003. pH, dissolved oxygen, and adsorption effects on metal removal in anaerobic bioreactors. J. Environ. Qual. 32: 1212–1221.

Zarzo, D., López, A., Campos, E., Nieto, J., Macías, F., García, M., Mateos, F., Belmonte, A., 2016. Research and development project for sustainable treatment of acid mine drainage water. In: Proc. of the Water in Mining, May 18-20, Santiago, Chile.

Zagury, G.J., Kulnieks, V., Neculita, C.M., 2006. Characterization and reactivity assessment of organic substrates for sulphate-reducing bacteria in acid mine drainage treatment. Chemosphere 64: 944–954.

Zipper, C. and Skousen, J., 2014. Passive treatment of acid mine drainage, in: Jacobs, J.A., Lehr, J. H., Testa, S.M. (Eds.), Acid mine drainage, rock drainage, and acid sulfate soils: Causes, Assessment, prediction, prevention, and remediation, John Wiley & Sons, Inc., Hoboken, NJ (USA), pp. 339–353.

Zipper, C., Skousen, J., Jage, C., 2011. Passive treatment of acid-mine drainage. Communications and Marketing, College of Agriculture and Life sciences. Publication 460-133, Virginia, PT, USA. 15p.

CHAPITRE V

SCALE EFFECT ASSESSMENT OF PASSIVE MULTI-STEP SYSTEMS AND NEW DESIGN CRITERIA FOR THE TREATMENT OF IRON-RICH ACID MINE DRAINAGE[3]

Ce chapitre a été soumis en août 2017 dans la revue *Environmental Science and Pollution Research.*

[3] Rakotonimaro, T.V., Neculita, C.M., Bussière, B., Genty, T., Zagury, G.J., 2017. Scale effect assessment of passive multi-step treatment and new design criteria for the treatment of iron rich acid mine drainage. *Environmental Science and Pollution Research* (soumis).

5.1 Résumé

Les filières de traitement passif du drainage minier acide (DMA) ferrifère fonctionnent généralement de manière satisfaisante à l'échelle de laboratoire. Cependant, leur application sur le terrain a montré des différences significatives, en particulier sur les paramètres hydrauliques. Dans cette étude, une évaluation de l'effet d'échelle a été effectuée par une comparaison des expériences à l'échelle du laboratoire et d'une étude de terrain, suivi d'une identification des facteurs et paramètres potentiellement responsable des variations notées. Ainsi, trois scénarios de filières ont été réalisés avec des réacteurs en colonnes de 10,7L, composés de substrats alcalins dispersés (SAD), de drains anoxiques dolomitiques et de réacteurs passifs biochimiques (RPB). Le système à l'échelle de terrain était composé de deux RPB séparés par un réacteur à cendre de bois. Les paramètres identifiés, qui pourraient influencer la différence de performance entre les expériences à l'échelle de laboratoire et à l'échelle de terrain, sont la conductivité électrique, la concentration en SO_4^{2-}, le débit (Q) et la conductivité hydraulique saturée (k_{sat}). Q semblait être le principal facteur qui a contrôlé la performance du traitement sur le terrain. Pour une filière efficace utilisant des unités SAD et RPB, des critères de conception supplémentaires, prenant en compte les concentrations en Fe et SO_4^{2-}, ainsi que de k_{sat}, sont recommandés. Ainsi, le traitement du DMA ferrifère avec des filières nécessite une $k_{sat} > 10^{-3}$cm/s. De plus, dans un RPB, des charges de Fe <26 g/m^3 substrat/j et de SO_4^{2-} <110 g/m^3 substrat/j sont proposées. Si une unité de CB-DAS devait être utilisée comme prétraitement avant un RPB, des charges de 260 g Fe/m^3/j et de 407 g SO_4^{2-}/m^3/j sont attendues. Une étude plus étendue sur le terrain devrait être entreprise avant la construction d'une filière de traitement passif du DMA ferrifère à grande échelle.

5.2 Abstract

Multi-step passive systems for the treatment of iron-rich acid mine drainage (Fe-rich AMD) perform satisfactorily at the laboratory scale. However, their field-scale application has revealed dissimilarities in performance, particularly with respect to hydraulic parameters. In this study, a scale effect assessment was undertaken through a comparison of laboratory-scale and field-scale experiments, followed by identification of factors potentially responsible for any recorded variations in performance. Three laboratory-scale multi-step treatment scenarios, involving a combination of dispersed alkaline substrate (DAS) units, anoxic dolomitic drain, and passive biochemical reactors (PBRs), were set-up in 10.7 L columns. The field-scale treatment was comprised of two PBRs separated by a wood ash (WA) reactor.

The parameters identified as possibly influencing the performances of the laboratory-scale and field-scale experiments were: the electrical conductivity, Fe and SO_4^{2-} concentrations, flow rate (Q), and saturated hydraulic conductivity (k_{sat}). Q seemed to be the main factor that controlled the performance of the on-site treatment. For an efficient multi-step system using DAS-based units and PBRs, additional design criteria, including the k_{sat} and Fe and SO_4^{2-} concentrations, are recommended. Treatment of Fe-rich AMD with multi-step systems requires $k_{sat} > 10^{-3}$ cm/s. In a PBR, loadings of Fe <26 g/m^3 substrate/d and of SO_4^{2-} <110 g/m^3 substrate/d are proposed. If a WA-DAS unit were to be used as pre-treatment prior to a PBR, rates of 260 g Fe/m^3/d and 407 g SO_4^{2-}/m^3/d would be expected. Mesocosm testing is recommended prior construction of full-scale system for the treatment of Fe-rich AMD.

Keywords: Passive treatment, design, scale effect, acid mine drainage, dispersed alkaline substrate

5.3 Introduction

Multi-step passive treatment systems are currently recommended for the treatment of highly contaminated acid mine drainage (AMD) due to the limited long-term efficiencies of single-unit systems (Zipper et al. 2011). Such multi-step systems are comprised of combinations of chemical and biological treatment units (USEPA, 2014; Skousen et al. 2017). Some multi-step treatment systems may involve the grouping of dispersed alkaline substrate (DAS; i.e., mixtures of coarse-grained materials, such as wood wastes, and neutralizing materials, including calcite and magnesia) units with cascade aeration (Rötting et al. 2008a) or with decantation pond steps (Caraballo et al. 2009, 2011; Macías et al. 2012a, 2012b). Others combine passive biochemical reactors (PBRs) with anoxic limestone drains (ALDs; Figueroa et al. 2007; Prasad and Henry, 2009), wood ash (WA; Genty, 2012; Genty et al. 2016), or peat biofilters (Clyde et al. 2016). Passive multistage co-treatment of AMD with municipal wastewater has also been attempted (Strosnider et al. 2013). A multi-step treatment system often includes a pretreatment unit in order to reduce high metal concentrations and acidity loads, as well as to protect and sustain the effectiveness of the subsequent unit(s) (Macías et al. 2012b; Genty, 2012).

Conventionally, when designing passive treatment systems, several factors must be considered, including: 1) water chemistry, including metal and acid loads (Hedin et al. 1994, 2010; Bernier et al. 2001; Rötting et al. 2008a; McCauley et al. 2009; Skousen et al. 2017); 2) hydraulic retention time (HRT) (Rötting et al. 2008a; Neculita et al. 2008; Hedin et al. 2013); and 3) reactive mixture composition (Waybrant et al. 1998; Zagury et al. 2006; Neculita et al. 2011; Yim et al. 2015). Acidity and available space are generally used for sizing (Hedin et al. 2010). As specific examples, ALDs are designed to treat contaminated water at an initial acidity <150 mg/L $CaCO_3$ and required a minimum HRT of 14 h (Hedin et al. 1994). In addition, iron load was recommended to be 10 g $Fe/m^2/d$ and 20 g $Fe/m^2/d$ for acidic and alkaline waters,

respectively. In the same study, for alkaline waters, the acceptable load of acidity was <300 mg/L $CaCO_3$, at a flow rate 6.6 L/min.

With respect to PBR systems, reactive mixtures are generally comprised of, at a minimum, a substrate, a neutralizing agent, and an inert material (e.g., sand or gravel; to improve hydraulics; Cocos et al. 2002; Zagury et al. 2006; Neculita et al. 2011; Genty et al., 2017a). In addition, experience and practice have demonstrated that Fe concentrations in influents should not exceed 500 mg/L when a single PBR is used (Neculita et al. 2008). However, a difference in performance is usually observed upon scaling up from the laboratory to the field (Rötting et al. 2008a). In laboratory testing, high efficiencies (>96%) of passive multi-step systems treating Fe-rich AMD have been observed when initial Fe concentrations are <500 mg/L (Champagne et al. 2005; Prasad and Henry, 2009). When Fe concentrations are >500 mg/L, the long-term performance (84 to 238 days) of these systems declines significantly (as low as 33%; Genty, 2012). Similar results have been observed in field-scale pilot systems, with efficiencies of up to 99.9% when Fe <300 mg/L (Macías et al. 2012a, 2012b), which decreased to 20−78% at 300−2000 mg/L Fe (Rötting et al. 2008a; Caraballo et al. 2009, 2011; Genty et al. 2016). Thus, solely regarding the Fe removal, the efficiency of laboratory-scale vs field-scale systems could be different by a factor of 1.2−4.8, at Fe concentrations above 300 mg/L, depending on the type of units used in a multi-step treatment system. Therefore, the design of passive treatment systems varies according to the water quality. Some studies reported that the acceptable iron load was to be 10 g $Fe/m^2/d$ and 20 g $Fe/m^2/d$ for acidic and alkaline waters, respectively (Hedin et al. 1994). In the same study, for alkaline waters, the acceptable load of acidity was <300 mg/L $CaCO_3$, at a flow rate 6.6 L/min. Regarding the hydraulics, laboratory testing showed little variation in the saturated hydraulic conductivity (k_{sat}; Genty, 2012) and, despite the slow but progressive decrease over time, clogging issues generally did not occur (Rötting et al. 2007; Genty, 2012). Oppositely, changes in flow rate, preferential

flow, and partial clogging have been demonstrated in field-scale systems (Rötting et al. 2007, 2008a; Genty et al. 2016).

These discrepancies suggest that further study is required to identify and understand the factors that control the performance of passive treatment systems at different scales. In the laboratory, detecting problems is relatively easy because controlled conditions allow for the collection of high-quality data that can provide information on the primary issues, as well as the potential concerns that could arise in the field. However, field conditions are prone to changes (either predictable or not), including: seasonal temperature variations, metal loading rate changes, and gas lock-up. One example of inconsistency in the performance between laboratory-scale and field-scale experiments was a multi-step treatment system (composed of two PBRs separated by one unit of wood ash for the treatment of Fe-rich AMD) tested first in the laboratory, as batch and column reactors, then scaled up as a field-scale pilot system at Lorraine mine in Québec, Canada (Genty, 2012; Genty et al. 2016; 2017a; 2017b). Results obtained from the laboratory testing showed that Fe removal efficiency was ~97% (Genty, 2012), whereas in the field, surface overflow occurred one year after installation and Fe removal efficiency was ~66% (Genty et al. 2016). Due to this hydraulic issue, further laboratory studies to improve the system were undertaken by testing the performance of DAS mixtures as components in a potential passive treatment system that could be used at the Lorraine mine site (Rakotonimaro et al. 2016; 2017).

The objective of the present study was to assess the scale effects that cause differences in the performances of laboratory- and field-scale passive treatment systems, specifically in the case of the Lorraine mine site. The assessment of scale effects was made with respect to the efficiency (i.e., input vs output) and stability (efficiency over time) of the system. A comparison between the efficiency of the laboratory vs field experiments was undertaken and new design criteria are proposed which may be useful in the construction of efficient multi-step passive treatment systems with respect to Fe-rich AMD.

5.4 Materials and methods

5.4.1 Laboratory testing

5.4.1.1 Multi-step columns: design, set-up and operating conditions

Five columns (14 cm in diameter and 70 cm height; total volume = 10.7 L) were set-up to simulate various multi-step treatment systems. The columns were filled with different mixtures (Table 5.1): three were type DAS (two of WA50 and one of C50), one dolomitic rock (DOL), and one type commonly used in PBRs (70% w/w dry organic materials and 30% w/w inorganic materials).

Table 5.1 Compositions of mixtures filling the columns

Mixture	WA50	C50	PBR	DOL
	%v/v		% w/w	
Composition				
Structural agent				
Sand	-	-	10	-
Cellulosic wastes				
Wood chips	50	50	40	-
Organic wastes				
Chicken manure	-	-	20	-
Compost	-	-	10	-
Neutralizing agents				
Wood ash	50	-	-	-
Calcite	-	50	20	-
Dolomite	-	-	-	100
Total	*100*	*100*	*100*	*100*
HRT (days)	3	3	5	3

During batch testing, the two DAS mixtures (WA50 and C50) were found to be particularly efficient for the pre-treatment of Fe-rich AMD (Rakotonimaro et al. 2016). Additionally, all of the mixtures were effective in removing Fe (up to 91%) and were

stable in terms of their hydraulic parameters during over 30–63 days of testing in smaller (1 L) columns (Rakotonimaro et al. 2017). Previous studies reported that using dolomite has the advantage of limiting the formation of precipitates (e.g., gypsum) and should be used as polishing treatment (Potgieter-Vermaak et al. 2006; Huminicki and Rimstidt, 2008; Genty et al. 2012; Rakotonimaro et al. 2016).

The reactive mixture in each column was then placed between two layers of gravel (≈ 5 cm thick) and fine-mesh geotextiles at the top and bottom prior to being sealed.

Following construction, the PBR was saturated with Postgate B medium, which was prepared in deionized water with the following composition: 3.5 g/L sodium lactate (or 4.67 mL lactate liquid, 56.8%); 2.0 g/L $MgSO_4 \cdot 7H_2O$; 1.0 g/L NH_4Cl; 1.27 g/L $CaSO_4 \cdot 2H_2O$; 1.0 g/L yeast extract; 0.5 g/L KH_2PO_4; 0.5 g/L $FeSO_4 \cdot 7H_2O$; 0.1 g/L thioglycolic acid; and 0.1 g/L ascorbic acid (Postgate, 1984). Prior to starting the continuous feed of AMD, the bioreactor was incubated for 2 weeks (the acclimation period) with the medium, then acclimated with diluted AMD (3:1 deionized water to AMD) for another week. This procedure allows SRB to grow and produce enough sulfides and alkalinity in order to avoid a sudden exposure to the high acid and metal loads such as those present in AMD (Tsukamoto and Miller, 1999).

The tested AMD (Table 5.2), which composition simulated effluents from the abandoned Lorraine mine site (Québec, Canada), was prepared bi-monthly in a 60 L reservoir and pumped upward with calibrated Masterflex peristaltic pumps to feed the columns.

Table 5.2 Composition of Fe-rich AMD used to feed the multi-step columns

Elements	Concentration (mg/L)	Source
Al^{3+}	1.6 ± 0.6	$Al_2(SO_4)_3 \cdot 18H_2O$
Fe^{2+}/Fe^{3+}	2350 ± 330	$FeSO_4 \cdot 7H_2O$
Mg^{2+}	33.5 ± 3.8	$MgSO_4 \cdot 7H_2O$
Mn^{2+}	8.2 ± 1.0	$MnSO_4 \cdot H_2O$
Ni^{2+}	0.7 ± 0.4	$NiSO_4 \cdot 6H_2O$
Pb^{2+}	0.2 ± 0.1	$Pb(NO_3)_2$
Zn^{2+}	0.2 ± 3.0	$ZnSO_4 \cdot 7H_2O$
Ca^{2+}	430 ± 5	$CaSO_4 \cdot 2H_2O$
SO_4^{2-}	5073 ± 407	N/A[1]
pH	3.04 ± 0.45	N/A

[1] N/A- Not applicable, reagents were under the form of soluble sulfate

This water quality is typical of AMD from hard rock mines in Canada (Aubertin et al. 2002). However, the pH of AMD at the Lorraine site is around 5.8 (Genty et al. 2016), while during laboratory testing, no adjustment of the pH was undertaken.

Three multi-step scenarios (LM-1, LM-2, and LM-3) were tested (Fig. 5.1; Fig. C1); each scenario was comprised of one (WA50) or two pre-treatment units (WA50A and WA50B), one basic treatment unit (PBR), and/or one polishing unit (DOL or C50).

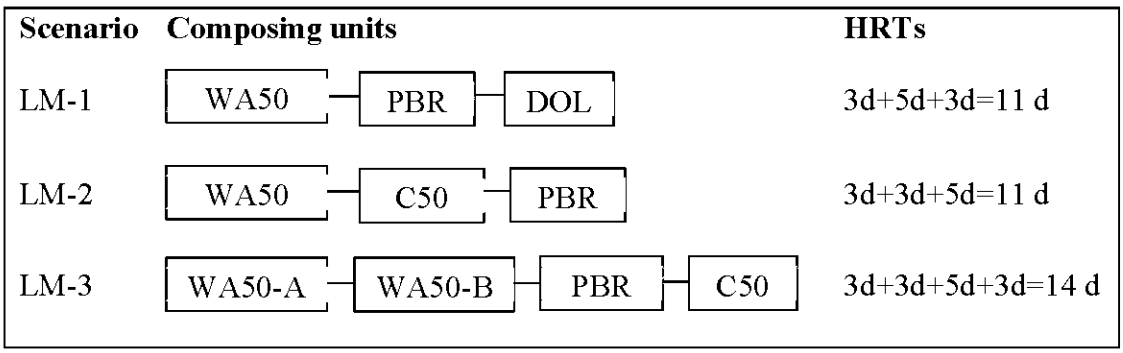

Figure 5.1 Schematic representation of the multi-step treatment scenarios tested in the laboratory

Scenarios LM-1 and LM-2 were tested over a period of 10 weeks, while LM-3 was tested for 15 weeks. All units in the columns were started at 3 d of HRT, except for the PBR units that had an HRT of 5 d. Thus, the total HRTs of scenarios LM-1, LM-2, and LM-3 were of 11 d, 11 d, and 14 d, respectively. The optimal HRT for the treatment of Fe-rich AMD in each unit was determined previously (Rakotonimaro et al. 2017). The orders of the units composing the scenarios were also established based on their performance and determination as either more suitable for pre-treatment, treatment, and/or polishing steps (Rakotonimaro et al. 2016; 2017). Configuration as separate units has the advantage of facilitating the maintenance (e.g., replacement of a deficient unit).

5.4.1.2 Monitoring of physicochemical, microbiological and hydraulic parameters

Effluent quality was monitored through weekly sampling and analysis of the physicochemical parameters, until a steady state was reached. These parameters included: pH, redox potential (ORP), electrical conductivity (EC), alkalinity, acidity, and the concentrations of total iron (Fe_t), ferrous iron (Fe^{2+}), sulphate (SO_4^{2-}), and dissolved oxygen (DO). Microbiological monitoring was also carried out and consisted of enumerating SRB and iron-reducing bacteria (IRB). Finally, the monitored hydraulic parameters included the k_{sat} and porosity (n).

Water pH was measured with an Orion 3-Star pH meter (GENEQ Inc.), while the EC was measured with a HACH Sension 1 electrode. The ORP was determined using a potentiometer (Sension1 POR HACH 51939-00) coupled with an internal Pt/Ag/AgCl electrode. DO concentrations were measured using a HACH-LDO10103 with HQ30d probe, which was calibrated with air-saturated water. Alkalinity and acidity were determined with a Metrohm Binkmann, 716 DMS Trinitro titrator (APHA, 2012). The concentrations of Fe_t, Fe^{2+}, and SO_4^{2-} were determined with filtered samples (0.45 µm), within 1–2 h after collection, using a DR/890 HACH colorimeter (Method 8008 - 1, 10

phenanthroline, Method 8146 - 1, 10 phenanthroline, and Method 8051 - barium chloride powder pillows for Fe_t, Fe^{2+}, and SO_4^{2-}, respectively) (HACH, 2013). Soluble sulfides (H_2S, HS^-, and S^{2-}) were analyzed immediately after sampling using a DR/890 HACH colorimeter (Method 8131- Methylene blue) (HACH, 2013). Total metal concentrations were analyzed by ICP-AES, on filtered (0.45 μm) and acidified (with 2% v/v HNO_3) samples. Metal removal efficiency, r (%), was calculated in the supernatant using the following equation:

$$r = [(C_x - C_{x+7})/ C_x] \times 100 \qquad (5.1)$$

where C_x and C_{x+7} are the metal concentrations (mg/L) at time x and $x + 7$ days, respectively.

Microbial counts in the effluents from the PBRs were performed at the beginning, during steady state, and the end of the testing period using the most probable number (MPN) method (ASTM, 1990; Cochran, 1950). To do so, tubes (5 replicates per dilution) were inoculated and incubated at 30°C for 21 d under anaerobic conditions for SRB counting. The growth of SRB was indicated by the presence of black FeS precipitate (Postgate, 1984); when the presence of black precipitate was not obvious, the presence of SRB was verified using $FeCl_3$/HCl and p-aminodimethylaniline dihydrochloride/HCl (ASTM, 1990). Enumeration of IRB was performed on 1 mL of liquid (or 1 g of soil sediment) added to each of 5 replicate glass tubes (containing 9 mL of culture medium, prepared in an anaerobic glove box). The inoculated serum tubes were then diluted tenfold using 1 mL syringes into another series of 5 serum tubes and repeated to get 10 to 12 serial dilutions. The tubes were incubated at 25°C for 28 d in an anaerobic chamber and, afterwards, the number of positive tubes was recorded. To determine if iron reduction had taken place, 0.2 mL of ferrozine reagent was injected into each serum bottle; the development of a purple color indicated a positive result (Gould et al. 2003).

The k_{sat} of each column was evaluated by using the falling head method (ASTM, 1995). The water was allowed to flow through the column under a falling head condition. Porosity was calculated as the ratio between void volume, which was calculated considering the specific gravity (G_s), and the total volume of the reactive mixture.

5.4.2 Field-scale pilot experiment

5.4.2.1 Site description and brief history of rehabilitation

The pilot-scale experiment was installed at the abandoned Lorraine mine site, which is located nearby the village of Latulipe in the Témiscamingue region of Québec, Canada (Fig. 5.2A). The site was exploited between 1964 and 1968 for Cu, Ni, Au, and Ag, and it produced about 600,000 tons of acid-generating tailings, rich in sulfide minerals, such as chalcopyrite, pyrite, pyrrhotite, and pentlandite (Bernier et al. 2001). These tailings (15−120 cm in depth) were left exposed for approximately 30 years in a pond with an area of about 15.5 ha, thus leading to the generation of Fe-rich AMD (Bernier et al. 2001; Genty et al. 2016).

In 1998, the site was rehabilitated using a 1.1 m thick multi-layer cover with capillary barrier effects (CCBEs) composed of (from the base to the top): 0.3 m of sand, 0.5 m of silt, and 0.3 m of sand and gravel (Bussière et al. 2009). The principle of the CCBE is based on the use of unsaturated soil properties to maintain the fine-grained layer at a sufficiently high degree of saturation to be used as an effective barrier to the ingress of oxygen (Bussière et al. 2003). The cover was placed over the severely weathered tailings in order to prevent oxygen from reaching the tailings and, thus, to limit further AMD production.

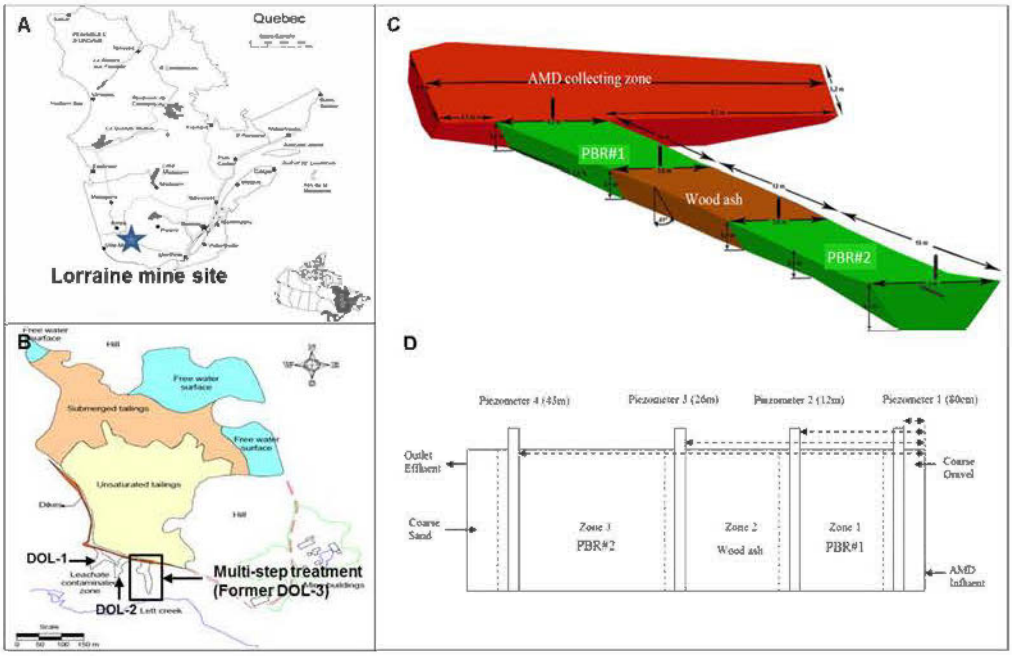

Figure 5.2 A) Map showing the location of Lorraine mine site; B) Plan view of the Lorraine multi-step treatment system (former DOL-3) and tailings pond; C) Model of the multi-step system; D) Layout of the sampling points (Nastev and Aubertin, 2000; Genty, 2012; Genty et al. 2016)

The reclamation system was proven to be effective as the pore water quality, i.e., AMD (pH <3 and 11 g/L Fe before installation of the CCBE) significantly improved (pH 5–6, about 2.5 g/L Fe) within 12 years of implementation (Genty et al. 2016). However, this this Fe-rich pore water could take a number of years before being completely discharged. Thus, passive systems for water treatment were also constructed.

5.4.2.2 Features and design of the existing passive treatment system

In 1998, one limestone drain and three anoxic dolomitic drains (DOL-1, -2, and -3) with impermeable walls were installed. The goal of these structures, which consisted of trenches (length 50−69 m, cross section area 1.68 m^2, mass of calcite or dolomite rocks of around 38.05−194.2 tons), was to treat the AMD flowing from beneath the

covered tailings (Fig. 5.2B). The trenches were isolated by a bentonitic geocomposite and covered with soil. The AMD flows into the drains by gravity and the neutralized effluent is discharged through a pipe and released directly into the environment (Potvin, 2009). In 2011, due to clogging issues, DOL-3 was replaced by a multi-step system (Fig. 5.2C). This system consists of three units (45 m length, 3.5 m width, and 1 m height) with a total volume of 158 m^3. The two units on the ends are PBRs (zone 1 and zone 3) which are filled with a mixture of organic materials and crushed limestone (Table 5.3), and the middle unit is comprised of wood ash (zone 2) (Fig. 5.2C, D). The estimated total HRT is 12 d.

Table 5.3 Characteristics of mixtures filling the three units composing the field multi-step system in the Lorraine mine site

Mixture	PBR#1 (P2)	WA (P3)	PBR#2 (P4)
	%w/w		
Composition			
Structural agent			
Sand	10	-	21
Cellulosic wastes			
Wood chips	18	-	36
Organic wastes			
Chicken manure	10	-	17
Compost	12	-	24
Neutralizing agents			
Wood ash	-	*100*	-
Calcite	50	-	2
Total	*100*	*100*	*100*
HRT (days)	3	3	5
Porosity (*n*)	0.41	0.47	0.46

The first PBR (PBR#1) was designed to neutralize acidity and partially remove metals, the wood ash reactor was used largely to decrease Fe concentrations, and the second PBR (PBR#2) functioned as a polishing treatment (Fig. 5.2D). The monitoring of the system started in October 2011, immediately after its construction. In 2012, due to a

low flow through the system, the mixtures in all three units were remixed and coarse rocks were added between each two units (Genty et al. 2016). Nevertheless, preferential flow and partial water bypassing the system was still observed (Fig. C2).

5.4.2.1 Field multi-step treatment (FM) monitoring

Sampling campaigns were performed yearly, during the summer, for over 5 years (2011–2016). Water was pumped from the four piezometers (P1 to P4) with a peristaltic pump connected to a generator (Fig. 5.2D). The flow (at the outlet), basic physicochemical parameters (pH, ORP, EC, and temperature), and piezometric head in the four piezometers were measured on site. The pH, EC, and temperature were measured with a portable multiparameter PCSTestr 35 and the ORP with an ORPTestr 10 (Oakton-Eutech instruments). Samples were preserved in pre-cleaned polyethylene bottles and transported on ice to the laboratory for alkalinity, acidity, and total metal analysis. In addition, water at the outlet of the system was collected and analyzed for total metal concentrations. Alkalinity, acidity, as well as the total metal concentrations were determined with the same methods as described for the laboratory samples.
The k_{sat} was determined by using Darcy's law (Eq. 5.2):

$$k_{sat}=Q/(A.dH/dL) \qquad (5.2)$$

where Q is the flow rate (m^3/s), A is the cross section of the reactor (m^2) and dH/dL is the hydraulic gradient (between P1 and the P4, in m/m).

5.5 Assessment of scale effects

As previously mentioned, the assessment of scale effects in the present study was performed with respect to efficiency (input vs output) and stability (efficiency over time). To do so, a comparison of efficiencies between the laboratory and field experiments was performed. The results were used to propose new design criteria that

could be useful for constructing an efficient multi-step system for the passive treatment of Fe-rich AMD.

5.5.1 Performance comparision of laboratory and field-scale tests

Calculated metal removal efficiencies (Eq. 5.1; considered as timeless and space-independent) were compared between the laboratory and field tests, and used to identify the parameters necessary to upscale the system. The appraisal considered the evolution of both the physicochemical and the hydraulic parameters during the treatment.

Statistical analysis was performed to compare the correlations between physicochemical parameters and metal concentrations, using variables such as pH, EC, metals (Al, Fe, Ca, Mg, Mn, Ni, Pb, Si, and Zn) and SO_4^{2-} concentrations. The results were interpreted according to two factors, F1 and F2. Principal component analysis, which was carried out using XLSTAT (18.06.36970), was used to determine the hypothetical variables (components) that could account for as much as possible of the variability in the multidimensional data (Maqsoud et al. 2016). Correlations between the variables and their dispersion, while preserving as much as possible relevant information, were then analyzed. This allowed for the evaluation and identification of any discrepancies between the most important variable regardless of the conditions and context of operation. Vector space was used to transform and reduce the dimensionality of the large data set. Thus, the obtained graphical projection (often in a circle radius) of the correlation value allows the large volume of original data to be interpreted in just a few variables (i.e., the principal components). The calculations are based on the Pearson's correlation coefficient (n). The greater the correlation value (closer to −1 or +1), the stronger the correlation between the variables and the factor.

5.5.2 Identification of new design criteria

After comparing the performances of the laboratory-scale and pilot field-scale systems, analyses based on observations and interpretations of the quantitative results were carried out. Firstly, the identification of the parameters that could drive any efficiency similarities or dissimilarities was carried out. Thereafter, these parameters allowed recording any changes in performance, including the lowest and highest performance, which were then used to establish new design criteria. Likewise, results from previous studies were used to validate the findings.

5.6 Results and discussion

The three laboratory-scale scenarios of multi-step systems showed that the efficiency (in terms of Fe removal) with two pre-treatment units was improved relative to single-unit systems. Scenario LM-3, which included two WA50 pre-treatment units, yielded higher efficiencies than either the LM-1 or LM-2 scenarios, as well as the field system.

5.6.1 Performance of laboratory-scale vs field-scale pilot experiments

Laboratory-scale and field-scale experiments were compared through their physicochemical characteristics, metal and SO_4^{2-} removal efficiencies, and evolution of hydraulic parameters.

5.6.1.1 Physicochemical quality

The pH of AMD increased from between 2.3 and 4.3 to between 5 and 8.21 for LM-1, 4.73 and 6.68 for LM-2, and 4.44 and 8.09 for LM-3 (Fig. 5.3).

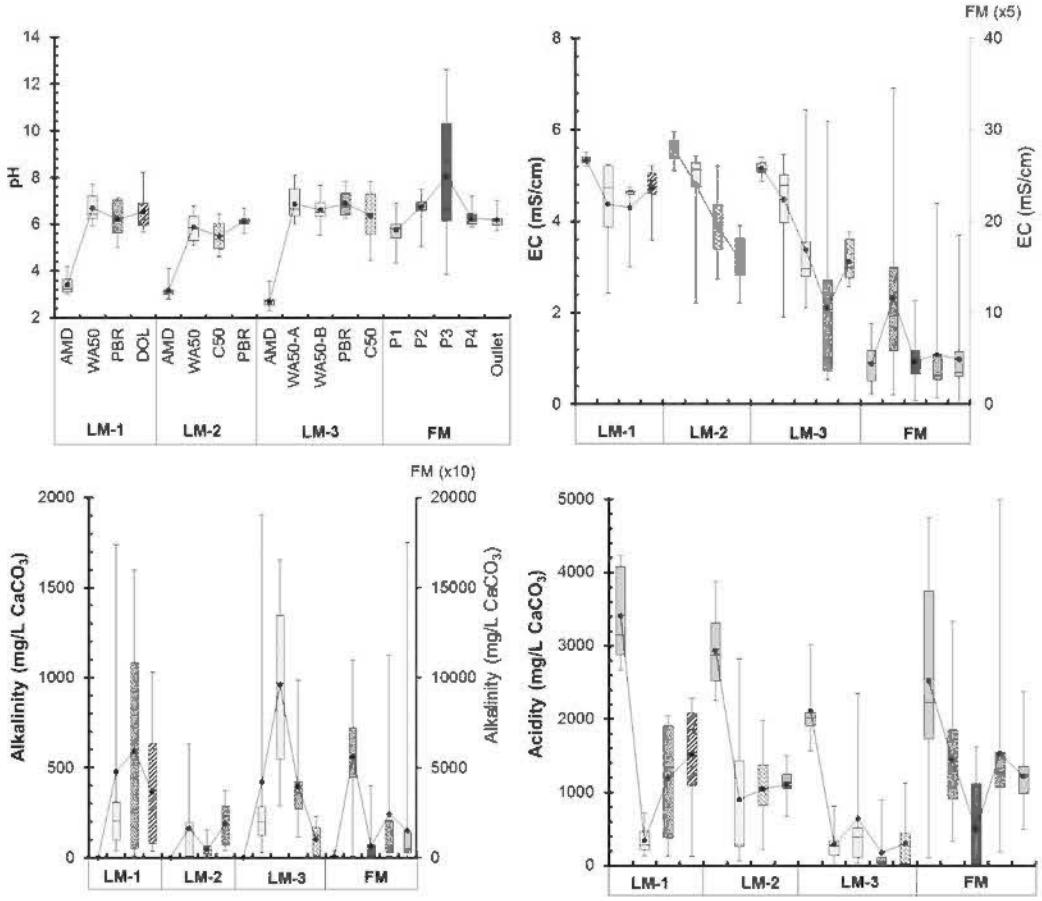

Figure 5.3 Box and whisker plots showing the comparison of physicochemical evolution (minimum, first quartile, median, third quartile, maximum, mean) of reactors during laboratory-scale and pilot field-scale experiments; ▭AMD, ⁘WA50, ▩ PBR, ▨ DOL, ▩ C50, ▩ WA, ▩ Outlet

On site, pH increased from a minimum of 4.33 to 5.73−7.01. A large, distinctive statistical distribution of pH values was observed in C50 (LM-3), and principally in P3 (FM), suggesting a variable increase in pH (Fig. 5.3). On the contrary, pH values recorded in the PBRs from laboratory and field experiments showed narrower distributions, with more consistent increases.

The EC values measured on site (in all sections) were five times higher than the laboratory values, regardless of the mass and volume of the substrates (Fig. 5.3). This

was attributed to a higher contamination of AMD on site, the decomposition of organic material, and the leaching of some metals from the reactive mixtures.

Despite the large distribution of the ORP values in the PBRs on site vs in the laboratory, the conditions appeared to be stable, with a mean of +37.5 mV in P2, +107 mV in P4, whereas they ranged between −79 and +141 mV all along the laboratory experiment (Tables 5.4, 5.5; Fig. C3).

Improved acid removal was found with two pre-treatment units of WA-DAS (98% in LM-3); however, the rapid decrease in alkalinity (down to ten times) would entail lower acid neutralization and potential re-dissolution of metals (Fig. C4). Similarly, the alkalinity in P3 decreased eight times the initial value (~4000 mg/L $CaCO_3$), followed by an increase in acidity by around 12% (Fig. 5.3).

Pre-treatment is crucial for a multi-step treatment system. Using a PBR as pre-treatment could be more advantageous than a DAS-based reactor because it can maintain continuous levels of alkalinity to keep up the constant input of acid and metal loads from AMD. Indeed, PBR#1 could produce higher alkalinity relative to WA-DAS reactors (1456 mg/L $CaCO_3$ vs ~475 mg/L $CaCO_3$, respectively).

When a single wood ash-based pre-treatment unit was used, >99.9% efficiency (Fe removal) was observed for a period of about 3 weeks in LM-1; however, efficiencies rapidly deteriorated (Fig. 5.4). This deterioration was accompanied by a decrease in pH and alkalinity, thus leading to a low Fe removal and an increase in Fe concentrations. Likewise, during year 3 of field testing, the acidity of the output from the wood ash unit (P3) was 3−66% higher than the input value. Therefore, the field experiments showed that Fe leaching occurred after wood ash unit's saturation. Consequently, the Fe leaching entailed an increase of the acidity in the following unit (i.e., PBR#2) by 10−68% (negative values in Table 5.5; Fig. 5.3). The increase in acidity could potentially be explained also by a lack of sufficient alkalinity in the PBR to buffer the acid produced during metal removal (Neculita et al. 2008). Indeed, all the soluble biogenic sulfides are consumed and alkalinity is depleted due to excess of dissolved

divalent metals while additional acidity could be generated (Johnson and Hallberg, 2005). In addition, SO_4^{2-} reduction was reported as an important source of alkalinity providing that some H_2S remains unreacted for metal retention (Dvorak et al. 1991). Hence, in order to compensate for the released acidity, the performance of the PBR would have to rely upon additional alkalinity provided by the alkaline agents in the substrate. This could explain the fact that when two WA-DAS pre-treatments were used, the following PBR (LM-3) presented a higher acidity removal (81%) (Fig. C4). Therefore, the concentrations of metals and SO_4^{2-} must be equally lowered.

Table 5.4 Efficiency comparison of laboratory-scale experiments of the multi-step passive treatment of ferriferous AMD

Parameters	LM-1			LM-2			LM-3			
	WA50-A	**PBR**	**DOL**	**WA50-A**	**C50**	**PBR**	**WA50-B**	**WA50-A**	**PBR**	**C50**
pH	5.95–7.7	5–7.13	5.67–8.21	5.1–6.77	4.62–6.44	5.62–6.68	6.01–8.09	5.54–7.66	6.26–7.84	4.44–7.82
ORP (mV)	+84	–47	–18	+141	+84	–29	+18	–79	+21	+81
EC (mS/cm)	4.37	4.30	4.73	4.79	3.91	3.16	4.3	3.44	1.95	2.92
Fe_t removal (%)	36	33	–9	21	71	16	91	52	61	–71 (1^{st} 10 weeks) 68 (last 6 weeks)
SO_4^{2-} removal (%)	20	23	–12	16	36	16	39	70	>99	–99.7
Acid removal (%)	32	30	–2	24	55	<5	90	28	81	–29
Alkalinity ($mgCaCO_3/L$)	39–1738	26–1597	36–1028	3–630	5–155	37–375	30–1905	289–1654	117–985	0–230

Table 5.5 Efficiency of field-scale experiment using multi-step passive treatment of ferriferous AMD

Parameters	P2	P3	P4	Outlet
pH	6.74	8.04	6.26	6.18
ORP (mV)	+37.5	+55	+107	+100
EC (mS/cm)	11.6	4.7	5.5	4.88
Fe_t removal (%)	93	99.2 (1st two years) −64 (last three years)	−70 (1st three years) 48 (last two years)	−27
SO_4^{2-} removal (%)	69	72.2 (1st year) −73 (last 4 years)	47	−11
Acid removal (%)	37	78 (1st three years) −24 (last two years)	−44 (1st four years) 22.4 (last one year)	34 (1st two years) −14 (last four years)
Alkalinity ($mgCaCO_3/L$)	62–11000	0–4000	63–11250	133–17500

5.6.1.1 Metal and sulfate removal

Scenario LM-1 showed the lowest Fe removal efficiency (53%) and LM-3 the highest (99%). LM-2 and FM tests showed similar efficiencies (≈75% in total from all units; Fig. 5.4). The WA50 pre-treatment unit removed up to 99% of Fe, but then decreased rapidly to 36% at an initial Fe concentration >2000 mg/L. However, at Fe <2000 mg/L, the same unit could maintain an efficiency of around 91% (Fig. C5). The performance of WA50 would be better relative to a 100% wood ash reactor (P3 in FM) since the efficiency of this latter was improved due to the preceding PBR#1 unit that lessen the contaminations (acid and metal loads). The WA50 reactors (in LM-3) could remove up to 427 g/m^3/d of Fe, and the following PBR could remove between 4 and 73 g Fe/m^3/d. In the same scenario, the highest efficiency in the PBR (up to 87% Fe removal) was recorded when acidity was lower than 300 mg/L as $CaCO_3$ (81% removal; Table 5.4). On site, PBR#1 removed 93% of Fe (initial concentration of 1715 ± 740 mg/L) even when exposed to acidities greater than 2500 mg/L $CaCO_3$. This was likely due to the presence of sufficient alkalinity, which would allow SRB to thrive. In samples collected on site, MPN analyses showed that SRB were present on the order of 10^6 cells/100 mL (Fig. C5).

SRB in PBRs are often outcompeted by IRB during the treatment of Fe-rich AMD, thus influencing Fe vs SO_4^{2-} removal (Rakotonimaro et al. 2017). Based on Fe concentrations in C50 (in LM-3, mean Fe = 562 mg/L) and P3 (in FM, mean Fe = 365 mg/L) (both units preceded a PBR), the development of IRB could have been promoted at Fe >300 mg/L and SRB could have been inhibited. The counts of SRB and IRB in LM-2 were similar (10^4–10^5 cells/100 mL), whereas in LM-3, significant differences were observed (10^4–10^5 cells/100 mL vs 200–5000 cells/100 mL for SRB and IRB, respectively; Fig. C5). A predominant bacterial reduction of Fe^{3+} could have increased Fe^{2+} concentration, thus triggering a low Fe removal. In addition, the low concentrations of S^{2-} (0.03–4.35 mg/L) during the experiment give an Fe^{2+}/H_2S ratio

>10, indicating the contribution of Fe reduction (Chapelle et al. 2009). Even though SRB were abundant, a shift in the relative importance of Fe reduction and SO_4^{2-} reduction could occur with respect to Fe concentration and alkalinity. During the transition process, an excess of Fe^{2+} would be consumed first, prior to reaching favorable conditions for SO_4^{2-} reduction (Fe^{2+}/H_2S = 0.3 ; Chapelle et al. 2009). In support of this assumption, Fe^{2+} removal observed during laboratory-based experiments indicated that a PBR removed between 18–42% of Fe when its initial value ranged between 200–500 mg/L and 16–21% of SO_4^{2-} when its initial concentration was >1000 mg/L (Fig. C5). However, at Fe <200 mg/L and SO_4^{2-}<1000 mg/L, removal was >97% and 71–99.2%, respectively. These findings show that the PBR was efficient when Fe <200 mg/L (Fe^{2+}/SO_4^{2-} <0.2).

Another noted similarity in all studied systems was the increase of Fe concentrations after treatment with PBRs, either in the polishing units (laboratory) or at the outlet (field). On site, Fe concentrations increased by 27% when the drainage waters were exposed to air (Table 5.5). Similarly, Fe concentrations increased by up to 71% in C50 in LM-3 (Table 5.4). This was most likely due to re-oxidation of Fe^{2+} because of high DO (Fig. C4), thus entailing further increases in acidity and dissolved metal concentrations. Therefore, a polishing treatment, which would produce enough alkalinity, is then suggested to be used following a PBR, if residual Fe concentrations exceed 25 mg/L. An ALD could be advantageous because it would produce alkalinity six to seven times higher compared to dolomite, depending on the grain size (Potgieter-Vermaak et al. 2006; Genty et al. 2012). Moreover, less surface area would be required (approximately two to four times less) since this study showed that a minimum HRT of 3 d was required to treat Fe-rich AMD with a DOL, whereas a HRT of only 15 h was required with an ALD (Hedin et al. 1994; Genty et al. 2012).

A solely DAS-based multi-step treatment system might be considered closely based on the efficiency reached from the two pre-treatment units in LM-2 and LM-3 (observed

Fe and SO_4^{2-} removal efficiencies were 76–99% and 46–74%, respectively; Fig. 5.4). However, the necessity of a frequent replacement of the reactive mixtures could occur due to saturation (Rötting et al. 2008a). Therefore, the lifespan of DAS columns would be extended when used to treat AMD with lower Fe contamination.

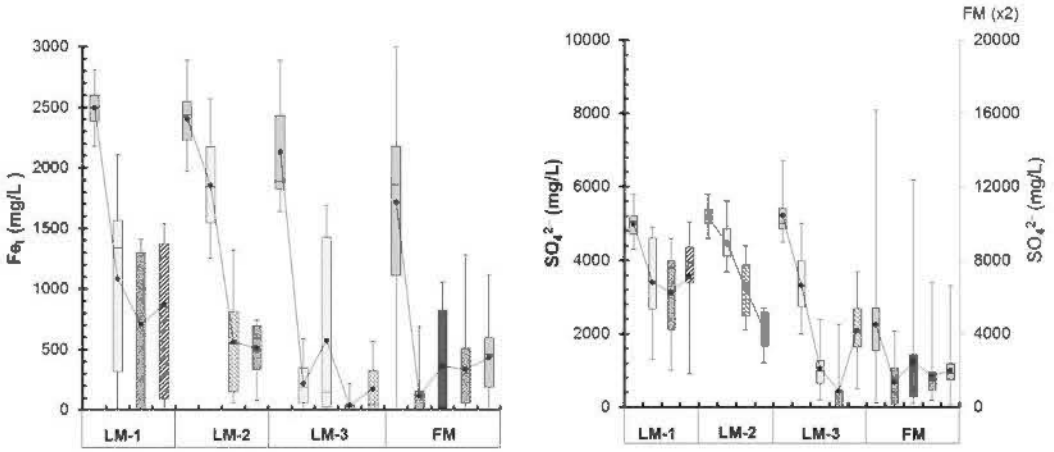

Figure 5.4 Box and whisker plots of Fe_t and SO_4^{2-} concentrations (minimum, 25% percentile, median, 75% percentile, maximum, mean) during laboratory-scale and field-scale experiments

All the treatments showed decreases in Al, Ni and Pb concentrations by 96%, >83%, and 52–92%, respectively (Fig. 5.5). In addition, these metals were removed early (>72%) in the first pre-treatment units (WA50 and PBR#1). However, initial concentrations of these metals were very low (<1 mg/L). The most significant Zn removal was observed in the PBR in scenario LM-2 (94%), which could be due to its adsorption onto Fe and Al (oxy) hydroxides. In the laboratory, the Mn was removed during the first phase of pre-treatment in the WA50 unit (up to 98%) due to the high pH values (>8). These findings are consistent with previous data reported by Genty (2012).

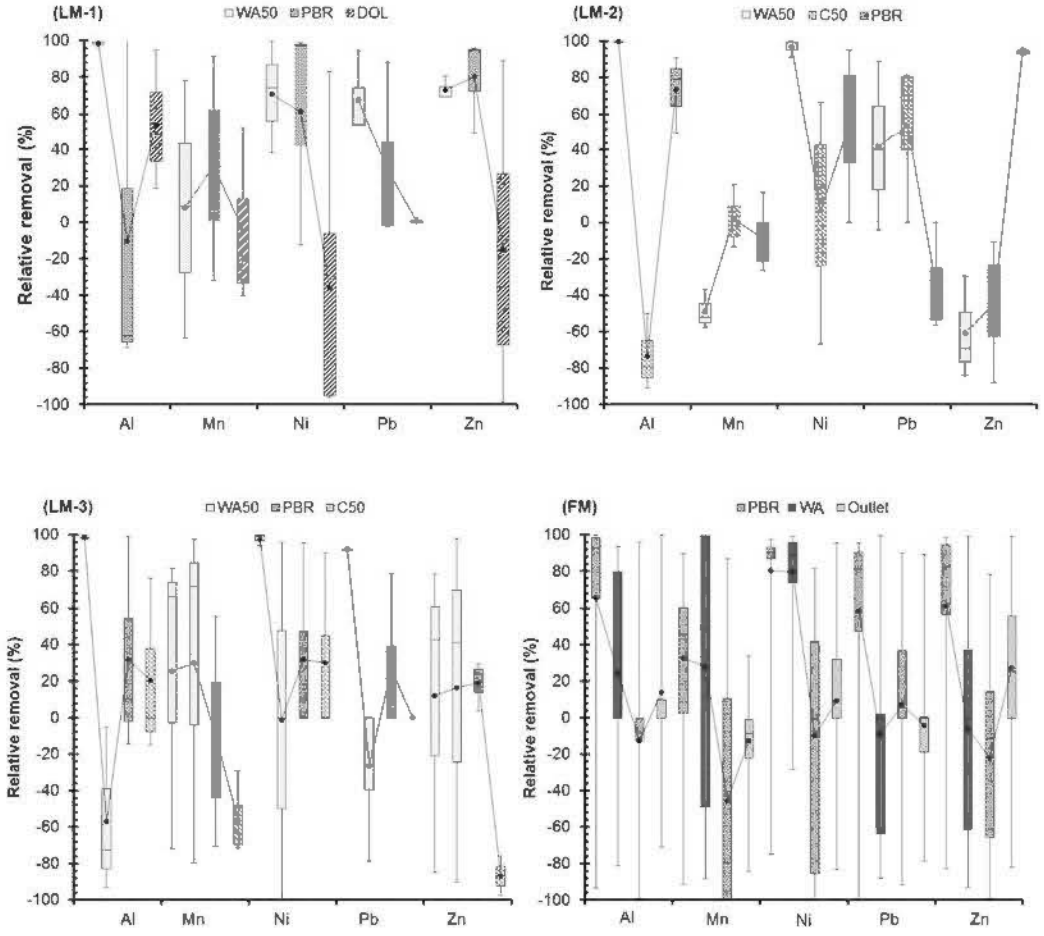

Figure 5.5 Box and whisker plots of relative metals removal (minimum, 25% percentile, median, 75% percentile, maximum, mean) during laboratory-scale and field-scale experiments

On site, during the first two years, Mn in P2 (PBR#1) was higher than in P1 (AMD), likely due to leaching from the materials composing the reactive mixture. However, after two years, it decreased down to around 50% probably because of the efficient performance of the previously installed CCBE (Bussière et al. 2003).

Statistical analyses showed that Fe concentrations were strongly correlated to Al, Ni, Pb and SO_4^{2-} (Table C1). Calculations between variables and factors indicated that the

variance represented by the factors F1 and F2 was 85% (variance by ouly F1 was 63% and F2 22%). Factor F1 was negatively correlated to Al, Fe, Ni, Pb, and SO_4^{2-} concentrations, as well as to EC. In contrast, factor F2 was positively correlated to concentrations of Mg, Mn, Zn, and SO_4^{2-} (Table C2). Factor F1 (Fig. 5.6), indicates an opposing spatial representation of the iulet waters (AMD-1, AMD-2, AMD-3, P1) and the outlet water collected from the multi-step treatment in the field and in the laboratory (FM, LM-1, LM-2, LM-3). Therefore, the F1 axis (y) separates the multi-step treatment that contains the lowest and the highest contamination. The F2 axis (x) indicates contrasting spatial representation between waters with high and low concentrations of metals and SO_4^{2-}. Thus, the same spatial representation points out that all the multi-step systems remove metals and SO_4^{2-} (Fig. 5.6). Accordingly, LM-1 and LM-2 are the two scenarios that removed the lowest amounts of Fe and SO_4^{2-} relative to FM and LM-3. In addition, LM-3 is diametrically opposed to LM-1; i.e., this scenario had the highest efficiency.

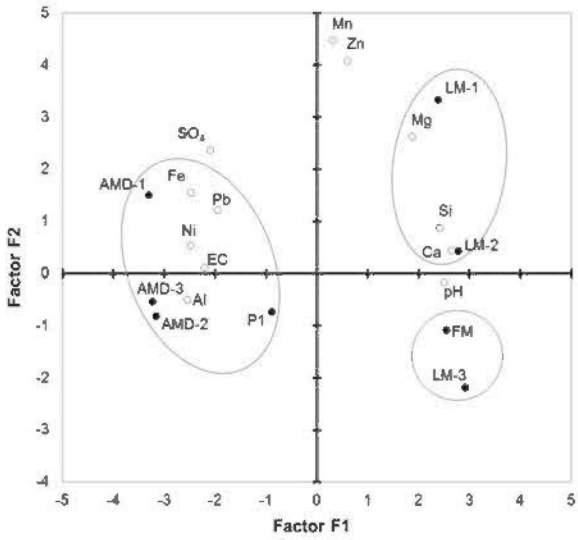

Figure 5.6 Principal component analysis of water collected during laboratory and field multi-step treatment experiments: projection of variables on the plane F1–F2

5.6.1.2 Evolution of hydraulic parameters

The estimated porosity varied from 0.40 (DOL) to 0.77 (WA50-A and WA50-B), while the initial flow rate (Q) ranged from 0.86 mL/min (DOL) to 1.6 mL/min (WA50-DAS). The k_{sat} values were 7.7 x 10^{-3} cm/s (WA50-A), 1.4 x 10^{-2} cm/s (WA50-B), 3 x 10^{-2} cm/s (C50), 1.1 x 10^{-3} cm/s (DOL), and 2.1 x10^{-2} cm/s (PBR). The evolution of Q and k_{sat} was recorded only for scenario LM-3. At the outlet of each unit, the Q decreased, entailing a decrease of 10^{-1} cm/s from the initial values of the k_{sat} (overall mean k_{sat} on the order of 10^{-3} cm/s). These results were consistent with what was found in previous studies (using both columns and medium size reactors) with k_{sat} values ranging on the order of 10^{-3} to 10^{-4} cm/s (Genty, 2012). This study supports the findings of previous works (Genty, 2012; Genty et al. 2017a) during which clogging issues and short-circuiting were not encountered during the laboratory experiments. Mineralogical analyses and modeling of secondary precipitates performed in previous studies showed the significant presence of Fe-oxides/hydroxides precipitates, which are less recalcitrant than gypsum, and thus may explain the lack of clogging (Rakotonimaro et al. 2017; Genty et al. 2017b).

On site, Q varied from 0.13 to 5 L/min (Fig. C6), where the third quartile indicated values less than 1.13 L/min (Fig. 5.7). The k_{sat} was estimated between 10^{-5}–4.4 x10^{-3} cm/s (Fig. 5.7) which could be 10^{-1} to 10^{-2} cm/s unit less than during laboratory experiment. Given the fact that the Q of the laboratory-based system was almost half of the estimated field rate (after excluding the scale of x1000), this difference showed that the changes in the hydraulic properties of the mixture were beneficial. According to the evolution of k_{sat} on site, a decrease on the order of 10^{-2} cm/s could be expected when the substrate has initial k_{sat} <10^{-3} cm/s. In this case, a correction factor of 1/100 could be applied between the laboratory and field k_{sat} values.

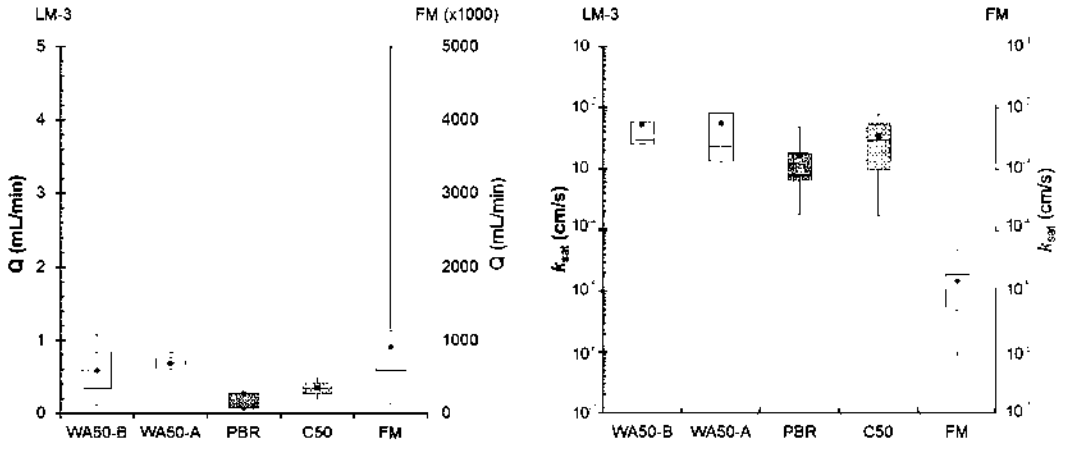

Figure 5.7 Box and whisker plots showing Q and k_{sat} (minimum, 25% percentile, median, 75% percentile, maximum, mean) during LM-3 and FM experiments

In summary, the differences in performance between the laboratory- and field-scale experiments could have been influenced by factors such as electrical conductivity, Q, k_{sat}, and Fe and SO_4^{2-} concentrations. Control over the operating conditions during laboratory experiments could have resulted in overestimation of the treatment systems' performance relative to the field experiments, where conditions are not controllable. For example, in the laboratory, constant temperatures would be expected and peristaltic pumps are used to control flow, while in the field, the temperature is determined by the weather and flow is gravitational.

5.6.2 Identification of new design criteria

The evolution of mixtures comprising the multi-step treatment units showed that the adjustment of the proportions is essential as it can change the hydraulic properties of the system. Indeed, when the amount of cellulosic wastes (porous materials) in the PBR mixture was increased (from 18% to >40%), n increased almost two times (0.41–0.46 on site vs 0.69 in laboratory) and the k_{sat} increased by 10 cm/s from its initial value (10^{-3} cm/s on site vs 10^{-2} cm/s in laboratory). At the same time, when the mixtures were

composed of more than 20% of alkaline agent, the PBR could produce constant alkalinity (about 376 mg $CaCO_3$/L), which was higher than the average alkalinity reported in a previous study (214 mg $CaCO_3$/L; Genty, 2012). Varying proportions of alkaline agents and/or porous organic materials in the mixture, with respect to initial Fe concentrations, are then strategically essential to maintaining a high k_{sat} value while preserving efficiency. Indeed, with less than 2% of limestone in a PBR (P4 in FM), Fe leaching was found during the first 3 years (9–100%). Oppositely, a PBR (laboratory experiments) comprised of 20% of an alkaline agent contributed to Fe removal (16–86%) throughout the duration of testing. Other studies showed that with limestone proportions between 5 and 12.5%, Fe removal was 94–99% (average initial concentration of 71 mg/L; McCauley et al. 2009). A higher amount of limestone (25%) was required to remove 78–98% of Fe with an input of 140 mg/L (Thomas and Romanek, 2002). This suggests that more than 20% of limestone could be required to remove around 200 mg/L of Fe in a PBR. The addition of organic porous media (40%) is also proposed in order to obtain a higher porosity and to minimize biomass fouling.

Following the efficiency comparison of the laboratory-based and field pilot experiments, Fe concentrations appeared to drive the performance of a multi-step treatment of Fe-rich AMD when other metal concentrations were significantly lower (or absent). The efficiency obtained during laboratory experiments, both this study and previous studies (Rötting et al. 2008a, 2008b), including one with medium size systems (2000 m^3, 12 d of HRT; Genty, 2012), indicated that a correction factor of 0.2–0.8 could be used to evaluate field performance. Amongst the probable factors that could drive this difference, particularly in the case of PBRs, is the variation of temperature since water temperature affects microbial activity and metabolic reaction rates unless additional sufficient carbon substrate is provided (Janin and Harrington, 2015). On site, no further addition of substrate was performed and the temperature varied from 2–24.5 °C whereas in the laboratory, temperature was relatively constant (~23 °C). Although the efficiency of PBRs reported in several studies varied, the results obtained

in this study suggested a design criteria for the treatment of Fe-rich AMD at Fe <26 g/m^3 substrate/d, and SO_4^{2-} <10 g/m^3 substrate/d. The rate was calculated according to equation 5.3 (Hedin et al. 1994):

$$Fe_{removed}\ (g/m^3\ substrate/d) = 1.44 \times Q\ (L/min) \times \Delta Fe\ (mg/L) / V\ (m^3) \qquad (5.3)$$

where Q is the flow rate, ΔFe is the difference between the Fe input and output, and V is the volume.

The concentration of other metals was low in the present study, but if significant (especially Al, which could precipitate at an early stage), they must be taken into account in the design criteria. Previous work suggested that Al loads should be <10 g Al/m^2/d (Rötting et al. 2008a). For a DAS reactor, Fe <150 g/m^3/d is proposed if used as a treatment system.

Localized dissolution of calcite in the DAS mixture could increase total porosity, but not necessarily effective porosity, which would simultaneously raise the k_{sat} (Rötting et al. 2015). Hence, the k_{sat} is apparently a more appropriate parameter that directly affects the long-term performance, as it is proportional to Q, which is in turn inversely proportional to the HRT [Q = (V_t x n) / HRT]. In the field, highly variable flow rates may result in significant changes in the HRT; i.e., increases or decreases in Q would translate to decreases or increases, respectively, in the HRT. Thus, only relying on the HRT, which considers the average Q as design criteria could bias the framework and the upscaling. Instead, the lowest and the highest measured (or estimated) Q values should be used to forecast the long-term performance and stability of a treatment system. The lowest Q could predict an optimum efficiency but may predispose the system to a shorter performance because of potentially higher loads. On the other hand, the highest Q could yield a minimum efficiency but would ensure a longer lifespan. This hypothesis is corroborated by the trend in k_{sat} values during the field pilot experiment, which showed a significant decrease (around 10^{-5} cm/s) at Q <0.5 L/min (Fig. 5.8). At the same time, the decline of k_{sat} appears to be related to the decrease in

Fe and SO_4^{2-} concentrations; i.e., the clogging could be due to mineral precipitates (e.g., metal sulfides, gypsum).

In this study, establishing the design according to the lowest and the mean value of Q measured on site is suggested. In addition, the design criteria should include the k_{sat}, as well as Fe and SO_4^{2-} concentrations. Moreover, a correction factor of at least 1/100 on the k_{sat} can be applied, based on values obtained in the laboratory vs field experiments, to predict the durability according to Q_{min}.

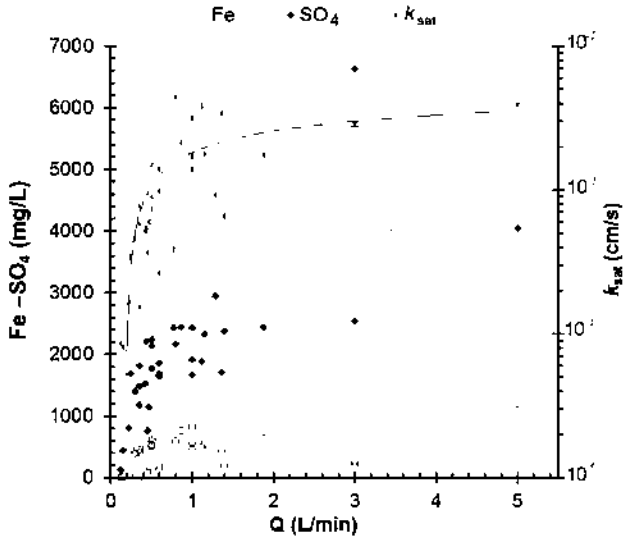

Figure 5.8 Concentrations of Fe, SO_4 (at the outlet) and k_{sat} values according to the measured flow (Q) during the field pilot experiment

5.7 Conclusion

The results of laboratory-based experiments (three scenarios, referred to as LM-1, LM-2, and LM-3; each comprised of one or two pre-treatment units, one basic treatment unit, and/or one polishing unit) and field-based pilot experiments (FM; comprised of two PBRs, separated by a wood ash reactor) were compared. The objective of the study was to evaluate the scale effects during the conversion of laboratory-scale to field-scale

multi-step passive treatment systems for Fe-rich AMD. Amongst the factors that could influence the differences in the performance of the laboratory-scale and field-scale systems are the EC, Q, k_{sat}, and Fe and SO_4^{2-} concentrations.

In the laboratory, the most efficient scenario (LM-3) removed up to 99% of the initial Fe over a period of 112 days. In the field, Fe removal was of 33–98.5% over a 5-year period. The most efficient pre-treatment units were the two WA50, with an overall Fe removal of 76–99.6%, in addition to 46–82% SO_4^{2-} removal. Consequently, the subsequent PBR could remove 86% Fe and >99% SO_4^{2-}. However, in long-term operation, using a WA50 reactor as a pre-treatment might be risky according to the on-site performance of the wood ash. This is because a rapid decrease in alkalinity could occur, thus resulting in a decline of efficiency (as found after 3 years in P3 unit of the field system). Hence, a pre-treatment unit that could provide continuous alkalinity, such as a PBR, is proposed instead. In this case, the mixture should be designed so that the reactor could produce sufficient and continuous alkalinity. On site, a mixture comprised of 50% of an alkaline agent, together with 30% of a porous organic material (to enhance the hydraulic parameters) proved efficient enough for Fe pretreatment over a 5-year period. However, when used as post-treatment to the wood ash reactor, a PBR with less than 2% of limestone (P4 in FM) showed Fe leaching during the first 3 years (9–100%). On the contrary, in laboratory testing, a mixture comprised of 20% limestone in a post-treatment PBR yielded steady Fe removal. In this latter case, the Fe load is suggested to be <26 g/m^3 substrate/d (Fe <200 mg/L) and SO_4^{2-} <110 g/ m^3 substrate/d. The evolution of the k_{sat} in the field system revealed that it was related to Fe and SO_4^{2-} concentrations, showing the potential for clogging because of mineral precipitates, which would result in an increase in HRT. Accordingly, upscaling from the laboratory to field-scale pilot treatment of Fe-rich AMD should consider design criteria based on Q, including k_{sat} (>10^{-3} cm/s), as well as Fe and SO_4^{2-} loads. Moreover, in order to predict the performance on site, a correction factor of 0.2–0.8 could be applied to Q and Fe removal, and a factor of at least 1/100 to k_{sat} values

measured in the laboratory. When designing a multi-step passive treatment system for Fe-rich AMD, a Fe pre-treatment unit is also recommended and should be operated under a high k_{sat} value and low HRT (with respect to Q) to minimize early clogging. However, validation of the results with other similar cases, as undertaken in this study, is necessary. Further studies investigating site-specific parameters that could cause a decrease of performance, such as the effects of ice cover, temperature, and the rate of substrate decomposition, should be undertaken.

Acknowledgements

This study was funded by the NSERC (Natural Sciences and Engineering Research Council of Canada), grant no. 469489-14, the MERN (Ministère de l'Énergie et des Ressources Naturelles – Québec's Ministry of Energy and Natural Resources), and the industrial partners of the RIME UQAT-Polytechnique Montreal, including Agnico Eagle, Canadian Malartic Mine, Iamgold, Raglan Mine-Glencore, and Rio Tinto. The authors want to thank sincerely Marc Paquin, Mélanie Bélanger, Patrick Bernèche, Joël Beauregard, Alain Perreault and Marouen Jouini for technical assistance during the laboratory and field experiments.

References

APHA (American Public Health Association) (2012) Alkalinity titration, standard methods for the examination of water and wastewater, 22nd edn. Greenberg A. (Eds.), Washington DC, USA

ASTM (American Society for Testing and Materials) (1990) Standard methods for sulphate reducing bacteria in water and water-formed deposit. In: Annual book of ASTM Standards, vol. 04.08. section D 4412–84, Washington, DC, pp 533–535

ASTM (American Society for Testing and Materials) (1995) Standard test method for permeability of granular soils. Annual book of ASTM Standards.08. D 2434 – 68, Philadelphia, PA, USA

Aubertin M, Bussière B, Bernier L (2002) Environnement et gestion des rejets miniers. Presses Internationales, Polytechnique Montréal, QC, Canada (in French)

http ://www.presses-polytechnique.ca/fr/environnement-et-gestion-des-rejets-miniers. Accessed 04 August 2017

Bernier L, Aubertin M, Dagenais AM, Bussière B, Bienvenu L, Cyr J (2001) Limestone drain design criteria in AMD passive treatment: theory, practice and hydrogeochemistry monitoring at Lorraine mine site, Temiscamingue. In: Proc. of the CIM Minespace 2001 annual meeting, technical paper n° 48, 9p

Bussière B, Potvin, R, Dagenais A-M, Aubertin M, Maqsoud A, Cyr J (2009) Restauration du site minier Lorraine, Latulipe, Québec : Résultats de 10 ans de suivi. Déchets- Revue francophone d'écologie industrielle 54: 49–64 (in French)

Bussière B, Aubertin M, Chapuis RP (2003) The behaviour of inclined covers used as oxygen barriers. Can Geotech J 40: 512–535

Caraballo MA, Macías F, Rötting TS, Nieto JM, Ayora C (2011) Long term remediation of highly polluted acid mine drainage: A sustainable approach to restore the environmental quality of the Odiel river basin. Environ Pollut 159 (12): 3613–3619

Caraballo MA, Rötting TS, Macías F, Nieto JM, Ayora C (2009) Field multi-step limestone and MgO passive system to treat acid mine drainage with high metal concentrations. Appl Geochem 24 (12): 2301–2311

Champagne P, Van Geel P, Parker W (2005) A Bench-scale assessment of a combined passive system to reduce concentrations of metals and sulphate in acid mine drainage. Mine Water Environ 24 (3): 124–133

Chapelle, FH, Bradley PM, Thomas MA, McMahon PB (2009) Distinguishing iron-reducing from sulfate-reducing conditions. Ground Water 47(2): 300–305

Clyde EJ, Champagne P, Jamieson HE, Gorman C, Sourial J (2016) The use of passive treatment for the mitigation of acid mine drainage at the Williams Brothers Mine (California): Pilot-scale study. J Clean Prod 130: 116–125

Cochran WG (1950) Estimation of bacterial densities by means of the most probable number. Biometrics 6: 105–116

Cocos IA, Zagury GJ, Clement B, Samson R (2002) Multiple factor design for reactive mixture selection for use in reactive walls in mine drainage treatment. Water Res 32: 167–177

Dvorak DH, Hedin RS, Edenborn HM, McIntire PE (1991) Treatment of metal-contaminated water using bacterial sulfate reduction: Results from pilot-scale reactors. In: Proc. of the National Meeting of the American Society of Mining and Reclamation (ASMR), May 14-17, Pittsburgh, PA, USA, pp 109–122

Figueroa L, Miller A, Zaluski M, Bless D (2007) Evaluation of a two-stage passive treatment approach for mining influenced waters. In: Proc. of the ASMR, June 2-7, Lexington, KY, USA, pp 238–247

Genty T, Bussière B, Benzaazoua M, Neculita CM, Zagury GJ (2017a) Changes in efficiency and hydraulic parameters during the passive treatment of acid mine drainage in biochemical reactors. Mine Water Environ (in corrections)

Genty T, Bussière B, Benzaazoua M, Neculita CM, Zagury GJ (2017b) Iron removal in highly contaminated acid mine drainage using passive biochemical reactors. Water Sci Technol (in press, doi: 10.2166/wst.2017.362)

Genty T, Bussière B, Paradie M, Neculita CM (2016) Passive biochemical treatment of ferriferous mine drainage: Lorraine mine site, Northern Québec, Canada. In: Proc. of the International Mine Water Association (IMWA), July 11-15, Leipzig, Germany

Genty T, Bussière B, Potvin R, Benzaazoua M, Zagury GJ (2012) Dissolution of calcitic marble and dolomitic rock in high iron concentrated acid mine drainage: Application to anoxic limestone drains. Environ Earth Sci 66: 2387–2401

Genty T (2012) Comportement hydro-bio-géo-chimique de systèmes passifs de traitement du drainage minier acide fortement contaminé en fer. PhD dissertation. Applied Sciences, RIME - UQAT, Rouyn-Noranda, QC, Canada, 270p (in French and English)

Gould WD, Stichbury M, Francis M, Lortie L, Blowes DW (2003) An MPN method for the enumeration of iron-reducing bacteria. In Proc. of the Mining and the environment III Conference. Laurentian University, Sudbury, ON, Canada, pp 25–28

HACH, 2013. Colorimeter procedures manual.

http://www.hach.com/quick.search-download.search.jsa?keywords=Colorimeter%20procedures%20manual. Accessed 04 August 2017

Hedin R, Weaver T, Wolfe N, Watzlaf G (2013) Effective passive treatment of coal mine drainage. Paper presented at the 35th annual National Association of Abandoned Mine Land Programs Conference, September 23, Daniels, WV, USA, 13p

Hedin RS, Weaver T, Wolfe N, Weaver K (2010) Passive treatment of acidic coal mine drainage: The Anna S mine passive treatment complex. Mine Water Environ 29: 165–175

Hedin RS, Watzlaf GR, Nairn RW (1994) Passive treatment of acid mine drainage with limestone. J Environ Qual 23: 1358–1345

Huminicki DMC, Rimstidt JD (2008) Neutralization of sulfuric acid solutions by calcite dissolution and the application to anoxic limestone drain design. Appl Geochem 23: 148–165

Janin A, Harrington J (2015) Performances of lab-scale anaerobic bioreactors at low temperature using Yukon native microorganisms. In: Proc. of Mine Water Solutions in Extreme Environments, April 12-15, Vancouver, Canada

Johnson DB, Hallberg KB (2005). Biogeochemistry of the compost bioreactor components of a composite acid mine drainage passive remediation system. Sci Total Environ 338: 81–93

Macías F, Caraballo MA, Rötting TS, Pérez-López R, Nieto JM, Ayora C (2012a) From highly polluted Zn-rich acid mine drainage to non-metallic waters: Implementation of a multi-step alkaline passive treatment system to remediate metal pollution. Sci Tot Environ 433: 323–330

Macías F, Caraballo MA, Nieto JM, Rötting TS, Ayora C (2012b) Natural pretreatment and passive remediation of highly polluted acid mine drainage. J Environ Manage 104: 93–100

Maqsoud A, Neculita CM, Bussière B, Benzaazoua M, Dionne J (2016) Impact of fresh tailing deposition on the evolution of groundwater hydrogeochemistry at the abandoned Manitou mine site, Québec, Canada. Environ Sci Pollut Res 23: 9054–9072

McCauley CA, O'Sullivan AD, Milke MW, Weber PA, Trumm DA (2009) Sulfate and metal removal in bioreactors treating acid mine drainage dominated with iron and aluminum. Water Res 43: 961–970

Nastev M, Aubertin M (2000) Hydrogeological modelling for the reclamation work at the Lorraine mine site Québec. In: Proc. of the 1st Joint IAH-CNC-CGS Groundwater Specialty Conference, Montreal, Canada, pp 311–318

Neculita CM, Yim GJ, Lee G, Ji SW, Jung JW, Park HS, Song H (2011) Comparative effectiveness of mixed organic substrates to mushroom compost for treatment of mine drainage in passive bioreactors. Chemosphere 83: 76-82

Neculita CM, Zagury GJ, Bussière B (2008) Effectiveness of sulfate-reducing passive bioreactors for treating highly contaminated acid mine drainage: I. Effect of hydraulic retention time. Appl Geochem 23: 3442–3451

Postgate JR (1984) The sulfate-reducing bacteria. 2nd edn. Cambridge University Press: Cambridge

Potgieter-Vermaak SS, Potgieter JH, Monama P, Van Grieken R (2006) Comparison of limestone, dolomite and fly ash as pre-treatment agents for acid mine drainage. Miner Eng 19: 454–462

Potvin R (2009) Évaluation à différentes échelles de la performance de systèmes de traitement passif pour les effluents fortement contaminés par le drainage minier

acide. PhD dissertation. Applied Sciences, UQAT, Rouyn-Noranda, QC, Canada, 335p (in French)

Prasad D, Henry JG (2009) Removal of sulphates acidity and iron from acid mine drainage in a bench scale biochemical treatment system. Environ Technol 30(2): 151–160.

Rakotonimaro TV, Neculita CM, Bussière B, Zagury GJ (2017) Comparative column testing of three reactive mixtures for the bio-chemical treatment of iron rich acid mine drainage. Miner Eng 11: 79–89

Rakotonimaro TV, Neculita CM, Bussière B, Zagury GJ (2016) Effectiveness of various dispersed alkaline substrates for the pretreatment of ferriferous acid mine drainage. Appl Geochem 73: 13–23

Rötting TS, Luquot L, Carrera J, Casalinuovo DJ (2015) Changes in porosity, permeability, water retention curve and reactive surface area during carbonate rock dissolution. Chem Geol 403: 86–98

Rötting TS, Caraballo MA, Serrano JA, Ayora C, Carrera J (2008a) Field application of calcite Dispersed Alkaline Substrate (calcite-DAS) for passive treatment of acid mine drainage with high Al and metal concentrations. Appl Geochem 23: 1660–1674

Rötting TS, Thomas RC, Ayora C, Carrera J (2008b) Passive treatment of acid mine drainage with high metal concentrations using dispersed alkaline substrate. J Environ Qual 37: 1741–1751

Rötting TS, Ayora C, Carrera J (2007) Chemical and hydraulic performance of "Dispersed Alkaline Substrate" (DAS) for passive treatment of acid mine drainage with high metal concentrations. In: Proc. of the IMWA, May 27-31, Cagliary, Italy

Strosnider WHJ, Nairn RW, Peer RAM, Winfrey BK (2013) Passive co-treatment of acid mine drainage and sewage: Anaerobic incubation reveals a regeneration technique and further treatment possibilities. Ecol Eng 610: 268–273

Skousen J, Zipper CE, Rose A, Ziemkiewicz PF, Nairn R, McDonald LM, Kleinmann RL (2017) Review of passive systems for acid mine drainage treatment. Mine Water Environ 36(1): 133–153

Thomas RC, Romanek CS (2002) Passive treatment of low-pH, ferric iron-dominated acid rock drainage in a vertical flow wetland II: metal removal. In: Proc. of the ASMR, June 9-13, Lexignton KY, USA, pp 752–775

Tsukamoto TK, Miller GC (1999) Methanol as a carbon source for microbiological treatment of acid mine drainage. Water Res 33: 1365–1370

USEPA (United States Environmental Protection Agency) (2014) Code of Federal Regulations: Part 434- Coal mining point source category BPT, BAT, BCT limitations and new source performance standards.

https://www.gpo.gov/fdsys/pkg/CFR-2014-title40-vol30/xml/CFR-2014-title40-vol30-part434.xml#seqnum434.33. Accessed 04 August 2017

Waybrant K, Ptacek C, Blowes D, Ptacek CJ (1998) Selection of reactive mixtures for use in permeable reactive walls for treatment of mine drainage. Environ Sci Technol 32: 1972–1979

Yim GJ, Ji SW, Cheong YW, Neculita CM, Song H (2015) The influences of the amount of organic substrate on the performance of pilot-scale passive bioreactors for acid mine drainage treatment. Environ Earth Sci 73: 4717–4727

Zagury GJ, Kulnieks VI, Neculita CM (2006) Characterization and reactivity assessment of organic substrates for sulphate reducing bacteria in acid mine drainage treatment. Chemosphere 64 (6): 944–954

Zipper C, Skousen J, Jage C (2011) Passive treatment of acid-mine drainage. Reclamation Guidelines for Surface Mined Land. Virginia Cooperative Extension Publication 460-133. Powell River Project, Blacksburg, VA, USA, 15p

CHAPITRE VI

DISCUSSION

L'objectif de cette étude était de réaliser des investigations plus poussées sur l'amélioration de la performance à long terme d'une filière de traitement passif, dans le but de fournir des critères de design additionnels pour la construction d'un système efficace pour traiter le DMA ferrifère. La performance d'un traitement passif du DMA ferrifère en utilisant une filière à base de mélanges SAD, composée de 3 à 4 unités, a donc été évaluée dans les chapitres 3 (essais en batch), 4 (essais en petites colonnes) et 5 (filières) de cette thèse.

Les résultats obtenus ont montré que l'utilisation de mélanges SAD dans une unité de prétraitement du Fe a effectivement été bénéfique pour la performance globale de la filière. De plus, l'étude sur la comparaison des filières à l'échelle de laboratoire et une filière à l'échelle pilote de terrain (chapitre 5) a permis de proposer des critères de conception utiles pour la construction à grande échelle d'une filière de traitement passif du DMA ferrifère.

Ce chapitre apporte plus de détails sur l'effet du prétraitement du Fe, notamment sur l'enlèvement des SO_4^{2-}, ainsi que les probables limites de l'utilisation des mélanges sélectionnés durant les tests batch (i.e. CB-SAD). De plus, les causes probables des problèmes d'écoulement de surface observés sur le terrain, qui n'ont pas été rencontrés durant les essais de laboratoire (effet d'échelle), sont également abordées. En outre, l'estimation préliminaire technico-économique d'une éventuelle installation d'une

filière à base de SAD et RPB sur un site minier dans la région d'Abitibi, situé à une distance de 30–1000 km des fournisseurs de matériaux, mérite également d'être discutée afin de déterminer l'avantage pratique de la construction d'une telle filière.

6.1 Prétraitement du Fe

Les mélanges SAD permettraient de limiter les problèmes d'enrobage et de colmatage communément rencontrés dans les systèmes de traitement passif et, donc, de limiter les problèmes hydrauliques. Ainsi, trois types de mélanges SAD composés de trois différents matériaux alcalins naturels (cendres de bois, calcite, dolomite), à différentes proportions (20, 50 et 80% v/v), ont été d'abord testés dans neuf réacteurs batch (chapitre 3). Ensuite, le mélange le plus performant, i.e. CB50 (50% de cendre de bois), ainsi que deux autres mélanges [C20 (20% de calcite) et C50 (50% calcite)] ont été testés dans des réacteurs colonnes (système continu) de 1, 5 L (chapitre 4) et de 10,7 L (chapitre 5) comme composants d'une unité de prétraitement/polissage.

Les résultats de caractérisation des mélanges lors des tests batch (chapitre 3) ont montré que les SAD composés de cendre de bois (CB-SAD) avaient une surface spécifique 17 à 60 fois supérieure (9,15–32,8 m^2/g) à ceux composés de calcite ou de dolomite (0,16–0,55 m^2/g), pouvant permettre une sorption plus importante. Ainsi, les mélanges de type CB-SAD étaient plus efficaces pour enlever le Fe (99,9%) par rapport aux calcite- et dolomite-SAD, dont l'efficacité différait seulement à très court terme (jusqu'à 66% dans calcite-SAD) mais était comparable à plus long terme. Les observations des solides après traitement ont fourni en partie une explication sur la différence de l'efficacité des mélanges CB-SAD. Selon les analyses au microscope électronique à balayage, des oxy-hydroxydes de Fe étaient trouvés autant sur les copeaux de bois que sur les cendres de bois et, chronologiquement, avant le gypse ($CaSO_4.2H_2O$). Il en est déduit qu'en plus des copeaux de bois qui permettaient l'accumulation des précipités sur leur surface, les cendres de bois pouvaient également

fournir des sites de sorption additionnels. Les précipités de Fe qui étaient principalement amorphes et de tailles microscopiques variables (allant jusqu'à l'ordre de nanomètre) ont probablement saturé en premier, de façon prépondérante, les sites de sorption. Dans le même temps, les particules de gypse plus grossières (jusqu'à 150 μm) étaient adsorbées sur les oxy-hydroxydes de Fe. En l'absence (ou en quantité négligeable) d'autres métaux (p. ex. : Al), l'enlèvement du Fe et des SO_4^{2-} était de ce fait fortement interdépendant, car les oxy-hydroxydes de Fe pouvaient non seulement adsorber les gypses mais également les ions SO_4^{2-}. En effet, des travaux précédents ont permis de trouver que l'affinité des anions adsorbés sur les oxydes de Fe était dans l'ordre suivant : $PO_4^{3-} > SO_4^{2-} > NO_3^- > Cl^-$ (Peacock et Rimmer, 2000). Ce phénomène fournit alors une explication sur le meilleur enlèvement de SO_4^{2-} par les CB-SAD. Par contre, avec les calcite- et dolomite-SAD, les SO_4^{2-} étaient principalement enlevés sous forme de particules de gypse, qui étaient déposées dans les macropores des grains de calcite et/ou de dolomite (chapitre 4). Dans ce cas, l'apport en Ca^{2+} et sa disponibilité (influencée par la cinétique de dissolution de la calcite/dolomite selon l'acidité à neutraliser) pourraient être également un facteur limitant l'enlèvement des SO_4^{2-}. Par conséquent, avec un mélange C20 exploité à un TRH de 2 j dans un réacteur en colonne (chapitre 4), une rapide diminution (de 38%) d'une concentration initiale d'environ 5000–6000 mg/L de SO_4^{2-} était atteinte. Ensuite, seulement moins de 8% était enlevée, phénomène probablement attribuable à la consommation de tous les ions de Ca^{2+} disponibles. Par contre, avec un SAD composé de >50% de calcite (C50), environ 36% de SO_4^{2-} (concentration initiale autour de 4000 mg/L) était enlevée de façon stable, à un TRH de 3 j (chapitre 5). Donc, à long terme, l'efficacité d'enlèvement des SO_4^{2-} par un mélange C50 était environ 4 à 5 fois supérieure par rapport à celle des mélanges SAD composés de moins de 50% de calcite (C20/C25) (chapitre 4; Rötting et al., 2008a).

Ainsi, le prétraitement du Fe améliorerait l'enlèvement des SO_4^{2-}, dont les facteurs limitants en utilisant les mélanges CB-SAD sont la disponibilité des sites de sorption,

tandis qu'avec les mélanges calcite- ou dolomite-SAD, la disponibilité des ions Ca^{2+} était plus importante.

Une unité de prétraitement du Fe à base de CB-SAD amènerait donc une meilleure performance à long terme d'une filière de traitement passif du DMA ferrifère. Cependant, basé sur la performance de l'unité de cendre de bois installée sur le terrain, un assez rapide épuisement de l'alcalinité d'un prétraitement à CB-SAD pourrait se produire, entraînant une augmentation de l'acidité et par la suite un relargage de métaux. Néanmoins, un réacteur composé de CB50 pourrait être utilisé comme prétraitement du DMA à une concentration initiale <1500 mg/L de Fe, avant un RPB. En effet, pour un TRH de minimum de 1 j (4 h de temps de contact ; chapitre 3), la concentration pouvait être réduite à 418–530 mg/L (enlèvement de 40–61%). Dans ce cas, il serait alors envisageable d'exploiter l'unité de prétraitement à un TRH de 1–2 j. Ceci éviterait la saturation précoce des mélanges par les précipités et, par la suite, la diminution de n et de k_{sat} serait retardée. Dans le cas où un RPB serait utilisé, c'est plus l'accumulation de la biomasse qui serait restreinte.
De plus, un réacteur à calcite-SAD (C50) précédant un RPB est aussi proposé comme prétraitement du DMA ferrifère ayant une concentration <1000 mg Fe/L, dont l'enlèvement attendu est de 27–96% (diminution Fe à 8–830 mg/L ; chapitre 5).

6.2 Effet d'échelle

Après avoir sélectionné les mélanges les plus performants selon les résultats des tests batch et choisi les TRH optimaux en système avec écoulement, différents scénarios de filières de traitement du DMA ferrifère, composés de réacteurs SAD (prétraitement/polissage) et RPB (enlèvement des SO_4^{2-}), ont été construits.
L'évolution des paramètres hydrauliques (n et k_{sat}) dans tous les réacteurs, que ce soit durant les tests en petites colonnes ou les tests en filière, démontrait que le risque de colmatage précoce était limité, dû probablement aux valeurs plus élevées de k_{sat}. Par

conséquent, le prétraitement du Fe a amélioré la performance du reste des composants d'une filière de traitement passif du DMA ferrifère.

La comparaison des essais en laboratoire et sur le terrain a permis de proposer de nouveaux critères de design pour la conception d'une filière de traitement du DMA riche en Fe, à savoir les concentrations du Fe et des SO_4^{2-}, et le k_{sat}. Toutefois, étant donné que le colmatage n'a pas été constaté durant les tests en petites colonnes et en filière, les questions liées à cette problématique n'ont pas été soulevées. De ce fait, une tentative d'explication sur les éventuelles causes des problèmes hydrauliques sur le terrain est discutée dans ce qui suit.

1) D'abord, la structure d'un système de traitement passif est agencée de façon à ce qu'un court-circuit ou un écoulement préférentiel soit évité. Ainsi, dans le cas d'une filière, l'unité de prétraitement est une préoccupation primordiale, car elle est le premier receveur d'eau et subit le plus grand flux par rapport au reste des composants. Elle sert souvent de façade de ralentissement ou de régulateur de débit d'entrée, surtout lorsque ce dernier est très élevé, pour évacuer la pression tout en permettant à l'eau de circuler à travers le système. Si l'efficacité d'enlèvement de métaux dans cette première unité est trop élevée, n ainsi que k_{sat} diminuent rapidement, entrainant une augmentation de la pression ou un écoulement en surface. Or, tant que la pression à l'entrée est la même qu'à la sortie, les fluides continuent de s'écouler, comme ce qui était constaté durant les essais en colonne (chapitres 4 et 5 ; Genty, 2012), mais ce n'est probablement pas le cas sur le terrain. Cette différence est vraisemblablement expliquée par le fait que l'écoulement de l'eau à travers les réacteurs au laboratoire était contrôlé par les pompes péristaltiques, tandis que la circulation de l'eau à travers le système de traitement passif sur le terrain repose sur l'écoulement gravitaire. Par conséquent, le débordement constaté est en partie expliqué par l'absence de pente suffisante (1%; Genty, 2012); le niveau d'eau dans la filière tendrait alors à atteindre celui à l'entrée (Fig. 6.1). Une pente de 11% pourrait être bénéfique pour le système, comme dans les drains dolomitiques utilisés sur le même site (DOL-1, DOL-2 ; Potvin, 2009), 10 fois

supérieur à celui de la filière (1%, Genty, 2012). Cette structure sans pente a pu augmenter le temps de contact dans le système, de même que la pression et subséquemment, la diminution de n et de k_{sat}, particulièrement dans la zone 3 (unité 3).

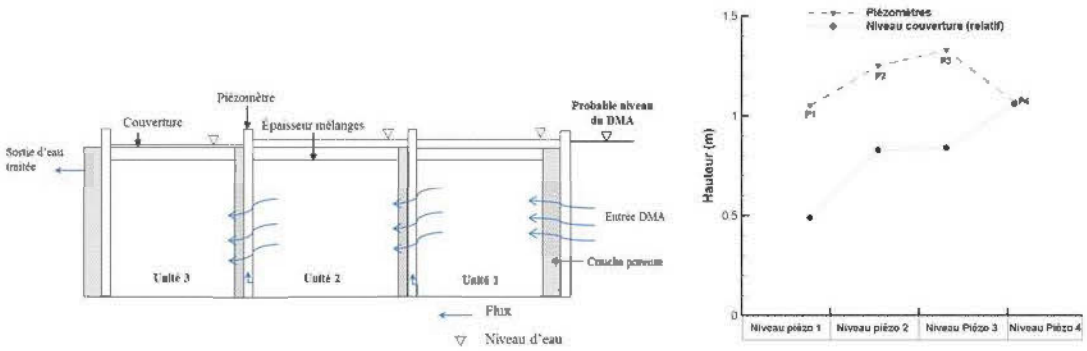

Figure 6.1 État actuel de la filière de traitement sur le site Lorraine : niveau d'eau dans les piézomètres et niveau relatif de la membrane (couverture)

2) Un deuxième facteur qui aurait contribué à cette submersion serait l'insuffisance de franc-bord ou une hauteur suffisante pour recevoir le surnageant ou pour dépasser le niveau probable d'entrée d'eau. Puisque les mélanges réactifs sont majoritairement composés de matière organique, ils sont perçus comme une éponge géante qui absorbe les précipités et l'eau jusqu'à saturation. Par conséquent, ils sont susceptibles à une perte de hauteur suite à la surcharge, notamment liée à la pression manométrique sur les mélanges lors de la saturation initiale, la perte de pression résultante de la production de gaz trop élevée, la décomposition de la matière organique et la charge de recouvrement de neige. En anticipant une éventuelle conséquence d'une charge élevée sur une filière, des essais de consolidation (ASTM, 2004) ont été réalisés sur trois mélanges frais (RPB, CB50, C50) utilisés pendant cette étude. Les résultats ont montré que les mélanges pouvaient perdre jusqu'à 63% de sa hauteur initiale ainsi qu'une diminution moyenne de n de 36%, selon la contrainte appliquée (Tableau 6.1 ; Fig. 6.2 a, b). Toutefois, même si un tassement pourrait se produire, l'utilisation des

mélanges de types SAD faciliterait l'écoulement dans un système de traitement passif du DMA ferrifère.

Tableau 6.1 Changement de hauteur (h), indice des vides (e), porosité (*n*) selon une valeur de contrainte appliquée

Contrainte (kPa)	RPB			CB50			C50		
	h réelle (cm)	**e**	***n***	**h réelle (cm)**	**e**	***n***	**h réelle (cm)**	**e**	***n***
1	3,07	4,73	0,83	3,06	4,45	0,82	3,07	2,28	0,70
12	3,03	4,66	0,82	3,02	4,38	0,81	3,04	2,25	0,69
25	2,99	4,59	0,82	2,98	4,31	0,81	3,04	2,25	0,69
50	2,94	4,50	0,82	2,65	3,72	0,79	3,03	2,24	0,69
100	2,72	4,07	0,80	2,28	3,06	0,75	2,61	1,80	0,64
200	2,02	2,78	0,74	1,75	2,11	0,68	2,24	1,39	0,58
400	1,14	1,13	0,53	1,12	1,00	0,50	1,96	1,10	0,52

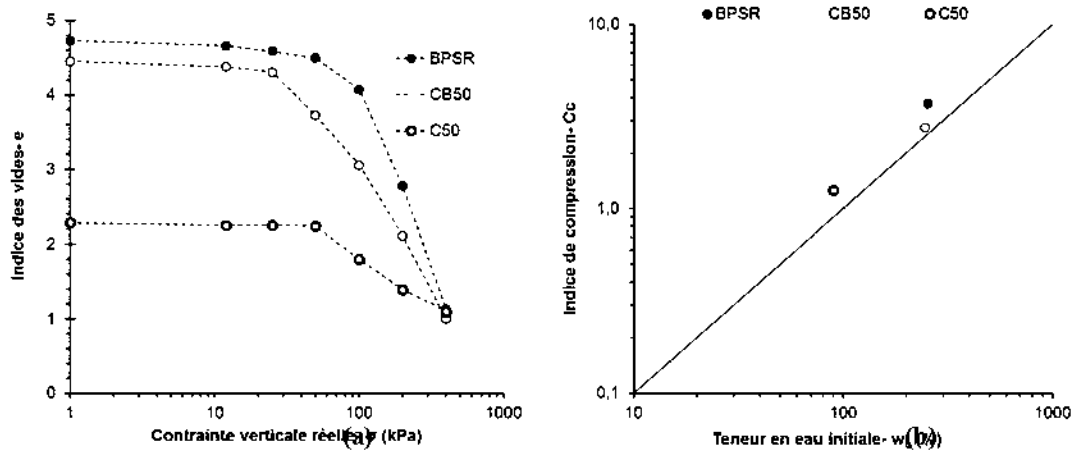

Figure 6.2 (a) Indice des vides (e) selon une contrainte verticale; (b) Indice de compression (Cc) en fonction de la teneur en eau

Une correction sur la surcharge portée par le système devrait donc inclure au moins le recouvrement de neige et la pression manométrique lors du design d'une filière de traitement passif à grande échelle.

6.3 Évaluation préliminaire technico-économique

Une des raisons principales pour choisir les systèmes de traitement passif est le coût qui est généralement 2–10 fois inférieur par rapport à celui des systèmes actifs à plus long terme (20–40 ans) (Hedin et al., 2013). La rentabilité économique d'un système passif est souvent calculée selon le coût de traitement d'une tonne d'acide par année ($/t/an) (Ziemckiewicz et al., 2003). Les coûts de construction d'une unité de traitement passif variaient de 10 565 à 94 515 $, avec un rapport coût/efficacité (en termes de neutralisation d'acide) de 59–1468 $/t/an (Skousen et Ziemckiewicz, 2005 ; Hedin et al., 2013). Les coûts d'investissement des systèmes de traitement passif étaient de 0,05–1,49 M$ (moyenne de 0,77 M$) (Zinck and Griffith, 2013 ; Grembi et al., 2015; Diloreto et al., 2016). Pour une filière à six unités, le capital requis est de 1,77 M$ (comprenant l'ingénierie, les permis et la gestion de projet) (Hedin et al., 2013; 2016). Une diminution de 19% peut être attendue si une valorisation des boues (récupération produits secondaires) est réalisée, selon le cas (Hedin, 2016). D'autres études montrent que la récupération de métaux dans les solides usés après traitement pouvait diminuer 30% du coût total (cycle de vie de 10 ans) ou 90% des frais de stockage (Bailey et al., 2016). Il a été également trouvé que la réduction du coût de transport pouvait diminuer de 50% les frais d'installation d'un système de traitement passif (voire pour un système actif) (Hengen et al., 2014). En général, le coût des matériaux utilisés dans les systèmes passifs est faible/négligeable mais le coût du transport peut augmenter significativement les montants de construction. Ainsi, pour estimer les coûts d'installation d'une filière de traitement passif de terrain, quelques étapes sont nécessaires, comprenant :

1) l'analyse de la qualité de l'eau ;

2) l'identification des types d'unité de traitement passif pouvant constituer les unités composants la filière ;

3) la mesure de l'espace disponible pour l'installation ;

4) l'inventaire des matériaux disponibles dans les plus proches points d'approvisionnement et l'estimation des distances ;

5) le choix des types d'unités composants la filière ;

6) le choix du nombre d'unités ;

7) la quantification des matériaux ;

8) la liste de la main d'œuvre nécessaire.

Enfin, une estimation du coût de construction d'une filière de terrain est présentée.

Au laboratoire, le coût d'analyse des échantillons était environ 2,85–30 $/analyse. Les mélanges réactifs utilisés provenaient du même lot que les précédentes expériences (Genty, 2012), desquelles quelques matériels étaient également réutilisés. La quantité de matériaux utilisés pour construire une filière de traitement du DMA ferrifère utilisant des réacteurs SAD et RPB (3 ou 4 unités) était environ 5,6 kg cendre de bois, 7,03 kg de copeaux de bois, 1,08 kg de fumier, 0,54 kg de compost, 0,54 kg de sable et 8,06 kg de calcite.

Sur le terrain, l'évaluation des coûts a été estimée à partir des coûts d'installation de la filière de traitement sur le site Lorraine. Le coût de transport des matériaux, variant de 3,28–484 $/km selon la distance de livraison et les fournisseurs, représenterait 3–7 fois le coût des mélanges (0–68 $/t). Ainsi, l'estimation du coût de construction d'une

filière de traitement passif sur le terrain pourrait être basée sur la distance du site par rapport aux localités de procuration de matériaux/matériels.

En prenant l'exemple d'une éventuelle installation d'une filière (p. ex. 3 à 4 unités et un volume de 158 m^3) à base de réacteurs SAD et RPB sur un site minier situé dans un périmètre de 30–1000 km des fournisseurs de matériaux/matériels dans la région d'Abitibi, une estimation des coûts totaux serait environ 40 000–110 000 $ (Tableau 6.2). Le montant total du coût d'installation d'une telle filière pourrait être 18–50% de moins que celui de la filière actuellement en place sur le site Lorraine (période de 5 ans) selon le nombre et le type d'unités utilisées.

Tableau 6.2 Estimation préliminaire des coûts de construction d'une filière à base de réacteurs SAD et RPB sur un site minier situé dans un périmètre de 30–1000 km des agglomérations et selon les fournisseurs de matériels

	Laboratoire				Terrain		
Unité	**Quantité de mélanges (kg)**	**Coût des mélanges et transport ($)**	**Analyses ($)**	**Divers($)**	**Quantité de mélanges (t)**	**Coût des mélanges + transport ($)**	**Installation et divers ($)**
CB50	3,8	0			39	2435	
RPB	5,4	0	2,85–30	200	39,22	4331	38 291–107 656
C50	8,6	0			38,12	1623,14	
Total	***17,8***	***0***	***540***	***200***	***116,34***	***8389,14***	***38 291–107 656***

CHAPITRE VII

CONCLUSIONS ET RECOMMANDATIONS

Bien que les études précédentes aient montré des résultats satisfaisants sur les filières de traitement passif du DMA ferrifère au laboratoire, les problèmes d'écoulement en surface constatés sur le terrain indiquaient que davantage de recherches étaient nécessaires. L'objectif principal de cette étude était donc de mener des études plus poussées pour améliorer la performance à long terme des filières de traitement passif du DMA ferrifère dans le but de proposer de nouveaux critères de design pour construire un système efficace. L'approche proposée pour atteindre cet objectif consistait à utiliser les mélanges réactifs composés de matériaux à haute porosité et à forte alcalinité comme composant d'une unité de prétraitement du Fe dans une filière. Ainsi, l'approche de recherche proposée était divisée en trois étapes :

1) Évaluation de l'efficacité des mélanges de types SAD pour le traitement du DMA ferrifère. Cette étape comprenait la caractérisation de ces mélanges et l'évaluation de leurs efficacités dans des réacteurs batch (sans écoulement) afin de sélectionner le(s) plus efficace(s) pour prétraiter le Fe dans le DMA ferrifère ;

2) Évaluation de l'efficacité du/des mélange(s) sélectionné(s) dans l'étape 1), ainsi qu'un autre mélange à utiliser dans un RPB dans des réacteurs de type colonnes (1,5 L) selon le/les TRH optimal/optimaux. Cette deuxième étape incluait également l'évaluation de la performance hydraulique de ces mélanges ;

3) Évaluation de l'effet d'échelle par comparaison des filières de laboratoire, construites en utilisant les résultats des étapes 1 et 2, avec la filière de terrain, afin de proposer de nouveaux critères de design pour construire une filière de traitement passif du DMA ferrifère.

Les principales conclusions et recommandations des trois grandes parties composantes de cette étude, à savoir les chapitres 3, 4, et 5 de la thèse, sont donc présentées dans ce qui suit.

7.1 Chapitre 3 –Essais batch

Les mélanges SAD ont été testés pour prétraiter le DMA ferrifère afin de limiter les problèmes d'enrobage et de colmatage communément rencontrés dans les traitements passifs. Trois types de SAD composés de matériaux alcalins naturels (cendres de bois, calcite, dolomie), à différentes proportions (20, 50, 80% v/v) et des substrats à grande surface spécifique (copeaux de bois) ont été testés dans neuf réacteurs batch. Les essais ont été réalisés en duplicata pendant une période de 91 j.

Les résultats sur la caractérisation des mélanges ont montré que les SAD composés de cendre de bois (CB-SAD) avaient une surface spécifique jusqu'à 60 fois plus grande que ceux composés de calcite ou de dolomite. Tous les mélanges CB-SAD pouvaient enlever jusqu'à 99,9% de Fe et 40% de SO_4^{2-}. L'efficacité des mélanges calcite-SAD et dolomite-SAD est comparable à long terme (16–27% Fe et <10% SO_4^{2-}) et ils pouvaient donc être substitués. Le Fe est principalement précipité sous forme d'oxydes/hydroxydes amorphes de taille <150µm, tandis que les SO_4^{2-} sont sous forme de particules grossières de gypse ($CaSO_4.2H_2O$).

Pour pouvoir utiliser les mélanges CB-SAD dans une unité de prétraitement avant un RPB qui requiert une concentration du Fe à moins de 500 mg/L, un temps de contact de 6–11 h était nécessaire. Les proportions d'agents alcalins dans les mélanges réactifs n'influencaient pas la quantité de Fe enlevée, ni l'augmentation du pH. Par contre, la

stabilité de l'efficacité du traitement pourrait être mise en cause. Toutefois, puisque le mélange CB-SAD avec une proportion de 80% de cendre de bois contenait une proportion élevée de fines, le mélange CB50 (avec 50% cendres de bois) était choisi comme compromis pour être utilisé dans une unité de prétraitement du Fe.

Cette partie de la thèse a montré que d'autres types d'agents alcalins moins coûteux (cendre de bois et dolomite) pourraient être utilisés comme substitution des agents alcalins conventionnels (MgO et calcite) dans les mélanges SAD. De plus, il a été remarqué que le CB-SAD pouvait enlever une quantité plus importante de Fe et de SO_4^{2-} par rapport aux types de SAD communs (calcite-SAD).

Toutefois, d'autres caractérisations des mélanges utilisés sont recommandées, particulièrement des mélanges CB-SAD, à savoir la capacité d'échange cationique, la capacité de sorption/désorption et la détermination du pH de la charge nulle de surface des matériaux.

7.2 Chapitre 4 – Essais en petites colonnes

Deux des mélanges testés durant les tests batch [CB50 et C20 (20% de calcite)] ont été choisis pour prétraiter le Fe. Un troisième mélange réactif composé de matériaux organiques (70%) et inorganiques (30%) a été testé dans un RPB, pour traiter les SO_4^{2-} à cause du traitement limité de ces derniers par les mélanges SAD. Une évaluation de l'efficacité et de la performance hydraulique de ces trois mélanges dans des réacteurs à colonnes exploités à différents TRH a été effectuée.

Les résultats obtenus dans ce chapitre ont permis de conclure que les réacteurs CB50 ont montré un meilleur enlèvement du Fe et des SO_4^{2-} (17–62% et 7,5–37%, respectivement) lorsque le TRH était de 5 j (CB50-5). Cependant, un TRH de 3 j est proposé pour un système à grande échelle pour limiter les espaces requis. Dans le même temps, les réacteurs C20 étaient efficaces seulement à très court terme (dans les premiers 7 j) et un TRH >2 j est requis pour traiter du DMA ferrifère. Ce mélange est

suggéré pour être utilisé dans un traitement de polissage, succédant un RPB. Enfin, l'enlèvement du Fe dans les RPB augmentait lorsque le TRH était doublé de 2,5 à 5 j (77 % et 91%, respectivement). Par contre, l'enlèvement des SO_4^{2-} diminuait de 91% à moins de 14%, suite à une probable compétition entre les BFR et les BSR à une concentration du Fe dans le DMA à traiter de 300 mg/L.

L'évolution des paramètres hydrauliques (n et k_{sat}) dans tous les réacteurs démontre que le risque de colmatage précoce était limité avec une évolution de k_{sat} initial de l'ordre de 10^{-2}cm/s qui diminuait seulement d'une unité de 10^{-1} ou 10^{-2} cm/s.

Cependant, les limites des méthodes utilisées durant la réalisation de ces tests amènent à recommander quelques points pour des travaux futurs :

- D'autres méthodes pour déterminer le TRH, tels les essais de traceurs, devraient être utilisées afin d'obtenir des résultats consistants ;

- Les bactéries ferri-réductrices (BFR) et les BSR ont été dénombrés par la méthode du nombre le plus probable (NPP), mais leur influence ne pouvait pas être testée. L'analyse de la déshydrogénase peut fournir des informations sur les effets de modification ou d'augmentation des activités microbiennes et pourrait différencier le comportement de ces deux types de bactéries dans le RPB lors du traitement du DMA ferrifère.

7.3 Chapitre 5– Filière

Les résultats obtenus durant les tests batch et petites colonnes ont permis de construire trois scénarios de filière de traitement du DMA ferrifère au laboratoire. Les objectifs de ce chapitre étaient de comparer les filières de laboratoire avec celle installée sur un site pilote afin d'évaluer l'effet d'échelle.

Les résultats sur l'évaluation d'effet d'échelle ont permis de conclure que les paramètres qui pourraient influencer la différence de performance entre les expériences

au laboratoire et à l'echelle de terrain sont la conductivité électrique, la concentration en Fe et SO_4^{2-}, le débit (Q) et la conductivité hydraulique saturée (k_{sat}).

L'efficacité d'une filière basée sur l'utilisation des mélanges SAD pouvait enlever jusqu'à 99% de Fe. Sur le terrain, l'efficacité de la filière était d'environ 75%. Ainsi, le prétraitement du Fe a amélioré effectivement la performance du reste des composants d'une filière de traitement passif du DMA ferrifère. Les meilleures performances de la filière ont été obtenues lorsque deux unités de prétraitement ont été utilisées avec une efficacité globale du Fe de 76–99,6% et 46–82% de SO_4^{2-}. Les unités de prétraitement les plus efficaces étaient les deux CB50 avec un enlèvement du Fe, à elles seules, de 82 et 79% de SO_4^{2-}. Par conséquent, le RPB qui les succédait pouvait traiter 86% de Fe et >99% de SO_4^{2-}. Toutefois, l'utilisation d'un réacteur à base de CB50 comme prétraitement pourrait être risquée, car l'évaluation de la performance du réacteur composé de cendres de bois (100%) sur le terrain laissait présager un rapide épuisement de l'alcalinité, entraînant une augmentation de l'acidité et, par la suite, un relargage de métaux. Néanmoins, un réacteur CB50 pourrait être utilisé comme prétraitement du DMA à une concentration initiale <1500 mg/L de Fe. Une unité de prétraitement de Fe devrait être également opérée sous une valeur élevée de k_{sat}, et à faible TRH (selon Q) pour minimiser un colmatage précoce.

La comparaison des essais en laboratoire et sur le terrain a également permis de constater que le débit (Q) est un paramètre majeur qui contrôle la performance d'une filière de traitement passif. Aussi, de nouveaux critères de design, incluant les concentrations du Fe et des SO_4^{2-}, et k_{sat} ont été proposés. Ainsi, une charge de Fe <150 g /m^3/j est proposée si un réacteur SAD est utilisé pour prétraiter un DMA ferrifère et moins de 26 g Fe /m^3substrat/j et de SO_4^{2-} <110 g/m^3substrat/j pour un RPB. De plus, les mélanges réactifs devraient avoir un k_{sat} >10^{-3}cm/s et pour un RPB, au moins 20% d'agents alcalins est suggéré. Un facteur de correction de 0,2–0,8 pourrait être appliqué sur la valeur de Q et l'enlèvement du Fe, et 1/100 sur le k_{sat} mesuré au laboratoire pour prédire la durabilité du traitement sur site.

Selon les résultats obtenus dans cette étude, un schéma conceptuel d'une filière de traitement passif du DMA ferrifère est proposé (Fig. 7.1).

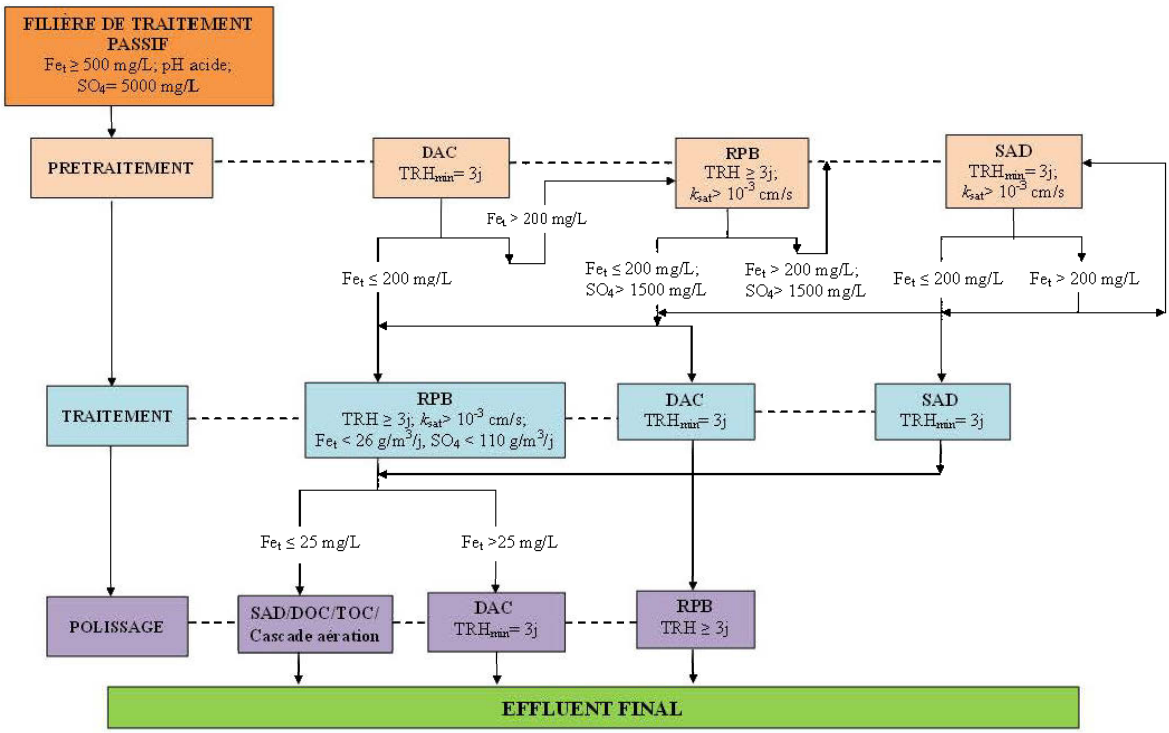

Figure 7.1 Schéma conceptuel d'une filière de traitement passif d'un DMA ferrifère

Enfin, suite à ce travail, des études supplémentaires sont suggérées, portant particulièrement sur les points suivants :

- Évaluation de l'effet de la température sur l'efficacité d'enlèvement du Fe ;
- Évaluation de l'effet de la pente sur une filière de traitement, soit par simulation numérique ou par des essais de laboratoire, où un écoulement qui simulerait celui du terrain est testé ;

- Instrumentation de la filière de terrain qui pourrait permettre de comprendre davantage le comportement continu réel du système de traitement et d'appréhender les problématiques de l'effet d'échelle ;

- Caractérisation des solides après traitement, que ce soit de ceux obtenus au laboratoire ou sur le terrain, en déterminant la spéciation des métaux par la procédure d'extraction séquentielle (Zagury et al., 1997) et l'analyse des métaux simultanément solubles avec sulfures acides volatils (Brouwer et al., 1994). Cette procédure permettrait de déterminer la stabilité et la mobilité des contaminants retenus par les constituants solides ainsi que de distinguer les différentes formes de liaisons possibles des espèces ;

- Mesure expérimentale de l'effet de l'enneigement sur le système de traitement par les essais de consolidation en comparant les résultats obtenus sur les matériaux initiaux et ceux obtenus sur les matériaux après traitement (fin de vie).

7.4 Dernières remarques

Les chapitres 3, 4 et 5 de la présente thèse ont apporté des éléments de réponse aux objectifs posés pour améliorer la performance des filières de traitement passif du DMA ferrifère. Les approches méthodologiques ont notamment permis de développer un mélange moins coûteux et efficace pour prétraiter le Fe. L'originalité de ce travail réside dans la proposition de nouveaux critères de design pour la construction d'une filière de traitement passif du DMA ferrifère, qui pourraient être validés avec d'autres qualités de DMA fortement contaminé. Cette étude a également permis de faire une comparaison concrète entre les essais au laboratoire et le système pilote de terrain, afin de comprendre d'autres aspects précédemment omis qui ont pu changer la performance d'une filière de traitement du DMA ferrifère. Ensuite, l'intégration des facteurs de correction sur la concentration du Fe, la conductivité hydraulique k_{sat} et du débit Q pour prédire le comportement à long terme peut être une approche innovante.

Enfin, cette étude suggère l'utilisation de deux unités de prétraitement du Fe afin d'optimiser la performance à long terme d'une filière de traitement du DMA ferrifère. Suite aux questions liées au devenir des solides post-traitements, une optimisation du design des filières, selon les conditions spécifiques de chaque site, afin de pouvoir récupérer des oxydes de Fe, pourrait être envisagée.

BIBLIOGRAPHIE GÉNÉRALE

Aitcin, P.C., Généreux, F., Jolicoeur, G., Maurice, M. (2012). Technologie des granulats, 3rd ed. Modulo, Montréal, QC, Canada, 352p.

Anello, G., Lamarche, P., Héroux, J.A. (2005). Reduction of hydraulic conductivity changes in an in-ground bioreactor. *Journal of Environmental Engineering and Science*, 4, 195–207.

APHA (American Public Health Association) (2012). Alkalinity titration, in Standard methods for the examination of water and wastewater (22ème edition). Greenberg A. (Eds), Washington DC, USA.

APHA (American Public Health Association) (2005). Titration method, in Standard methods for the examination of water and wastewater (19ème edition), Greenberg A. (Eds), Washington, DC, USA, pp. 161–166.

Arnold, D.E. (1991). Diversion wells-a low-cost approach to treatment of acid mine drainage. In: Proc. of the 12th West Virginia Surface Mine Drainage Task Force Symposium, April 3-4, Morgantown, WV, USA.

Asadi, A., Huat, B.K.B., Hanafi, M.M., Mohamed, T.A., Shariatmadari, N. (2009). Role of organic matter on electroosmotic properties and ionic modification of organic soils. *Geosciences Journal*, 13 (2), 175–181.

ASTM (American Society for Testing and Materials) (2004). Standard test methods for one-dimensional consolidation properties of soils using incremental loading. In: Book of Standards Vol. 04.08 (D2435).

ASTM (American Society for Testing and Materials) (1995). Standard test method for permeability of granular soils. In: Annual book of ASTM Standards.08. D 2434 – 68, Philadelphia, PA, USA.

ASTM (1990). Standard methods for sulphate reducing bacteria in water and water-formed deposit. In: Annual book of ASTM Standards, vol. 04.08. Section D 4412–84, Washington, DC, pp. 533–535.

Aubertin, M., Bussière, B., Zagury, G.J. (2010). La gestion des rejets miniers au Québec. L'état du Québec 2011, Institut du nouveau monde, *Boréal*, p. 225–232.

Aubertin, M., Bussière, B., Bernier, L. (2002). Environnement et gestion des rejets miniers. Presses Internationales, Polytechnique Montréal, QC, Canada. http://www.presses-polytechnique.ca/fr/environnement-et-gestion-des-rejets-miniers

Ayora, C., Caraballo, M.A., Macías, F., Rötting, T.S., Carrera, J., Nieto, J.-M. (2013). Acid mine drainage in the Iberian Pyrite Belt: 2. Lessons learned from recent passive remediation experiences, *Environmental Science and Pollution Research*, 20, 7837–7853.

Bailey, M.T., Gandy, C.J., Jarvis, A.P. (2016). Reducing life-cycle costs of passive mine water treatment by recovery of metals from treatment wastes. Drebenstedt, C., Michael, P. (Eds). In: Proc. of the International Mine Water Association (IMWA). July 11-15, Leipzig, Germany.

Bejan, D. et Bunce, N.J. (2015). Acid mine drainage: Electrochemical approaches to prevention and remediation of acidity and toxic metals. *Journal of Applied Electrochemistry*, 45, 1239–1254.

Bernier, L.R. (2005). The potential use of serpentinite in the passive treatment of acid mine drainage: batch experiments. *Environmental Geology*, 47, 670–684.

Bernier, L., Aubertin, M., Dagenais, A. M., Bussière, B., Bienvenu, L., Cyr, J. (2001). Limestone drain design criteria in AMD passive treatment: theory, practice and hydrogeochemistry monitoring at Lorraine mine site, Temiscamingue. In: Proc. of the CIM Minespace 2001 annual meeting, Technical paper n°48, 9p.

Biesinger, K.E. et Christensen, G.M., 1972. Effects and various metals on survival, growth, reproduction and metabolism of Daphnia magna. *Journal of the Fisheries Research Board of Canada*, 29, 1691–1700.

Bigham, J.M., Schwertmann, U., Traina, S.J., Winland, R.L., Wolf, M. (1996). Schwertmannite and chemical modeling of iron and sulfate waters. *Geochimica et Cosmochimica Acta*, 60 (12), 2111–2121.

Burgos, W.D., Senko, J.M., Bruns, M.A. (2008). Low pH Fe(II) oxidation incorporated into passive treatment. In: Proc. of the 29th WV Surface Mine Drainage Task Force Symposium, April 22-23, Morgantown, WV, USA.

Bussière, B., Potvin, R., Dagenais, A.-M., Aubertin, M., Maqsoud, A., Cyr, J. (2009). Restauration du site minier Lorraine, Latulipe, Québec : Résultats de 10 ans de suivi. *Déchets sciences et techniques,* 54, 49–64.

Bussière, B., Aubertin, M., Zagury, G.J., Potvin R., Benzaazoua, M. (2005). Principaux défis et piste de solution pour la restauration des aires d'entreposage de rejets miniers abandonnées. Symposium 2005 sur l'environnement et les mines, Rouyn Noranda. UQAT, Québec.

Bussière B., Aubertin, M., Chapuis, R.P. (2003). The behaviour of inclined covers used as oxygen barriers. *Canadian Geotechnical Journal*, 40, 512–535.

Caraballo, M.A., Macías, F., Nieto, J. M., Castillo, J., Quispe, D., Ayora, C. (2011a). Hydrochemical performance and mineralogical evolution of a dispersed alkaline substrate (DAS) remediating the highly polluted acid mine drainage in the full-scale passive treatment of Mina Esperanza (SW Spain). *American Mineralogist*, 96, 1270–1277.

Caraballo, M.A., Macías, F., Rötting, T.S., Nieto, J. M., Ayora, C. (2011b). Long term remediation of highly polluted acid mine drainage: A sustainable approach to restore the environmental quality of the Odiel river basin. *Environmental Pollution*, 159 (12), 3613–3619.

Caraballo, M.A., Rötting, T.S., Silva, V. (2010). Implementation of an MgO-based metal removal step in the passive treatment system of Shilbottle, UK: Column experiments. *Journal of Hazardous Materials*, 181 (1-3), 923–930.

Caraballo, M.A., Rötting, T.S, Macías, F., Nieto, J.M., Ayora, C. (2009). Field multi-step limestone and MgO passive system to treat acid mine drainage with high metal concentrations. *Applied Geochemistry*, 24 (12), 2301–2311.

Champagne, P., Van Geel, P., Parker, W. (2008). Impact of temperature and loading on the mitigation of AMD in peat biofilter columns. *Mine Water and the Environment*, 27, 225–240.

Champagne, P., Van Geel, P., Parker, W. (2005). A Bench-scale assessment of a combined passive system to reduce concentrations of metals and sulphate in acid mine drainage. *Mine Water and the Environment*, 24 (3), 124–133.

Chapelle, F.H., Bradley, P.M., Thomas, M.A., McMahon, P.B. (2009). Distinguishing iron-reducing from sulfate-reducing conditions. *Ground Water* 47(2), 300–305.

Chapelle, F.H. et Lovley, D.R. (1992). Competitive exclusion of sulfate reduction by Fe(III) - reducing bacteria: A mechanism for producing discrete zones of high-iron. *Ground Water*, 30 (1), 29–36.

Clyde, E.J., Champagne, P., Jamieson, H.E., Gorman, C., Sourial, J. (2016). The use of passive treatment for the mitigation of acid mine drainage at the Williams Brothers Mine (California): Pilot-scale study. *Journal of Cleaner Production*, 130, 116–125.

Cochran, W.G. (1950). Estimation of bacterial densities by means of the most probable number. *Biometrics*, 6, 105–116.

Cocos, I.A., Zagury, G.J., Clement, B., Samson, R. (2002). Multiple factor design for reactive mixture selection for use in reactive walls in mine drainage treatment. *Water Research*, 32, 167–177.

Cornell, R.M. et Schwertmann, U. (2003). The iron oxides: Structure, properties, reactions, occurrences, and uses (2ème edition). Wiley-VCH GmbH&Co. KGaA, Weinheim, Germany, 694 p.

Dar, S.A., Kleerebezem, R., Stams, A.J.M., Kuenen, J.G., Muyzer, G. (2008). Competition and coexistence of sulfate-reducing bacteria, acetogens and methanogens in a lab-scale anaerobic bioreactor as affected by changing substrate to sulfate ratio. *Applied Microbiology and Biotechnology*, 78(6), 1045−1055.

Deng, D., Weidhaas, J.L., Lin, L.-S. (2016). Kinetics and microbial ecology of batch sulfidogenic bioreactors for co-treatment of municipal wastewater and acid mine drainage. *Journal of Hazardous Materials*, 305, 200–208.

Diloreto, Z.A., Weber, P.A., Olds, W., Pope, J., Trumm, D., Chaganti, S.R., Heath, D.D., Weisner, C.G. (2016). Novel cost effective full scale mussel shell bioreactors for metal removal and acid neutralization. *Journal of Environmental Management*, 183 (3), 601−612.

Diz, H.R., Novak, J.T., Rimstidt, F.D. (1999). Iron precipitation kinetics in synthetic acid mine drainage. *Mine Water and the Environment*, 18 (1), 1−14.

Dvorak, D.H., Hedin, R.S., Edenborn, H.M., McIntire, P.E. (1991). Treatment of metal-contaminated water using bacterial sulfate reduction: Results from pilot-scale reactors. In: Proc. of the National Meeting of the American Society of

Mining and Reclamation (ASMR), May 14-17, Pittsburgh, PA, USA, pp. 109–122.

El Gheriany, I.A., Bocioaga, D., Hay, A.G., Ghiorse, W.C., Shuler, M.L., Lion, L.W. (2009). Iron requirement for Mn(II) oxidation by Leptothrix discophora SS-1. *Applied and Environmental Microbiology*, 75(5), 1229–1235.

Figueroa, L., Miller. A., Zaluski, M., Bless, D. (2007). Evaluation of a two-stage passive treatment approach for mining influenced waters. In: Proc. of the ASMR. June 2-7, Lexington, KY, USA, pp. 238–247.

Florence, K., Sapsford, D., Wolkersdorfer, C. (2015). Mechanisms of iron removal during passive treatment of AMD in a vertical flow reactor. In: Proc. of the International Conference on Acid Roch Drainage (ICARD) & IMWA Annual Conference, April 21-24, Santiago, Chile.

Gazea, B., Adam, K., Kontopoulos, A. (1996). A review of passive systems for the treatment of acid mine drainage. *Minerals Engineering*, 9, 23–42.

Genty, T., Bussière, B., Benzaazoua, M., Neculita, C.M., Zagury, G.J. (2017a) Changes in efficiency and hydraulic parameters during the passive treatment of ferriferous acid mine drainage in biochemical reactors. *Mine Water and the Environment* (in corrections).

Genty, T., Bussière, B., Benzaazoua, M., Neculita, C.M., Zagury, G.J. (2017b). Iron removal in highly contaminated acid mine drainage using passive biochemical reactors. *Water Science and Technology* (in press, doi: 10.2166/wst.2017.362).

Genty, T., Bussière, B., Paradie, M., Neculita, C.M. (2016). Passive biochemical treatment of ferriferous mine drainage: Lorraine mine site, Northern Quebec, Canada. In: Proc. of the IMWA, July 11-15, Leipzig, Germany.

Genty, T. (2012). Comportement hydro-bio-géo-chimique de systèmes passifs de traitement du drainage minier acide fortement contaminé en fer. Thèse de

doctorat, Institut de recherche en mines et environment (IRME)-Université du Québec en Abitibi-Témiscamingue (UQAT), Rouyn-Noranda, QC, Canada, 270p.

http://depositum.uqat.ca/id/eprint/269http://depositum.uqat.ca/id/eprint/269.

Genty, T., Bussière, B., Potvin, R., Benzaazoua, M., Zagury, G.J. (2012a). Dissolution of calcitic marble and dolomitic rock in high iron concentrated acid mine drainage: Application to anoxic limestone drains. *Environmental Earth Sciences*, 66, 2387–2401.

Genty, T., Bussière, B., Potvin, R., Benzaazoua, M., Zagury, G.J. (2012b). Capacity of wood ash filters to remove iron from acid mine drainage: Assessment of retention mechanism. *Mine Water and the Environment*, 31 (4), 273–286.

Genty, T., Bussière, B., Zagury, G.J., Benzaazoua, M. (2010). Passive treatment of high-iron acid mine drainage using sulphate reducing bacteria: Comparison between eight biofilter mixtures. Wolkersdorfer & Freund (Eds). In: Proc. of the IMWA, September 5-9, Sydney, NS, Canada.

Gibert, O., De Pablo, J., Cortina, J., Ayora, C. (2004). Chemical characterisation of natural organic substrates for biological mitigation of acid mine drainage. *Water Research*, 38, 4186– 4196.

Gould, W. D., Stichbury, M., Francis, M., Lortie, L., Blowes, D. W. (2003). An MPN method for the enumeration of iron-reducing bacteria. In Proc. of Mining and the environment III Conference. Laurentian University, Sudbury, ON, Canada, pp. 25–28.

Grembi, J., A., Sick, B.A., Brennan, R.A. (2015). Remediation of high-strength mine-impacted water with mixed organic substrates containing crab shell and spent mushroom compost. *Journal of Environmental Engineering*, 142 (2), 10p.

Haakensen, M., Pittet, V., Spacil, M.M., Castle, J.W., Rodgers Jr, J.H. (2015). Key aspects for successful design and implementation of passive water treatment systems. *Journal of environmental solutions for oil, gas, and mining*, 1(1), 59–81.

HACH, 2013. Colorimeter procedures manual. http://www.hach.com/quick.search-download.search.jsa?keywords=Colorimeter%20procedures%20manual

Hammarstrom, J.M., Sibrell, P.L., Belkin, H.E. (2003). Characterization of limestone reacted with acid-mine drainage in a pulsed limestone bed treatment system at the Friendship Hill National Historical Site, Pennsylvania, USA. *Applied Geochemistry*, 18, 1705–1721.

Hao, O.J., Chen, J.M., Huang, L., Buglass, R.L. (1996). Sulfate reducing bacteria: Critical reviews. *Environmental Science and Technology*, 26,155−187.

Hedin, R.S. (2016). Long term minimization of mine water treatment costs through passive treatment and production of a sealable iron oxide sludge. Drebenstedt, C., Paul, M. (Eds). In: Proc. of the IMWA, July 11-15, Freiberg, Germany.

Hedin, R., Weaver, T., Wolfe, N., Watzlaf, G. (2013). Effective passive treatment of coal mine drainage. In: Proc. of the 35th Annual National Association of Abandoned Mine Land Programs Conference, September 22-25, Daniels, WV, USA.

Hedin, R.S., Weaver, T., Wolfe, N., Weaver, K. (2010). Passive treatment of acidic coal mine drainage: The Anna S mine passive treatment complex. *Mine Water and the Environment*, 29, 165–175.

Hedin, R.S., Watzlaf, G.R., Nairn, R.W. (1994). Passive treatment of acid mine drainage with limestone. *Journal of Environmental Quality*, 23, 1358–1345.

Hengen, T.J., Squillace, M.K., O'Sullivan, A.D., Stone, J.J. (2014). Life cycle assessment analysis of active and passive acid mine drainage treatment technologies. *Resources, Conservation and Recycling*, 86, 160–167.

Hilton, T. 2005. Low pH-iron oxidation. In: Proc. of the 26th West Virginia Surface Mine Drainage Task Force Symposium, April 19-20, Morgantown, WV, USA.

Huminicki, D.M.C. et Rimstidt, J.D. (2008). Neutralization of sulfuric acid solutions by calcite dissolution and the application to anoxic limestone drain design. *Applied Geochemistry*, 23,148–165.

Hustwit, C.C., Ackman, T.E., Erickson, P.M. (1992). The role of oxygen transfer in acid mine drainage treatment. *Water Environment Research*, 64, 817–823.

Janin, A. et Harrington, J. (2015). Performances of lab-scale anaerobic bioreactors at low temperature using Yukon native microorganisms. In: Proc. of Mine Water Solutions in Extreme Environments. April 12-15, Vancouver, Canada.

Jeen, S.-W. et Mattson, B. (2016). Evaluation of layered and mixed passive treatment systems for acid mine drainage. *Environmental Technology*, 37 (22), 2835–2851.

Jennings, S.R. et Jacobs, J.A. (2014). Overview of acid drainage prediction and prevention. In: Acid mine drainage, rock drainage, and acid sulfate soils: Causes, assessment, prediction, prevention, and remediation, Jacobs, J.A., Lehr, J.H., Testa, S. M. (Eds), John Wiley & Sons, Inc., Hoboken, NJ (USA), pp. 205–215.

Johnson, D.B. et Hallberg, K.B. (2005a). Acid mine drainage remediation options: A review. *Science of the Total Environment*, 338, 3–14.

Johnson, D.B. et Hallberg K.B. (2005b). Biogeochemistry of the compost bioreactor components of a composite acid mine drainage passive remediation system. *Science of the Total Environment*, 338, 81–93.

Kagambega, N., Galvez, R., Ouattara, A., Laflamme, M. (2014). Assessment of the neutralizing capacity of high purity dolomite on the highly polluted acid mine drainage. *International Journal of Environmental Engineering*, 1(3), 120–129.

Kalin, M., Fyson, A., Wheeler, W.N. (2006). The chemistry of conventional and alternative treatment systems for the neutralization of acid mine drainage. *Science of the Total Environment,* 366, 395–408.

Kepler, D.A. et McCleary, E.C. (1997). Passive aluminum treatment successes. In: Proc. of the NAAMLP, August 17–20, Davis, WV, USA. 7p.

King, D.W., Aldrich, R.A., Charnecki, S.E. (1993). Photochemical redox cycling of iron in NaCl solutions. *Marine Chemistry*, 44(2-4), 105–120.

Kirby, C.S., Thomas, H.M., Southam, G., Donald, R. (1999). Relative contributions of abiotic and biological factors in Fe(II) oxidation in mine drainage. *Applied Geochemistry*, 14, 511–530.

Kleinmann, R.L.P., Crerar, D.A., Pacellil, R.R. (1981). Biogeochemistry of acid mine drainage and a method to control acid formation. *Minerals Engineering*, 33(3), 300–305.

KTH, 2013. Visual MINTEQ, Version 3.0: a Window Version of MINTEQA2. http://vminteq.lwr.kth.se/.

Lewis, A.E. (2010). Review of metal sulphide precipitation. *Hydrometallurgy*, 104(2), 222–234.

Lovley, D.R. et Phillips, E.J.P. (1987). Competitive mechanisms for inhibition of sulfate reduction and methane production in the zone of ferric iron reduction in sediments. *Applied and Environmental Microbiology*, 53(11), 2636–2641.

Lovley, D.R. et Phillips, E.J.P. (1986). Organic matter mineralization with reduction of ferric iron in anaerobic sediments, *Applied and Environmental Microbiology*, 51 (4): 683–689.

Lozano, A., Ayora, C., Macias, F., Nieto, J.M., Gomez-Arias, A., Castillo, J., Van Heerden, E. (2015). Sulphate removal from acid mine drainage: Evaluation of granular $BaCO_3$ with column experiments. *Macla*, 20, 83–84.

Macías, F., Caraballo, M. A., Rötting, T.S., Pérez-López, R., Nieto, J.M., Ayora, C. (2012a). From highly polluted Zn-rich acid mine drainage to non-metallic waters: Implementation of a multi-step alkaline passive treatment system to remediate metal pollution. *Science of the Total Environment*, 433, 323–330.

Macías, F., Caraballo, M.A., Nieto, J.M., Rötting, T.S., Ayora, C. (2012b). Natural pretreatment and passive remediation of highly polluted acid mine drainage. *Journal of Environmental Management*, 104, 93–100.

Maqsoud, A., Neculita, C.M., Bussière, B., Benzaazoua, M., Dionne, J. (2016). Impact of fresh tailing deposition on the evolution of groundwater hydrogeochemistry at the abandoned Manitou mine site, Quebec, Canada. *Environmental Science and Pollution Research*, 23, 9054–9072.

Maree, J.P., Du Plessis, P., Van der Walt, C.J. (1992). Treatment of acidic effluents with limestone instead of lime. *Water Science and Technology*, 26 (1-2), 345–355.

Martin, T.R., et Holdich, D.M. (1986). The acute lethal toxicity of heavy metals to peracarid crustaceans (with particular reference to fresh-water asellids and gammarids). *Water Research*, 20, 1137–1147.

McCauley, C.A., O'Sullivan, A.D., Milke, M.W., Weber, P.A., Trumm, D.A. (2009). Sulfate and metal removal in bioreactors treating acid mine drainage dominated with iron and aluminum. *Water Research*, 43, 961–970.

McClurg, S.E., Petty, J.T., Mazik, P.M., Clayton, J.L. (2007). Stream ecosystem response to limestone treatment in acid impacted watersheds of the Allegheny Plateau. *Ecological Applications*, 17, 1087–1104.

MDDELCC (Ministère du Développement Durable de L'environnement et Lutte contre les Changements Climatiques) (2012). Directive 019 sur l'industrie minière, 105p.

MERN (Ministère des Ressources Naturelles) (1997). Guide et modalités de préparation du plan et exigences générales en matière de restauration des sites miniers au Québec, 64p.
https://mern.gouv.qc.ca/publications/mines/restauration/restauration-guifrmin.pdf

Moncur, M.C, Ptacek, C.J., Blowes, D.W., Jambor, J.L. (2005). Release, transport and attenuation of metals from an old tailings impoundment. *Applied Geochemistry*, 20 (3), 639–659.

Moore, J.W. (1991). Inorganic contaminants of surface water. Springer-Verlag, 1st ed. NY, USA.

Nastev, M. et Aubertin, M. (2000). Hydrogeological modelling for the reclamation work at the Lorraine mine site Québec. In: Proc. of the 1st Joint IAH-CNC-CGS Groundwater Specialty Conference, Montreal, Canada, pp. 311–318.

Neculita, C.M. et Rosa, E. (2017). Challenges of manganese removal in mine drainage and potential impacts of untreated effluents on the quality of natural waters. *Science of the Total Environment* (submitted, July 12).

Neculita, C.M., Yim, G.-J., Lee, G., Ji, S-W., Jung, J.-W., Park, H.-S., Song, H. (2011). Comparative effectiveness of mixed organic substrates to mushroom compost for treatment of mine drainage in passive bioreactors. *Chemosphere*, 83, 76-82.

Neculita, C.M., Zagury, G.J., Bussière, B. (2008a). Effectiveness of sulfate-reducing passive bioreactors for treating highly contaminated acid mine drainage: I. Effect of hydraulic retention time. *Applied Geochemistry*, 23, 3442–3451.

Neculita, C.M., Zagury, G.J., Bussière, B. (2008b). Effectiveness of sulfate-reducing passive bioreactors for treating highly contaminated acid mine drainage: II. Metal

removal mechanisms and potential mobility. *Applied Geochemistry*, 23, 3442–3451.

Neculita, C.M. et Zagury, G.J. (2008). Biological treatment of highly contaminated acid mine drainage in batch reactors: Long-term treatment and reactive mixture characterization. *Journal of Hazardous Materials*, 157, 358–366.

Neculita, C.M, Zagury G. J., Bussière, B. (2007). Passive treatment of AMD in the bioreactors using sulfate-reducing bacteria: Critical review and research needs. *Journal of Environmental Quality*, 36(1), 1–16.

Neuman, D.R., Brown, P.J., Jennings, S.R. (2014). Metals associated with acid rock drainage and their effect on fish health and ecosystems. In: Acid mine drainage, rock drainage, and acid sulfate soils: Causes, assessment, prediction, prevention, and remediation, Jacobs, J.A., Lehr J.H., Testa S. M. (Eds), John Wiley & Sons, Inc., Hoboken, NJ (USA), pp.139–169.

Nordstrom, D.K., Blowes, D.W., Ptacek, C.J. (2015). Hydrogeochemistry and microbiology of mine drainage: An update. *Applied Geochemistry*, 57, 3–16.

Nordstrom, D.K., Alpers, C.N., Ptacek, C.J., Blowes, D.W. (2000). Negative pH and extremely acidic mine waters from Iron Mountain California. *Environmental Science and Technology*, 34, 254–2582.

Nordstrom, D.K. et Alpers, C.N. (1999). Negative pH, efflorescent mineralogy, and consequences for environmental restoration at the Iron Mountain Superfund site, California. In: Proc. of the National Academy of Sciences, 96, 3455–3462.

Oh, C., Ji, S., Cheong, Y., Yim, G., Hong, J.-H. (2016). Evaluation of design factors for cascade aerator to enhance efficiency of oxidation pond for ferruginous mine drainage. *Environmental Technology*, 37 (19), 2483–2493.

Oh, C. Yu, C., Cheong, Y., Yim, G., Song, H., Hong, J.-H., Ji, S. (2015). Efficiency assessment of cascade aerator in a passive treatment system for Fe (II) oxidation

in ferruginous mine drainage of net alkaline. *Environmental Earth Eciences*, 73 (9), 5363–5373.

Orakwue, E.O., Asokbunyarat, V., Rene, E.R., Lens, P.N.L., Annachhatre, A. (2016). Adsorption of iron (II) from acid mine drainage contaminated groundwater using coal fly ash, coal bottom ash, and bentonite clay. *Water, Air and Soil Pollution*, 227 (3), 74.

Peacock, S. et Rimmer, D.L. (2000). The suitability of an iron-rich gypsum by-product as a soil amendment. *Journal of Environmental Quality*, 29, 1969–1975.

Phippen, B., Hovath, C., Nordin, R., Nagpal, N. (2008). Ambient water quality guidelines for iron. Overview report 978-0-7726-5990-3, 48p.

Postgate, J.R. (1984). The sulfate-reducing bacteria (2ème edition). Cambridge University Press, Cambridge.

Potgieter-Vermaak, S.S., Potgieter, J.H., Monama, P., Van Grieken, R. (2006). Comparison of limestone, dolomite and fly ash as pre-treatment agents for acid mine drainage. *Minerals Engineering*, 19, 454–462.

Potts, P.J. (1987). A handbook of silicate rock analysis, Blakie & Son Ltd. 622p.

Potvin, R. (2009). Évaluation à différentes échelles de la performance de systèmes de traitement passif pour les effluents fortement contaminés par le drainage minier acide. Thèse de doctort. Sciences appliquées, UQAT, Rouyn-Noranda, QC, Canada, 335p.

http://www.env.gov.bc.ca/wat/wq/BCguidelines/iron/iron_tech.pdf

Power, I.M., Wilson, S., Thom, J.M., Dipple, G.M., Southam, G. (2007). Biologically induced mineralization of dypingite by cyanobacteria from an alkaline wetland near Atlin, British Columbia, Canada. *Geochemical Transactions*, 8: 13.

Prasad, D., et Henry, J.G., 2009. Removal of sulphates, acidity and iron form from acid mine drainage in a bench scale biochemical system. *Environmental Technology*, 30 (2), 151–160.

Rakotonimaro, T.V., Neculita, C.M., Bussière, B., Zagury, G.J. (2017). Comparative column testing of three reactive mixtures for the bio-chemical treatment of iron rich acid mine drainage. *Minerals Engineering*, 111, 79–89.

Rakotonimaro, T.V., Neculita, C.M., Bussière, B., Zagury, G.J. (2016a). Recovery and reuse of sludge from active and passive treatment of mine drainage-impacted waters: a review. *Environmental Science and Pollution Research*, 24 (1), 73–91.

Rakotonimaro, T.V., Neculita, C.M., Bussière, B., Zagury, G.J. (2016b). Effectiveness of various dispersed alkaline substrates for the pretreatment of ferriferous acid mine drainage. *Applied Geochemistry*, 73: 13–23.

Rose, A.W., Shah, P.J., Means, B. (2003a). Case studies of limestone bed passive systems for manganese removal from acid mine drainage. In: Proc. of the 20th ASMR, June 3-6, Billings, MT, USA.

Rose, A.W., Means, B., Shah, P. (2003b). Methods for passive removal of manganese from acid mine drainage. In: Proc. of the 24th West Virginia Surface Mine Drainage Task Force Symposium, April 15, Morgantown, WV, USA.

Rötting, T.S., Luquot, L., Carrera, J., Casalinuovo, D.J. (2015). Changes in porosity, permeability, water retention curve and reactive surface area during carbonate rock dissolution. *Chemical Geology*, 403, 86–98.

Rötting, T.S., Caraballo, M.A., Serrano, J.A., Ayora, C., Carrera, J. (2008a). Field application of calcite Dispersed Alkaline Substrate (calcite-DAS) for passive treatment of acid mine drainage with high Al and metal concentrations. *Applied Geochemistry*, 23, 1660–1674.

Rötting, T.S., Thomas, R.C., Ayora, C., Carrera, J. (2008b). Passive treatment of acid mine drainage with high metal concentrations using dispersed alkaline substrate. *Journal of Environmental Quality*, 37, 1741– 1751.

Rötting, T.S., Ayora, C., Carrera, J. (2008c). Improved passive treatment of high Zn and Mn concentrations using caustic magnesia (MgO): particle size effects. *Environmental Science and Technology*, 42, 9370–9377.

Rötting, T.S., Ayora, C., Carrera, J. (2007). Chemical and hydraulic performance of "Dispersed Alkaline Substrate" (DAS) for passive treatment of acid mine drainage with high metal concentrations. In: Proc. of the IMWA, May 27-31, Cagliary, Italy.

Rötting, T.S., Jordi C., Ayora, C. (2006). Use of caustic magnesia to remove cadmium, nickel, and cobalt from water in passive treatment systems: column experiments. *Environmental Science and Technology*, 40, 6438–6443.

Sahoo, P.K., Kim, K., Equeenuddin, Sk. Md., Powell, M.A. (2013). Current approaches for mitigating acid mine drainage. In: Reviews of environmental contamination and toxicology, Whitacre, D.M., Bennett, E.R., Doerge, D.R. (Eds), NY (USA), 226: 1–32.

Santomartino, S. et Webb, J.A. (2007). Estimating the longevity of limestone drains in treating acid mine drainage containing high concentrations of iron. *Applied Geochemistry*, 2, 2344–2361.

Schwertmann, U. et Carlson, L. (2005). The pH-dependent transformation of schwertmannite to goethite at 25 °C. *Clay Minerals*, 40, 63–66.

Sibrell, P.L., Denholm, C., Dunn, M. (2013). Case study: Field trial of pulsed limestone well. National meeting of the ASMR, June 1-6, Barnhisel, R.I. (Eds), Lexignton, PA, USA.

Simón, M., Martín, F., García, I., Bouza, P., Dorronsoro, C., Aguilar, J. (2005). Interaction of limestone grains and acidic solutions from the oxidation of pyrite tailings. *Environmental Pollution*, 135 (1), 65–72.

Singh, N.B. et Middendorf, B. (2007). Calcium sulphate hemihydrate hydration leading to gypsum crystallization. *Progress in Crystal Growth and Characterization of Materials*, 53, 57–77.

Skousen, J., Zipper, C.E., Rose, A., Ziemkiewicz, P.F., Nairn, R., McDonald, L.M., Kleinmann, R.L. (2017). Review of passive systems for acid mine drainage treatment. *Mine Water and the Environment*, 36 (1), 133–153.

Skousen, J. et Ziemkiewicz, P. (2005). Performance of 116 Passive Treatment Systems for Acid Mine Drainage. National Meeting of the ASMR, June 19-23, Lexington, KY, USA, 31p.

Song, H., Yim, G.J., Ji, S.W., Nam, I.-H., Neculita, C.M., Lee, G. (2012a). Performance of mixed organic substrates during treatment of acidic and moderate mine drainage in column bioreactors. *Journal of Environmental Engineering*, 138 (10), 1077-1084.

Song, H., Yim, G.-J., Ji, S.-W., Neculita, C.M., Hwang, T. (2012b) Pilot-scale passive bioreactors for the treatment of acid mine drainage: Efficiency of mushroom compost vs. mixed substrates for metal removal. *Journal of Environmental Management*, 111, 150–158.

Sparks, D.L. (2003). Environmental soil chemistry (2ème edition). Academic Press, San Diego, CA, USA, 352p.

Strosnider, W.H.J., Nairn, R.W., Peer, R.A.M., Winfrey, B.K. (2013). Passive co-treatment of Zn-rich acid mine drainage and raw municipal wastewater. *Journal of Geochemical Exploration*, 125, 110–116.

Taylor, J., Pape, S., Murphy, N. (2005). A summary of passive and active treatment technologies for acid and metalliferous drainage (AMD). 5th Australian Workshop on acid drainage, August 29-31, Fremantle, Western Australia. 49p.

Taylor, S.W. et Jaffé, P.R. (1990). Biofilm growth and the related changes in the physical properties of a porous medium: 1. Experimental investigation. *Water Resources Research*, 26, 2153–2159.

Thomas, R.C. et Romanek, C.S. (2002). Passive treatment of low-pH, ferric iron-dominated acid rock drainage in a vertical flow wetland II: metal removal. In: Proc. of the ASMR, June 9-13, Lexignton KY, USA, pp.752–775.

Tsukamoto, T.K. et Miller, G.C. (1999). Methanol as a carbon source for microbiological treatment of acid mine drainage. *Water Research*, 33, 1365–1370.

URS (United Registrar of Systems) (2003). Passive and semi-active treatment of acid rock drainage from metal mines-state of the practice. Prepared for US Army Corps of Engineers, Portland, ME.

USEPA (United States Environmental Protection Agency) (2014a). Code of Federal Regulations: Part 434- Coal mining point source category BPT, BAT, BCT limitations and new source performance standards.
https://www.gpo.gov/fdsys/pkg/CFR-2014-title40-vol30/xml/CFR-2014-title40-vol30-part434.xml#seqnum434.33.

USEPA (United States Environmental Protection Agency) (2014b). Reference Guide to Treatment Technologies for Mining-influenced Water. EPA 542-R-14-001, 94p.

USGS (United States Geological Survey) (2015).
http://wwwbrr.cr.usgs.gov/projects/GWC_coupled/phreeqc/index.html

USGS (U.S. Geological Survey) (1962). Chemistry of iron in natural water. Geological Survey water-supply paper 1459. United States Governmental Printing Office, Washignton, USA.

Utgikar, V.P., Harmon, S.M., Chaudary, N., Tabak, H.H., Govind, R., Haines, J.R. (2002). Inhibition of sulfate-reducing bacteria by metal sulfide formation in bioremediation of acid mine drainage. *Environmental Toxicology*, 17 (1), 40–48.

Van Bodegom, P.M., Scholten, J.C., Stams, A.J. (2004). Direct inhibition of methanogenesis by ferric iron. *FEMS Microbiology Ecology*, 49, 261–268.

Vasquez, Y., Escobar, M.C., Saez, J., Quiceno-Vallejo, M.F., Neculita, C.M., Arbeli, Z., Roldan, F. (2017) Effect of hydraulic retention time on the microbial community in biochemical passive reactors during treatment of acid mine drainage. *Bioresource Technology* (submitted, July 17).

Vasquez, Y., Escobar, María, C., Neculita, C. M., Arbeli, Z., Roldan, F. (2016a). Biochemical passive reactors for treatment of acid mine drainage: Effect of hydraulic retention time on changes in efficiency, composition of reactive mixture, and microbial activity. *Chemosphere*, 153, 244–253.

Vasquez, Y., Escobar, María, C., Neculita, C. M., Arbeli, Z., Roldan, F. (2016b). Selection of reactive mixture for biochemical passive treatment of acid mine drainage. *Environmental Earth Sciences*, 75, 576.

Watzlaf, G.R. (2004). Treatment of high-flow, low-iron mine drainage with a semi-passive system. In: Proc. of the National Meeting of the ASMR, Morgantown, WV, USA. pp. 1962–1973.

Watzlaf, G.R., Schroeder, K.T., Kleinmann, R.L., Kairies, C.L., Nairn, R.W. (2004). The passive treatment of coal mine drainage. USDOE/NETL Report 2004/1202. U.S. Department of Energy, Washington, DC, USA. 72 p.

Watzlaf, G.R., Schroeder, K.T., Kairies, C.L. (2000). Long-term performance of anoxic limestone drains. *Mine Water and the Environment*, 19, 98–110.

Waybrant, K., Ptacek, C., Blowes, D. (2002). Treatment of mine drainage using permeable reactive barriers: column experiments. *Environmental Science and Technology*, 36, 1349–1356.

Waybrant, K., Ptacek, C., Blowes, D., Ptacek, C.J. (1998). Selection of reactive mixtures for use in permeable reactive walls for the treatment of acid mine drainage. *Environmental Science and Technology*, 32, 1972–1979.

WHO (World Health Organization) (2011). Guidelines for drinking-water quality (4ème edition)
http://www.who.int/water_sanitation_health/publications/2011/dwq_guidelines/en/.

Widdel, F. (1988). Microbiology and ecology of sulfate-and sulfur- reducing bacteria. AJB Zehn der (Eds). Biology of anaerobic microorganism. NY, USA. pp. 469–586.

Willow, M.A. et Cohen, R.R.H. (2003). pH, dissolved oxygen, and adsorption effects on metal removal in anaerobic bioreactors. *Journal of Environmental Quality*, 32, 1212–1221.

Wolfe, N., Hedin, B., Weaver, T. (2010). Sustained treatment of AMD containing Al and Fe^{3+} with limestone aggregate. In: Proc. of the IMWA, September 5-9, Wolkersdorfer & Freund (Eds), Sydney, NS, Canada. pp. 29–32.

Yim, G.-J., Ji, S.-W., Cheong, Y.-W., Neculita C.M., Song, H. (2015). The influences of the amount of organic substrate on the performance of pilot-scale passive bioreactors for acid mine drainage treatment. *Environmental Earth Sciences*, 73, 4717-4727.

Younger, P.L., Banwart, S.A., Hedin, R.S. (2002). Passive treatment of polluted mine waters, in: Mine water: Hydrology, pollution, remediation. Kluwer Academic Publishers, Norwell, MA, USA. pp. 311–393.

Zagury, G.J., Neculita, C., Bussière, B. (2007). Passive treatment of acid mine drainage in bioreactors: short review, applications, and research needs. The 60th Canadian Geotechnical Conference & 8th Joint CGS/IAH-CNC Groundwater Conference, October 21-24, Ottawa, ON, Canada.

Zagury, G.J., Kulnieks, V.I., Neculita, C.M. (2006). Characterization and reactivity assessment of organic substrates for sulphate reducing bacteria in acid mine drainage treatment. *Chemosphere*, 64 (6), 944–954.

Zarzo, D., López, A., Campos, E., Nieto, J., Macías, F., García, M., Mateos, F., Belmonte, A. (2016). Research and development project for sustainable treatment of acid mine drainage water. In: Proc. of the Water in Mining, May 18-20, Santiago, Chile.

Zhang, T., Tu, Z., Lu, G., Duan, X., Yi, X., Guo, C., Dang, Z. (2017). Removal of heavy metals from acid mine drainage using chicken eggshells in column mode. *Journal of Environmental Management*, 188, 1–8.

Zhang, L., Keller, J., Yuan, Z. (2009). Inhibition of sulfate-reducing and methanogenic activities of anaerobic sewer biofilms by ferric iron dosing. *Water Research*, 43, 4123–4132.

Ziemkiewicz, P.F. et Brant, D. (1997). The Casselman river restoration project. In: Proc. of the 18th WV Surface Mine Drainage Task Force Symposium, Morgantown, WV, USA.

Ziemkiewicz, P.F., Skousen, J.G., Brant, D.L., Sterner, P.L., Lovett, R.J. (1997). Acid mine drainage treatment with armored limestone in open limestone channels. *Journal of Environmental Quality*, 26(4), 1017–1024.

Zinck, J. et Griffith, W. (2013). Review of acidic drainage treatment and sludge management operations, MEND Report 3.43.1. CANMET-MMSL, 101p. http://mend-nedem.org/wp-content/uploads/3.43.1_ReviewMineDrainageTreatmentSludge.pdf

Zipper, C. et Skousen, J. (2014). Passive treatment of acid mine drainage. In: Acid mine drainage, rock drainage, and acid sulfate soils: Causes, Assessment, prediction, prevention, and remediation. Jacobs, J.A., Lehr, J. H., Testa, S.M. (Eds), John Wiley & Sons, Inc., Hoboken, NJ, USA, pp. 339–353.

Zipper, C., Skousen, J., Jage, C. (2011). Passive treatment of acid-mine drainage. Communications and Marketing, College of Agriculture and Life sciences. Publication 460-133, Virginia, PT, USA, 15p.

Zipper, C.E. et Skousen, J. (2010). Influent water quality affects performance of passive treatment systems for acid mine drainage. *Mine Water and the Environment*, 29, 135–143.

ANNEXE A

COMPLÉMENTS DE DONNÉES SUR LES ESSAIS BATCH

Table A.1 Chemical characteristics of wood ash, calcite and dolomite used in batch testing (Genty et al., 2012a; 2012b)

Characteristics	Wood ash	Calcite	Dolomite
Mineral composition by XRD (%w/w)			
Calcite	n.q.	95	<1
Dolomite	n.q.	0	75
Quartz	n.q.	2.5	15
Hornblende	n.q.	2.5	0
Muscovite	n.q.	<1*	9
Kutnahorite	n.q.	<1	0.5
Magnesite	n.q.	<1	0.5
Element abundance by ICP-AES (%w/w)			
Ca	12.3	35	16.5
Mg	1.4	0.5	8.7
Al	2.3	0.01	0.9
Mn	0.2	0.006	0.038
Fe	1.5	0.7	0.7
S	0.2	0.5	0.03

*Method detection limit; n.q: not quantified

Table A.2 Estimated calculations of Fe removal from ferriferous AMD with different type of DAS

Reactors	Time (days)	Number of days, *A*	Initial Fe concentration (mg/L), *B*	Final Fe concentration (mg/L), *C*	Mass of Fe introduced in reactors (mg), *D*	Mass of Fe in effluent (mg), *E*	Estimated precipitated Fe in reactor (mg), *F*	Fe precipitated (%),*G*	Fe precipitation rate (mg Fe/d), *H*
WA20	0-7	7	2760	1.1	1678.08	0.67	1677.41	99.9	239.63
	7-21	14	229	137	147.25	88.09	59.16	42.9	4.23
	21-70	49	384	281	251.52	184.06	67.47	27.0	1.38
	70-91	21	388	350	241.72	218.05	23.67	25.8	1.13
Total after 91 days					2318.57	490.86	1827.71	Ave. 48.9	246.36
WA50	0-7	7	2760	0.3	1656.00	0.16	1655.84	99.9	236.55
	7-21	14	197.5	163	118.50	97.80	24.84	17.5	1.48
	21-70	49	362	262	217.20	157.20	75.00	27.6	1.22
	70-91	21	325	235	195.00	141.00	68.40	27.7	2.57
Total after 91 days					2186.70	396.16	1824.08	Ave. 43.2	241.82
WA80	0-7	7	2760	0.1	1656.00	0.06	1655.94	100.0	236.55
	7-21	14	205.4	154	139.67	104.72	34.95	25.0	1.77
	21-70	49	322	192	231.84	138.24	93.60	40.4	1.53
	70-91	21	162	73	108.54	48.91	59.63	55.0	3.26
Total after 91 days					2136.05	291.93	1844.12	Ave. 55.1	243.11
C20	0-7	7	2760	1750	1490.40	945.00	545.40	36.6	77.91
	7-21	14	1977	1533	1067.58	828	240	22.5	-2.97
	21-70	49	2058	1902	1115.44	1030.88	84.55	7.6	1.73
	70-91	21	1735	1633	867.50	816.50	51.00	5.9	2.43
Total after 91 days					2525.43	3901.54	639.37	Ave. 18.15	79.10
C50	0-7	7	2760	2270	1656.00	1362.00	294.00	17.8	42.00
	7-21	14	2135	1605	1093.68	823	271.11	25	2.27
	21-70	49	1991	1834	1051.25	968.35	82.90	7.9	1.69
	70-91	21	1772	1662	839.93	787.79	52.14	6.2	2.48
Total after 91 days					4640.85	4180.04	460.81	Ave. 14.2	48.44

C80	0-7	7	2760	2340	1501.44	1272.96	228.48	15.2	32.64
	7-21	14	2310	1721	1196.58	891.48	305.10	25.5	21.79
	21-70	49	2012	1771	1046.24	920.92	125.32	12.0	2.56
	70-91	21	1265	1203	598.35	569.02	29.33	4.9	1.40
Total after 91 days					4342.61	3654.38	228.48	Ave. 14.4	58.39
D20	0-7	7	2760	2155	1380.00	1077.50	302.50	21.9	43.21
	7-21	14	2201	2115	1188.54	1142.10	46.44	3.9	3.32
	21-70	49	2146	2046	1073.00	1023.00	50.00	4.7	1.02
	70-91	21	1835	1665	825.75	749.25	76.50	9.3	3.64
Total after 91 days					4467.29	3991.85	475.44	Ave. 9.9	51.19
D50	0-7	7	2760	2400	1338.60	1164.00	174.60	13.0	24.94
	7-21	14	2448	2289	1260.72	1178.84	81.89	6.5	5.85
	21-70	49	2016	1920	1042.27	992.64	49.63	4.8	1.01
	70-91	21	1612	1393	757.64	654.71	102.93	13.6	4.90
Total after 91 days					4399.23	3990.19	409.05	Ave. 9.5	36.71
D80	0-7	7	2760	2365	1490.40	1277.10	213.30	14.3	30.47
	7-21	14	2431	2275	1312.74	1228.50	84.24	6.4	6.017
	21-70	49	1906	1690	975.87	865.28	110.59	11.3	2.25
	70-91	21	1015	797	471.98	370.61	101.37	21.5	4.83
Total after 91 days					4250.99	3741.49	509.50	Ave. 13.4	43.57

Volume (*V*): 500-610mg/L; *D=B* x *V*; *E=C* x *V*; *F= D-E*; *G=(F/D)* x 100; *G= H/A*

Table A.3 Fe removal during the first 12 h in WA-DAS reactors (first set)

Reactors	Time (hours)	Number of hours, *A*	Initial Fe concentration (mg/L), *B*	Final Fe concentration (mg/L), *C*	Mass of Fe introduced in reactors (mg), *D*	Mass of Fe in effluent (mg), *E*	Estimated precipitated Fe in reactor (mg), *F*	Fe precipitated (%),*G*	Fe precipitation rate (mgFe/h), *H*
	0-1	1	2592	992	1555	595	960	61.7	
	1-2	1	992	920	595	552	43	7.3	
	2-3	1	920	840	552	504	48	8.7	
	3-4	1	840	565	504	339	165	32.7	
WA20	4-6	2	565	680	339	408	-69	-20.4	106.7
	6-8	2	680	575	408	345	63	15.4	
	8-9	1	575	496	345	298	47	13.74	
	9-11	2	496	470	298	282	16	5.2	
	11-12	1	470	458	282	275	7	2.6	
Total		12					1280	Ave. 14	
	0-1	1	2592	816	1555	490	1066	68.5	
	1-2	1	816	670	490	402	88	17.9	
	2-3	1	670	544	402	326	76	18.8	
	3-4	1	544	440	326	264	62	19.1	
WA50	4-6	2	440	408	264	245	19	7.3	119.4
	6-8	2	408	328	245	197	48	19.6	
	8-9	1	328	304	197	182	14	7.3	
	9-11	2	304	278	182	167	16	8.6	
	11-12	1	278	204	167	122	44	26.6	
Total		12					1433	Ave. 21.5	
	0-1	1	2592	448	1555	269	1286	82.7	
	1-2	1	448	120	269	72	197	73.2	
	2-3	1	120	216	72	130	-58	-80.0	
	3-4	1	216	116	130	70	60	46.3	
WA80	4-6	2	116	70	70	42	28	39.7	128.6
	6-8	2	70	64	42	38	4	9.3	
	8-9	1	64	57	38	34	4	10.2	
	9-11	2	57	108	34	65	-31	-89.5	
	11-12	1	108	21	65	13	52	80.6	
Total		12					1543	Ave. 19	

Volume (*V*): 600mg/L; *D*=*B* x *V*; *E*=*C* x *V*; *F*= *D*-*E*; *G*=(*F*/*D*) x 100; *G*= *H*/*A*

Table A.4 Fe removal in the first 12 h in WA-DAS reactors (second set)

Reactors	Time (hours)	Number of hours, *A*	Initial Fe concentration (mg/L), *B*	Final Fe concentration (mg/L), *C*	Mass of Fe introduced in reactors (mg), *D*	Mass of Fe in effluent (mg), *E*	Estimated precipitated Fe in reactor (mg), *F*	Fe precipitated (%),*G*	Fe precipitation rate (mg Fe/h), *H*
	0-1	1	2524	1800	1514	1080	434	28.7	
	1-2	1	1800	1150	1080	690	390	36.1	
	2-3	1	1150	1504	690	902	-212	-30.8	
	3-4	1	1504	1460	902	876	26	2.9	
WA20	4-6	2	1460	1175	876	705	171	19.5	89.4
	6-8	2	1175	1150	705	690	15	2.1	
	8-9	1	1150	1488	690	893	-203	-29.3	
	9-11	2	1488	1100	893	660	233	26.1	
	11-12	1	1100	736	660	442	218	33.1	
Total		12					1280	Ave. 5.5	
	0-1	1	2400	1300	1440	780	660	45.8	
	1-2	1	1300	850	780	510	270	34.6	
	2-3	1	850	1080	510	648	-138	-27.1	
	3-4	1	1080	630	648	378	270	41.7	
WA50	4-6	2	630	838	378	503	-125	-32.9	93.3
	6-8	2	838	720	503	432	71	14.0	
	8-9	1	720	592	432	355	77	17.8	
	9-11	2	592	430	355	258	97	27.4	
	11-12	1	430	535	258	321	-63	-24.4	
Total		12					1433	Ave. 11	
	0-1	1	2380	1240	1428	744	684	47.9	
	1-2	1	1240	940	744	564	180	24.2	
	2-3	1	940	740	564	444	120	21.3	
	3-4	1	740	520	444	312	132	29.7	
WA80	4-6	2	520	480	312	288	24	7.7	109
	6-8	2	480	340	288	204	84	29.2	
	8-9	1	340	488	204	293	-89	-43.5	
	9-11	2	488	244	293	146	146	50.0	
	11-12	1	244	200	146	120	26	18.0	
Total		12					1543	Ave. 20.5	

Volume (*V*): 600mg/L; *D*=*B* x *V*; *E*=*C* x *V*; *F*= *D*-*E*; *G*=(*F*/*D*) x 100; *G*= ***H***/*A*

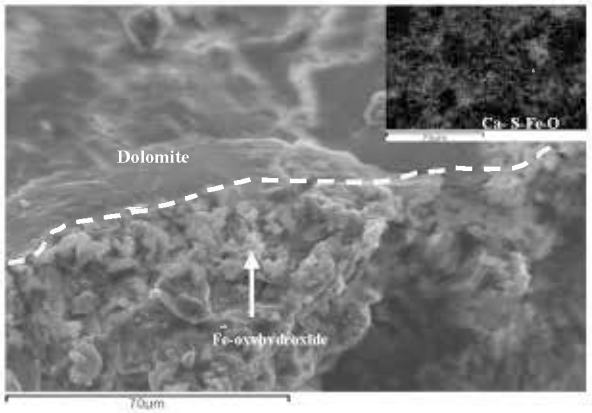

Figure A.1 SEM-EDS images showing the coating with calcium sulfate and Fe-oxyhydroxides of the surface of dolomite from D80 after the batch testing

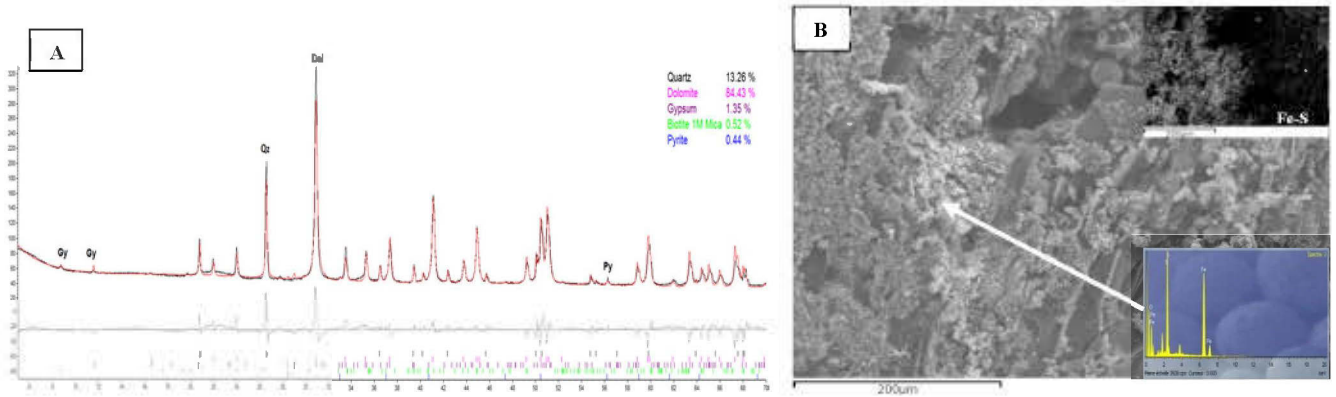

Figure A.2 (A) Diffractogram showing the presence of gypsum and pyrite as the secondary crystallized minerals in D50, (B) SEM-EDS images of Fe-oxyhydroxides and pyrite on the surface of wood chips in WA80

ANNEXE B

COMPLÉMENTS DE DONNÉES SUR LES ESSAIS EN PETITES COLONNES

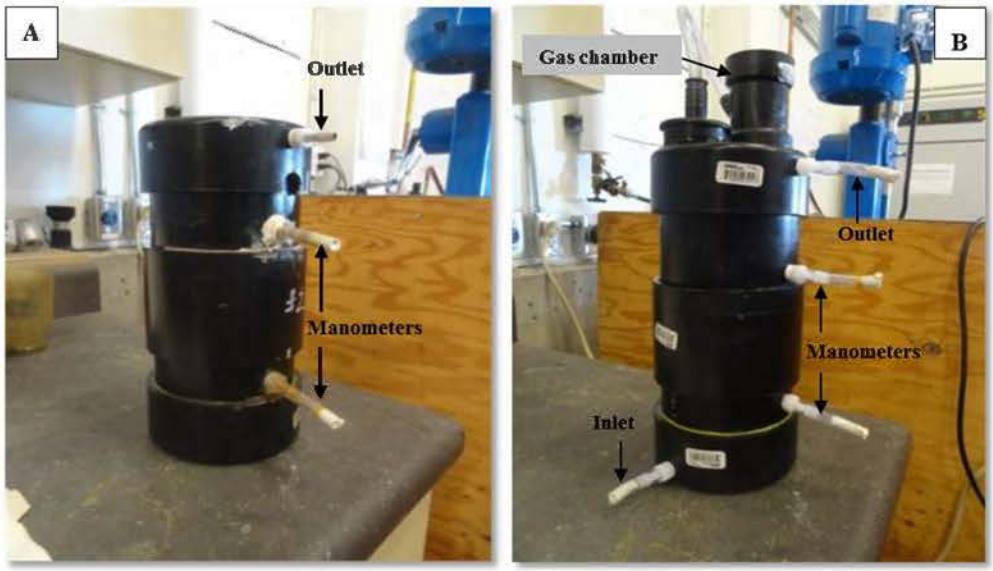

Figure B.1 Design of columns materials for: (A) Dispersed Alkaline Substrate (DAS) reactors and (B) Passive Biochemical Reactors (PBRs)

Table B.1 Comparison of wood ash-based mixtures with a previous studies

Mixture	#1	#4	#5	WA-DAS
	Genty et al., 2012b			*This study*
Mixtures				
Wood ash	100%	40%	70%	50%
Sand	-	60%	30%	-
Wood chips	-	-	-	50%
Hydraulic characteristics				
Estimated porosity	0.47	0.44	0.44	0.74
k_{sat} (cm/s)	5.0×10^{-3}–3.1×10^{-2}			1.6×10^{-3}–1.2×10^{-2}
Mixtures performance				
HRT (d*.)	5.3	5	5.1	1,2,3,5
Optimal efficiency				
Fe removal (%)	>99.8% (108d.)	>99.9% (60d.)	>99.9% (67d.)	>99.9% (2,4,12,16d.)
SO_4^{2-} removal (%)	44	43	49	44,43, 48,63
Steady state				
Fe removal	-	-	-	8.5,33, 44, 62% (12, 26, 30, 30d.)
SO_4^{2-} removal (%)	-	-	-	<8,23, 35 (12, 26, 30d.)

*days

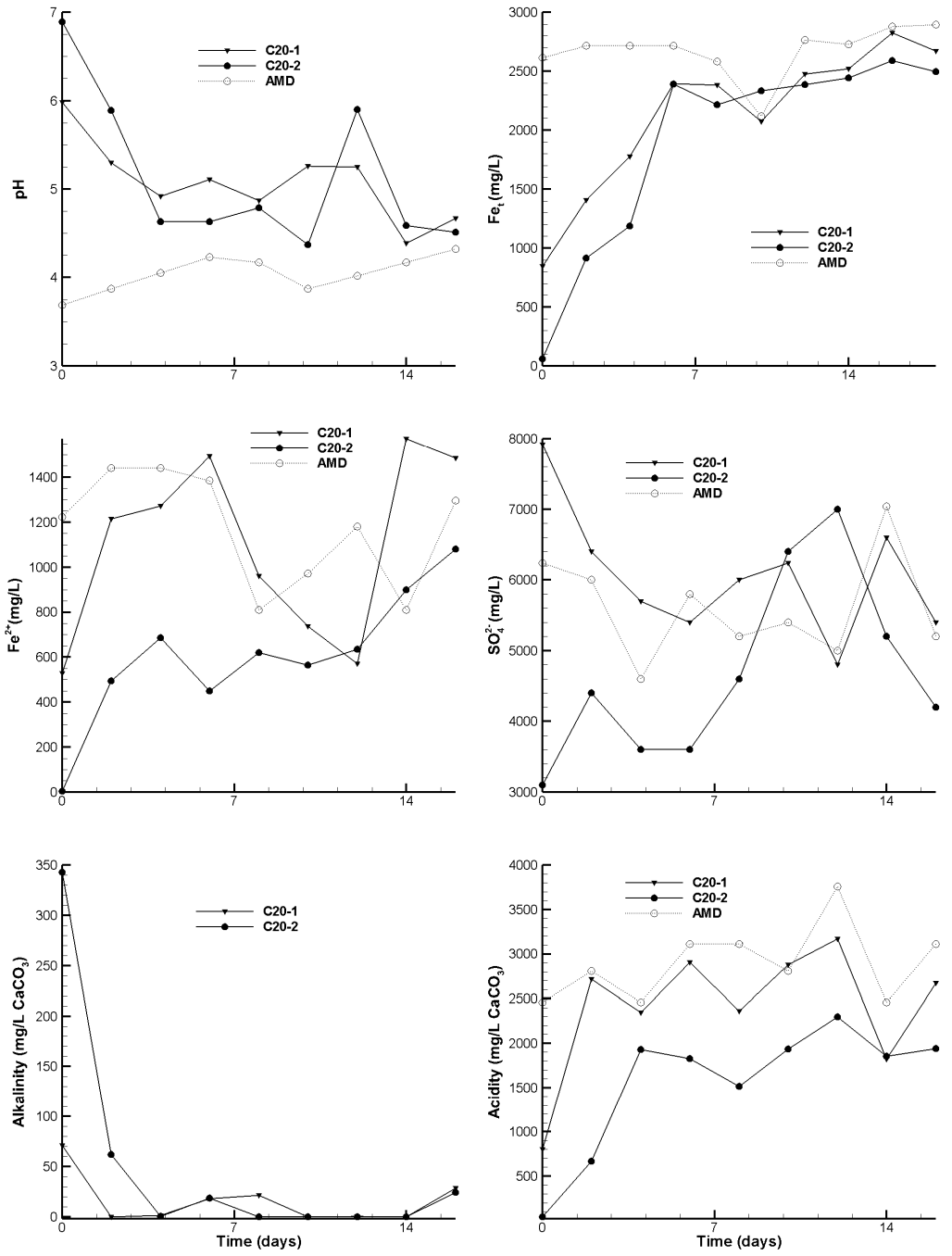

Figure B.2 Evolution of physicochemical parameters in the calcite-DAS reactors during column testing

Table B.2 Saturated indices (SI) of the possible mineral phases calculated with PHREEQC code with respect to physicochemical parameters in water from WA50-3 reactor and R5

Phase	Chemical formula	SI	
		W50-3	R5
Alunite (Na)	$NaAl_3(SO_4)_2\ (OH)_6$	1.59	4.65
Boemhite	AlO(OH)	2.56	2.65
Corundum	Al_2O_3	1.99	2.16
Cerussite	$PbCO_3$	0.20	−2.77
Dawsonite	$NaAlCO_3(OH)_2$	−0.67	2.66
Diaspore	AlO(OH)	3.34	3.42
Ferrihydrite	$Fe\ (OH)_3$	4.95	2.37
Ferrite (Mn)	$MnFe_2O_4$	9.87	3.96
FeS	FeS	−53.49	−46.75
Gibbsite	$Al(OH)_3$	2.48	2.57
Goethite	FeOOH	7.64	5.06
Greigite	Fe_3S_4	−199.98	−173.46
Gypsum	$CaSO_4.2H_2O$	0.18	0.03
Hematite	Fe_2O_3	16.03	10.87
Jacobsite	$Mn(FeO_2)_2$	9.03	3.12
Jarosite (Pb)	$Pb0.5Fe_3(SO_4)_2\ (OH)_6$	9.51	0.54
Lepidocrocite	FeOOH	6.12	3.54
Magnesioferrite	$MgFe_2O_4$	5.99	0.39
Magnetite	Fe_3O_4	15.86	9.13
Mackinawite	FeS	−52.93	−46.19
$NiFe_2O_4$	$NiFe_2O_4$	12.21	4.68
Rhodochrosite	$MnCO_3$	0.06	−0.27
Schwertmannite	$Fe_8O_8\ (OH)_6\ SO_4.\ nH_2O$	41.68	21.36
Siderite	$FeCO_3$	1.29	0.77

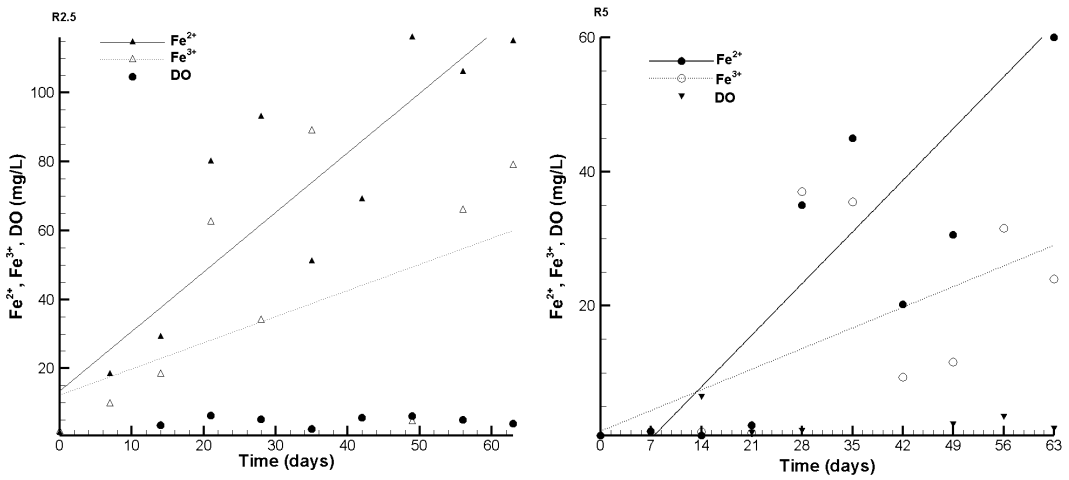

Figure B.3 Evolution of Fe^{2+}, Fe^{3+}, and DO concentrations in R2.5 and R5

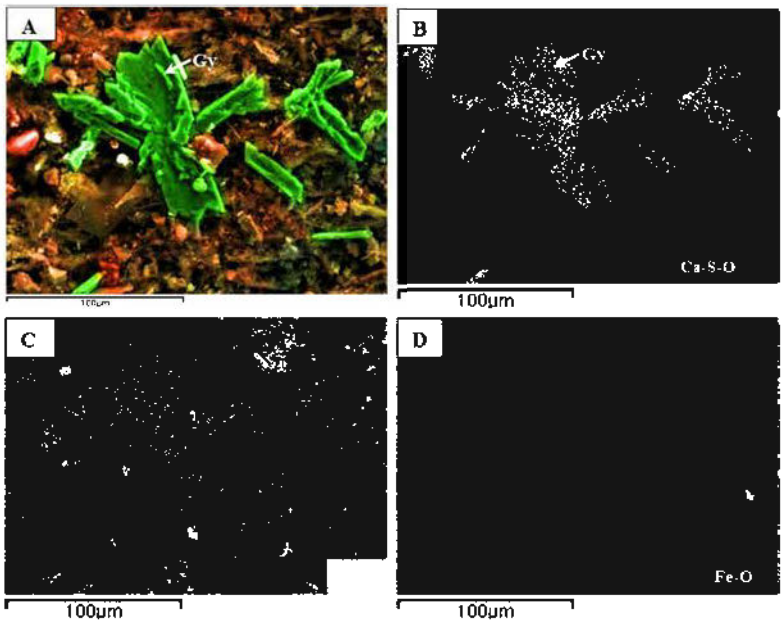

Figure B.4 SEM-EDS images of minerals observed at the bottom layer of WA50-3 (0-10 cm): (A) Cameo image of euhedral gypsum (Gy in green color) on a Fe-oxide/hydroxide layer (red-brownish); (B) SEM-EDS picture of sulfate included in gypsum; (C) Image of Ca in excess forming a second layer on top of the Fe-oxides/hydroxides; (D) Thin layer of Fe-oxides/hydroxides under gypsum crystal

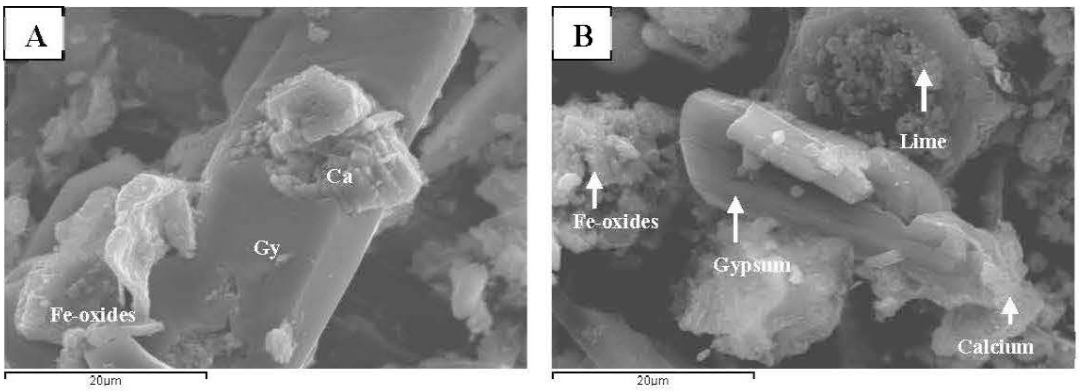

Figure B.5 SEM images of spent reactive mixture from the WA50-3 reactor: (A) Crystal growth of gypsum (Gy) with an abscess of calcium at the 0-10 cm bottom layer, (B) Grouping of precipitates including Fe-oxides, gypsum, lime and excess of calcium observed at the 15-20 cm top layer

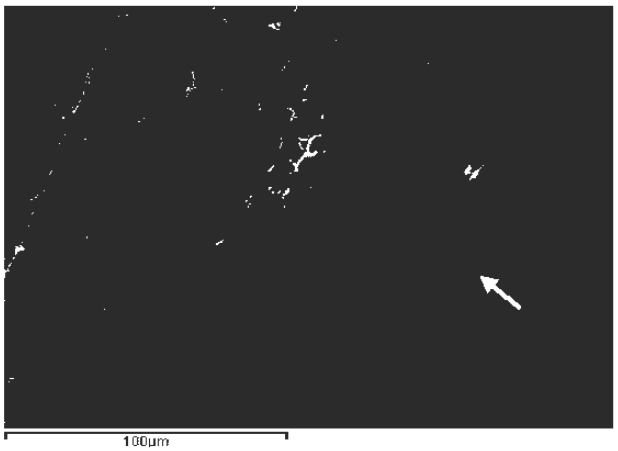

Figure B.6 Rosette-like carbonate mineral containing Mn and Ni observed at the bottom layer (0-5cm) of the spent reactive mixture recovered from the WA50-3 reactor

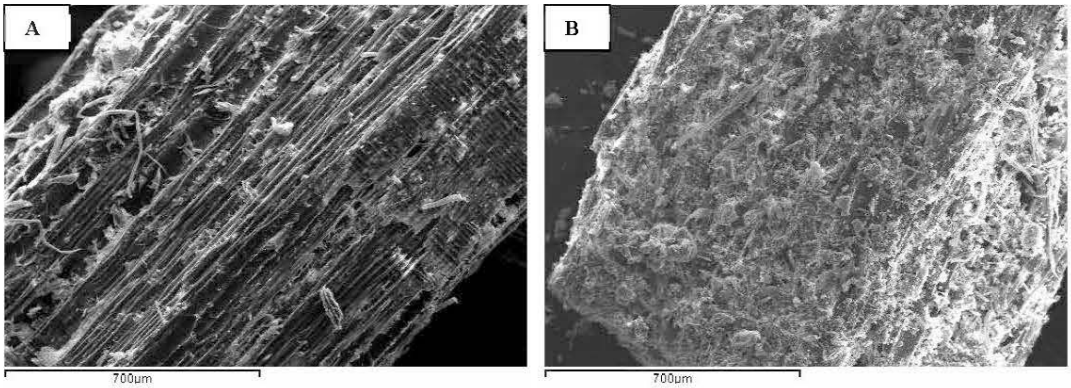

Figure B.7 SEM images of (A) Wood chips before treatment with PBRs, (B) Wood chips collected at the bottom layer (0-5cm) of PBRs operated at HRT of 5 d fouled with precipitates containing Fe, Mn, S, Ca.

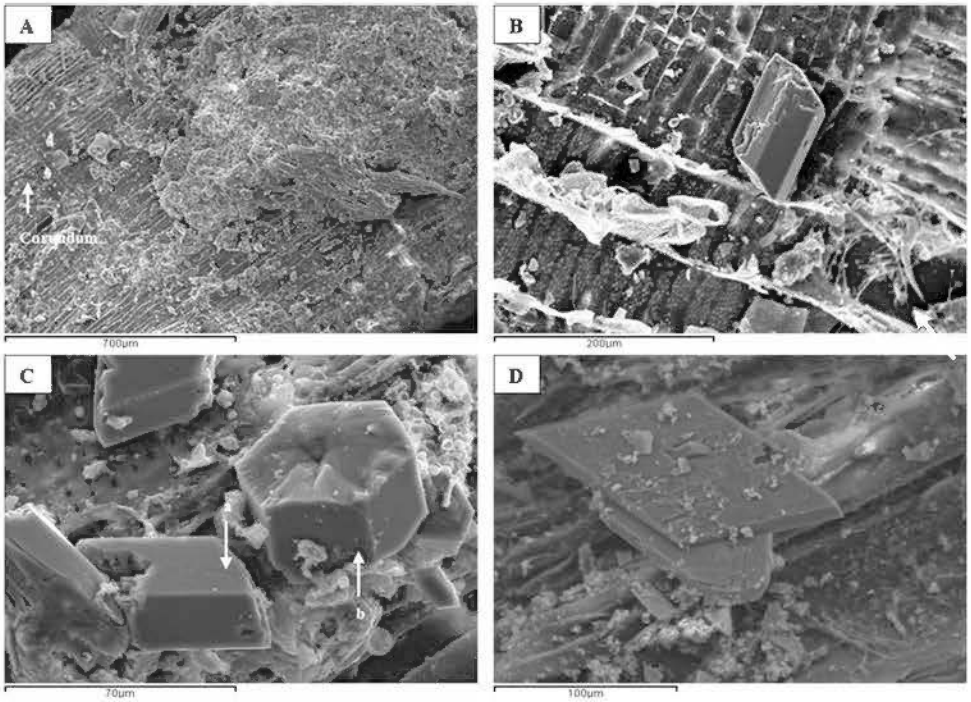

Figure B.8 SEM images of minerals observed from spent reactive mixture in R5, at the top layer (15-20 cm) and at the bottom layer (0-10 cm): (A) Wood chips fouled with Fe-oxides/hydroxides with small particles of corundum; (B) Euhedral gypsum with fine particle of aluminum hydroxide; (C) a. Interlaced block of calcium sulfate– b. Crystal of γ- hemihydrate gypsum; (D) Plate-like gypsum

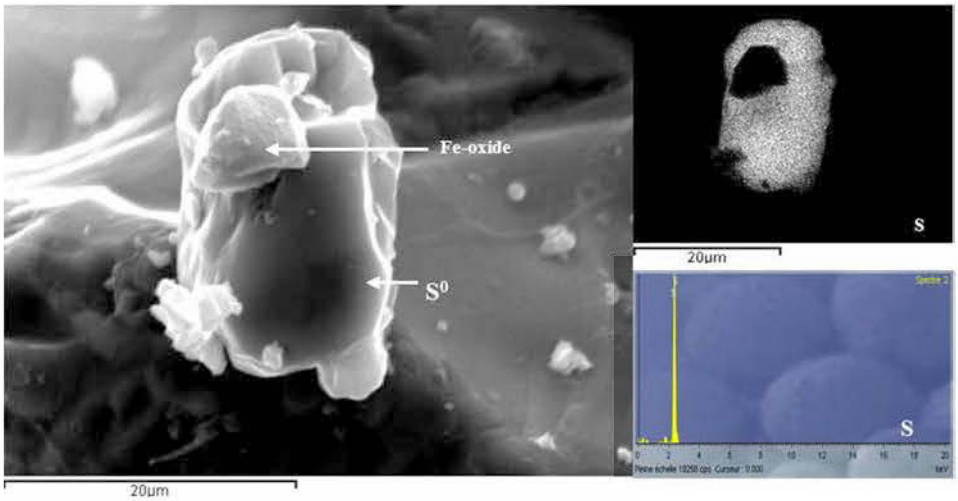

Figure B.9 SEM-EDS image of native sulfur S^0 with particle of Fe-oxide covered with calcium at the bottom layer (0-10 cm) of spent reactive mixture from R5

ANNEXE C

COMPLÉMENTS DE DONNÉES SUR LES ESSAIS EN FILIÈRE ET LES TRAVAUX DE TERRAIN

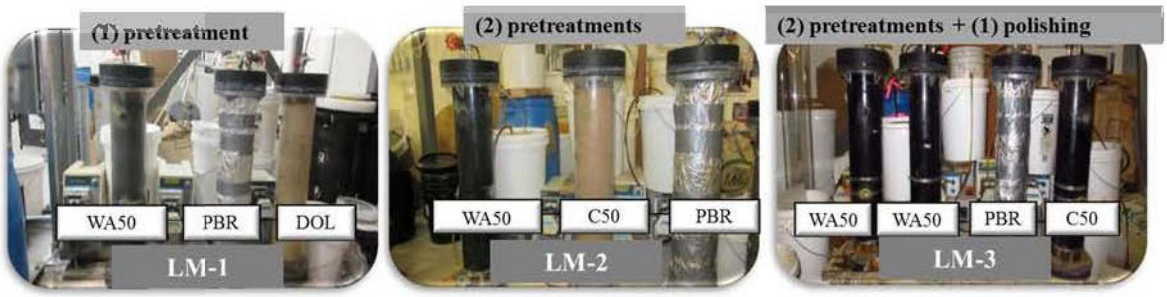

Figure C.1 Configuration of the three scenarios (LM-1, LM-2, LM-3) of multi-step systems during laboratory experiments

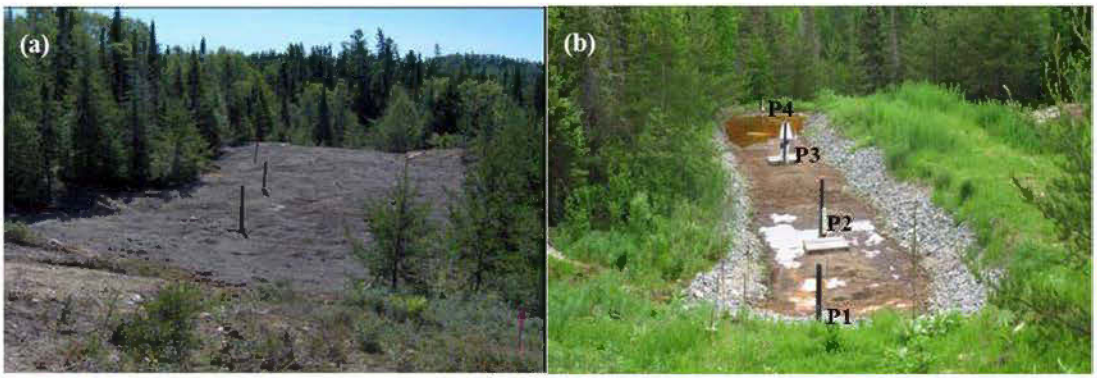

Figure C.2 Multi-step passive treatment system composed of two PBRs separated by a wood ash unit, in 2011, just after installation (a), and in 2016 (b) (Photos: Genty, 2012; Rakotonimaro, 2016)

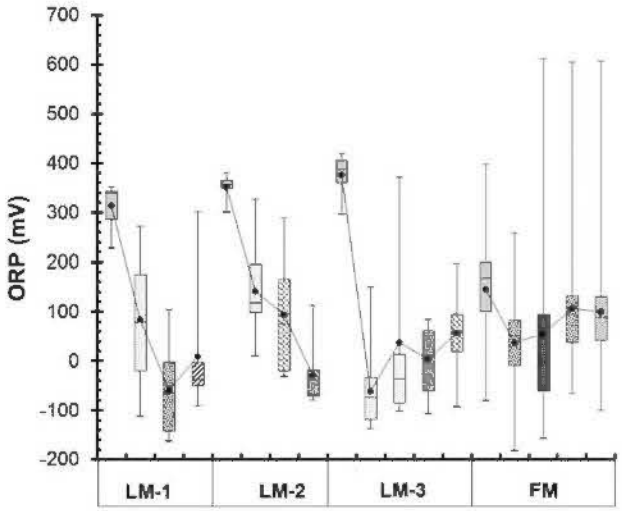

Figure C.3 Comparison of ORP values during laboratory (LM-1, LM-2, LM-3) and field pilot (FM) experiments

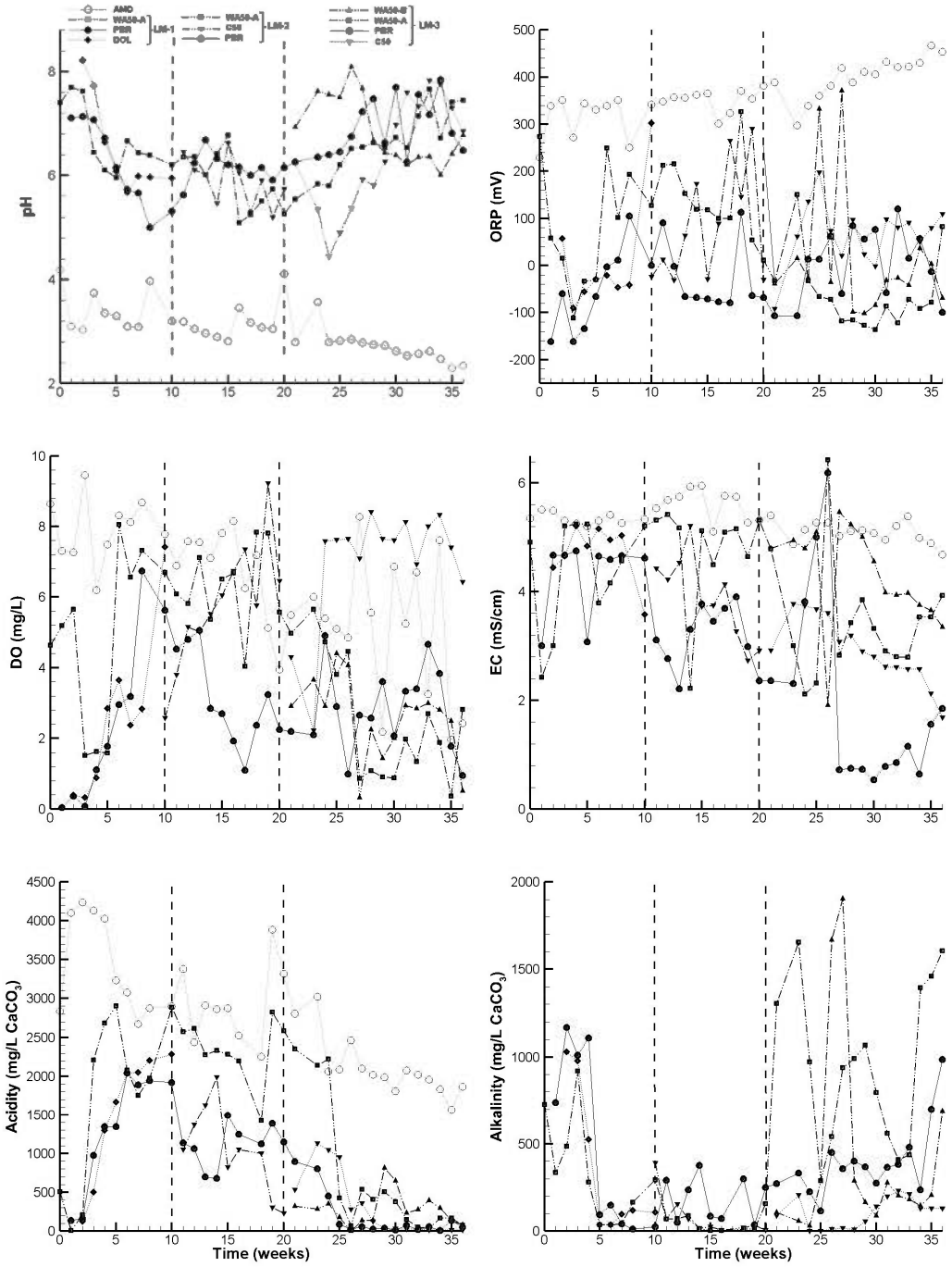

Figure C.4 Evolution of physicochemical parameters (pH, ORP, EC, DO, alkalinity, acidity) during the three laboratory scenarios of multi-step treatment systems (LM-1, LM-2, LM-3) experiments

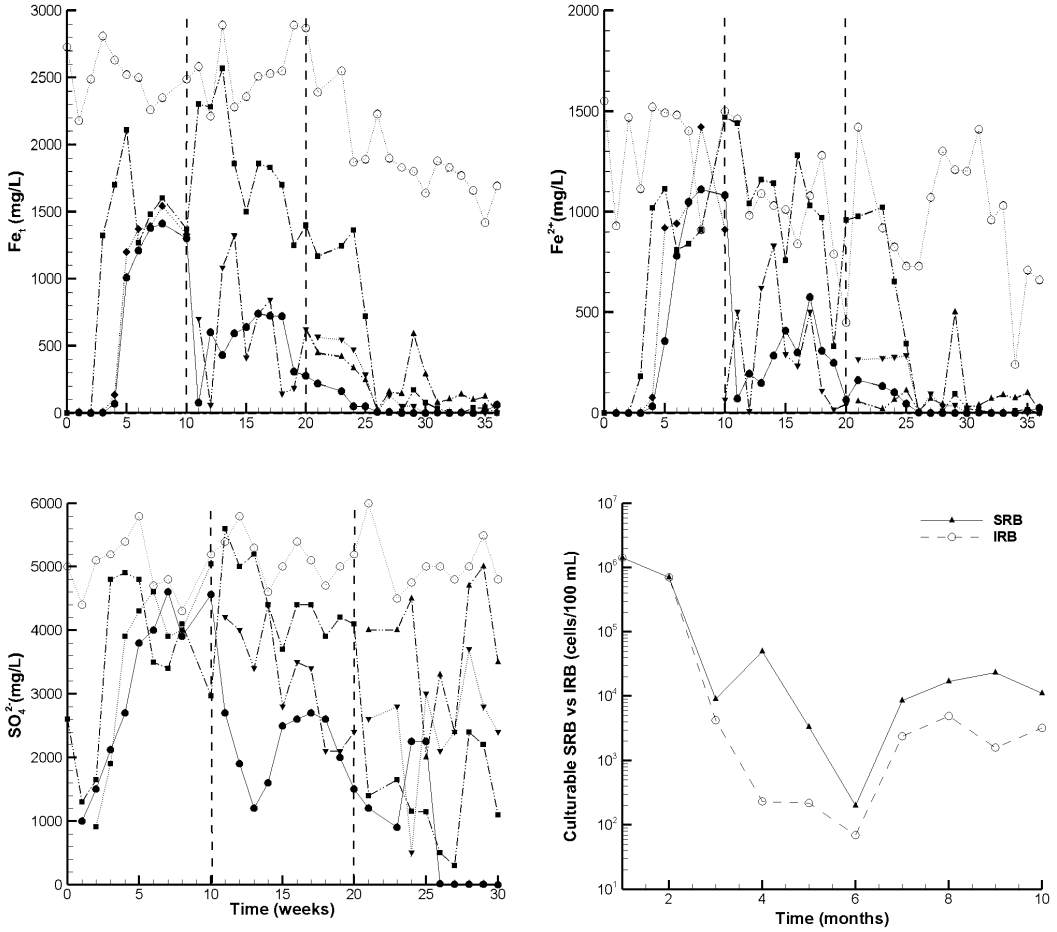

Figure C.5 Evolution of Fe_t, Fe^{2+}, SO_4^{2-} concentrations, and microbial counts during laboratory multi-step treatment (LM-1, LM-2, LM-3) experiments

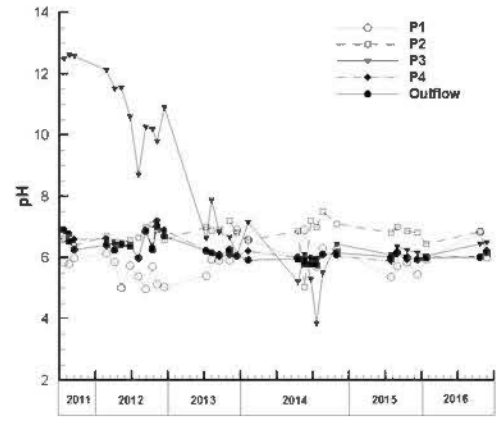
P1
P2
P3
P4
Outflow
pH
2011
2012
2013
2014
2015
2016

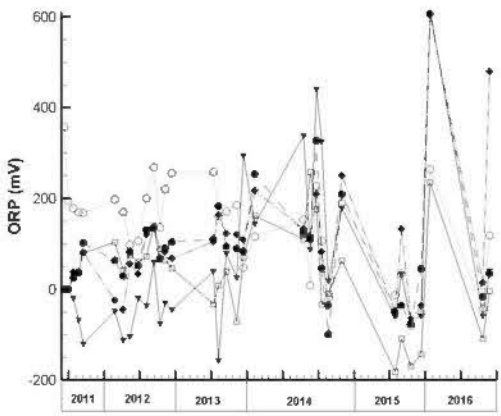
ORP (mV)
2011
2012
2013
2014
2015
2016

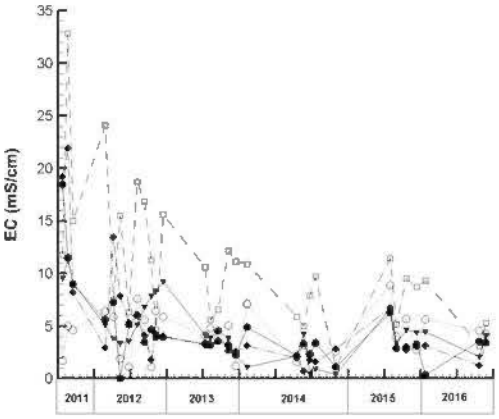
EC (mS/cm)
2011
2012
2013
2014
2015
2016

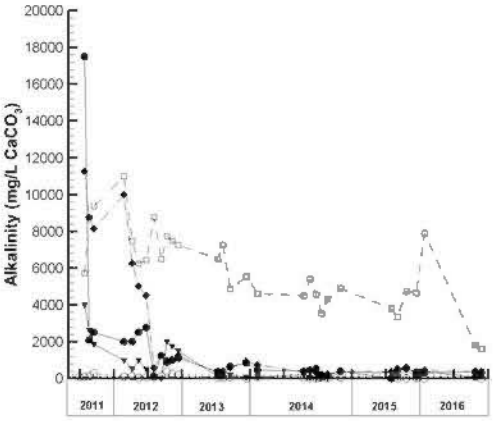
Alkalinity (mg/L CaCO3)
2011
2012
2013
2014
2015
2016

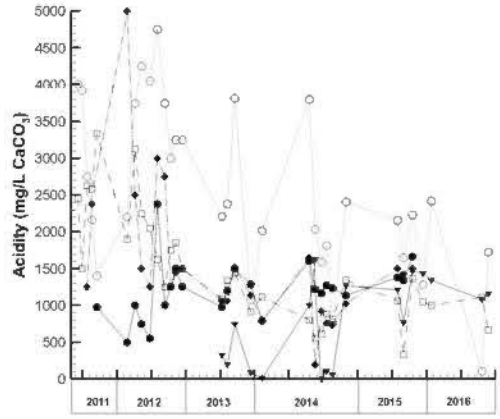
Acidity (mg/L CaCO3)
2011
2012
2013
2014
2015
2016

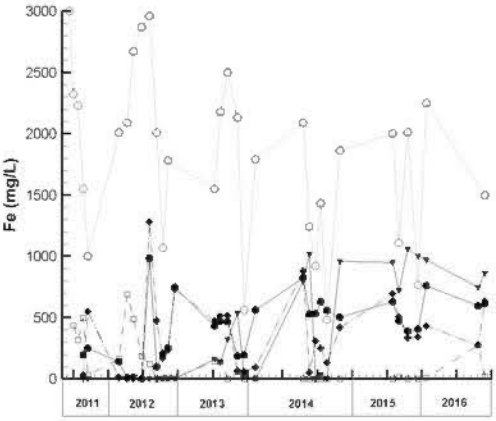
Fe (mg/L)
2011
2012
2013
2014
2015
2016

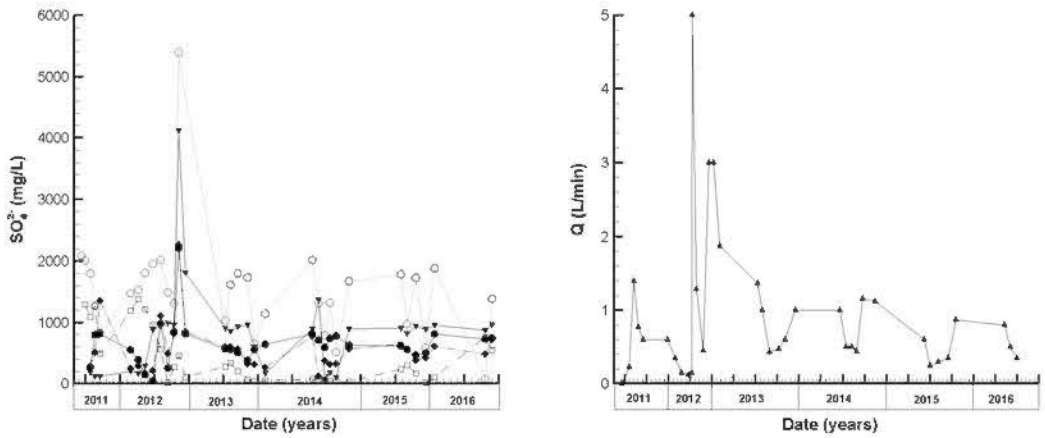

Figure C.6 Evolution of physicochemical parameters (pH, ORP, EC, alkalinity, acidity), Fe_t and SO_4^{2-} concentrations and flow rate (Q) during five years monitoring of the field pilot experiment

Table C.1 Correlation between chemical parameters of treated water collected from the lab-based and field multi-step treatment experiments

	Al	**Ca**	**Fe**	**Mg**	**Mn**	**Ni**	**Pb**	**SO4**	**Si**	**Zn**	**pH**	**EC**
Al	1											
Ca	-0.960	1										
Fe	0.804	-0.852	1									
Mg	-0.672	0.685	-0.456	1								
Mn	-0.175	0.210	0.221	0.622	1							
Ni	0.777	-0.903	0.889	-0.580	-0.026	1						
Pb	0.506	-0.621	0.804	-0.423	0.123	0.796	1					
SO4	0.706	-0.675	0.918	-0.310	0.448	0.691	0.755	1				
Si	-0.899	0.915	-0.714	0.809	0.266	-0.809	-0.457	-0.569	1			
Zn	-0.302	0.273	0.066	0.618	0.900	-0.047	-0.035	0.219	0.224	1		
pH	-0.971	0.949	-0.811	0.559	0.034	-0.816	-0.473	-0.706	0.897	0.116	1	
EC	0.775	-0.839	0.792	-0.327	-0.109	0.762	0.598	0.589	-0.558	-0.270	-0.756	1

Bold numbers indicate that the elements are highly correlated

Table C.2 Correlation between variables and factors (F1 and F2) from treated water collected during laboratory and field multi-step treatment experiments

	Factor F1	Factor F2
Al	**-0.946**	-0.108
Ca	0.982	0.097
Fe	**-0.912**	0.340
Mg	0.690	**0.576**
Mn	0.113	**0.979**
Ni	**-0.925**	0.118
Pb	**-0.728**	0.267
SO_4	**-0.780**	**0.518**
Si	**0.892**	0.193
Zn	0.220	**0.895**
pH	**0.926**	-0.034
EC	**-0.821**	0.026

Bold numbers indicate high correlation

ANNEXE D

ARTICLE DE REVUE SUR LE CHAPITRE 3 (ESSAIS BATCH)

(FICHIERS SUR CD-ROM)

ANNEXE E

ARTICLE DE REVUE SUR LE CHAPITRE 4 (ESSAIS COLONNES)

(FICHIERS SUR CD-ROM)

ANNEXE F

ARTICLE DE CONFÉRENCE (ENVIROMINE 2015, LIMA, PÉROU)

(FICHIERS SUR CD-ROM)

ANNEXE G

PROTOCOLES, PHOTOS ET RÉSULTATS BRUTS DES ESSAIS DE LABORATOIRE

(FICHIERS SUR CD-ROM)